MITOCHONDRIAL DISORDERS: BIOCHEMICAL AND MOLECULAR BASIS OF DISEASE

EDITED BY: Al-Walid Mohsen, Grant M. Hatch, Guilhian Leipnitz and Ronald Wanders

PUBLISHED IN: Frontiers in Genetics, Frontiers in Pediatrics and Frontiers in Cell and Developmental Biology

frontiers Research Topics

frontiers

ISSN 1664-8714
ISBN 978-2-88974-021-5
DOI 10.3389/978-2-88974-021-5

About Frontiers

Frontiers is more than just an open-access publisher of scholarly articles: it is a pioneering approach to the world of academia, radically improving the way scholarly research is managed. The grand vision of Frontiers is a world where all people have an equal opportunity to seek, share and generate knowledge. Frontiers provides immediate and permanent online open access to all its publications, but this alone is not enough to realize our grand goals.

Frontiers Journal Series

The Frontiers Journal Series is a multi-tier and interdisciplinary set of open-access, online journals, promising a paradigm shift from the current review, selection and dissemination processes in academic publishing. All Frontiers journals are driven by researchers for researchers; therefore, they constitute a service to the scholarly community. At the same time, the Frontiers Journal Series operates on a revolutionary invention, the tiered publishing system, initially addressing specific communities of scholars, and gradually climbing up to broader public understanding, thus serving the interests of the lay society, too.

Dedication to Quality

Each Frontiers article is a landmark of the highest quality, thanks to genuinely collaborative interactions between authors and review editors, who include some of the world's best academicians. Research must be certified by peers before entering a stream of knowledge that may eventually reach the public - and shape society; therefore, Frontiers only applies the most rigorous and unbiased reviews.
Frontiers revolutionizes research publishing by freely delivering the most outstanding research, evaluated with no bias from both the academic and social point of view. By applying the most advanced information technologies, Frontiers is catapulting scholarly publishing into a new generation.

What are Frontiers Research Topics?

Frontiers Research Topics are very popular trademarks of the Frontiers Journals Series: they are collections of at least ten articles, all centered on a particular subject. With their unique mix of varied contributions from Original Research to Review Articles, Frontiers Research Topics unify the most influential researchers, the latest key findings and historical advances in a hot research area! Find out more on how to host your own Frontiers Research Topic or contribute to one as an author by contacting the Frontiers Editorial Office: frontiersin.org/about/contact

MITOCHONDRIAL DISORDERS: BIOCHEMICAL AND MOLECULAR BASIS OF DISEASE

Topic Editors:
Al-Walid Mohsen, University of Pittsburgh, United States
Grant M. Hatch, University of Manitoba, Canada
Guilhian Leipnitz, Federal University of Rio Grande do Sul, Brazil
Ronald Wanders, University of Amsterdam, Netherlands

Citation: Mohsen, A.-W., Hatch, G. M., Leipnitz, G., Wanders, R., eds. (2021). Mitochondrial Disorders: Biochemical and Molecular Basis of Disease. Lausanne: Frontiers Media SA. doi: 10.3389/978-2-88974-021-5

Table of Contents

frontiers in Genetics

EDITORIAL
published: 19 November 2021
doi: 10.3389/fgene.2021.769770

Editorial: Mitochondrial Disorders: Biochemical and Molecular Basis of Disease

Guilhian Leipnitz[1], Grant M. Hatch[2], Al-Walid Mohsen[3] and Ronald J. A. Wanders[4]*

[1]Post-Graduation Program in Biological Sciences, Biochemistry, Department of Biochemistry, Universidade Federal do Rio Grande do Sul, Porto Alegre, Brazil, [2]Department of Pharmacology and Therapeutics, University of Manitoba, Winnipeg, MB, Canada, [3]Division of Genetic and Genomic Medicine, Department of Pediatrics, School of Medicine, University of Pittsburgh, Pittsburgh, PA, United States, [4]Laboratory Genetic Metabolic Diseases, Departments Pediatrics, Emma Children Hospital and Clinical Chemistry, Amsterdam University Medical Center, Amsterdam, Netherlands

Keywords: mitochondrial disorders, case report, treatment, pathophysiology, reaction mechanism

Editorial on the Research Topic

Mitochondrial Disorders: Biochemical and Molecular Basis of Disease

Mitochondria are dynamic, double-membrane organelles that play an essential function in cellular energy metabolism, in which the citric acid cycle, fatty acid β-oxidation, and oxidative phosphorylation act in concert to generate most of the ATP in cells. However, in the last few decades, mitochondria have been reported to execute and regulate many other functions, including ATP production, metabolism of amino acids, lipids and nucleotides, iron-sulfur cluster synthesis, calcium homeostasis, and programmed cell death. Healthy mitochondria take up calcium not only to regulate their own intrinsic metabolism and stimulate the production of ATP, but also to buffer cytosolic calcium rises that occur during normal cell functioning (Dard et al., 2020). However, calcium influx beyond the buffering capacity of mitochondria, as well as reactive oxygen overproduction, trigger mitochondrial permeability transition that may cause apoptosis (Vercesi et al., 2018).

For maintenance of normal mitochondrial functionality, this organelle depends on a delicate balance between fission and fusion (mitochondrial dynamics). The fusion and fission cycle consists, respectively, of the formation of an elongated organelle by fusing two or more mitochondria and by the division of one mitochondrion into two daughter mitochondria (Tilokani et al., 2018). While mitofusins 1 and 2 and optic atrophy 1 protein mediate fusion of the outer and inner mitochondrial membrane, correspondingly, dynamin-related protein 1 is considered a crucial player in the fission process, forming oligomers around mitochondria to constrict them (Tilokani et al., 2018).

The pivotal role of mitochondria for cellular survival is highlighted by the variety of diseases that are associated with mitochondrial dysfunction. In this sense, mitochondrial inherited genetic disorders, which may be caused either by mutations in nuclear genes or mitochondrial DNA encoding mitochondrial proteins, usually affect multiple tissues, typically those which are highly dependent on aerobic metabolism (Gorman et al., 2016; Ferreira and van Karnebeek, 2019; Wajner, 2019). While primary defects are characterized by disturbances in oxidative phosphorylation and other energy generating pathways, secondary mitochondrial diseases result from the toxic influences of endogenous metabolites to the mitochondria and/or cell physiology in general. In this topic "Mitochondrial Disorders: Biochemical and Molecular Basis of Disease", we provide a collection of nine articles covering diverse aspects of primary and secondary mitochondrial disorders.

The pathophysiology of mitochondrial disorders is the main theme of two articles. Amaral and Wajner review the toxic effects of fatty acids accumulating in fatty acid oxidation disorders causing impairment of mitochondrial bioenergetics and calcium homeostasis and inducing permeability

OPEN ACCESS

Edited and reviewed by:
Erica E. Davis,
Ann & Robert H. Lurie Children's Hospital of Chicago, United States

****Correspondence:***
Guilhian Leipnitz
guilhian@ufrgs.br

Specialty section:
This article was submitted to Genetics of Common and Rare Diseases, a section of the journal Frontiers in Genetics

Received: *02 September 2021*
Accepted: *26 October 2021*
Published: *19 November 2021*

Citation:
Leipnitz G, Hatch GM, Mohsen A-W and Wanders RJA (2021) Editorial: Mitochondrial Disorders: Biochemical and Molecular Basis of Disease. Front. Genet. 12:769770. doi: 10.3389/fgene.2021.769770

transition pore opening. The group of Dr. Schwarz (Mellis et al.) shows alterations of mitochondrial dynamics in embryonic fibroblasts prepared from *Suox*$^{-/-}$ mice (isolated sulfite oxidase deficiency model) and fibroblasts from patients with molybdenum cofactor deficiency (*MOCS1A, MOCCS1B, MOCS2*, and *GPHN* genes), indicating that disturbances in the mitochondrial network are involved in the pathophysiology of these disorders.

The elucidation of the reaction mechanism of mitochondrial enzymes may help to understand the biochemical abnormalities associated with mitochondrial disorders. In this regard, the article by Leung et al. provides evidence that glycine cleavage system H protein (GCSH) has an additional role beyond being a component of the glycine cleavage system, a protein complex that decarboxylates glycine. The study demonstrates that loss of GCSH causes embryonic death of homozygous *Gcsh* null mice, unlike animals with a deficiency of the other proteins belonging to the glycine cleavage system, which are compatible with embryonic survival. Furthermore, Cronan reviews the reaction mechanism of lipoic acid metabolism enzymes with the aim to better understand the biochemistry and physiology of mitochondrial disorders that affect the assembly of this coenzyme on its cognate enzyme proteins.

In addition, different models for mitochondrial disease research are reviewed by the group of Dr. Sánchez-Alcázar (Povea-Cabello et al.), with emphasis on direct cellular reprogramming. Another article by Schlieben and Prokisch (2020) gives an overview of the mitochondrial disease associated genes, with focus on the classification of these disorders according to the functional roles of deficient proteins, with implications for diagnosis. This topic also includes a perspective article on the outcome of triheptanoin in treating long chain fatty acid oxidation disorders, with special emphasis on the cardiomyopathy and hypoglycemia observed in affected patients (Sklirou et al.).

Finally, two articles present case reports of primary mitochondrial disorders. Kušíková et al. (2021) give a brief review on the mitochondrial disorder caused by mutations in *VARS2*, which encodes the mitochondrial valyl-tRNA synthetase, and presents a patient with a new missense biallelic variant leading to a novel phenotypic presentation. Moreover, (Yan et al.) report the first three Chinese cases of combined oxidative phosphorylation deficiency 23 (COXPD23), which is caused by mutations in *GTPBP3*, as well as genotype-phenotype correlations of these patients.

In conclusion, this topic provides a valuable collection of articles revealing important aspects of the genetic and biochemical basis and pathophysiology of mitochondrial disorders. While most articles emphasize bioenergetic dysfunction as a fundamental mechanism in mitochondrial disorders, this topic also explores the involvement of other mitochondrial functions and processes that are impaired in these pathologies, such as calcium homeostasis, mitochondrial dynamics, and permeability transition. We hope that the articles presented here stimulate future studies not only focused on the expansion of current knowledge but also on the development of novel adjuvant therapeutic strategies with the aim to provide new treatment options and/or to prevent these devastating conditions.

AUTHOR CONTRIBUTIONS

GL, GMH, A-WM, and RW wrote and reviewed the editorial.

ACKNOWLEDGMENTS

The guest editors wish to thank all the authors and reviewers for their valuable contributions to this Research Topic.

REFERENCES

Dard, L., Blanchard, W., Hubert, C., Lacombe, D., and Rossignol, R. (2020). Mitochondrial Functions and Rare Diseases. *Mol. Aspects Med.* 71, 100842. doi:10.1016/j.mam.2019.100842

Ferreira, C. R., and van Karnebeek, C. D. M. (2019). Inborn Errors of Metabolism. *Handb Clin. Neurol.* 162, 449–481. doi:10.1016/B978-0-444-64029-1.00022-9

Gorman, G. S., Chinnery, P. F., DiMauro, S., Hirano, M., Koga, Y., McFarland, R., et al. (2016). Mitochondrial Diseases. *Nat. Rev. Dis. Primers.* 2, 16080. doi:10.1038/nrdp.2016.80

Kušíková, K., Feichtinger, R. G., Csillag, B., Kalev, O. K., Weis, S., Duba, H. C., et al. (2021). Case Report and Review of the Literature: A New and a Recurrent Variant in the VARS2 Gene Are Associated With Isolated Lethal Hypertrophic Cardiomyopathy, Hyperlactatemia, and Pulmonary Hypertension in Early. *Infancy. Front. Pediatr.* 9, 660076. doi:10.3389/fped.2021.660076

Schlieben, L. D., and Prokisch, H. (2020). The Dimensions of Primary Mitochondrial Disorders. *Front. Cell. Dev. Biol.* 8, 600079. doi:10.3389/fcell.2020.600079

Tilokani, L., Nagashima, S., Paupe, V., and Prudent, J. (2018). Mitochondrial Dynamics: Overview of Molecular Mechanisms. *Essays Biochem.* 62 (3), 341–360. doi:10.1042/EBC20170104

Vercesi, A. E., Castilho, R. F., Kowaltowski, A. J., de Oliveira, H. C. F., de Souza-Pinto, N. C., Figueira, T. R., et al. (2018). Mitochondrial Calcium Transport and the Redox Nature of the Calcium-Induced Membrane Permeability Transition. *Free Radic. Biol. Med.* 129, 1–24. doi:10.1016/j.freeradbiomed.2018.08.034

Wajner, M. (2019). Neurological Manifestations of Organic Acidurias. *Nat. Rev. Neurol.* 15 (5), 253–271. doi:10.1038/s41582-019-0161-9

Conflict of Interest: The authors declare that the research was conducted in the absence of any commercial or financial relationships that could be construed as a potential conflict of interest.

frontiers in Genetics

MINI REVIEW
published: 21 May 2020
doi: 10.3389/fgene.2020.00510

Progress in the Enzymology of the Mitochondrial Diseases of Lipoic Acid Requiring Enzymes

*John E. Cronan**

B103 Chemical and Life Sciences Laboratory, Departments of Microbiology and Biochemistry, University of Illinois at Urbana-Champaign, Urbana, IL, United States

Three human mitochondrial diseases that directly affect lipoic acid metabolism result from heterozygous missense and nonsense mutations in the *LIAS*, *LIPT1*, and *LIPT2* genes. However, the functions of the proteins encoded by these genes in lipoic acid metabolism remained uncertain due to a lack of biochemical analysis at the enzyme level. An exception was the LIPT1 protein for which a perplexing property had been reported, a ligase lacking the ability to activate its substrate. This led to several models, some contradictory, to accommodate the role of LIPT1 protein activity in explaining the phenotypes of the afflicted neonatal patients. Recent evidence indicates that this LIPT1 protein activity is a misleading evolutionary artifact and that the physiological role of LIPT1 is in transfer of lipoic acid moieties from one protein to another. This and other new biochemical data now define a straightforward pathway that fully explains each of the human disorders specific to the assembly of lipoic acid on its cognate enzyme proteins.

Keywords: lipoic acid, lipoate assembly, pyruvate dehydrogenase, α-ketoglutarate dehydrogenase, glycine cleavage system, LIPT1, LIPT2, LIAS

OPEN ACCESS

Edited by:
Al-Walid Mohsen,
University of Pittsburgh, United States

Reviewed by:
Sandro Ghisla,
University of Konstanz, Germany
J. Kalervo Hiltunen,
University of Oulu, Finland
Ronald Wanders,
University of Amsterdam, Netherlands

***Correspondence:**
John E. Cronan
jecronan@illinois.edu

Specialty section:
This article was submitted to Genetic Disorders, a section of the journal Frontiers in Genetics

Received: *06 March 2020*
Accepted: *27 April 2020*
Published: *21 May 2020*

Citation:
Cronan JE (2020) Progress in the Enzymology of the Mitochondrial Diseases of Lipoic Acid Requiring Enzymes. Front. Genet. 11:510. doi: 10.3389/fgene.2020.00510

INTRODUCTION

Lipoic acid is an enzyme cofactor that plays a key role in mitochondrial metabolism. All of the mammalian proteins involved in lipoic acid assembly and utilization are located in the mitochondria. The cofactor is covalently attached to subunits of enzymes involved in central pathways of mitochondrial energy and carbon metabolism and thus defects in the synthesis and attachment of lipoic acid have dire effects on human health (Mayr et al., 2014; Tort et al., 2016).

DISEASE MANIFESTATIONS

Neonatal patients suffering from mutations in the genes encoding the enzymes of lipoate assembly show defective respiration, accumulation of toxic levels of specific amino acids, and generally die early in life (Mayr et al., 2014; Tort et al., 2016). Note that this review will not discuss the clinical aspects of these diseases but will focus on the biochemistry of lipoic acid assembly. Reviews that discuss the diagnosis and treatment of these disorders are: (Mayr et al., 2014; Tort et al., 2016). Mutations that result in iron–sulfur cluster biosynthesis deficiencies that affect the activity of lipoic acid synthase (LIAS) (**Table 1**), the enzyme that inserts the lipoate sulfur atoms, will not be discussed because their effects are not specific to lipoic acid synthesis; other key enzymes (e.g., complexes II and III of the respiratory chain) are also affected.

TABLE 1 | The nonenclature differences in *E. coli, B. subtilis* and humans.

Protein	*E. coli*	*B. subtilis*	*H. sapiens*
Lipoyl Synthase	LipA	LipA	LIAS
Octanoyl-transferase	LipB	LipM	LIPT2
Glycine H Protein	GcvH	GcvH	GCSH
Amidotransferase	none	LipL	LIPT1
Lipoate ligase	LiplA	LipJ	none

The key enzymes that require lipoic acid for activity are pyruvate dehydrogenase, the enzyme required for entry of carbon into the citric acid cycle and α-ketoglutarate dehydrogenase, an enzyme at the midpoint of the citric acid cycle plus the glycine cleavage system. Two other dehydrogenases, the branched chain keto acid dehydrogenase required for degradation of branched-chain amino acids and the α-oxo(keto)adipate dehydrogenase of lysine degradation also require lipoic acid for activity. However, although accumulation of branched-chain amino acids and lysine in body fluids of patients have been reported (Mayr et al., 2011, 2014), enzymological studies have generally focused on the pyruvate and α-ketoglutarate dehydrogenase due to their key roles in energy production. The loss of these two dehydrogenases short-circuits the citric acid cycle, resulting in severe respiratory deficiency and extreme muscle weakness (Mayr et al., 2014; Tort et al., 2016). Lack of glycine cleavage activity additionally results in elevated brain glycine levels which can result in a host of neurological disorders, including neurodegeneration, encephalopathy, and neonatal-onset epilepsy (Mayr et al., 2014; Tort et al., 2016; Stowe et al., 2018). In general, the first indicator of defective lipoic acid metabolism is the presence of very high levels of lactate (resulting from reduction of the pyruvate that accumulates due to loss pyruvate dehydrogenase activity) in urine and other bodily fluids. Subsequent measurement of body fluid glycine levels consigns the patients into two classes (Tort et al., 2016). Normal glycine levels demonstrate that the glycine cleavage system is functional whereas abnormally high glycine levels indicate that glycine cleavage is defective. Tissue fibroblasts (and/or liver biopsy tissue) derived from the patients are then assayed for the cognate enzyme activities plus the levels of lipoylation of the cognate enzyme proteins. Patients that display absent or low lipoylation of all three enzymes have mutations in either of two genes *LIAS* or *LIPT2* whereas patients that retain glycine cleavage activity are mutant in a third gene, *LIPT1* (Mayr et al., 2014; Tort et al., 2016; **Table 1**). The phenotypes of the two classes of patients could be explained by a simple model in which LIAS and LIPT2 are required for lipoic acid synthesis whereas LIPT1 is not required (demonstrated by the normally lipoylated glycine cleavage system H protein (GCSH) of *LIPT1* patients). Since it was clear that LIAS was the sulfur insertion enzyme (Mayr et al., 2011), LIPT2 could be assigned a role in providing the substrate of LIAS whereas LIPT1 would function to relay lipoyl groups from GCSH to the pyruvate and α-ketoglutarate dehydrogenases. (Note that the protein products of the genes have the same name as the encoding gene except that protein names lack italics.) However, there was no precedent for such a pathway in nature and the LIPT1 protein had an enzymatic activity that muddled this simple model. It now seems clear that this misleading enzyme activity is an evolutionary artifact (see below).

The Pathway of Lipoic Acid Assembly and Attachment to the Cognate Proteins

The background of the lipoic acid assembly and attachment pathway is required to place the products of these genes in context. In bacteria *de novo* synthesized lipoic acid attached to its cognate enzyme proteins (lipoyl modification) was shown to arise by a markedly unusual pathway: lipoyl groups are assembled on the cognate enzyme proteins (**Figure 1**). Although this was first uncovered by genetic and biochemical analysis in bacteria (see below), the bacterial and human proteins are members of the same protein family (see below). The "backbone" of lipoic acid is octanoic acid, an eight-carbon fatty acid synthesized by a distinct mitochondrial fatty acid synthesis system. The relevant form of octanoic acid is that attached to a small carrier protein of fatty acid synthesis called acyl carrier protein (ACP). The chemical linkage that couples octanoate to ACP greatly facilitates transfer of the octanoyl group to the glycine cleavage H protein (GCSH) where the covalently bound octanoyl groups are converted to lipoyl groups by insertion of the two sulfur atoms required for function of the cognate enzymes. Following sulfur insertion lipoyl groups are relayed to the E2 subunits of the two dehydrogenases. The human pathway of **Figure 1** has been validated by direct enzyme assays of the proteins and their activity in a reconstituted human pathway (Cao et al., 2018). Hence GCSH functions both in glycine cleavage and in assembly of lipoyl moieties. Indeed, bacterial strains that lack GCSH are defective in both glycine cleavage and lipoic acid assembly (Christensen et al., 2011; Cao et al., 2018).

The Pathway Explains the Metabolic Defects Seen in Neonatal Patients

Given the pathway (**Figure 1**) we can now interpret the biochemical phenotypes of the patients. LIPT2 and LIAS proteins are required for lipoic acid assembly because LIPT2 is the enzyme that transfers octanoyl groups from ACP to GCSH to provide the substrate for sulfur insertion by LIAS. Hence patients defective in either of these genes have undetectable or severely decreased levels of all lipoylated proteins and undergo the severe respiratory deficiency and extreme muscle weakness due to citric acid cycle disfunction plus the neurological impairments caused by glycine accumulation in the brain (Tort et al., 2016). In contrast LIPT1 patients generally suffer only the respiratory and muscle weakness problems because GCSH is lipoylated and glycine is cleaved (Tort et al., 2016). The two dehydrogenase proteins lack lipoylation because LIPT1 is the enzyme that transfers lipoyl groups from lipoyl-GCSH to the dehydrogenase proteins. Hence, glycine cleavage is normal and most of these patients escape the neurological problems resulting from glycine accumulation. However, there are reports of neurological involvements in LIPT1 patients (Soreze et al., 2013; Tache et al., 2016; Stowe et al., 2018) which remain unexplained.

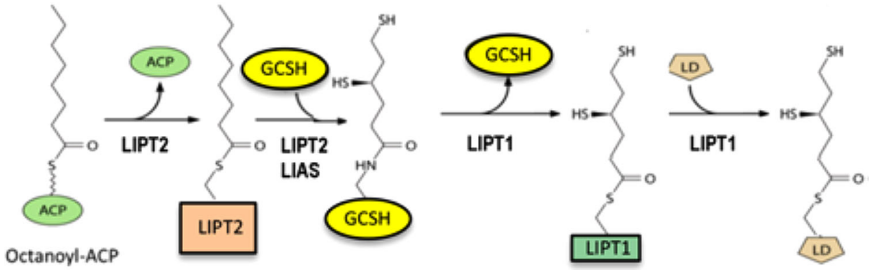

FIGURE 1 | The human pathway of assembly of lipoyl moieties on its cognate proteins. LIPT2 utilizes octanoyl-ACP synthesized by the mitochondrial fatty acid synthesis system to modify GCSH. The reaction proceeds via a LIPT2 acyl enzyme intermediate as shown. The octanoyl-GCSH is then converted to lipoyl-GCSH by LIAS catalyzed sulfur insertion. LIPT1 then transfers the lipoyl moiety from GCSH to form an acyl enzyme intermediate. This in turn is attacked by a specific lysine reside of the lipoyl domain (LD) of the N-termini of the E2 subunits of the dehydrogenases or GCSH to give the active modified enzymes.

The Misleading Defective Ligase Activity of the LIPT1 Protein

Beginning in 1969 Japanese investigators began study of lipoic acid attachment to the glycine cleavage H protein of various vertebrates (Fujiwara et al., 1994, 1996, 1997, 2001). They identified a puzzling enzyme encoded the by the human *LIPT1* gene that could transfer the activated intermediate lipoyl-AMP to the H protein. However, the origin of lipoyl-AMP remained a mystery. Since classical ligases in general use ATP to activate the substrate to be ligated as well as perform the transfer of the substrate to the acceptor molecule, the protein seemed a peculiar "half ligase" unable to activate its substrate. This was in contrast to an early report that lipoate was readily attached to pyruvate dehydrogenase in an ATP-requiring reaction that proceeded through a lipoyl-AMP intermediate (Reed et al., 1958) in bacterial extracts. However, since the preparations were only partially purified, the activity could have been due to more than one protein. In 1994 the first homogenous bacterial lipoate ligase was reported (the LplA of *E. coli*) and unlike the mammalian and avian proteins, it performed the full ligase reaction: incubations containing lipoate and ATP resulted in formation of lipoyl-AMP and the lipoyl moiety was then transferred to the cognate acceptor proteins with release of AMP (Morris et al., 1994). Curiously, this *E. coli* protein aligned readily with the vertebrate LIPT1 proteins except for the C-terminal 25% of the proteins at which point the sequences diverged greatly (Fujiwara et al., 2001). Subsequent crystal structures of the *E. coli* LplA and bovine LIPT1 proteins showed that although the N-terminal 75% of the protein structures could be superimposed, the two C-terminal domains were positioned very differently (Fujiwara et al., 2007, 2010). Subsequent studies of other lipoate ligases indicated that the C-terminal domain is required for lipoyl-AMP synthesis consistent with the lack of this activity in the vertebrate proteins (Christensen and Cronan, 2009; Cao and Cronan, 2015). Despite the inability of the vertebrate proteins to perform the overall ligase reaction, several investigators assigned it a role in scavenging dietary lipoate which argued that feeding lipoate to patients should bypass genetic defects in lipoate assembly.

Insights From Studies in Mammals, Yeast and Bacteria

The first indication that lipoate supplementation was unable to reverse the genetic defects in lipoic acid metabolism came from studies of *LIAS* knockout mice (Yi and Maeda, 2005). Despite supplementation of the diets of the heterozygous mothers with lipoic acid during pregnancy, all homozygous *LIAS* null embryos died *in utero* and were reabsorbed This was consistent with the findings that lipoic acid supplementation of the diets of human *LIAS, LIPT1*, and *LIPT2* patients or of their fibroblast cultures failed to alleviate the physiological and biochemical effects of the mutant genes (Baker et al., 2014; Tort et al., 2014, 2016; Tsurusaki et al., 2015). Lipoate is known to rapidly enter the bloodstream (Teichert et al., 2003) and thus it should have been available if a fully competent ligase existed. Additional mouse and tissue culture studies also clearly demonstrated the inability of supplemented lipoic acid to become attached to the key lipoic acid modified proteins of central metabolism (Witkowski et al., 2007; Feng et al., 2009; Smith et al., 2012).

Two genetic selections gave *E. coli* mutants devoid of ligase activity due to disruption of the encoding gene, *lplA*. These selections were done based on the premise that the ligase played a role in lipoic acid synthesis but this soon found not to be the case. The mutant bacteria had normal levels of lipoylated enzymes and grew normally (Morris et al., 1994). Further work showed that the physiological function of *E. coli* lipoate ligase (LplA) was to scavenge lipoic acid from the environment, an advantage for an enteric bacterium. These data led to a new hypothesis in which octanoyl-ACP was the substrate for sulfur insertion. Prior studies had isolated mutants that required lipoic acid for growth and these fell into two classes, those lacking the sulfur insertion enzyme (LipA, a homolog of LIAS) and an enzyme (LipB, a homolog of LIPT2) (**Table 1**) that transferred either lipoic acid or octanoic acid from their ACP thioesters to pyruvate dehydrogenase (Cronan, 2016). Although study of these enzymes led to the first synthesis of lipoic acid *in vitro*, (Miller et al., 2000) the putative lipoyl-ACP reaction intermediate could not be detected. The reason for this result became clear when LipB mutants were found to grow with

octanoic acid supplementation in place of the usual lipoic acid supplementation (Zhao et al., 2003). Moreover, octanoate-dependent growth required LplA ligase activity. Hence, the combination of octanoate supplementation and ligase activity bypassed the lack of LipB transferase activity (Zhao et al., 2003). The most straightforward interpretation of these results was that lipoyl moieties were assembled on the cognate enzyme proteins. That is, octanoyl groups became covalently attached to the dehydrogenase and were then converted to lipoyl moieties by the LipA sulfur insertion enzyme. Hence there was no lipoyl-ACP intermediate to be detected! This "on-site" assembly was a striking departure from the usual pathway of other attached cofactors (e.g., biotin) which are fully assembled and then transferred onto the cognate protein. The pathway of lipoyl-protein assembly was quickly validated by *in vivo* and *in vitro* studies in several laboratories (Booker, 2004; Cicchillo et al., 2004; Bryant et al., 2006; Douglas et al., 2006). Hence *E. coli* lipoyl assembly requires only two enzymes, the LipB octanoyl transferase and the sulfur insertion enzyme, LipA.

Lipoic acid assembly has also been studied in the yeast, *Saccharomyces cerevisiae* mainly by genetic studies and immunological assays of protein lipoylation (Sulo and Martin, 1993; Schonauer et al., 2008). The picture that emerged is consistent with the human pathway (see below). However, the yeast proteins involved in lipoate assembly form intractable inclusion bodies when expressed in *E. coli* or in a yeast expression system (Hermes and Cronan, 2013). Hence minimal *in vitro* enzymology has been done and that was done with proteins refolded from inclusion bodies, a serious caveat (Hermes and Cronan, 2013). Given the lack of direct demonstrations of the enzymatic activities of the proteins, the yeast pathway lacks the biochemical grounding of the human pathway. An unexplained facet is that most of the yeast lipoic acid synthesis mutants were originally isolated as strains defective in processing of mitochondrial RNAs (Sulo and Martin, 1993; Schonauer et al., 2008).

The Human Pathway Is Remarkably Similar to That Used by Gram-Positive Bacteria and Probably by Yeast

The gram-positive bacterium, *Bacillus subtilis,* was studied because it lacked a gene that encoded a recognizable LipB-like octanoyl transferase although the bacterium had a *lipA* gene, disruption of which resulted in a growth requirement for lipoic acid (Martin et al., 2009). The ability to use exogenous lipoic acid argued that the bacterium must have a functional lipoate ligase. However, analysis of the *B. subtilis* genome showed not one but three genes encoding putative lipoate ligases, albeit they had only low sequence identity with *E. coli* LplA. One of these genes encoded a ligase (LplJ) that functionally replaced LplA in *E. coli* (Martin et al., 2011) whereas a second putative ligase gene encoded an octanoyl transferase (LipM) that had no ligase activity (Christensen and Cronan, 2010). The protein encoded by third ligase candidate gene, LipL, also lacked ligase activity and seemed an enigma, although its inactivation resulted in a growth requirement for lipoic acid. A series of biochemical experiments with purified proteins presented the perplexing result that the *B. subtilis* LipM octanoyl transferase was unable to transfer octanoate from octanoyl-ACP to its native pyruvate dehydrogenase E2 subunit, although it was active with a foreign (*E. coli*) pyruvate dehydrogenase subunit (Christensen et al., 2011). These results argued that a factor or factors was missing. Two were found: GcvH, the GCSH and the enigmatic third ligase candidate, LipL (Christensen et al., 2011). Biochemical analyses showed that the LipM octanoyl transferase attached an octanoyl moiety to GcvH which LipA converted to a lipoyl group. LipL then transferred the lipoyl group from GcvH to the dehydrogenase proteins (Christensen et al., 2011). This was the first biochemical evidence for "lipoyl relay," the process used in the human and yeast pathways. Indeed, the human pathway reaction scheme given in **Figure 1** can describe that of *B. subtilis* given substitution of LipM for LIPT2, GcvH for GCSH, and LipL for LIPT1.

DISCUSSION

Evolutionary Considerations

Why is lipoic acid assembled on its cognate enzymes rather than on octanoyl ACP? A good rationale is economy: the levels of cognate proteins to be modified dictate that the cell can make only the amount of lipoic acid required; no excess is made.

Is there an explanation for why lipoyl moieties are relayed from the glycine cleavage H protein to the dehydrogenase rather than directly assembled on the dehydrogenases? A persuasive argument put forth by Braakman and Smith (2014) is that lipoyl relay seems be a "make-do" device that arose when primitive bacteria having the glycine cleavage H protein as the sole lipoylated protein acquired lipoate-requiring dehydrogenases.

All of the enzymes that transfer octanoate or lipoate are related by their structures but with little sequence conservation and comprise a protein family (Pfam PF03099). Crystal structures show that the lipoate ligases (LplA, LplJ), the octanoyl transferases (LIPT2, LipB, LipM), and the lipoyl relay enzymes (LIPT1 and LipL) are all constructed on the same structural scaffold albeit with only minimal amino acid sequence conservation (generally 15–25%) (Cronan, 2016). Sometimes the scaffold has given rise to the same enzyme activity by seemingly different routes. An example is the two bacterial octanoyl transferases (LipB and LipM) which have their active site cysteine residues lie on different loops of the scaffold (Christensen and Cronan, 2010). The Pfam PF03099 scaffold is also found in the biotin protein ligases that attach biotin to its cognate proteins. The fact that proteins having similar sequences (e.g., LplA and LIPT1) can have different enzyme activities makes assignment of functions based solely on sequence comparisons perilous.

Why has LIPT1 retained a partial lipoate ligase reaction when it clearly functions as an amidotransferase that transfers lipoate from GCSH to the dehydrogenases E2 subunits? The answer seems to lie in a newly appreciated aspect of enzyme evolution called "moonlighting"; a protein can acquire a new enzymatic activity while fully or partially retaining its original activity (Copley, 2012, 2014; Jeffery, 2018, 2019). That is, mutations

can enhance the moonlighting function without concomitant elimination of the ancestral function. The original ancestor of LIPT1 seems likely to have been a fully functional lipoate ligase like LplA encoded by the genome of the bacterial endosymbiont that became the mitochondrion. In this scenario the price for retooling the ligase into an amidotransferase was that the carboxyl terminus lost the ability to activate lipoate to lipoyl-AMP and the protein became a "half-ligase" and (temporarily?) retained the partial ligase activity. In other words, the lipoyl-transfer activity is an evolutionary remnant, an aspect often seen in moonlighting proteins (Copley, 2014; Jeffery, 2018). Note that moonlighting as been observed for medically important proteins (Sriram et al., 2005; Houten, 2017) and the possibility that moonlighting could complicate understanding of single gene Mendelian inherited disorders has been raised (Sriram et al., 2005; Franco-Serrano et al., 2018). Indeed, the partial LIPT1 ligase activity markedly hindered our understanding the human pathway of lipoyl-protein assembly.

The Future?

Although the biochemistry and physiology of the human disorders of lipoic acid metabolism is now understood this knowledge offers few approaches to ameliorate the suffering of these patients (as is the case with other mitochondrial diseases). At present this reviewer can offer only the remote possibility of introducing a bacterial ligase into the mitochondria perhaps by inserting a modified ligase gene into the nuclear genome. The encoded ligase would carry an N-terminal sequence targeting it to the mitochondria. The *E. coli* lipoate ligase is known to modify human lipoyl enzymes (Quinn, 1997).

AUTHOR CONTRIBUTIONS

JC wrote the entire manuscript and takes full responsibility for the contents.

FUNDING

The research from this laboratory discussed herein was supported by Grant AI15650 from the National Institutes of Allergy and Infection Diseases, National Institutes of Health.

REFERENCES

Baker, P. R., Friederich, M. W., Swanson, M. A., Shaikh, T., Bhattacharya, K., Scharer, G. H., et al. (2014). Variant non ketotic hyperglycinemia is caused by mutations in LIAS, BOLA3 and the novel gene GLRX5. *Brain* 137, 366–379. doi: 10.1093/brain/awt328

Booker, S. J. (2004). Unraveling the pathway of lipoic acid biosynthesis. *Chem. Biol.* 11, 10–12. doi: 10.1016/j.chembiol.2004.01.002

Braakman, R., and Smith, E. (2014). Metabolic evolution of a deep-branching hyperthermophilic chemoautotrophic bacterium. *PLoS One* 9:e87950. doi: 10.1371/journal.pone.0087950

Bryant, P., Kriek, M., Wood, R. J., and Roach, P. L. (2006). The activity of a thermostable lipoyl synthase from Sulfolobus solfataricus with a synthetic octanoyl substrate. *Anal. Biochem.* 351, 44–49. doi: 10.1016/j.ab.2006.01.023

Cao, X., and Cronan, J. E. (2015). The Streptomyces coelicolor lipoate-protein ligase is a circularly permuted version of the *Escherichia coli* enzyme composed of discrete interacting domains. *J. Biol. Chem.* 290, 7280–7290. doi: 10.1074/jbc.M114.626879

Cao, X., Hong, Y., Zhu, L., Hu, Y., and Cronan, J. E. (2018). Development and retention of a primordial moonlighting pathway of protein modification in the absence of selection presents a puzzle. *Proc. Natl. Acad. Sci. U.S.A.* 115, 647–655. doi: 10.1073/pnas.1718653115

Christensen, Q. H., and Cronan, J. E. (2009). The Thermoplasma acidophilum LplA-LplB complex defines a new class of bipartite lipoate-protein ligases. *J. Biol. Chem.* 284, 21317–21326. doi: 10.1074/jbc.M109.015016

Christensen, Q. H., and Cronan, J. E. (2010). Lipoic acid synthesis: a new family of octanoyltransferases generally annotated as lipoate protein ligases. *Biochemistry* 49, 10024–10036. doi: 10.1021/bi101215f

Christensen, Q. H., Martin, N., Mansilla, M. C., De Mendoza, D., and Cronan, J. E. (2011). A novel amidotransferase required for lipoic acid cofactor assembly in *Bacillus subtilis*. *Mol. Microbiol.* 80, 350–363. doi: 10.1111/j.1365-2958.2011.07598.x

Cicchillo, R. M., Iwig, D. F., Jones, A. D., Nesbitt, N. M., Baleanu-Gogonea, C., Souder, M. G., et al. (2004). Lipoyl synthase requires two equivalents of S-adenosyl-L-methionine to synthesize one equivalent of lipoic acid. *Biochemistry* 43, 6378–6386. doi: 10.1021/bi049528x

Copley, S. D. (2012). Moonlighting is mainstream: paradigm adjustment required. *Bioessays* 34, 578–588. doi: 10.1002/bies.201100191

Copley, S. D. (2014). An evolutionary perspective on protein moonlighting. *Biochem. Soc. Trans.* 42, 1684–1691. doi: 10.1042/BST20140245

Cronan, J. E. (2016). Assembly of lipoic acid on its cognate enzymes: an extraordinary and essential biosynthetic pathway. *Microbiol. Mol. Biol. Rev.* 80, 429–450. doi: 10.1128/MMBR.00073-15

Douglas, P., Kriek, M., Bryant, P., and Roach, P. L. (2006). Lipoyl synthase inserts sulfur atoms into an octanoyl substrate in a stepwise manner. *Angew. Chem. Int. Ed. Engl.* 45, 5197–5199. doi: 10.1002/anie.200601910

Feng, D., Witkowski, A., and Smith, S. (2009). Down-regulation of mitochondrial acyl carrier protein in mammalian cells compromises protein lipoylation and respiratory complex I and results in cell death. *J. Biol. Chem.* 284, 11436–11445. doi: 10.1074/jbc.M806991200

Franco-Serrano, L., Huerta, M., Hernandez, S., Cedano, J., Perez-Pons, J., Pinol, J., et al. (2018). Multifunctional proteins: involvement in human diseases and targets of current drugs. *Protein J.* 37, 444–453. doi: 10.1007/s10930-018-9790-x

Fujiwara, K., Hosaka, H., Matsuda, M., Okamura-Ikeda, K., Motokawa, Y., Suzuki, M., et al. (2007). Crystal structure of bovine lipoyltransferase in complex with lipoyl-AMP. *J. Mol. Biol.* 371, 222–234. doi: 10.1016/j.jmb.2007.05.059

Fujiwara, K., Maita, N., Hosaka, H., Okamura-Ikeda, K., Nakagawa, A., and Taniguchi, H. (2010). Global conformational change associated with the two-step reaction catalyzed by *Escherichia coli* lipoate-protein ligase A. *J. Biol. Chem.* 285, 9971–9980. doi: 10.1074/jbc.M109.078717

Fujiwara, K., Okamura-Ikeda, K., and Motokawa, Y. (1994). Purification and characterization of lipoyl-AMP:N epsilon-lysine lipoyltransferase from bovine liver mitochondria. *J. Biol. Chem.* 269, 16605–16609.

Fujiwara, K., Okamura-Ikeda, K., and Motokawa, Y. (1996). Lipoylation of acyltransferase components of alpha-ketoacid dehydrogenase complexes. *J. Biol. Chem.* 271, 12932–12936. doi: 10.1074/jbc.271.22.12932

Fujiwara, K., Okamura-Ikeda, K., and Motokawa, Y. (1997). Lipoate addition to acyltransferases of alpha-keto acid dehydrogenase complexes and H-protein of glycine cleavage system. *Methods Enzymol.* 279, 184–193. doi: 10.1016/s0076-6879(97)79022-0

Fujiwara, K., Takeuchi, S., Okamura-Ikeda, K., and Motokawa, Y. (2001). Purification, characterization, and cDNA cloning of lipoate-activating enzyme from bovine liver. *J. Biol. Chem.* 276, 28819–28823. doi: 10.1074/jbc.M101748200

Hermes, F. A., and Cronan, J. E. (2013). The role of the *Saccharomyces cerevisiae* lipoate protein ligase homologue, Lip3, in lipoic acid synthesis. *Yeast* 30, 415–427. doi: 10.1002/yea.2979

Houten, S. M. (2017). Protein moonlighting in inborn errors of metabolism: the case of the mitochondrial acylglycerol kinase. *J. Inherit. Metab. Dis.* 40, 755–756. doi: 10.1007/s10545-017-0090-y

Jeffery, C. J. (2018). Protein moonlighting: what is it, and why is it important? *Philos. Trans. R. Soc. Lond. B Biol. Sci.* 373:20160523. doi: 10.1098/rstb.2016.0523

Jeffery, C. J. (2019). Multitalented actors inside and outside the cell: recent discoveries add to the number of moonlighting proteins. *Biochem. Soc. Trans.* 47, 1941–1948. doi: 10.1042/BST20190798

Martin, N., Christensen, Q. H., Mansilla, M. C., Cronan, J. E., and De Mendoza, D. (2011). A novel two-gene requirement for the octanoyltransfer reaction of *Bacillus subtilis* lipoic acid biosynthesis. *Mol. Microbiol.* 80, 335–349. doi: 10.1111/j.1365-2958.2011.07597.x

Martin, N., Lombardia, E., Altabe, S. G., De Mendoza, D., and Mansilla, M. C. (2009). A lipA (yutB) mutant, encoding lipoic acid synthase, provides insight into the interplay between branched-chain and unsaturated fatty acid biosynthesis in *Bacillus subtilis*. *J. Bacteriol.* 191, 7447–7455. doi: 10.1128/JB.01160-09

Mayr, J. A., Feichtinger, R. G., Tort, F., Ribes, A., and Sperl, W. (2014). Lipoic acid biosynthesis defects. *J. Inherit. Metab. Dis.* 37, 553–563.

Mayr, J. A., Zimmermann, F. A., Fauth, C., Bergheim, C., Meierhofer, D., Radmayr, D., et al. (2011). Lipoic acid synthetase deficiency causes neonatal-onset epilepsy, defective mitochondrial energy metabolism, and glycine elevation. *Am. J. Hum. Genet.* 89, 792–797. doi: 10.1016/j.ajhg.2011.11.011

Miller, J. R., Busby, R. W., Jordan, S. W., Cheek, J., Henshaw, T. F., Ashley, G. W., et al. (2000). *Escherichia coli* LipA is a lipoyl synthase: in vitro biosynthesis of lipoylated pyruvate dehydrogenase complex from octanoyl-acyl carrier protein. *Biochemistry* 39, 15166–15178. doi: 10.1021/bi002060n

Morris, T. W., Reed, K. E., and Cronan, J. E. (1994). Identification of the gene encoding lipoate-protein ligase A of *Escherichia coli*. Molecular cloning and characterization of the lplA gene and gene product. *J. Biol. Chem.* 269, 16091–16100.

Quinn, J. (1997). Lipoylation of acyltransferase components of 2-oxo acid dehydrogenase complexes. *Methods Enzymol.* 279, 193–202. doi: 10.1016/s0076-6879(97)79023-2

Reed, L. J., Leach, F. R., and Koike, M. (1958). Studies on a lipoic acid-activating system. *J. Biol. Chem.* 232, 123–142.

Schonauer, M. S., Kastaniotis, A. J., Hiltunen, J. K., and Dieckmann, C. L. (2008). Intersection of RNA processing and the type II fatty acid synthesis pathway in yeast mitochondria. *Mol. Cell. Biol.* 28, 6646–6657. doi: 10.1128/MCB.01162-08

Smith, S., Witkowski, A., Moghul, A., Yoshinaga, Y., Nefedov, M., De Jong, P., et al. (2012). Compromised mitochondrial fatty acid synthesis in transgenic mice results in defective protein lipoylation and energy disequilibrium. *PLoS One* 7:e47196. doi: 10.1371/journal.pone.0047196

Soreze, Y., Boutron, A., Habarou, F., Barnerias, C., Nonnenmacher, L., Delpech, H., et al. (2013). Mutations in human lipoyltransferase gene LIPT1 cause a Leigh disease with secondary deficiency for pyruvate and alpha-ketoglutarate dehydrogenase. *Orphanet. J. Rare Dis.* 8:192. doi: 10.1186/1750-1172-8-192

Sriram, G., Martinez, J. A., Mccabe, E. R., Liao, J. C., and Dipple, K. M. (2005). Single-gene disorders: what role could moonlighting enzymes play? *Am. J. Hum. Genet.* 76, 911–924. doi: 10.1086/430799

Stowe, R. C., Sun, Q., Elsea, S. H., and Scaglia, F. (2018). LIPT1 deficiency presenting as early infantile epileptic encephalopathy, Leigh disease, and secondary pyruvate dehydrogenase complex deficiency. *Am. J. Med. Genet A* 176, 1184–1189. doi: 10.1002/ajmg.a.38654

Sulo, P., and Martin, N. C. (1993). Isolation and characterization of LIP5. A lipoate biosynthetic locus of *Saccharomyces cerevisiae*. *J. Biol. Chem.* 268, 17634–17639.

Tache, V., Bivina, L., White, S., Gregg, J., Deignan, J., Boyadjievd, S. A., et al. (2016). Lipoyltransferase 1 gene defect resulting in fatal lactic acidosis in two siblings. *Case Rep. Obstet. Gynecol.* 2016:6520148. doi: 10.1155/2016/6520148

Teichert, J., Hermann, R., Ruus, P., and Preiss, R. (2003). Plasma kinetics, metabolism, and urinary excretion of alpha-lipoic acid following oral administration in healthy volunteers. *J. Clin. Pharmacol.* 43, 1257–1267. doi: 10.1177/0091270003258654

Tort, F., Ferrer-Cortes, X., and Ribes, A. (2016). Differential diagnosis of lipoic acid synthesis defects. *J. Inherit. Metab. Dis.* 39, 781–793. doi: 10.1007/s10545-016-9975-4

Tort, F., Ferrer-Cortes, X., Thio, M., Navarro-Sastre, A., Matalonga, L., Quintana, E., et al. (2014). Mutations in the lipoyltransferase LIPT1 gene cause a fatal disease associated with a specific lipoylation defect of the 2-ketoacid dehydrogenase complexes. *Hum. Mol. Genet.* 23, 1907–1915. doi: 10.1093/hmg/ddt585

Tsurusaki, Y., Tanaka, R., Shimada, S., Shimojima, K., Shiina, M., Nakashima, M., et al. (2015). Novel compound heterozygous LIAS mutations cause glycine encephalopathy. *J. Hum. Genet.* 60, 631–635. doi: 10.1038/jhg.2015.72

Witkowski, A., Joshi, A. K., and Smith, S. (2007). Coupling of the de novo fatty acid biosynthesis and lipoylation pathways in mammalian mitochondria. *J. Biol. Chem.* 282, 14178–14185. doi: 10.1074/jbc.M701486200

Yi, X., and Maeda, N. (2005). Endogenous production of lipoic acid is essential for mouse development. *Mol. Cell. Biol.* 25, 8387–8392. doi: 10.1128/MCB.25.18.8387-8392.2005

Zhao, X., Miller, J. R., Jiang, Y., Marletta, M. A., and Cronan, J. E. (2003). Assembly of the covalent linkage between lipoic acid and its cognate enzymes. *Chem. Biol.* 10, 1293–1302. doi: 10.1016/j.chembiol.2003.11.016

Conflict of Interest: The author declares that the research was conducted in the absence of any commercial or financial relationships that could be construed as a potential conflict of interest.

frontiers in Cell and Developmental Biology

REVIEW
published: 26 November 2020
doi: 10.3389/fcell.2020.600079

The Dimensions of Primary Mitochondrial Disorders

Lea D. Schlieben[1,2] *and Holger Prokisch*[1,2]*

[1] School of Medicine, Institute of Human Genetics, Technical University of Munich, Munich, Germany, [2] Institute of Neurogenomics, Helmholtz Zentrum München, Munich, Germany

The concept of a mitochondrial disorder was initially described in 1962, in a patient with altered energy metabolism. Over time, mitochondrial energy metabolism has been discovered to be influenced by a vast number of proteins with a multitude of functional roles. Amongst these, defective oxidative phosphorylation arose as the hallmark of mitochondrial disorders. In the premolecular era, the diagnosis of mitochondrial disease was dependent on biochemical criteria, with inherent limitations such as tissue availability and specificity, preanalytical and analytical artifacts, and secondary effects. With the identification of the first mitochondrial disease-causing mutations, the genetic complexity of mitochondrial disorders began to unravel. Mitochondrial dysfunctions can be caused by pathogenic variants in genes encoded by the mitochondrial DNA or the nuclear DNA, and can display heterogenous phenotypic manifestations. The application of next generation sequencing methodologies in diagnostics is proving to be pivotal in finding the molecular diagnosis and has been instrumental in the discovery of a growing list of novel mitochondrial disease genes. In the molecular era, the diagnosis of a mitochondrial disorder, suspected on clinical grounds, is increasingly based on variant detection and associated statistical support, while invasive biopsies and biochemical assays are conducted to an ever-decreasing extent. At present, there is no uniform biochemical or molecular definition for the designation of a disease as a "mitochondrial disorder". Such designation is currently dependent on the criteria applied, which may encompass clinical, genetic, biochemical, functional, and/or mitochondrial protein localization criteria. Given this variation, numerous gene lists emerge, ranging from 270 to over 400 proposed mitochondrial disease genes. Herein we provide an overview of the mitochondrial disease associated genes and their accompanying challenges.

Keywords: mitochondrial disease, genetics, mutation, diagnostic, challenges

OPEN ACCESS

Edited by:
Guilhian Leipnitz, Federal University of Rio Grande do Sul, Brazil

Reviewed by:
Massimo Zeviani, University of Padua, Italy
Yolanda Cámara, Vall d'Hebron Research Institute (VHIR), Spain

***Correspondence:**
Holger Prokisch
prokisch@helmholtz-muenchen.de

Specialty section:
This article was submitted to Mitochondrial Research, a section of the journal Frontiers in Cell and Developmental Biology

Received: *28 August 2020*
Accepted: *06 November 2020*
Published: *26 November 2020*

Citation:
Schlieben LD and Prokisch H (2020) The Dimensions of Primary Mitochondrial Disorders. Front. Cell Dev. Biol. 8:600079. doi: 10.3389/fcell.2020.600079

Abbreviations: ACAD9, Acyl-CoA dehydrogenase family member 9; ATP, adenosine triphosphate; CPEO, chronic progressive external ophthalmoplegia; FA, Friedreich ataxia; KSS, Kearns-Sayre syndrome; LHON, Leber's hereditary optic neuropathy; MELAS, mitochondrial encephalopathy, lactic acidosis and stroke-like episodes; MIDD, maternally inherited diabetes and deafness; mtDNA, mitochondrial DNA; MT-ND4, mitochondrially encoded NADH:ubiquinone oxidoreductase; MT-RNR2, mitochondrially encoded 16S rRNA; MT-TL1, mitochondrially encoded tRNA leucine 1; nDNA, nuclear DNA; NGS, next generation sequencing; OMIM, Online Mendelian Inheritance in Man; OXPHOS, oxidative phosphorylation; PDHA1, pyruvate dehydrogenase E1 subunit alpha 1; RNA-seq, RNA sequencing; TCA cycle, tricarboxylic acid cycle; tRNA, transfer RNA; VUS, variant of unknown significance; WES, whole-exome-sequencing; WGS, whole-genome-sequencing.

INTRODUCTION

Mitochondria are dynamic ubiquitous organelles with innumerable functions in various cellular and metabolic pathways. Energy production via the oxidative phosphorylation (OXPHOS) represents the most prominent function of mitochondria (Duchen, 2004). Consisting of five protein complexes and two electron carriers embedded in the inner mitochondrial membrane, the OXPHOS generates ∼ 90% of the body's energy. An electrochemical gradient across the inner mitochondrial membrane is the driving force of adenosine triphosphate (ATP) synthesis by the fifth OXPHOS complex (ATP synthetase) (Papa et al., 2012). Mitochondria also have a decisive contribution to other cellular processes, such as initiation of apoptotic cell death, calcium homeostasis, heme and iron-sulfur cluster biosynthesis, and amino acid and lipid metabolism (Nunnari and Suomalainen, 2012; Gorman et al., 2016).

Nucleated cells of multicellular eukaryotes contain hundreds to thousands of mitochondria, with numbers varying among different tissues depending on energy demand (Cole, 2016). Uniquely, mitochondria have retained their own DNA, the mitochondrial DNA (mtDNA), a circular, double-stranded genome consisting of 37 genes, with each mitochondrion containing 2–10 copies of mtDNA (Anderson et al., 1981; Keogh and Chinnery, 2015). The 37 genes in total encode 13 proteins involved in OXPHOS, 22 mitochondrial tRNAs, and two subunits of the mitochondrial ribosomes. The additionally required ∼ 1500 proteins of the mitochondrial proteome are encoded by the nuclear genome and actively imported into the mitochondria (Pagliarini et al., 2008; Calvo et al., 2016; Alston et al., 2017). Unlike the nuclear DNA (nDNA), which displays Mendelian inheritance patterns, inheritance of mtDNA is exclusively maternal while paternal mtDNA is degraded after fertilization (Al Rawi et al., 2011).

MITOCHONDRIAL DISORDERS

The term "mitochondrial disorder" refers to a large group of genetically defined disorders, leading to direct defects of the pyruvate root of the OXPHOS (DiMauro and Garone, 2010; Mancuso et al., 2017; Stenton and Prokisch, 2020). The clinical diagnosis of individuals with mitochondrial disease poses a major challenge to physicians. Considering the presence of mitochondria in all nucleated cells, clinical symptoms can selectively involve only a single organ or be multisystemic affecting predominantly, but not exclusively, organs with the highest energy requirements, such as the heart, brain, and skeletal muscles. Moreover, the age of disease presentation can vary substantially. Clinical features are manifold and often overlap with other systemic or neurological diseases (Ng and Turnbull, 2016). Many common clinical symptoms, such as short stature, migraine, diabetes mellitus, and blindness, are not specific to mitochondrial disorders, and are also prevalent in the population. They may therefore present due to the primary genetic defect or as an unrelated clinical entity. Only a fraction of individuals display a unique combination of clinical manifestations belonging to a distinct clinical syndrome described more frequently, such as mitochondrial encephalopathy, lactic acidosis and stroke-like episodes (MELAS), chronic progressive external ophthalmoplegia (CPEO), maternally inherited diabetes and deafness (MIDD), and Leber's hereditary optic neuropathy (LHON). The clinical course and mortality rates of affected individuals vary widely owing to the heterogenous disease manifestations, with pediatric disease onset often being multisystemic and rapidly progressive in association with high mortality rates (Gorman et al., 2016).

The concept of mitochondrial disorders was initially described in Luft et al. (1962) on the basis of clinical, biochemical, and morphological evidence. In this premolecular era, mitochondriopathies were grouped into general biochemical pathways, such as defects in the substrate transport, tricarboxylic acid (TCA) cycle, or the pyruvate dehydrogenase complex. The term "mitochondrial disorder" has been employed for describing defects in the mitochondrial OXPHOS (DiMauro and Garone, 2010). At present, however, no consensus on uniform and standardized biochemical criteria for the definition of mitochondriopathies exists. Mitochondrial diseases are suspected on clinical grounds, but muscle biopsies and biochemical markers are necessary to validate the suspicion (Koenig, 2008; DiMauro, 2011). Biochemical screening methods for mitochondrial biomarkers in blood, urine, and spinal fluid, typically include the measurement of pyruvate and lactate, amino acids, urine organic acids, and plasma acylcarnitines. More recently, biochemical screenings also include new biomarkers for mitochondrial diseases, such as FGF-21 and GDF-15 (Suomalainen et al., 2011; Parikh et al., 2015; Montero et al., 2016). All of these biochemical measurements can be indicators for the presence of a mitochondriopathy, however, given the suboptimal specificity and sensitivity of these biomarkers, the confirmation of a specific diagnosis is challenging. In addition, no uniform or standardized guidelines for the biochemical evaluation of a suspected disease exist and multiple biochemical assays are conducted in several laboratories, ranging from single enzyme measures to metabolic flow or ATP production measurements in fresh or frozen tissues processed following various protocols (Haas et al., 2008). Given their post-mitotic properties, skeletal muscle biopsies are the tissue of choice and are the most commonly sampled in biochemical analyses (Phadke, 2017). Normal biochemical findings do not rule out an OXPHOS deficiency in other tissues or a defect not examined in the artificial system, such as a cofactor malfunction, if the cofactor was supplemented in the assay. At the same time, it has become apparent that in some patients the significantly reduced activity in the conducted assay is not always attributable to a defect in the OXPHOS enzymes, but to secondary mitochondrial dysfunctions or artifacts of the biochemical measurements. The secondary involvement of mitochondria in diseases is thus not considered as primary mitochondriopathy (Mancuso et al., 2017). Disorders contributing to secondary mitochondrial dysfunctions are being detected with an increasing frequency, making the diagnosis of mitochondrial disorders based on biochemical

findings in tissues evermore challenging (Niyazov et al., 2016; Parikh et al., 2019).

The molecular era of mitochondrial medicine began in 1988 with the description of the first disease-causing mutation in the mtDNA (Holt et al., 1988; Wallace et al., 1988; Zeviani et al., 1988). Since then, the identification of pathogenic variants has become the essential key for the molecular genetic confirmation of clinically suspected mitochondrial disorders and genetic definition of mitochondriopathies has subsequently gained increasing relevance over biochemical definition. Due to the mtDNA encoding only OXPHOS proteins and additional genetic elements required for mtDNA replication, transcription and translation of those peptides, an undisputed fact was that diseases associated with pathogenic variants of the mtDNA are mitochondrial disorders. Primary mitochondrial disorders are, however, also caused by pathogenic variants in nDNA encoded genes functionally relevant for the mitochondrial OXPHOS. The dual genetic control of mitochondria means that mutations can follow all possible modes of inheritance: maternal, autosomal-recessive, autosomal-dominant, and X-linked. For both, nDNA and mtDNA, pathogenic variants can occur *de novo* (DiMauro et al., 2004).

Although mutations in mitochondrial disease genes are individually rare, mitochondrial disorders represent the largest group of inborn errors of metabolism, with a collective lifetime risk of 1.6 in 5,000 (Ferreira et al., 2019; Tan et al., 2020). To date, pathogenic variants in more than 400 genes, of both mitochondrial and nuclear origin, have been ascribed as causes of mitochondriopathies (Frazier et al., 2019; Falk, 2020; Rahman, 2020; Stenton and Prokisch, 2020).

In patients with mtDNA encoded disease, inheritance and clinical presentation are further complicated by the presence of multiple mtDNA copies, both wild-type and mutant, in each cell (Larsson and Clayton, 1995). The level of this so called "heteroplasmy" often needs to exceed a tissue specific threshold to cause a biochemical defect and an associated mitochondrial disorder. Such threshold levels have been shown to vary widely between different tissues and mtDNA mutations. The level of heteroplasmy is not only associated with variable clinical manifestations but also disease severity (Khan et al., 2015; Grady et al., 2018). Insufficient genotype-phenotype correlation, even within defined clinical syndromes, are additional complications in the genetics of mitochondrial diseases (French et al., 2019). Leigh syndrome, a progressive neurodegenerative disorder in childhood, exemplifies the genetic heterogeneity of mitochondriopathies as it is associated with defects in more than 90 different genes (Rahman et al., 2017). Conversely, the straightforward association of a single gene with a defined clinical presentation and mode of inheritance is uncommon in mitochondrial diseases. A classic example displaying the genetic pleiotropy of mitochondrial disorders is the most common disease-causing mtDNA mutation m.3243A > G in *MT-TL1* causing a wide range of phenotypes, including MELAS, CPEO, and MIDD (Nesbitt et al., 2013).

This immense clinical and genetic heterogeneity of mitochondrial disorders, in conjunction with inadequate genotype-phenotype correlations, makes the reliable diagnosis of patients a demanding task, requiring extensive expertise of clinicians from all specialties. Many patients thus undergo a diagnostic odyssey with a multitude of consultations, conflicting diagnoses, and repeated, often invasive tests (Grier et al., 2018).

Although remarkable progress has been made in the field of mitochondrial medicine, the complexity of mitochondrial diseases continues to add to a shortage of therapeutic options for patients. The incomplete understanding of disease pathomechanisms, the rareness of the individual diseases, the inaccessibility of the double-membraned mitochondrion for a number of drugs, as well as the small number of biomarkers and outcome measures to demonstrate treatment effects, have contributed to a lack of licensed curative therapies for patients. Many early attempts at therapy development have sought to improve the function of the respiratory chain, by administering cofactor supplements such as carnitine, niacin, and thiamine (Pfeffer et al., 2013). With the exception of a few of these deficiencies in the biosynthesis or transport of cofactors and vitamins (Koch et al., 2017), the majority of patients still receive only symptomatic and supportive treatments, such as exercise, hearing aids, or reduction of toxic metabolites (Distelmaier et al., 2017; Hirano et al., 2018; Pitceathly et al., 2020). Thanks to technological advances, however, the knowledge of mitochondrial diseases is improving. This knowledge, coupled with the collection of larger cohorts of patients in to registries, enables an increasing number of clinical trials to be conducted, with many more expected in the next years.

DEVELOPMENTS IN THE MOLECULAR DIAGNOSTICS OF MITOCHONDRIAL DISORDERS

The molecular era of mitochondrial medicine began in 1988 with the discovery of the first pathogenic variants causing mitochondrial disease. Within 1 year large-scale deletions in the mtDNA causing mitochondrial myopathy (MIM 251900) or Kearns-Sayre syndrome (KSS, MIM 530000) shortly followed by an mtDNA point mutation in *MT-ND4* causing LHON (MIM 5350000), were identified (Holt et al., 1988; Wallace et al., 1988; Zeviani et al., 1988). With the discovery of pathogenic variants in the mitochondrial genome, the suspicion of a mitochondrial disorder based on clinical and biochemical markers could be unambiguously confirmed. Given the small size of the mitochondrial genome, the last decade of the first millennium in mitochondrial research was dominated by discoveries of pathogenic variants in the mtDNA (DiMauro and Garone, 2010). Mitochondrial disease associated mutations have now been reported for almost all 37 mtDNA genes. The only exception is *MT-RNR2,* for which proof of pathogenicity has not yet been sufficiently validated (Lott et al., 2013). Mutations in the mtDNA, however, could not explain the entire heritability of mitochondrial disorders and shortly after the identification of the first pathogenic mtDNA variants as genetic causes of mitochondrial diseases, the first nuclear encoded cause, defects in the X-chromosomal encoded gene *PDHA1,* was reported (Endo et al., 1989). Already, this first nuclear encoded defect

exceeded the strict biochemical concept of impaired OXPHOS for mitochondrial diseases by a dysfunction in the PDH. However, the classification of PDH deficiencies as mitochondrial diseases is undisputed.

The identification of pathogenic variants in the mtDNA and nDNA guided the beginning of the genetic era of diagnostics in suspected mitochondrial disease. Traditionally, molecular diagnoses of suspected mitochondrial disorders relied upon clinical phenotyping and blood, urine, and skeletal muscle tests evaluating the biochemical evidence of mitochondrial defects. Biochemical screening studies then guided targeted candidate gene sequencing of patient cohorts with similarities in the clinical and biochemical phenotype. The limited association of single genes with recognizable clinical presentations, in combination with the large number of mitochondrial disease genes, often made the sequencing of individual genes a laborious and time-consuming approach. Hence, candidate gene sequencing is effective only for clear clinical phenotypes explained by a low number of distinct pathogenic variants, due to the technique being sensitive enough for variant detection and segregation analysis.

In the last decade, the restricted analysis of the genome by conventional candidate gene sequencing methods was overcome with the advent of whole-exome sequencing (WES) and whole-genome sequencing (WGS), both serving to study the genetic background of this disease group (Haack et al., 2012). Advances in the next generation sequencing (NGS) technology have remarkably reduced the cost and workload of sequencing and laboratory protocols, allowing the implementation of these methods into routine diagnostics at many centers, and the analysis of large patient cohorts (Stenton and Prokisch, 2020; Wetterstrand, 2020). Capturing data on all genes allows us to identify not only known pathogenic variants, but also other outcomes including: (1) novel variants in mitochondrial disease genes, (2) suspected pathogenic variants in candidate genes, (3) variants in disease genes not associated with mitochondrial disease yet with a similar phenotypic presentation, and (4) a number of variants of uncertain significance (VUS). Thereby, WES and WGS do not only help to distinguish mitochondrial from non-mitochondrial disorders presenting clinically as mitochondriopathy, but also help to identify mitochondrial diseases in patients not suspected of having mitochondrial dysfunction. As the number of examined genes increases, more rare variants can be discovered, requiring interpretation of their clinical relevance.

Since the detection of the first mitochondrial disease gene *ACAD9* by NGS in 2010, the number of reported mitochondrial disease genes has duplicated, exemplifying the technology's diagnostic power (Haack et al., 2010). In the pre-NGS era approximately five mitochondrial disease genes were reported annually, increasing to over 15 genes annually after the advent of NGS methods in 2010 (Stenton and Prokisch, 2020). Application of WES and WGS in patients with suspected mitochondrial disease for whom extensive prior clinical analysis had failed to return a diagnosis achieves diagnostic yields of approximately 50% (Taylor et al., 2014; Wortmann et al., 2015; Kohda et al., 2016; Pronicka et al., 2016). The success of unbiased NGS methods results in the less frequent analysis of invasive skeletal muscle biopsies. By reducing the frequency of biochemical examinations, the classic definition of a mitochondrial disease is further neglected leading to the argument for utilization of genetic definitions (Wortmann et al., 2017). In line with the concept that mtDNA mutations cause an OXPHOS disease, mutations in nuclear genes with products considered functionally relevant for the OXPHOS, covering mtDNA replication and transcription, mitochondrial translation and pyruvate oxidation root, are classified as causes of mitochondrial diseases, not always associated with an OXPHOS deficiency in all patients.

Increasing integration of WES and WGS into routine diagnostics of mitochondrial diseases improved diagnostic rates remarkably. Nevertheless, a significant number of patients with suspected mitochondrial disease do not receive a genetic diagnosis due to challenges in variant detection and interpretation. Other methods contribute to closing the diagnostic gap further.

For the interpretation of VUS new tools are becoming useful in the diagnosis of Mendelian diseases. Quantification of the gene products can help to interpret unclear pathogenic variants in case they result in reduced levels of proteins, making proteomics a powerful tool to complement the genetic analysis. Moreover, recent studies demonstrate that whole transcriptome sequencing (RNA-seq) increases the power and sensitivity of detection and interpretation of the large number of VUS identified by DNA sequencing. RNA-seq provides insight into the transcripts of a tissue at a specific time point and is an additional tool following exome sequencing to analyze unsolved cases by high-throughput functional characterization of variants. Of rare disease patients remaining undiagnosed by DNA analysis, by providing evidence for the pathogenicity of variants, RNA-seq allows an additional 17.5% of investigated patients to reach a genetic diagnosis (Cummings et al., 2016; Kremer et al., 2017; Frésard et al., 2019; Gonorazky et al., 2019; Lee et al., 2020).

Despite the potential of such multi-omic approaches to further increase the diagnostic yield, the most commonly used method in current practice for evaluating the pathogenicity of VUS and the impact on OXPHOS remains to be the biochemical examination of tissue biopsies, though we expect this to change in the future.

Taken together, despite the major technological advances in diagnostic tools for rare diseases, the lack of genotype-phenotype correlations, the genetic heterogeneity and the presence of VUS in patients with mitochondrial disease imply that the confirmation of a specific diagnosis often remains a challenge.

DEFINITION OF MITOCHONDRIAL DISEASE GENES

With the increased utilization of sequencing technologies, it is now possible to provide a molecular diagnosis to a large fraction of patients with mitochondrial disease. As a result, mitochondriopathies are meanwhile frequently defined by their genetic cause rather than by biochemical deficiencies.

The number of nuclear genes associated with mitochondrial function is estimated to be ∼1500 (Calvo et al., 2016). So far, 376

of these genes have been associated with human mitochondrial disorders in total and as the routine use of NGS technologies grows, this number is expected to continuously increase (Frazier et al., 2019; Falk, 2020; Rahman, 2020; Stenton and Prokisch, 2020). Due to the capacity to detect pathogenic variants in genes so far not linked to mitochondrial disorders, the criteria for which genes should be classified as associated with a mitochondriopathy are now the subject to discussion.

Considering the mitochondrial disease gene lists of four different publications released within the last year, the number of disease associated genes varied between 289 and 384: (1) Frazier et al. (2019), 289 genes, (2) Rahman (2020), 384 genes, (3) updated list of Stenton and Prokisch (2020), 343 genes, and (4) Falk (2020), 313 genes. Within these four lists, a total of 413 distinct mitochondrial disease associated genes were reported. Amongst these 413 genes, just 272 genes were included by all authors (**Figure 1**), illustrating their diversity. The following could be the reasons for the differences in the classification.

Firstly, the existing biochemical definition, that a mitochondrial disease must lead to direct OXPHOS defects, implies that the encoded protein is generally localized in the mitochondrion with very few exceptions. Using MitoCarta2.0, an inventory of the mitochondrial proteome, to examine the mitochondrial localization, 13% (54/413 genes) of the proteins encoded by the named genes are not listed (**Figure 2**). Though the two mitochondrial rRNAs and 22 mitochondrial tRNAs are not mentioned in MitoCarta2.0 due to their non-protein-coding properties, they also have a mitochondrial localization. No standardized definitions exist on whether gene products have to be located within the mitochondrion, on the mitochondrial membrane and responsible for the mitochondrial transport, or outside the mitochondrion and responsible for the mitochondrial metabolism, such as *RRM2B* (Bourdon et al., 2007; Chen et al., 2019). For instance, defects in the cytosolic tRNA synthetase *IARS*, necessary for the synthesis of nuclear-encoded mitochondrial proteins, are not regarded as a cause of primary mitochondrial disease, despite the fact of being associated with an OXPHOS defect (Kopajtich et al., 2016). Additionally, knowledge of mitochondrial proteins listed in MitoCarta2.0 inventory (released in 2016) is increasing over time, representing one reason why some proteins with a mitochondrial localization are not yet listed. To name an example, *TRMT5* was reported concurrently (Powell et al., 2015), making regular updates essential and to our knowledge currently in preparation.

Importantly, though defects in all 413 genes have been ascribed in the literature as associated with mitochondrial

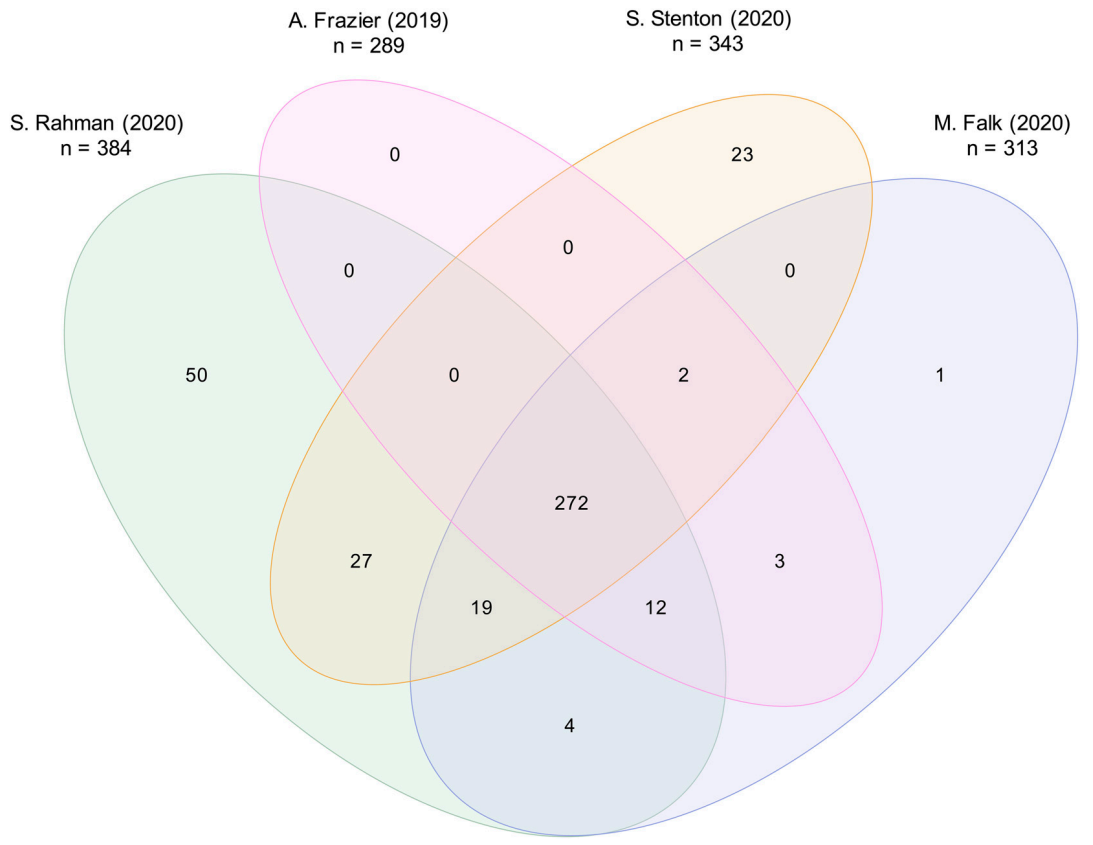

FIGURE 1 | Comparison of four distinct mitochondrial disease gene lists. Mitochondrial disease gene lists of (1) Frazier et al. (2019), listing 289 genes, (2) Rahman (2020), 384 genes, (3) Stenton and Prokisch (2020), 343 genes, and (4) Falk (2020), 313 genes, were compared. A total of 413 distinct genes was reported. A core of 272 mitochondrial disease genes was listed by all four authors.

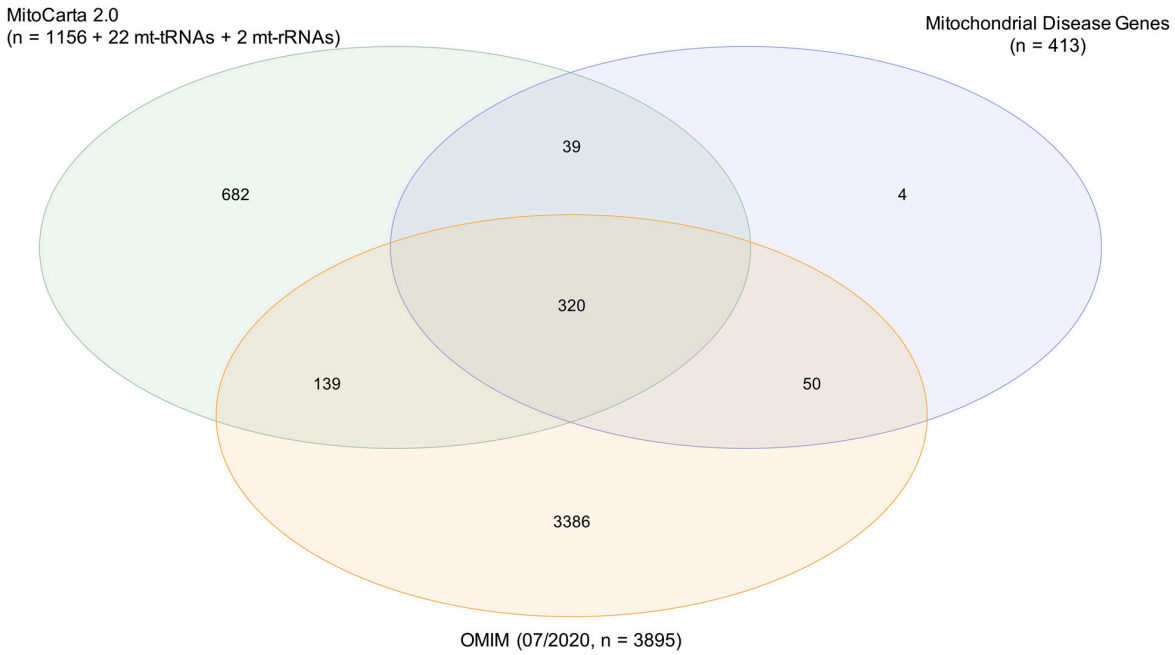

FIGURE 2 | Characterization of mitochondrial disease genes. Mitochondrial localization of encoded proteins was examined by using the mitochondrial proteome inventory MitoCarta2.0 (1156 genes). The 22 mitochondrial tRNAs and 2 mitochondrial rRNAs were also considered as mitochondrially localized. A total of 87% (359/413 genes) of mitochondrial disease genes were located in the mitochondrion. Annotation in the database OMIM (07/2020) served as prove for the pathogenicity of genes. A total of 90% (370/413 genes) of mitochondrial disease genes were annotated in OMIM with an associated phenotype and mode of inheritance.

disorders, 43 (10%) genes are not yet annotated in OMIM[1] as disease genes with an associated phenotype and mode of inheritance (status 07/2020) (**Figure 2**). Differences in the published mitochondrial disease gene lists and OMIM could be due to difficulties in assessing the evidence for inclusion and exclusion criteria. However, the evidence criteria to be fulfilled for annotation in OMIM are to our knowledge not consistent and their absence in OMIM is likely due to a work overload. Typically, description of a single case is not sufficient to define a genotype-phenotype association, but this seems not to be the limitation for the inclusion into OMIM, as for example in *TXN2* (Holzerova et al., 2016). As most knowledge databases, OMIM is dynamic and though regularly updated there may be a time-lag in inclusion, so that recently discovered disease genes may not yet be annotated in OMIM. References with evidence of pathogenicity were found in the literature for 40 of 43 mitochondrial disease genes not yet annotated in OMIM (**Supplementary Table 1**).

Taken together, although the biochemical definition of mitochondrial disorders relies on a defective OXPHOS, no gold standards have been developed for the classification of mitochondrial diseases. The annotation of proteins and disorders in MitoCarta2.0 and OMIM may contribute to the differences in the published disease gene lists.

Secondly, with increasing knowledge of the molecular, biochemical, and clinical basis of diseases, a clear definition of mitochondrial disorders becomes more complex. A wide array of proteins with a multitude of functional roles influence the functionality of the OXPHOS, impeding the biochemical definition and leading to an accelerated implementation of the genetic definition (**Figure 3**).

According to the functional roles of the encoded proteins, mitochondrial disease genes can be divided into seven subsets: (1) OXPHOS subunits, assembly factors, and electron carriers (112/413 genes), (2) mitochondrial DNA replication and expression (104/413 genes), (3) mitochondrial dynamics, homeostasis, and quality control (55/413 genes), (4) metabolism of substrates (57/413 genes), (5) metabolism of cofactors (49/413 genes), (6) metabolism of toxic compounds (10/413 genes), and (7) others/unknown function (26/413 genes) (**Figure 4**; **Supplementary Table 2**). Novel diseases associated with genes functionally assigned to the first or second subcategory of mitochondrial disease genes can be classified as mitochondrial diseases, as already accepted for pathogenic mtDNA variants. A mitochondrial localization of the encoded proteins is most likely. Genes within these functional categories not yet associated with mitochondriopathies represent strong prospective candidates. Proteins of the third category, mitochondrial dynamics, homeostasis, or quality control have generic mitochondrial functions, whose malfunction can directly or indirectly impair the mitochondrial energy metabolism. Diseases associated with a direct impairment of these functions are also commonly considered as mitochondriopathy. However, genetic defects in *PINK* or *PRKN*, which affect the mitochondrion but represent a specific subgroup of the disease categorized

[1]Online Mendelian Inheritance in Man, OMIM®. McKusick-Nathans Institute of Genetic Medicine, Johns Hopkins University (Baltimore, MD). https://omim.org/ (accessed July 15, 2020).

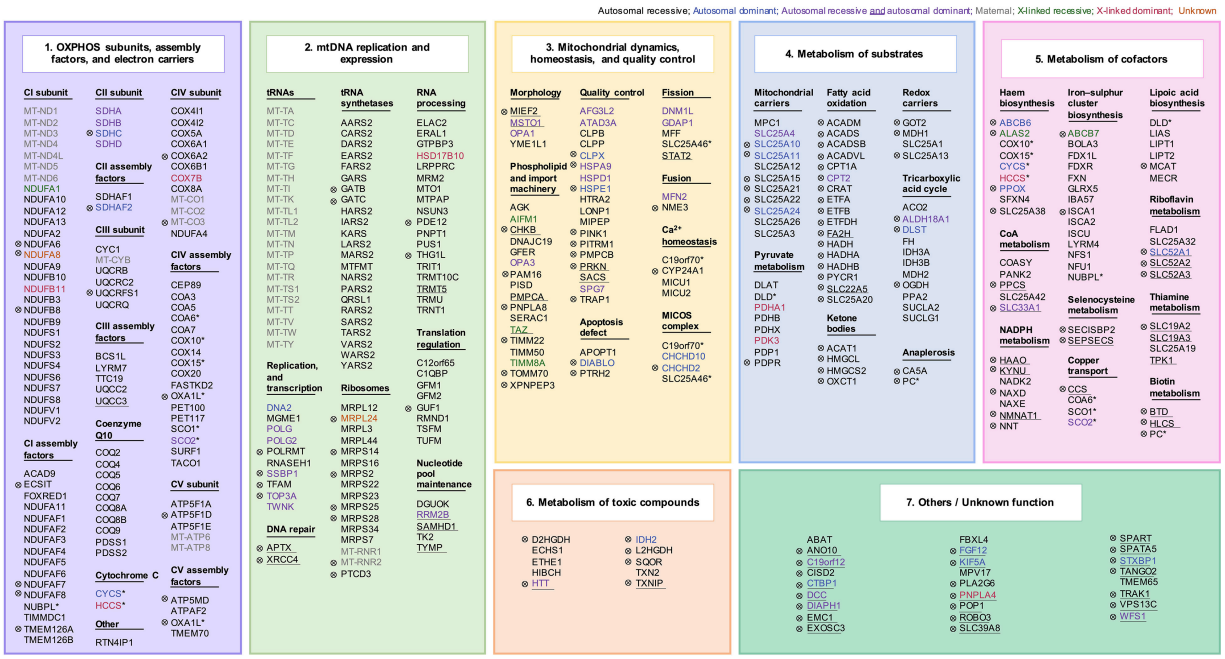

FIGURE 3 | Mitochondrial disease genes. An association with mitochondrial disorders has been reported for 413 genes. Genes were grouped into subcategories according to their function: (1) OXPHOS subunits, assembly factors, and electron carriers (112/413 genes), (2) mitochondrial DNA replication and expression (104/413 genes), (3) mitochondrial dynamics, homeostasis, and quality control (55/413 genes), (4) metabolism of substrates (57/413 genes), (5) metabolism of cofactors (49/413 genes), (6) metabolism of toxic compounds (10/413 genes), and (7) others (26/413 genes). The mode of inheritance is indicated by color. A total of 13 genes have more than one mitochondrial function, indicated by an asterisk. Genes not included in the core set of all four publications (141/413 genes) are indicated by a sign (⊗). Genes encoding proteins not localized to the mitochondrion according to MitoCarta2.0 are highlighted with an underscore (54/413 genes).

as Parkinson disease are an exception (Shimura et al., 2000; Valente et al., 2004). Besides the energy production via the OXPHOS, other aerobic energy metabolisms, such as the TCA cycle, pyruvate metabolism, or fatty acid oxidation, are part of the mitochondrial function and this metabolism of substrates required for the OXPHOS represents category four. Diseases associated with genes involved in the TCA cycle or the pyruvate metabolism are commonly considered as mitochondrial disorders. Defective PDH function is a prime example for not causing a classic OXPHOS dysfunction but being accepted as mitochondrial disease due to a defective oxidative decarboxylation of pyruvate (Brown et al., 1994). In contrast, functional subgroups of the mitochondrial substrate metabolism, such as fatty acid oxidation, ketone bodies, and anaplerosis, are controversially disputed as causative factors of mitochondriopathies as pathogenic mutations affect the mitochondrial energy metabolism but usually do not cause an OXPHOS deficiency. The OXPHOS requires at least ten cofactors (category 5). Dysfunctional OXPHOS due to cofactor deficiencies is generally regarded as a cause of mitochondriopathies. The association of a gene with a mitochondrial disorder is debated if the encoded protein is not located to the mitochondrion, such as with riboflavin transporters in the plasma membrane. Nevertheless, defects of the riboflavin transporters finally entail a lack of riboflavin in the mitochondrion and an associated impairment of mitochondrial function (Udhayabanu et al., 2017). In addition, certain mitochondrial diseases can arise from toxic metabolites that attack the respiratory chain. The latter group (category 7) comprises mainly proteins with a function outside the mitochondrion or a function not yet fully known. Disruptions in their function can, however, indirectly provoke mitochondrial dysfunctions posing the question as to what the main effect of a gene is.

The pathways currently reported in the context of mitochondrial disorders are presumably not yet complete and ongoing research in the field will continue to expand this list, just as knowledge about the localization and function of proteins is equally dynamic. Given the dynamic nature of mitochondrial disease genes, genes such as *MRPL24* (Di Nottia et al., 2020) may not yet be annotated in OMIM or included in all scientific publications. Furthermore, we are constantly discovering new factors involved in mitochondrial function further enriching the list of mitochondrial disease associated genes.

Taken together, the high level of clinical and genetical complexity, in combination with the absence of reliable biomarkers, resulted in the unavailability of a precise biochemical and genetic definition of mitochondrial disorders. No uniform and standardized definitions, regarding the pathogenicity, the presence of an OXPHOS defect, and the mitochondrial localization, have been provided to classify a gene or variant as a cause of mitochondriopathies (Haas et al., 2008). Moreover, diagnosis of mitochondrial disorders is increasing based on gene function, and a biochemical defect cannot be detected in all patients with pathogenic variants, further

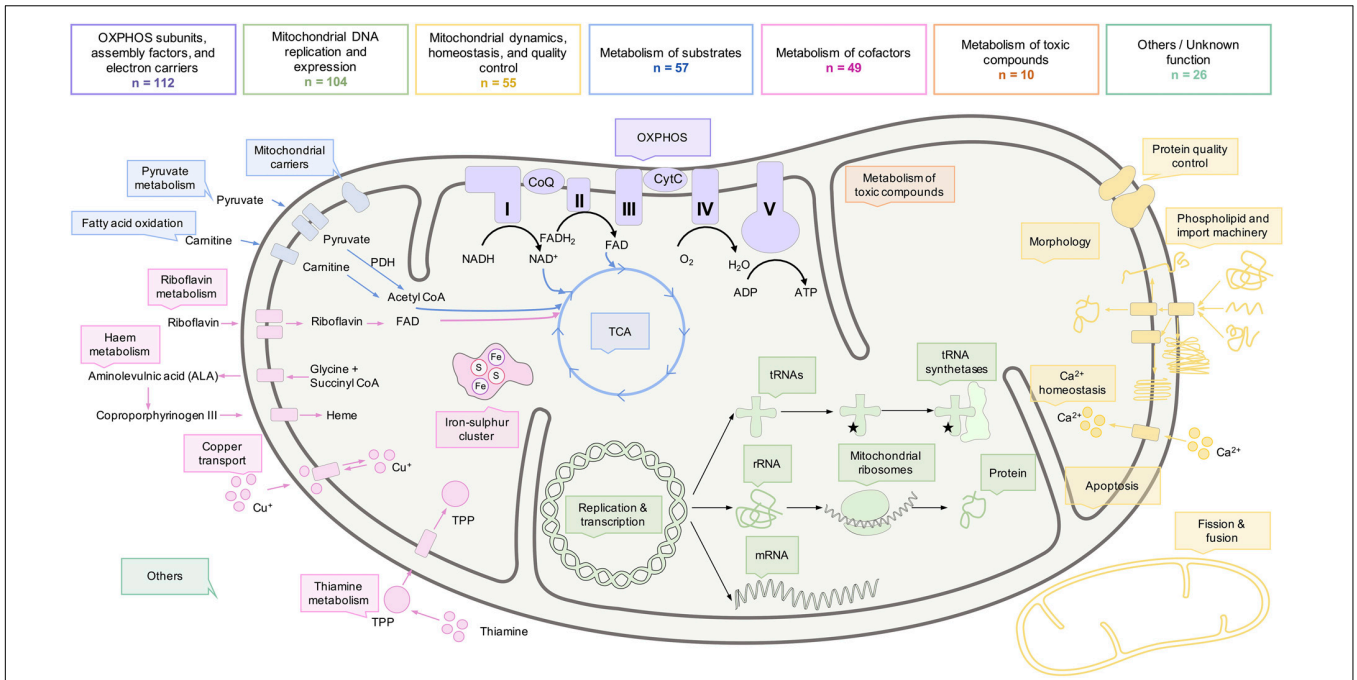

FIGURE 4 | Functional roles of mitochondria and the biochemical processes within a mitochondrion. Although the OXPHOS is considered as the hallmark of mitochondria, multiple proteins with a wide range of functional roles influence the metabolism of mitochondria. Some of the functions and biochemical processes of mitochondria, commonly defective in mitochondrial diseases, are illustrated here. The number of mitochondrial disease genes implicated in the biochemical pathways is indicated. Genes with multiple functions were only listed within one category.

complicating the definition of mitochondrial diseases. All these aspects for the inclusion and exclusion of mitochondrial disease genes can be assessed differently, and consequently lead to different gene lists, ranging from 270 to over 400 disease genes.

FUTURE PERSPECTIVES

With steadily growing utilization and further advancement of sequencing methodologies, the number of pathogenic variants and genes associated with mitochondrial disease will constantly rise. Raising the question of whether a precise definition of mitochondrial disease genes is indeed useful, and whether it is of importance to speak of 270 or 400 genes.

For patients with a constellation of symptoms indicating mitochondrial dysfunction in the absence of clear pathogenic variants and biochemical defects, it is recommended to avoid the diagnostic term "possible" mitochondrial disease (Parikh et al., 2019). Instead, in patients remaining without diagnosis, the focus should be on the description of the clinical manifestation. In fact, with regard to the rarity of mitochondrial diseases, the suspicion of a mitochondrial disorder should qualify for the inclusion into mitochondrial patient registries. Through the acquisition of patient data, patient registers are a powerful tool whose analytical statistical significance increases with a growing number of patients included. As research on such registries is ongoing, the chances of finding a molecular diagnosis or assessing the effectiveness of therapies will improve in the future. For patients suspected of having a mitochondrial disease, inclusion into patient registries not only provides diagnostic advantages, but also enables psychological support for the patients. The collaboration of clinicians and researchers facilitates an exchange of data worldwide, accelerates gene discoveries, and improves our understanding of genotype-phenotype correlations. This provides the opportunity to coordinate sufficiently powered clinical trials (Schon et al., 2020). The emergence of national mitochondrial patient registers over the last few years (e.g., mitoNET, MITOCON, NAMDC) has not only enabled large-scale NGS studies to be conducted to further clarify genotype-phenotype correlation (Altmann et al., 2016). It also offers other benefits such as in conducting natural history studies, in the preparation of intervention studies, the establishment of biobanks, and in increasing public and clinical awareness. Meanwhile, GENOMIT, a global mitochondrial patient registry with eight partners, in Germany, Austria, France, Italy, United Kingdom, Japan, and the United States, has been established. This global exchange of information will enable tremendous progress in this complex disease.

CONCLUSION

Mitochondrial disorders are associated with an increasingly large number of heterogenous clinical and molecular presentations. By moving further into the genomic and multi-omic diagnostic era, the diagnosis of a mitochondrial disease on the basis

of conventional biochemical definitions is increasingly being challenged. The function of mitochondria in many cellular activities and pathways contributes to the complexity in defining a single list of mitochondrial disease genes. Therefore, instead of adhering to an overly precise disease definition, the generous inclusion of patients with suspected mitochondrial disease, based on clinical and genetic evidence, into global patient registries appears to be more practicable and also beneficial to the field. The enlargement of global patient registries not only permits psychological support for patients, but also helps to combine clinical and genetic data in order to be able to analyze disease pathomechanisms in greater detail. Within the framework of the associated research studies, the establishment of genetic and biochemical criteria for the specific definition of mitochondrial diseases lends itself to the formation of clear patient groups. Moreover, advancements in diagnostic techniques are further unraveling the underlying causes of mitochondrial disease and will hopefully pave the way for the development of powerful treatments or curative agents for patients.

AUTHOR CONTRIBUTIONS

This article was written by LS under the guidance of HP.

FUNDING

This work was supported by the BMBF (German Federal Ministry of Education and Research) through mitoNET German Network for Mitochondrial Diseases [grant number 01GM1906B (to HP)], PerMiM Personalized Mitochondrial Medicine [grant number 01KU2016A (to HP)], and GENOMIT European Network for Mitochondrial Disease [grant number 01GM1920A (to HP)].

ACKNOWLEDGMENTS

We thank Dr. Johannes Mayr for his contribution to our mitochondrial disease gene list.

SUPPLEMENTARY MATERIAL

The Supplementary Material for this article can be found online at: https://www.frontiersin.org/articles/10.3389/fcell.2020.600079/full#supplementary-material

Supplementary Table 1 | Evidence for pathogenicity for 45 published mitochondrial disease genes not listed in OMIM.

Supplementary Table 2 | Current list of published mitochondrial disease genes.

REFERENCES

Al Rawi, S., Louvet-Valle, D. A., Sachese, M., CUletto, E., Hajar, C., Mayr, J. A., et al. (2011). Postfertilization autophagy of sperm. *Science* 334, 1144–1147. doi: 10.1126/science.1211878

Alston, C. L., Rocha, M. C., Lax, N. Z., Turnbull, D. M., and Taylor, R. W. (2017). The genetics and pathology of mitochondrial disease. *J. Pathol.* 241, 236–250. doi: 10.1002/path.4809

Altmann, J., Büchner, B., Nadaj-Pakleza, A., Schäfer, J., Jackson, S., Lehmann, D., et al. (2016). Expanded phenotypic spectrum of the m.8344A>G "MERRF" mutation: data from the German mitoNET registry. *J. Neurol.* 263, 961–972. doi: 10.1007/s00415-016-8086-3

Anderson, S., Bankier, A. T., Barrell, B. G., de Bruijn, M. H. L., Coulson, A. R., and Drouin, J. (1981). Sequence and organization of the human mitochondrial genome. *Nature* 290, 457–465. doi: 10.1038/290457a0

Bourdon, A., Minai, L., Serre, V., Jais, J. P., Sarzi, E., Aubert, S., et al. (2007). Mutation of RRM2B, encoding p53-controlled ribonucleotide reductase (p53R2), causes severe mitochondrial DNA depletion. *Nat. Genet.* 39, 776–780. doi: 10.1038/ng2040

Brown, G. K., Otero, L. J., LeGris, M., and Brown, R. M. (1994). Pyruvate dehydrogenase deficiency. *J. Med. Genet.* 31, 875–879. doi: 10.1136/jmg.31.11.875

Calvo, S. E., Clauser, K. R., and Mootha, V. K. (2016). MitoCarta2.0: an updated inventory of mammalian mitochondrial proteins. *Nucleic Acids Res.* 44, D1251–D1257. doi: 10.1093/nar/gkv1003

Chen, Y. F., Lin, I. H., Guo, Y. R., Chiu, W. J., Wu, M. S., Jia, W., et al. (2019). Rrm2b deletion causes mitochondrial metabolic defects in renal tubules. *Sci. Rep.* 9:13238. doi: 10.1038/s41598-019-49663-3

Cole, L. W. (2016). The evolution of per-cell organelle number. *Front. Cell Dev. Biol.* 4:85. doi: 10.3389/fcell.2016.00085

Cummings, B. B., Marshall, J. L., Tukiainen, T., Lek, M., Donkervoort, S., Foley, A. R., et al. (2016). Improving genetic diagnosis in mendelian disease with transcriptome sequencing genotype-tissue expression consortium. *Sci. Transl. Med.* 5209, 1–12. doi: 10.1101/074153

Di Nottia, M., Marchese, M., Verrigni, D., Mutti, C. D., Torraco, A., Oliva, R., et al. (2020). A homozygous MRPL24 mutation causes a complex movement disorder and affects the mitoribosome assembly. *Neurobiol. Dis.* 141:104880. doi: 10.1016/j.nbd.2020.104880

DiMauro, S. (2011). A history of mitochondrial diseases. *J. Inherit. Metab. Dis.* 34, 261–276. doi: 10.1007/s10545-010-9082-x

DiMauro, S., and Garone, C. (2010). Historical perspective on mitochondrial medicine. *Dev. Disabil. Res. Rev.* 16, 106–113. doi: 10.1002/ddrr.102

DiMauro, S., Tay, S., and Mancuso, M. (2004). Mitochondrial encephalomyopathies: diagnostic approach. *Ann. N. Y. Acad. Sci.* 1011, 217–231. doi: 10.1196/annals.1293.022

Distelmaier, F., Haack, T. B., Wortmann, S. B., Mayr, J. A., and Prokisch, H. (2017). Treatable mitochondrial diseases: cofactor metabolism and beyond. *Brain* 140:e11. doi: 10.1093/brain/aww303

Duchen, M. R. (2004). Mitochondria in health and disease: perspectives on a new mitochondrial biology. *Mol. Aspects Med.* 25, 365–451. doi: 10.1016/j.mam.2004.03.001

Endo, H., Hasegawa, K., Narisawa, K., Tada, K., Kagawa, Y., and Ohta, S. (1989). Defective gene in lactic acidosis: abnormal pyruvate dehydrogenase E1 alpha-subunit caused by a frame shift. *Am. J. Hum. Genet.* 44, 358–364.

Falk, M. J. (2020). *Mitochondrial Disease Gene Compendium - From Genes to Clinical Manifestations*. Cambridge, MA: Academic Press.

Ferreira, C. R., van Karnebeek, C. D. M., Vockley, J., and Blau, N. (2019). A proposed nosology of inborn errors of metabolism. *Genet. Med.* 21, 102–106. doi: 10.1038/s41436-018-0022-8

Frazier, A. E., Thorburn, D. R., and Compton, A. G. (2019). Mitochondrial energy generation disorders: genes, mechanisms, and clues to pathology. *J. Biol. Chem.* 294, 5386–5395. doi: 10.1074/jbc.R117.809194

French, C. E., Delon, I., Dolling, H., Sanchis-Juan, A., Shamardina, O., Mégy, K., et al. (2019). Whole genome sequencing reveals that genetic conditions are frequent in intensively ill children. *Intensive Care Med.* 45, 627–636. doi: 10.1007/s00134-019-05552-x

Frésard, L., Smail, C., Ferraro, N. M., Teran, N. A., Li, X., Smith, K. S., et al. (2019). Identification of rare-disease genes using blood transcriptome sequencing and large control cohorts. *Nat. Med.* 25, 911–919. doi: 10.1038/s41591-019-0457-8

Gonorazky, H. D., Naumenko, S., Ramani, A. K., Nelakuditi, V., Mashouri, P., Wang, P., et al. (2019). Expanding the boundaries of RNA sequencing as a

diagnostic tool for rare mendelian disease. *Am. J. Hum. Genet.* 104, 466–483. doi: 10.1016/j.ajhg.2019.01.012

Gorman, G. S., Chinnery, P. F., DiMauro, S., Hirano, M., Koga, Y., McFarland, R., et al. (2016). Mitochondrial diseases. *Nat. Rev. Dis. Prim.* 2, 1–23. doi: 10.1038/nrdp.2016.80

Grady, J. P., Pickett, S. J., Ng, Y. S., Alston, C. L., Blakely, E. L., Hardy, S. A., et al. (2018). mt DNA heteroplasmy level and copy number indicate disease burden in m.3243A>G mitochondrial disease. *EMBO Mol. Med.* 10, 1–13. doi: 10.15252/emmm.201708262

Grier, J., Hirano, M., Karaa, A., Shepard, E., and Thompson, J. L. P. (2018). Diagnostic odyssey of patients with mitochondrial disease results of a survey. *Neurol. Genet.* 4:e230. doi: 10.1212/NXG.0000000000000230

Haack, T. B., Danhauser, K., Haberberger, B., Hoser, J., Strecker, V., Boehm, D., et al. (2010). Exome sequencing identifies ACAD9 mutations as a cause of complex i deficiency. *Nat. Genet.* 42, 1131–1134. doi: 10.1038/ng.706

Haack, T. B., Haberberger, B., Frisch, E. M., Wieland, T., Iuso, A., Gorza, M., et al. (2012). Molecular diagnosis in mitochondrial complex I deficiency using exome sequencing. *J. Med. Genet.* 49, 277–283. doi: 10.1136/jmedgenet-2012-100846

Haas, R. H., Parikh, S., Falk, M. J., Saneto, R. P., Wolf, N. I., Darin, N., et al. (2008). The in-depth evaluation of suspected mitochondrial disease. *Mol. Genet. Metab.* 94, 16–37. doi: 10.1016/j.ymgme.2007.11.018

Hirano, M., Emmanuele, V., and Quinzii, C. M. (2018). Emerging therapies for mitochondrial diseases. *Essays Biochem.* 62, 467–481. doi: 10.1042/EBC20170114

Holt, I. J., Harding, A. E., and Morgan-Hughes, J. A. (1988). Deletions of muscle mitochondrial DNA in patients with mitochondrial myopathies. *Nature* 331, 717–719. doi: 10.1038/331717a0

Holzerova, E., Danhauser, K., Haack, T. B., Kremer, L. S., Melcher, M., Ingold, I., et al. (2016). Human thioredoxin 2 deficiency impairs mitochondrial redox homeostasis and causes early-onset neurodegeneration. *Brain* 139, 346–354. doi: 10.1093/brain/awv350

Keogh, M. J., and Chinnery, P. F. (2015). Mitochondrial DNA mutations in neurodegeneration. *Biochim. Biophys. Acta Bioenerg.* 1847, 1401–1411. doi: 10.1016/j.bbabio.2015.05.015

Khan, N. A., Govindaraj, P., Meena, A. K., and Thangaraj, K. (2015). Mitochondrial disorders: challenges in diagnosis & treatment. *Indian J. Med. Res. Suppl.* 141, 13–26. doi: 10.4103/0971-5916.154489

Koch, J., Mayr, J. A., Alhaddad, B., Rauscher, C., Bierau, J., Kovacs-Nagy, R., et al. (2017). CAD mutations and uridine-responsive epileptic encephalopathy. *Brain* 140, 279–286. doi: 10.1093/brain/aww300

Koenig, M. K. (2008). Presentation and diagnosis of mitochondrial disorders in children. *Pediatr. Neurol.* 38, 305–313. doi: 10.1016/j.pediatrneurol.2007.12.001

Kohda, M., Tokuzawa, Y., Kishita, Y., Nyuzuki, H., Moriyama, Y., Mizuno, Y., et al. (2016). A comprehensive genomic analysis reveals the genetic landscape of mitochondrial respiratory chain complex deficiencies. *PLoS Genet.* 12:e1005679. doi: 10.1371/journal.pgen.1005679

Kopajtich, R., Murayama, K., Janecke, A. R., Haack, T. B., Breuer, M., Knisely, A. S., et al. (2016). Biallelic IARS mutations cause growth retardation with prenatal onset, intellectual disability, muscular hypotonia, and infantile hepatopathy. *Am. J. Hum. Genet.* 99, 414–422. doi: 10.1016/j.ajhg.2016.05.027

Kremer, L. S., Bader, D. M., Mertes, C., Kopajtich, R., Pichler, G., Iuso, A., et al. (2017). Genetic diagnosis of Mendelian disorders via RNA sequencing. *Nat. Commun.* 8, 1–11. doi: 10.1038/ncomms15824

Larsson, N. G., and Clayton, D. A. (1995). Molecular genetic aspects of human mitochondrial disorders. *Annu. Rev. Genet.* 29, 151–178. doi: 10.1146/annurev.ge.29.120195.001055

Lee, H., Huang, A. Y., Wang, L., Kai, Y. A. J., Renteria, G., Eskin, A., et al. (2020). Diagnostic utility of transcriptome sequencing for rare Mendelian diseases. *Genet. Med.* 22, 490–499. doi: 10.1038/s41436-019-0672-1

Lott, M. T., Leipzig, J. N., Derbeneva, O., Michael Xie, H., Chalkia, D., Sarmady, M., et al. (2013). MtDNA variation and analysis using Mitomap and Mitomaster. *Curr. Protoc. Bioinform.* 44, 1.23.1–26. doi: 10.1002/0471250953.bi0123s44

Luft, R., Ikkos, D., Palmieri, G., Ernster, L., and Afzelius, B. (1962). A case of severe hypermetabolism of nonthyroid origin with a defect in the maintenance of mitochondrial respiratory control: a correlated clinical, biochemical, and morphological study. *J. Clin. Invest.* 41, 1776–1804. doi: 10.1172/jci104637

Mancuso, M., McFarland, R., Klopstock, T., Hirano, M., Artuch, R., Bertini, E., et al. (2017). International workshop: outcome measures and clinical trial readiness in primary mitochondrial myopathies in children and adults. Consensus recommendations. 16-18 November 2016, Rome, Italy. *Neuromuscul. Disord.* 27, 1126–1137. doi: 10.1016/j.nmd.2017.08.006

Montero, R., Yubero, D., Villarroya, J., Henares, D., Jou, C., Rodríguez, M. A., et al. (2016). GDF-15 is elevated in children with mitochondrial diseases and is induced by mitochondrial dysfunction. *PLoS One* 11:e148709. doi: 10.1371/journal.pone.0148709

Nesbitt, V., Pitceathly, R. D. S., Turnbull, D. M., Taylor, R. W., Sweeney, M. G., Mudanohwo, E. E., et al. (2013). The UK MRC mitochondrial disease patient cohort study: clinical phenotypes associated with the m.3243A>G mutation - implications for diagnosis and management. *J. Neurol. Neurosurg. Psychiatry* 84, 936–938. doi: 10.1136/jnnp-2012-303528

Ng, Y. S., and Turnbull, D. M. (2016). Mitochondrial disease: genetics and management. *J. Neurol.* 263, 179–191. doi: 10.1007/s00415-015-7884-3

Niyazov, D. M., Kahler, S. G., and Frye, R. E. (2016). Primary mitochondrial disease and secondary mitochondrial dysfunction: importance of distinction for diagnosis and treatment. *Mol. Syndromol.* 7, 122–137. doi: 10.1159/000446586

Nunnari, J., and Suomalainen, A. (2012). Mitochondria: in sickness and in health. *Cell* 148, 1145–1159. doi: 10.1016/j.cell.2012.02.035.Mitochondria

Pagliarini, D. J., Calvo, S. E., Chang, B., Sheth, S. A., Vafai, S. B., Ong, S. E., et al. (2008). A mitochondrial protein compendium elucidates complex I disease biology. *Cell* 134, 112–123. doi: 10.1016/j.cell.2008.06.016

Papa, S., Martino, P. L., Capitanio, G., Gaballo, A., De Rasmo, D., Signorile, A., et al. (2012). "The oxidative phosphorylation system in mammalian mitochondria," in *Advances in Experimental Medicine and Biology*, eds R. Scatena, P. Bottoni, and B. Giardina (Dordrecht: Springer), 3–37. doi: 10.1007/978-94-007-2869-1_1

Parikh, S., Goldstein, A., Koenig, M. K., Scaglia, F., Enns, G. M., Saneto, R., et al. (2015). Diagnosis and management of mitochondrial disease: a consensus statement from the mitochondrial medicine society. *Genet. Med.* 17, 689–701. doi: 10.1038/gim.2014.177

Parikh, S., Karaa, A., Goldstein, A., Bertini, E. S., Chinnery, P. F., Christodoulou, J., et al. (2019). Diagnosis of possible' mitochondrial disease: an existential crisis. *J. Med. Genet.* 56, 123–130. doi: 10.1136/jmedgenet-2018-105800

Pfeffer, G., Horvath, R., Klopstock, T., Mootha, V. K., Suomalainen, A., Koene, S., et al. (2013). New treatments for mitochondrial disease—no time to drop our standards. *Nat. Rev. Neurol.* 9, 474–481. doi: 10.1038/nrneurol.2013.129

Phadke, R. (2017). Myopathology of adult and paediatric mitochondrial diseases. *J. Clin. Med.* 6:64. doi: 10.3390/jcm6070064

Pitceathly, R., Keshavan, N., Rahman, J., and Rahman, S. (2020). Moving towards clinical trials for mitochondrial diseases. *J. Inherit. Metab. Dis.* 1–20. doi: 10.1002/jimd.12281 [Epub ahead of print].

Powell, C. A., Kopajtich, R., D'Souza, A. R., Rorbach, J., Kremer, L. S., Husain, R. A., et al. (2015). TRMT5 mutations cause a defect in post-transcriptional modification of mitochondrial tRNA associated with multiple respiratory-chain deficiencies. *Am. J. Hum. Genet.* 97, 319–328. doi: 10.1016/j.ajhg.2015.06.011

Pronicka, E., Piekutowska-Abramczuk, D., Ciara, E., Trubicka, J., Rokicki, D., Karkucinska-Wieckowska, A., et al. (2016). New perspective in diagnostics of mitochondrial disorders: two years' experience with whole-exome sequencing at a national paediatric centre. *J. Transl. Med.* 14, 1–19. doi: 10.1186/s12967-016-0930-9

Rahman, J., Noronha, A., Thiele, I., and Rahman, S. (2017). Leigh map: a novel computational diagnostic resource for mitochondrial disease. *Ann. Neurol.* 81, 9–16. doi: 10.1002/ana.24835

Rahman, S. (2020). Mitochondrial disease in children. *J. Intern. Med.* 287, 609–633. doi: 10.1111/joim.13054

Schon, K. R., Ratnaike, T., van den Ameele, J., Horvath, R., and Chinnery, P. F. (2020). Mitochondrial diseases: a diagnostic revolution. *Trends Genet.* 36, 702–717. doi: 10.1016/j.tig.2020.06.009

Shimura, H., Hattori, N., Kubo, S. I., Mizuno, Y., Asakawa, S., Minoshima, S., et al. (2000). Familial Parkinson disease gene product, parkin, is a ubiquitin-protein ligase. *Nat. Genet.* 25, 302–305. doi: 10.1038/77060

Stenton, S. L., and Prokisch, H. (2020). Genetics of mitochondrial diseases: identifying mutations to help diagnosis. *eBio Med.* 56:102784. doi: 10.1016/j.ebiom.2020.102784

Suomalainen, A., Elo, J. M., Pietiläinen, K. H., Hakonen, A. H., Sevastianova, K., Korpela, M., et al. (2011). FGF-21 as a biomarker for muscle-manifesting mitochondrial respiratory chain deficiencies: a diagnostic study. *Lancet Neurol.* 10, 806–818. doi: 10.1016/S1474-4422(11)70155-7

Tan, J., Wagner, M., Stenton, S. L., Strom, T. M., Wortmann, S. B., Prokisch, H., et al. (2020). Lifetime risk of autosomal recessive mitochondrial disorders calculated from genetic databases. *eBio Med.* 54:102730. doi: 10.1016/j.ebiom.2020.102730

Taylor, R. W., Pyle, A., Griffin, H., Blakely, E. L., Duff, J., He, L., et al. (2014). Use of whole-exome sequencing to determine the genetic basis of multiple mitochondrial respiratory chain complex deficiencies. *JAMA* 312, 68–77. doi: 10.1001/jama.2014.7184

Udhayabanu, T., Manole, A., Rajeshwari, M., Varalakshmi, P., Houlden, H., and Ashokkumar, B. (2017). Riboflavin responsive mitochondrial dysfunction in neurodegenerative diseases. *J. Clin. Med.* 6:52. doi: 10.3390/jcm6050052

Valente, E. M., Abou-Sleiman, P. M., Caputo, V., Muqit, M. M. K., Harvey, K., Gispert, S., et al. (2004). Hereditary early-onset Parkinson's disease caused by mutations in PINK1. *Science* 304, 1158–1160. doi: 10.1126/science.1096284

Wallace, D. C., Singh, G., Lott, M. T., Hodge, J. A., Schurr, T. G., Lezza, A. M., et al. (1988). Mitochondrial DNA mutation associated with Leber's hereditary optic neuropathy. *Science* 242, 1427–1430. doi: 10.1126/science.3201231

Wetterstrand, K. (2020). *DNA Sequencing Costs: Data from the NHGRI Genome Sequencing Program (GSP)*. Available online at: www.genome.gov/sequencingcostsdata (accessed August 13, 2020).

Wortmann, S. B., Koolen, D. A., Smeitink, J. A., van den Heuvel, L., and Rodenburg, R. J. (2015). Whole exome sequencing of suspected mitochondrial patients in clinical practice. *J. Inherit. Metab. Dis.* 38, 437–443. doi: 10.1007/s10545-015-9823-y

Wortmann, S. B., Mayr, J. A., Nuoffer, J. M., Prokisch, H., and Sperl, W. (2017). A Guideline for the diagnosis of pediatric mitochondrial disease: the value of muscle and skin biopsies in the genetics era. *Neuropediatrics* 48, 309–314. doi: 10.1055/s-0037-1603776

Zeviani, M., Moraes, C. T., DiMauro, S., Nakase, H., Bonilla, E., Schon, E. A., et al. (1988). Deletions of mitochondrial DNA in Kearns-Sayre syndrome. *Neurology* 38, 1339–1339. doi: 10.1212/WNL.38.9.1339

Conflict of Interest: The authors declare that the research was conducted in the absence of any commercial or financial relationships that could be construed as a potential conflict of interest.

frontiers in Genetics

REVIEW
published: 27 November 2020
doi: 10.3389/fgene.2020.598976

Recent Advances in the Pathophysiology of Fatty Acid Oxidation Defects: Secondary Alterations of Bioenergetics and Mitochondrial Calcium Homeostasis Caused by the Accumulating Fatty Acids

Alexandre Umpierrez Amaral[1,2]* *and Moacir Wajner*[1,3,4]

[1] *Programa de Pós-Graduação em Ciências Biológicas: Bioquímica, Instituto de Ciências Básicas da Saúde, Universidade Federal do Rio Grande do Sul, Porto Alegre, Brazil,* [2] *Departamento de Ciências Biológicas, Universidade Regional Integrada do Alto Uruguai e das Missões, Erechim, Brazil,* [3] *Departamento de Bioquímica, Instituto de Ciências Básicas da Saúde, Universidade Federal do Rio Grande do Sul, Porto Alegre, Brazil,* [4] *Serviço de Genética Médica, Hospital de Clínicas de Porto Alegre, Porto Alegre, Brazil*

OPEN ACCESS

Edited by:
Grant M. Hatch, University of Manitoba, Canada

Reviewed by:
Jerry Vockley, University of Pittsburgh, United States
Peter Bross, Aarhus University, Denmark
Sander Michel Houten, Icahn School of Medicine at Mount Sinai, United States

***Correspondence:**
Alexandre Umpierrez Amaral
alexandreamaral@uricer.edu.br

Specialty section:
This article was submitted to Genetics of Common and Rare Diseases, a section of the journal Frontiers in Genetics

Received: *26 August 2020*
Accepted: *03 November 2020*
Published: *27 November 2020*

Citation:
Amaral AU and Wajner M (2020) Recent Advances in the Pathophysiology of Fatty Acid Oxidation Defects: Secondary Alterations of Bioenergetics and Mitochondrial Calcium Homeostasis Caused by the Accumulating Fatty Acids. Front. Genet. 11:598976. doi: 10.3389/fgene.2020.598976

Deficiencies of medium-chain acyl-CoA dehydrogenase, mitochondrial trifunctional protein, isolated long-chain 3-hydroxyacyl-CoA dehydrogenase, and very long-chain acyl-CoA dehydrogenase activities are considered the most frequent fatty acid oxidation defects (FAOD). They are biochemically characterized by the accumulation of medium-chain, long-chain hydroxyl, and long-chain fatty acids and derivatives, respectively, in tissues and biological fluids of the affected patients. Clinical manifestations commonly include hypoglycemia, cardiomyopathy, and recurrent rhabdomyolysis. Although the pathogenesis of these diseases is still poorly understood, energy deprivation secondary to blockage of fatty acid degradation seems to play an important role. However, recent evidence indicates that the predominant fatty acids accumulating in these disorders disrupt mitochondrial functions and are involved in their pathophysiology, possibly explaining the lactic acidosis, mitochondrial morphological alterations, and altered mitochondrial biochemical parameters found in tissues and cultured fibroblasts from some affected patients and also in animal models of these diseases. In this review, we will update the present knowledge on disturbances of mitochondrial bioenergetics, calcium homeostasis, uncoupling of oxidative phosphorylation, and mitochondrial permeability transition induction provoked by the major fatty acids accumulating in prevalent FAOD. It is emphasized that further *in vivo* studies carried out in tissues from affected patients and from animal genetic models of these disorders are necessary to confirm the present evidence mostly achieved from *in vitro* experiments.

Keywords: fatty acid oxidation defects, bioenergetics, calcium homeostasis, mitochondrial permeability transition, mitochondrial functions

FATTY ACID OXIDATION DEFECTS

Mitochondrial fatty acid oxidation is critical to provide ATP to mitochondria-enriched tissues with high energy demand, including the heart, skeletal muscle, and liver. Mutations in genes expressing enzymes or transport proteins involved in this catabolic pathway cause the fatty acid oxidation defects (FAOD) that are biochemically characterized by accumulation of specific patterns of fatty acids and acylcarnitine derivatives. Patients typically manifest hypoglycemia, cardiomyopathy, hepatopathy, recurrent rhabdomyolysis, and encephalopathy, whose pathogenesis is still poorly known, although energy deprivation secondary to blockage of fatty acid degradation seems to play an important role.

Deficiencies of medium-chain acyl-CoA dehydrogenase (MCAD), mitochondrial trifunctional protein (MTP), isolated long-chain 3-hydroxyacyl-CoA dehydrogenase (LCHAD), and very long-chain acyl-CoA dehydrogenase (VLCAD) are the most common of these diseases. During acute episodes of metabolic decompensation usually associated with infections or fasting, the affected patients present hypoglycemia, encephalopathy, cardiomyopathy, rhabdomyolysis, and hepatopathy. Interestingly, during these catabolic crises, there is a high release of fatty acids from the adipose tissue and a significant increase of the accumulating fatty acids and derivatives due to the enzymatic defects, therefore suggesting the toxicity of these compounds (Rinaldo et al., 2002; Kompare and Rizzo, 2008; Olpin, 2013; Knottnerus et al., 2018; Anderson et al., 2020).

Medium-chain acyl-CoA dehydrogenase-deficient patients are generally asymptomatic, but 20–40% of them develop severe symptomatology along life during an acute episode of metabolic decompensation commonly triggered by prolonged fasting or infections (Merritt and Chang, 2019). During crises, they present hypoketotic hypoglycemia, vomiting that may progress to seizures and coma as well as elevation of liver enzymes and hepatomegaly, whereas a considerable percentage of them may have a fatal outcome (Grosse et al., 2006; Merritt and Chang, 2019; Anderson et al., 2020). Recurrent rhabdomyolysis is remarkably rare in this disease (Ruitenbeek et al., 1995; Schatz and Ensenauer, 2010), although long-term neurological complications are observed in up to 10–30% of patients (Maier, 2015). Tissue (blood) accumulation of medium-chain fatty acids (MCFA), especially octanoic acid (OA), decanoic acid (DA), and cis-4-decenoic acid (cDA), as well as their corresponding acylcarnitine derivatives hexanoylcarnitine, octanoylcarnitine (OC), decanoylcarnitine (DC), and cis-4-decenoylcarnitine and acylglycines (hexanoylglycine, suberylglycine, and phenylpropionylglycine) in urine is detected especially during episodes of acute metabolic decompensation (Dobrowolski et al., 2017; Anderson et al., 2020).

Mitochondrial trifunctional protein comprises three enzyme activities that catalyze the second, third, and fourth step of mitochondrial fatty acid oxidation cycle, namely, long-chain enoyl-CoA hydratase, LCHAD, and long-chain ketoacyl-CoA thiolase. Two inherited diseases are caused by defects of this complex protein, the isolated LCHAD deficiency and MTP deficiency. Long-chain 3-hydroxyacyl-CoA dehydrogenase deficiency is caused by a common mutation (c.1528 G > C) in the HADHA gene, whereas all other HADHA and HADHB mutations in this complex enzyme lead to MTP deficiency (De Biase et al., 2017).

Untreated MTP and LCHAD deficiencies have high mortality and morbidity. The clinical features are usually manifested during fasting or metabolic stress triggered by common illness and mainly affect the heart and skeletal muscles that are highly dependent on fatty acids for their energy needs (Sykut-Cegielska et al., 2011; De Biase et al., 2017; Lotz-Havla et al., 2018). Individuals with MTP deficiency usually present a severe neonatal early onset form with elevated mortality caused by cardiomyopathy, as well as peripheral neuropathy, whereas patients with LCHAD deficiency commonly have a moderate late-onset phenotype with cardiomyopathy, retinal disease, and peripheral neuropathy during adulthood. Patients affected by these diseases may also present with hepatopathy and episodes of rhabdomyolysis during situations of intense lipolysis (Rocchiccioli et al., 1990; Tyni et al., 1997; Den Boer et al., 2002, 2003; Moczulski et al., 2009; De Biase et al., 2017). Long-term complications include rhabdomyolysis, cardiomyopathy, peripheral neuropathy, and retinopathy (Karall et al., 2015; Lotz-Havla et al., 2018). High levels of the long-chain 3-hydroxy fatty acids (LCHFA), 3-hydroxytetradecanoic acid (3HTA), 3-hydroxypalmitic acid (3HPA), and 3-hydroxytetradecanedioic acid (3HTDA) and their respective carnitine by-products accumulate in the patients, with 3-hydroxypalmitoylcarnitine (C16–OH) and 3-hydroxyoleoylcarnitine (C18:1–OH) being the primary biomarkers characteristically found at high concentrations in their blood (Hagenfeldt et al., 1990; Costa et al., 1998; Jones et al., 2001; Hintz et al., 2002; Olpin, 2005; Sander et al., 2005). High amounts of triglycerides containing long-chain fatty acids (LCFA) have been also shown in LCHAD-deficient patients (McCoin et al., 2016).

Very long-chain acyl-CoA dehydrogenase is the first and rate-limiting intramitochondrial step in the mitochondrial oxidation of LCFA. The deficiency of this enzyme activity causes the most prevalent defect of LCFA β-oxidation. The affected patients commonly manifest hypoglycemia, cardiomyopathy, and recurrent rhabdomyolysis. Hypoglycemia usually occurs during 2–4 years of life, whereas rhabdomyolysis is manifested later, and cardiomyopathy can occur at any age. Patients may present three different clinical phenotypes: (a) a severe early onset manifestation with life-threatening cardiomyopathy

Abbreviations: CAC, citric acid cycle; cDA, cis-4-decenoic acid; Cis-5, cis-5-tetradecenoic acid; DA, decanoic acid; DRP1, dynamin-related protein 1; FAOD, fatty acid oxidation disorders; 3HTA, 3-hydroxytetradecanoic acid; 3HTDA, 3-hydroxytetradecanedioic acid; 3HPA, 3-hydroxypalmitic acid; MCAD, medium-chain acyl-CoA dehydrogenase; MCFA, medium-chain fatty acids; MCT, medium-chain triglycerides; LCAC, long-chain acylcarnitines; LCFA, long-chain fatty acids; LCHAD, long-chain 3-hydroxyacyl-CoA dehydrogenase; LCHFA, long-chain 3-hydroxy fatty acids; $\Delta\Psi m$, mitochondrial membrane potential; MCU, mitochondrial calcium uniporter; MFN1, mitofusin 1; MFN2, mitofusin 2; MTP, mitochondrial trifunctional protein; mPT, mitochondrial permeability transition; Myr, myristic acid; OA, octanoic acid; OPA1, optic atrophy 1; OXPHOS, oxidative phosphorylation; PGC-1α, peroxisome proliferator-activated receptor gamma coactivator 1-alpha; PINK1, PTEN-induced putative kinase 1; ROS, reactive oxygen species; SIRT1, sirtuin 1; VLCAD, very long-chain acyl-CoA dehydrogenase.

associated with arrhythmias, hypotonia, hepatomegaly, and intermittent hypoglycemia, (b) an early childhood presentation with hypoketotic hypoglycemia associated with liver alterations and hepatomegaly, or (c) a late-onset myopathic form with recurrent episodes of rhabdomyolysis and muscle pain usually induced by exercise (Spiekerkoetter, 2010; Diekman et al., 2014; Katz et al., 2017; Leslie et al., 2019; Rovelli et al., 2019). Recurrent rhabdomyolysis is a common and acute complication of this disease and should be treated with hydration and alkalization of the urine to prevent acute renal failure secondary to myoglobinuria. Elevated levels of myristic (Myr) and cis-5-tetradecenoic (Cis-5) acids, as well as their acylcarnitine derivatives tetradecenoyl-L-carnitine (C14:1), tetradecadienyl-L-carnitine (C14:2), tetradecanoyl-L-carnitine (C14), and dodecanoyl-L-carnitine (C12), are commonly found in blood (McHugh et al., 2011).

The diagnosis of MCAD, LCHAD/MTP, and VLCAD deficiencies is mainly performed by the detection of high concentrations of characteristic acylcarnitines in blood. The determination of enzyme activities in lymphocytes and/or fibroblasts and molecular analyses of mutations may be necessary for diagnosis confirmation. Since early diagnosis and prompt treatment are available in MCAD, LCHAD/MTP, and VLCAD deficiencies, these diseases have been included in the expanded newborn screening programs, allowing a much better outcome for the affected patients by significantly reducing morbidity and mortality (Wilcken et al., 2007; Spiekerkoetter et al., 2010; Maguolo et al., 2020).

The current treatments for these diseases include frequent meals and avoidance of catabolic stress situations caused by prolonged fasting or infectious illness. Fatty acid restriction, allied to medium-chain triglycerides (MCT) formulas and essential fatty acids to LCHAD/MTP and VLCAD deficiencies, as well as high oral or intravenous glucose administration to sustain anabolism is also critical in these disorders. The objective is therefore preventing hypoketotic hypoglycemia and metabolite accumulation. L-Carnitine supplementation should be used mainly to correct L-carnitine deficiency, but its beneficial effect to significantly increase the urinary excretion of potentially toxic fatty acids has still to be demonstrated (Spiekerkoetter et al., 2009, 2010). More recently, clinical trials have shown that bezafibrate, an agonist of peroxisome-proliferating activator receptor that increases mitochondrial biogenesis and the gene expression of mitochondrial fatty acid oxidation enzymes, may be useful in VLCAD (Yamada et al., 2018; Shiraishi et al., 2019) and MTP (Suyama et al., 2020) deficiencies. However, the clinical efficacy of bezafibrate is still disputed and needs to be further confirmed (Ørngreen et al., 2014, 2015). Furthermore, replacement of long-chain triglycerides by MCT and replenishment of citric acid cycle (CAC) intermediates by the seven-carbon fatty acid triglyceride (C7) triheptanoin to support ATP production have been recently demonstrated to improve the clinical outcome of these patients (Gillingham et al., 2017; Vockley et al., 2017, 2019).

Treatment is effective to decrease mortality and morbidity for most FAOD, although it does not completely prevent long-term systemic and neurological complications. It is therefore expected that elucidation of the exact underlying mechanisms of pathogenesis of these disorders will potentially help in the development of novel treatments to improve the quality of life of the affected patients. In particular, observations of mitochondrial biochemical and morphological abnormalities in highly mitochondria-enriched tissues of MCAD-, LCHAD/MTP-, and VLCAD-deficient patients, such as the heart, liver, and skeletal muscle, indicate that disturbances of mitochondrial functions are probably involved in their pathophysiology. The present review will mainly focus on recent evidence indicating secondary alterations of important mitochondrial properties caused by major fatty acids accumulating in these disorders.

MITOCHONDRIAL FUNCTIONS: BIOENERGETICS AND CALCIUM HOMEOSTASIS

The mitochondria are dynamic organelles with essential roles in cellular physiology, particularly in tissues with high energy demand and oxidative metabolism, such as the heart, skeletal muscle, liver, and brain. The mitochondria regulate ATP production, redox status, cytosolic calcium concentrations, and apoptosis-induced cell death. These mitochondrial functions are closely associated with efficient dynamic processes, such as mitochondrial fission and fusion, biogenesis, and mitophagy.

Mitochondrial fatty acid oxidation is the main source of ATP generation in the heart, skeletal muscle, and liver. Acetyl-CoA originated from fatty acid degradation is oxidized in the CAC, providing the electrons to form NADH and $FADH_2$, which are transferred through the respiratory chain complexes in the electron transfer system. Protons are pumped into the mitochondrial intermembrane space, generating an electrochemical gradient (mitochondrial membrane potential, $\Delta\Psi m$). The energy of the electrochemical gradient is used by ATP synthase to support ATP production, and the whole process is called oxidative phosphorylation (OXPHOS; Nicholls and Ferguson, 2013).

Calcium regulates a significant number of critical intracellular events necessary to cell survival, particularly in the heart, skeletal muscle, and liver (Rizzuto et al., 2012). The mitochondria continuously promote calcium influx down the electrochemical gradient through the mitochondrial calcium uniporter (MCU) and efflux by the Na^+/Ca^{2+} and H^+/Ca^{2+} exchangers, contributing together with the endoplasmic reticulum to maintain the cytosolic concentrations of this ion that would be adequate for cell functioning (De Stefani et al., 2016). At physiological or pathological situations of calcium overload, the capacity of the mitochondria to retain calcium is particularly important (Williams et al., 2013; Granatiero et al., 2017; Nicholls, 2017).

Mitochondrial permeability transition (mPT) pore opening in the inner mitochondrial membrane occurs when the threshold of mitochondrial calcium retention capacity is exceeded. Mitochondrial permeability transition pore opening is deleterious to cell functioning and survival mainly due to non-selective mitochondrial permeabilization that leads to significant calcium, glutathione, and NADH and NAD(P)H

release, inducing mitochondrial swelling, ΔΨm dissipation, disruption of ATP synthesis, and finally apoptotic cell death (Rasola and Bernardi, 2011; Bernardi and von Stockum, 2012; Giorgio et al., 2018).

Mitochondrial calcium homeostasis represents an important regulatory mechanism in muscular tissue physiology, being extremely important for normal cardiomyocyte (Drago et al., 2012; Eisner, 2014; Kohlhaas et al., 2017) and myocyte (Yi et al., 2011; Eisner, 2014) functioning. Dysregulation of intracellular calcium concentration due to mitochondrial dysfunction associated with mPT induction has been related to cardiac diseases (Gordan et al., 2016; Bravo-Sagua et al., 2017) and suggested as a pathophysiologic event leading to rhabdomyolysis (Hamel et al., 2015). Disturbance of mitochondrial calcium homeostasis and mPT pore opening has also been demonstrated to be involved in liver diseases (Ferreira et al., 2003; Brenner et al., 2013; Go et al., 2015).

On the other hand, balanced mitochondrial fusion (elongation) and fission (fragmentation) is essential for normal mitochondrial morphology, distribution, and function, being also necessary in response to the variable physiological demands of the cell (El-Hattab et al., 2018). These processes can restore or remove defective mitochondria and are mainly coordinated by the pro-fusion mitochondrial proteins optic atrophy 1 (OPA1), mitofusin 1 (MFN1), and mitofusin 2 (MFN2), as well as by the cytosolic pro-fission dynamin-related protein 1 (DRP1; Burté et al., 2015). The quantity and the quality of the mitochondria are regulated by the equilibrium between their formation (biogenesis) and removal (mitophagy). Upregulation of biogenesis improves mitochondrial function and has been related to various proteins, such as the peroxisome proliferator-activated receptor gamma coactivator 1-alpha (PGC-1α) and sirtuin 1 (SIRT1), whereas mitophagy is dependent on the PTEN-induced putative kinase 1 (PINK1; Ploumi et al., 2017). PTEN-induced putative kinase 1 is highly expressed in injured mitochondria with collapsed ΔΨm, recruiting and activating mitophagy-related proteins, particularly ubiquitin ligase parkin. It is noteworthy that the defects in mitochondrial dynamics result in the impairment of mitochondrial bioenergetics and calcium homeostasis, potentially leading to cell death (Pernas and Scorrano, 2016; Kowaltowski et al., 2019). Furthermore, failure in mitochondrial dynamics has been related to various pathological processes, including myopathies, cardiomyopathy, hepatopathy, neurodegeneration, diabetes, and cancer (Archer, 2013; Vásquez-Trincado et al., 2016; Bartsakoulia et al., 2018; Mansouri et al., 2018; Ji and Yeo, 2019).

FATTY ACID OXIDATION DEFECTS AND MITOCHONDRIAL ABNORMALITIES

Table 1 summarizes the biochemical and morphological evidence of mitochondrial abnormalities in patients, genetic knockout mice, and cultured cell models of MCAD, LCHAD/MTP, and VLCAD deficiencies.

Increased lactate formation commonly results from the impairment of mitochondrial bioenergetics, with lactic acidosis being therefore considered a biochemical hallmark of mitochondrial disorders (Kerr, 1991; Zeviani and Di Donato, 2004). However, it should be noted that, apart from being indicative of altered mitochondrial functions, lactic acidemia may be also a consequence of decreased lactate utilization due to liver dysfunction as found in some FAOD, particularly during episodes of metabolic decompensation. Patients with these diseases also present episodes of rhabdomyolysis that signalize severe disturbance of mitochondrial functions (Nance and Mammen, 2015). Oxidative stress has been also associated with mitochondrial dysfunction (Wang et al., 2014; Kudryavtseva et al., 2016; Rose et al., 2018) due to impairment of the mitochondrial electron flow through the respiratory chain, resulting in increased electron loss and subsequent reactive oxygen species (ROS) generation (Lambert and Brand, 2009; Nickel et al., 2014).

Although uncommon, lactic acidosis (Feillet et al., 2003), oxidative stress (Derks et al., 2014; Najdekr et al., 2015), and rhabdomyolysis (Ruitenbeek et al., 1995; Schatz and Ensenauer, 2010) have been observed in some patients with MCAD deficiency, particularly during episodes of metabolic decompensation. Reduced mitochondrial oxygen consumption, decreased respiratory chain complex protein levels, and increased ROS production were also found in fibroblasts from MCAD-deficient patients and in MCAD knockout 143B osteosarcoma cells (Lim et al., 2018), supporting a role for the disruption of bioenergetics and of redox homeostasis in the pathogenesis and progression of this disorder.

On the other hand, abnormal mitochondrial morphology and altered biochemical markers of mitochondrial functions, reflecting an impairment of bioenergetics, were commonly reported in isolated LCHAD and MTP deficiencies. In this scenario, lactic acidemia (Tyni et al., 1996; Ventura et al., 1998; Das et al., 2000; Enns et al., 2000), as well as rhabdomyolysis (Olpin, 2005; Diekman et al., 2014), mitochondrial morphological abnormalities, and inhibition of the respiratory chain electron flow (Tyni et al., 1996; Das et al., 2000; Enns et al., 2000; Hintz et al., 2002), was observed in skeletal muscle and cultured fibroblasts from patients with these diseases. Decreased mitochondrial oxygen consumption and reduced ATP synthesis were also detected in the fibroblasts of MTP-deficient patients (Lefort et al., 2017). Furthermore, an interesting study utilizing LCHAD-deficient fibroblasts demonstrated a dysregulation of the mitochondrial fusion/fission machinery as revealed by a decreased MFN2/DRP1 ratio, leading to the accumulation of fragmented mitochondria due to increased fission (Hagenbuchner et al., 2018). Mitochondrial swelling and distortion (Ibdah et al., 2001), as well as induction of oxidative stress, have been also reported in the liver of LCHAD-deficient mice (Ibdah et al., 2005).

As regards to VLCAD deficiency, lactic acidosis (Ventura et al., 1998) and rhabdomyolysis (Roe et al., 2002; Engbers et al., 2005; Diekman et al., 2014) were found in a considerable number of patients with this disorder. Decreased mitochondrial respiration associated with low ATP levels, as well as increased

TABLE 1 | Mitochondrial biochemical and morphological abnormalities observed in patients and genetic models of MCAD, LCHAD/MTP and VLCAD deficiencies.

FAOD		Evidence of mitochondrial abnormalities		References
MCAD deficiency	Patients	Fibroblasts	↓ Mitochondrial oxygen consumption ↓ Respiratory chain complexes protein levels	Lim et al., 2018
		Blood	Lactic acidemia ↑ Oxidative stress	Feillet et al., 2003 Derks et al., 2014; Najdekr et al., 2015
		Skeletal muscle	Rhabdomyolysis	Ruitenbeek et al., 1995; Schatz and Ensenauer, 2010
	Genetic model	MCAD knockout 143B osteosarcoma cells	↓ Mitochondrial oxygen consumption ↓ Respiratory chain complexes protein levels	Lim et al., 2018
LCHAD/MTP deficiencies	Patients	Fibroblasts	↓ Mitochondrial oxygen consumption ↓ ATP synthesis ↓ MFN2/DRP1 ratio (increased fission) ↑ ROS production	Lefort et al., 2017 Lefort et al., 2017 Hagenbuchner et al., 2018 Hagenbuchner et al., 2018
		Blood	Lactic acidemia	Tyni et al., 1996; Ventura et al., 1998; Das et al., 2000; Enns et al., 2000
		Skeletal muscle	Rhabdomyolysis Mitochondrial abnormalities and respiratory chain inhibition	Olpin, 2005; Diekman et al., 2014 Tyni et al., 1996; Enns et al., 2000; Das et al., 2000
	Genetic model	Mouse liver	↑ Oxidative stress Mitochondrial swelling and distortion	Ibdah et al., 2005 Ibdah et al., 2001
VLCAD deficiency	Patients	Fibroblasts	↓ Mitochondrial oxygen consumption ↓ ATP synthesis ↑ ROS generation ↑ MFN1 levels (increased fusion)	Seminotti et al., 2019
		Cardiomyocytes	↑ Intracellular calcium concentrations	Knottnerus et al., 2020
		Blood	Lactic acidemia	Ventura et al., 1998
		Skeletal muscle	Rhabdomyolysis	Roe et al., 2002; Engbers et al., 2005; Diekman et al., 2014
	Genetic model	Mouse brown adipose tissue	↑ Resting respiration (uncoupling of OXPHOS)	Exil et al., 2006
		Mouse heart	↓ Citric acid cycle intermediates ↓ Phosphocreatine/ATP ratio ↓ ATP production	Bakermans et al., 2013; Gaston et al., 2020 Tucci et al., 2014 Xiong et al., 2014

DRP1: dynamin-related protein 1; FAOD: fatty acid oxidation defects; LCHAD: long-chain 3-hydroxyacyl-CoA dehydrogenase; MCAD: medium-chain acyl-CoA dehydrogenase; MTP: mitochondrial trifunctional protein; MFN1: mitofusin 1; MFN2: mitofusin 2; ROS: reactive oxygen species; OXPHOS: oxidative phosphorylation; VLCAD: very long-chain acyl-CoA dehydrogenase.

ROS generation, was verified in the fibroblasts of VLCAD-deficient patients (Seminotti et al., 2019). These fibroblasts revealed elevated mitochondrial mass and fusion, as well as an increased expression of MFN1, indicating alterations of mitochondrial dynamics besides the disruption of the endoplasmic reticulum–mitochondria crosstalk that is involved in cytosolic calcium homeostasis (Seminotti et al., 2019). This is in line with the observations of increased intracellular calcium concentrations that were correlated with fatty acid intermediate accumulation in fibroblasts from VLCAD-deficient patients differentiated into cardiomyocytes (Knottnerus et al., 2020). Furthermore, results obtained in the genetic mice model of VLCAD deficiency showed bioenergetics disruption. Thus, increased resting respiration suggesting uncoupling of OXPHOS was found in brown adipose tissue (Exil et al., 2006), and decreased phosphocreatine/ATP ratio (Tucci et al., 2014), ATP production (Xiong et al., 2014), and CAC intermediate pools (Bakermans et al., 2013; Gaston et al., 2020) were demonstrated in the heart of these animals.

DISTURBANCE OF MITOCHONDRIAL BIOENERGETICS AND CALCIUM HOMEOSTASIS CAUSED BY THE MAJOR FATTY ACIDS ACCUMULATING IN FATTY ACID OXIDATION DEFECTS

The pathophysiology of tissue damage in patients with MCAD, LCHAD/MTP, and VLCAD deficiencies has not yet been well established, although energy deprivation caused by fatty acid oxidation blockage, leading to hypoketotic hypoglycemia and sequestration of CoA and L-carnitine, was presumed to be mainly involved in the pathogenesis of these disorders (Spiekerkoetter and Wood, 2010; Olpin, 2013). More recently, alternative pathogenetic mechanisms have been hypothesized to contribute to their symptomatology, more particularly the toxicity of the accumulating metabolites. This is in accordance with the observations that clinical worsening occurs during stress catabolic situations characterized by intense lipolysis leading to the massive production of these compounds (Gregersen and Olsen, 2010; Olpin, 2013; Tein, 2013; Knottnerus et al., 2018).

In particular, there is mounting evidence of bioenergetics impairment in tissues that primarily consume fatty acids for their energy needs in patients and in the genetic models of MCAD, LCHAD/MTP, and VLCAD deficiencies (**Table 1**). **Tables 2–4** summarize the updated data showing that the major metabolites, particularly MCFA, LCHFA, and LCFA, accumulating in these disorders provoke alterations of mitochondrial functions in the heart, liver and skeletal muscle of rats and also in cultured cell lines, mainly impairing mitochondrial bioenergetics and calcium homeostasis by distinct mechanisms. It is emphasized that, overall, the doses of the accumulating metabolites used in most of these studies were similar to the levels described in the blood of affected patients during metabolic decompensation. However, a significant impairment of mitochondrial functions was also achieved with lower concentrations of these compounds in LCHAD/MTP and VLCAD deficiencies that better approach the levels found in blood during periods of stable disease, therefore suggesting the chronic toxicity of these compounds in these inherited deficiencies.

Thus, OA, DA, and cDA, the MCFA that most commonly accumulate in MCAD deficiency, were shown to provoke mitochondrial dysfunction in the liver and skeletal muscle of rats. OA and DA were shown to inhibit the activities of the respiratory chain complexes I–III and II–III in rat liver, as well as of complex IV in the liver and skeletal muscle, besides inducing oxidative stress in these tissues (Scaini et al., 2012). In addition, DA and cDA severely inhibited ATP-linked (ADP-stimulated) and maximal (CCCP-stimulated) mitochondrial oxygen consumption, increased resting respiration (induced by the ATP synthase inhibitor oligomycin), and inhibited complexes II–III and IV activities, indicating metabolic inhibition and uncoupling of OXPHOS that lead to energy deficiency besides provoking a disruption of redox homeostasis in isolated liver mitochondria (Amaral et al., 2016). It is noteworthy that, in the same study, it was shown that DA and cDA decreased $\Delta\Psi m$ and matrix NAD(P)H content and stimulated the opening of cyclosporin A-sensitive mPT pore. Calcium retention capacity was also decreased by DA and cDA, probably as a result of mPT induction in the liver mitochondria (Amaral et al., 2016). Other studies reported that OA and DA caused $\Delta\Psi m$ dissipation in hepatocytes (Rial et al., 2018) and induced apoptosis in adipocytes (Yang et al., 2009), whereas OA was demonstrated to decrease the ATP/O ratio in perfused liver, indicating OXPHOS impairment (Gallis et al., 2007). In contrast, the carnitine derivatives of the corresponding MCFA tested, OC and DC, caused no changes in the mitochondrial parameters evaluated, implying that medium-chain acylcarnitine derivatives do not disturb these mitochondrial functions. This is consistent with a recent study showing no alterations of OC and DC on mitochondrial respiration in fibroblasts (Lefort et al., 2017).

As regards to LCHFA, it was demonstrated that 3HTA and 3HPA, which mostly accumulate in tissues and biological fluids of patients affected by LCHAD or MTP deficiencies, decrease $\Delta\Psi m$, matrix NAD(P)H content, calcium retention capacity, and ATP synthesis besides inducing mitochondrial swelling in calcium-loaded liver and heart mitochondria (Cecatto et al., 2015; Hickmann et al., 2015). It was proposed that these effects were due to the induction of cyclosporin A-sensitive mPT pore opening as well as due to uncoupling and to the metabolic inhibition caused by these fatty acids (Cecatto et al., 2015; Hickmann et al., 2015). Similar results were achieved in cultured cell lines from the heart and liver (Cecatto et al., 2018b), as well as in skeletal muscle mitochondria and permeabilized muscle fibers (Cecatto et al., 2016). Altered mitochondrial membrane fluidity caused by the LCHFA was also shown in the skeletal muscle (Cecatto et al., 2016). However, the corresponding dicarboxylic 3HTDA caused no effect on these parameters, implying a selective toxicity of monocarboxylic LCHFA (Cecatto et al., 2015, 2016; Hickmann et al., 2015).

Disruption of mitochondrial functions has also been suggested as a relevant pathomechanism involved in the cardiomyopathy, hepatopathy, and myopathy in VLCAD deficiency since high

TABLE 2 | Major metabolites accumulating in MCAD deficiency disturb mitochondrial bioenergetics and calcium homeostasis in liver and skeletal muscle of rats, as well as in cultured cell lines.

FAOD	Accumulating metabolites	Disturbance of mitochondrial bioenergetics and calcium homeostasis		References
MCAD deficiency	OA	Liver supernatants	↓ Complexes I-III, II-III and IV activities	Scaini et al., 2012
			↑ Oxidative stress	Scaini et al., 2012
			↓ ATP/O ratio	Gallis et al., 2007
		Skeletal muscle supernatants	↓ Complex IV activity	Scaini et al., 2012
			↑ Oxidative stress induction	
		Hepatocytes	↓ $\Delta\Psi m$	Rial et al., 2018
		Adipocytes	↑ Apoptosis	Yang et al., 2009
	OC	Liver mitochondria	No alterations	Amaral et al., 2016
		Fibroblasts	No alterations	Lefort et al., 2017
	DA	Liver supernatants	↓ Complexes I-III, II-III and IV activities	Scaini et al., 2012
			↑ Oxidative stress	
		Skeletal muscle supernatants	↓ Complex IV activity	Scaini et al., 2012
			↑ Oxidative stress	
		Liver mitochondria	↓ Complexes II-III and IV activities	Amaral et al., 2016
			↑ Oxidative stress	
			↓ ATP-linked and maximal respiration	
			↑ Resting respiration (uncoupling of OXPHOS)	
			↓ $\Delta\Psi m$ and matrix NAD(P)H concentrations	
			↓ Calcium retention capacity	
			Induction of mPT pore opening	
		Hepatocytes	↓ $\Delta\Psi m$	Rial et al., 2018
		Adipocytes	↑ Apoptosis	Yang et al., 2009
	DC	Liver mitochondria	No alterations	Amaral et al., 2016
		Fibroblasts	No alterations	Lefort et al., 2017
	cDA	Liver mitochondria	↓ Complexes II-III and IV activities	Amaral et al., 2016
			↑ Oxidative stress	
			↓ ATP-linked and maximal respiration	
			↑ Resting respiration (uncoupling of OXPHOS)	
			↓ $\Delta\Psi m$ and matrix NAD(P)H concentrations	
			↓ Calcium retention capacity	
			Induction of mPT pore opening	

cDA: cis-4-decenoic acid; DA: decanoic acid; DC: decanoylcarnitine; FAOD: fatty acid oxidation defects; MCAD: medium-chain acyl-CoA dehydrogenase; $\Delta\Psi m$: mitochondrial membrane potential; mPT: mitochondrial permeability transition; OA: octanoic acid; OC: octanoylcarnitine; OXPHOS: oxidative phosphorylation.

TABLE 3 | Major metabolites accumulating in LCHAD/MTP deficiencies disturb mitochondrial bioenergetics and calcium homeostasis in heart, liver and skeletal muscle of rats, as well as in cultured cell lines.

FAOD	Accumulating metabolites	Disturbance of mitochondrial bioenergetics and calcium homeostasis		References
LCHAD/MTP deficiencies	3HTDA	Heart, liver and skeletal muscle mitochondria	No alterations	Hickmann et al., 2015; Cecatto et al., 2015; Cecatto et al., 2016
	3HTA/3HPA	Heart mitochondria	↓ $\Delta\Psi$m and matrix NAD(P)H concentrations ↑ Swelling ↓ Calcium retention capacity ↓ ATP production - Induction of mPT pore opening	Cecatto et al., 2015
		Cardiomyocytes	↓ ATP-linked and maximal respiration ↑ Resting respiration (uncoupling of OXPHOS)	Cecatto et al., 2018b
		Liver mitochondria	↓ ATP-linked and maximal respiration ↑ Resting respiration (uncoupling of OXPHOS) ↓ $\Delta\Psi$m and matrix NAD(P)H concentrations ↓ Calcium retention capacity ↑ Swelling Induction of mPT pore opening	Hickmann et al., 2015
		Hepatocytes	↓ ATP-linked and maximal respiration ↑ Resting respiration (uncoupling of OXPHOS)	Cecatto et al., 2018b
		Skeletal muscle mitochondria	↓ ATP-linked and maximal respiration ↑ Resting respiration (uncoupling of OXPHOS) ↓ $\Delta\Psi$m and matrix NAD(P)H concentrations ↓ Calcium retention capacity ↓ Mitochondrial membrane fluidity Induction of mPT pore opening	Cecatto et al., 2016
		Skeletal muscle fibers	↓ ATP-linked and maximal respiration	Cecatto et al., 2016

FAOD: fatty acid oxidation defects; 3-HTDA: 3-hydroxytetradecanedioic acid; 3-HTA: 3-hydroxytetradecanoic acid; 3HPA: 3-hydroxypalmitic acid; LCHAD: long-chain 3-hydroxyacyl-CoA dehydrogenase; $\Delta\Psi$m: mitochondrial membrane potential; mPT: mitochondrial permeability transition; MTP: mitochondrial trifunctional protein; OXPHOS: oxidative phosphorylation.

TABLE 4 | Major metabolites accumulating in VLCAD deficiency disturb mitochondrial bioenergetics and calcium homeostasis in heart, liver and skeletal muscle of rats, as well as in cultured cell lines.

FAOD	Accumulating metabolites	Disturbance of mitochondrial bioenergetics and calcium homeostasis		References
VLCAD deficiency	Myr/Cis-5	Heart mitochondria	↓ Complex I activity ↓ ATP-linked and maximal respiration ↑ Resting respiration (uncoupling of OXPHOS) ↓ $\Delta\Psi$m and matrix NAD(P)H concentrations ↓ ATP production ↓ Calcium retention capacity Induction of mPT pore opening	Cecatto et al., 2018a
		Heart fibers	↓ ATP-linked and maximal respiration	Cecatto et al., 2018a
		Cardiomyocytes	↓ ATP-linked and maximal respiration ↑ Resting respiration (uncoupling of OXPHOS) ↓ $\Delta\Psi$m	Cecatto et al., 2018a
		Liver mitochondria	↓ Complex I-III activity ↓ ATP-linked and maximal respiration ↑ Resting respiration (uncoupling of OXPHOS) ↓ $\Delta\Psi$m ↓ ATP production ↑ Swelling ↑ Cytochrome c release ↓ Calcium retention capacity Induction of mPT pore opening	Cecatto et al., 2020 Cecatto et al., 2020 Cecatto et al., 2020; Wieckowski and Wojtczak, 1998; Bodrova et al., 2000 Cecatto et al., 2020 Bodrova et al., 2003; Cecatto et al., 2020
		Hepatocytes	↓ ATP-linked and maximal respiration ↑ Resting respiration (uncoupling of OXPHOS)	Cecatto et al., 2020
		Skeletal muscle mitochondria	↓ Complex I-III and α-KGDH activity ↓ ATP-linked and maximal respiration ↑ Resting respiration (uncoupling of OXPHOS) ↓ $\Delta\Psi$m ↓ ATP production ↓ Calcium retention capacity Induction of mPT pore opening	Cecatto et al., 2019
		Skeletal muscle fibers	↓ ATP-linked and maximal respiration ↑ Resting respiration (uncoupling of OXPHOS)	Cecatto et al., 2019
	C14:1/C16:1 LCAC	Cardiomyocytes	Induction of apoptosis and necrosis	Hoffmann et al., 2014
		Fibroblasts	↓ Resting respiration ↓ $\Delta\Psi$m	Lefort et al., 2017 Nguyen et al., 2017
		Heart mitochondria	↓ ATP-linked respiration ↑ ROS generation ↓ Calcium retention capacity	Liepinsh et al., 2016 Baydoun et al., 1988; De Villiers and Lochner, 1986
		Cardiomyocytes	Disturbance of cell calcium homeostasis	Berezhnov et al., 2008
		Myocytes	Disturbance of cell calcium homeostasis	McCoin et al., 2015b
		Heart sarcoplasmic reticulum	Disturbance of cell calcium homeostasis	Yamada et al., 2000

Cis-5: cis-5-tetradecenoic acid; FAOD: fatty acid oxidation defects; LCAC: long-chain acylcarnitines; $\Delta\Psi$m: mitochondrial membrane potential; mPT: mitochondrial permeability transition; Myr: myristic acid; OXPHOS: oxidative phosphorylation; VLCAD: very long-chain acyl-CoA dehydrogenase.

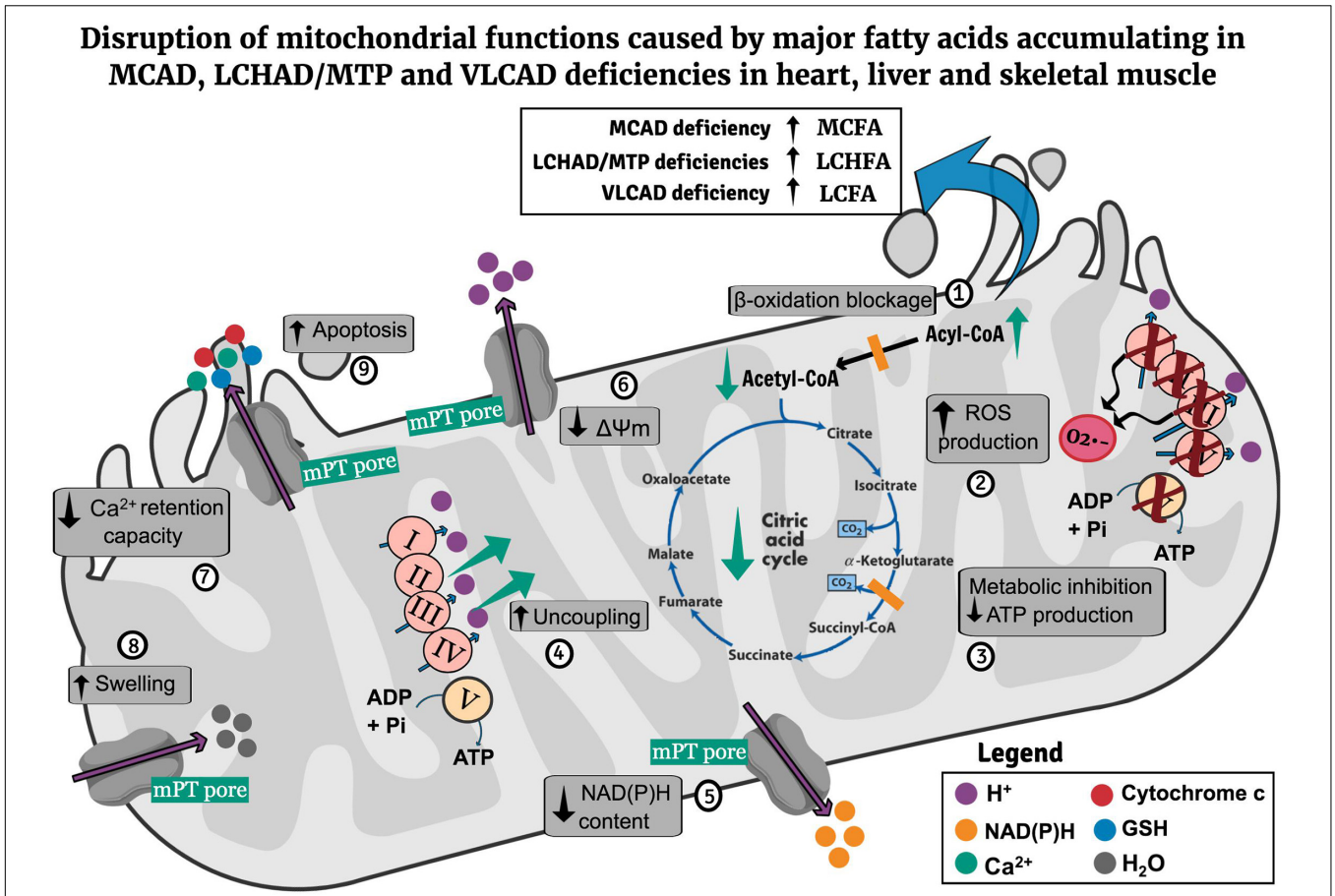

FIGURE 1 | Potential pathomechanisms of mitochondrial dysfunction in the heart, liver, and skeletal muscle in MCAD, LCHAD/MTP, and VLCAD deficiencies. Mitochondrial β-oxidation blockage leads to the matrix accumulation of MCFA (MCAD deficiency), LCHFA (LCHAD/MTP deficiencies), and LCFA (VLCAD deficiency) as well as CoA depletion (1). The accumulating fatty acids inhibit respiratory chain complexes activities, leading to ROS generation (2), cause metabolic inhibition due to decrease of respiratory chain and citric acid cycle activities compromising ATP synthesis (3), uncouple oxidative phosphorylation (4), activate the mPT pore opening, provoking a decrease of mitochondrial NAD(P)H content (5), ΔΨm (6), and mitochondrial Ca^{2+} retention capacity (7), and induce mitochondrial swelling (8). Finally, mPT induction also promotes cytochrome c release, possibly contributing to apoptosis induction (9). CoA, coenzyme A; LCFA, long-chain fatty acids; LCHAD, long-chain hydroxyacyl-CoA dehydrogenase; LCHFA, long-chain 3-hydroxy fatty acids; MCAD, medium-chain acyl-CoA dehydrogenase; MCFA, medium-chain fatty acids; ΔΨm, mitochondrial membrane potential; mPT, mitochondrial permeability transition; MTP, mitochondrial trifunctional protein; ROS, reactive oxygen species; VLCAD, very long-chain acyl-CoA dehydrogenase.

concentrations of Myr and Cis-5, which mostly accumulate in this disorder, were shown to be toxic to mitochondrial functions by impairing bioenergetics and calcium homeostasis. In particular, previous works performed in isolated liver mitochondria showed that Myr uncouples OXPHOS through the involvement of the dicarboxylate carrier (Wieckowski and Wojtczak, 1998) and of the ANT (Bodrova et al., 2000). Induction of mPT pore opening was also demonstrated to be caused by Myr (Bodrova et al., 2003). Recent studies demonstrated that, apart from Myr, pathological concentrations of Cis-5 disturb mitochondrial bioenergetics and calcium homeostasis in the heart, liver, and skeletal muscle (Cecatto et al., 2018a, 2019, 2020). These results were obtained in different tissue preparations, such as isolated mitochondria, permeabilized cardiomyocytes and hepatocytes, and heart fibers. Myr and Cis-5 also inhibited complex I–III and α-ketoglutarate dehydrogenase activities and altered mitochondrial respiration, behaving as metabolic inhibitors and uncouplers of OXPHOS, leading to ATP depletion besides reducing ΔΨm and matrix NAD(P)H content. These LCFA also induced cyclosporin A-sensitive mPT in the presence of calcium, causing mitochondrial ΔΨm dissipation, reduction of calcium retention capacity, swelling, and cytochrome c release. These observations are in accordance with a previous study showing that monounsaturated LCFA (C14:1 and C16:1) accumulating in VLCAD deficiency decrease ΔΨm and induce apoptosis and necrosis in cardiomyocytes (Hoffmann et al., 2014). On the other hand, the toxicity of long-chain acylcarnitines (LCAC) was reported to be involved in long-chain FAOD pathogenesis (McCoin et al., 2015a, 2019). In particular, it was demonstrated that LCAC disturb cell calcium homeostasis in myocytes (McCoin et al., 2015b), cardiomyocytes (Berezhnov et al., 2008), and heart

sarcoplasmic reticulum (Yamada et al., 2000) besides decreasing resting respiration (Lefort et al., 2017) and provoking $\Delta\Psi m$ dissipation (Nguyen et al., 2017) in fibroblasts. LCAC were also shown to reduce calcium retention capacity (De Villiers and Lochner, 1986; Baydoun et al., 1988), inhibit ATP-linked respiration, and generate ROS in the heart mitochondria (Liepinsh et al., 2016).

Figure 1 illustrates the main mechanisms of mitochondrial dysfunction caused by major fatty acids that accumulate in MCAD, LCHAD/MTP, and VLCAD deficiencies.

CONCLUDING REMARKS

Mounting evidence of altered mitochondrial morphology, functions, and dynamics has been recently described in various tissues of patients with MCAD, LCHAD/MTP, and VLCAD deficiencies and in the genetic models of these diseases, suggesting that impairment of mitochondrial homeostasis may play a relevant role in the pathogenesis of these disorders. In particular, the major accumulating MCFA, LCHFA, and LCFA were demonstrated to severely disturb mitochondrial bioenergetics and calcium homeostasis *in vitro* in highly oxidative mitochondria-enriched tissues, such as the heart, liver, and skeletal muscle. These fatty acids behaved as metabolic inhibitors, uncouplers of OXPHOS, and inductors of mPT pore opening. It is therefore presumed that these pathomechanisms probably contribute to the mitochondrial alterations observed in patients and animal models with these pathological conditions. Interestingly, severe cardiomyopathy, hepatopathy, and skeletal muscle alterations are mainly manifested during catabolic stress situations in which the concentrations of the characteristic fatty acids dramatically increase in tissues and biological fluids, therefore supporting an acute toxicity for these endogenous compounds. However, the present evidence of bioenergetics disruption caused by the accumulating metabolites must be interpreted with caution since most available data were achieved by *in vitro* assays. Further studies performed preferentially *in vivo* in animal models and in patients affected by FAOD are therefore necessary to further clarify the underlying mechanisms of tissue damage in these disorders. Finally, it is expected that, besides restricting fat dietary intake and avoiding fasting, drugs that stimulate mitochondrial function such as bezafibrate and the anaplerotic compound triheptanoin may hopefully improve the clinical outcome of the affected patients (Gillingham et al., 2017; Vockley et al., 2017, 2019; Yamada et al., 2018; Shiraishi et al., 2019; Suyama et al., 2020).

AUTHOR CONTRIBUTIONS

Both authors planned and wrote the review article.

FUNDING

The research activity in the authors' laboratories was supported in part by research grants from Conselho Nacional de Desenvolvimento Científico e Tecnológico (CNPq)—425914/2016-0 and Fundação de Amparo à Pesquisa do Estado do Rio Grande do Sul (FAPERGS)—17/2551-0000800-6.

ACKNOWLEDGMENTS

We acknowledge the invaluable technical assistance of A.C. Roginski.

REFERENCES

Amaral, A. U., Cecatto, C., Da Silva, J. C., Wajner, A., Godoy, K. D. S., Ribeiro, R. T., et al. (2016). Cis-4-Decenoic and decanoic acids impair mitochondrial energy, redox and Ca2 + homeostasis and induce mitochondrial permeability transition pore opening in rat brain and liver: possible implications for the pathogenesis of MCAD deficiency. *Biochim. Biophys. Acta* 1857, 1363–1372. doi: 10.1016/j.bbabio.2016.05.007

Anderson, D. R., Viau, K., Botto, L. D., Pasquali, M., and Longo, N. (2020). Clinical and biochemical outcomes of patients with medium-chain acyl-CoA dehydrogenase deficiency. *Mol. Genet. Metab.* 129, 13–19. doi: 10.1016/j.ymgme.2019.11.006

Archer, S. L. (2013). Mitochondrial dynamics - mitochondrial fission and fusion in human diseases. *N. Engl. J. Med.* 369, 2236–2251. doi: 10.1056/NEJMra1215233

Bakermans, A. J., Dodd, M. S., Nicolay, K., Prompers, J. J., Tyler, D. J., and Houten, S. M. (2013). Myocardial energy shortage and unmet anaplerotic needs in the fasted long-chain acyl-Co a dehydrogenase knockout mouse. *Cardiovasc. Res.* 100, 441–449. doi: 10.1093/cvr/cvt212

Bartsakoulia, M., Pyle, A., Troncoso-Chandía, D., Vial-Brizzi, J., Paz-Fiblas, M. V., Duff, J., et al. (2018). A novel mechanism causing imbalance of mitochondrial fusion and fission in human myopathies. *Hum. Mol. Genet.* 27, 1186–1195. doi: 10.1093/hmg/ddy033

Baydoun, A. R., Markham, A., Morgan, R. M., and Sweetman, A. J. (1988). Palmitoyl carnitine: an endogenous promotor of calcium efflux from rat heart mitochondria. *Biochem. Pharmacol.* 37, 3103–3107. doi: 10.1016/0006-2952(88)90307-3

Berezhnov, A. V., Fedotova, E. I., Nenov, M. N., Kokoz, I. M., Zinchenko, V. P., and Dynnik, V. V. (2008). Destabilization of the cytosolic calcium level and cardiomyocyte death in the presence of long-chain fatty acid derivatives. *Biofizika* 53, 1025–1032. doi: 10.1134/S0006350908060183

Bernardi, P., and von Stockum, S. (2012). The permeability transition pore as a Ca2+ release channel: new answers to an old question. *Cell Calcium* 52, 22–27. doi: 10.1016/j.ceca.2012.03.004

Bodrova, M. E., Brailovskaya, I. V., Efron, G. I., Starkov, A. A., and Mokhova, E. N. (2003). Cyclosporin A-sensitive decrease in the transmembrane potential across the inner membrane of liver mitochondria induced by low concentrations of fatty acids and Ca2+. *Biochemistry* 68, 391–398. doi: 10.1023/A:1023691628110

Bodrova, M. E., Dedukhova, V. I., Samartsev, V. N., and Mokhova, E. N. (2000). Role of the ADP/ATP-antiporter in fatty acid-induced uncoupling of Ca2+-loaded rat liver mitochondria. *IUBMB Life* 50, 189–194. doi: 10.1080/152165400300001507

Bravo-Sagua, R., Parra, V., López-Crisosto, C., Díaz, P., Quest, A. F. G., and Lavandero, S. (2017). Calcium transport and signaling in mitochondria. *Compr. Physiol.* 7, 623–634. doi: 10.1002/cphy.c160013

Brenner, C., Galluzzi, L., Kepp, O., and Kroemer, G. (2013). Decoding cell death signals in liver inflammation. *J. Hepatol.* 59, 583–594. doi: 10.1016/j.jhep.2013.03.033

Burté, F., Carelli, V., Chinnery, P. F., and Yu-Wai-Man, P. (2015). Disturbed mitochondrial dynamics and neurodegenerative disorders. *Nat. Rev. Neurol.* 11, 11–24. doi: 10.1038/nrneurol.2014.228

Cecatto, C., Amaral, A. U., da Silva, J. C., Wajner, A., Schimit, M. O. V, da Silva, L. H. R., et al. (2018a). Metabolite accumulation in VLCAD deficiency markedly disrupts mitochondrial bioenergetics and Ca(2+) homeostasis in the heart. *FEBS J.* 285, 1437–1455. doi: 10.1111/febs.14419

Cecatto, C., Amaral, A. U., Roginski, A. C., Castilho, R. F., and Wajner, M. (2019). Impairment of mitochondrial bioenergetics and permeability transition induction caused by major long-chain fatty acids accumulating in VLCAD deficiency in skeletal muscle as potential pathomechanisms of myopathy. *Toxicol. Vitr.* 62:104665. doi: 10.1016/j.tiv.2019.104665

Cecatto, C., Amaral, A. U., Wajner, A., Wajner, S. M., Castilho, R. F., and Wajner, M. (2020). Disturbance of mitochondrial functions associated with permeability transition pore opening induced by cis-5-tetradecenoic and myristic acids in liver of adolescent rats. *Mitochondrion* 50, 1–13. doi: 10.1016/j.mito.2019.09.008

Cecatto, C., Godoy, K. D. S., da Silva, J. C., Amaral, A. U., and Wajner, M. (2016). Disturbance of mitochondrial functions provoked by the major long-chain 3-hydroxylated fatty acids accumulating in MTP and LCHAD deficiencies in skeletal muscle. *Toxicol. Vitr.* 36, 1–9. doi: 10.1016/j.tiv.2016.06.007

Cecatto, C., Hickmann, F. H., Rodrigues, M. D., Amaral, A. U., and Wajner, M. (2015). Deregulation of mitochondrial functions provoked by long-chain fatty acid accumulating in long-chain 3-hydroxyacyl-CoA dehydrogenase and mitochondrial permeability transition deficiencies in rat heart–mitochondrial permeability transition pore opening as a potential contributing pathomechanism of cardiac alterations in these disorders. *FEBS J.* 282, 4714–4726. doi: 10.1111/febs.13526

Cecatto, C., Wajner, A., Vargas, C. R., Wajner, S. M., Amaral, A. U., and Wajner, M. (2018b). High vulnerability of the heart and liver to 3-hydroxypalmitic acid-induced disruption of mitochondrial functions in intact cell systems. *J. Cell. Biochem.* 119, 7678–7686. doi: 10.1002/jcb.27115

Costa, C. G., Dorland, L., Tavares De Almeida, I., Jakobs, C., Duran, M., and Poll-The, B. T. (1998). The effect of fasting, long-chain triglyceride load and carnitine load on plasma long-chain acylcarnitine levels in mitochondrial very long-chain acyl-CoA dehydrogenase deficiency. *J. Inherit. Metab. Dis.* 21, 391–399. doi: 10.1023/A:1005354624735

Das, A. M., Fingerhut, R., Wanders, R. J. A., and Ullrich, K. (2000). Secondary respiratory chain defect in a boy with long-chain 3- hydroxyacyl-CoA dehydrogenase deficiency: possible diagnostic pitfalls. *Eur. J. Pediatr.* 159, 243–246. doi: 10.1007/s004310050063

De Biase, I., Viau, K. S., Liu, A., Yuzyuk, T., Botto, L. D., Pasquali, M., et al. (2017). Diagnosis, treatment, and clinical outcome of patients with mitochondrial trifunctional protein/long-chain 3-hydroxy acyl-CoA dehydrogenase deficiency. *JIMD Reports* 31, 63–71. doi: 10.1007/8904_2016_558

De Stefani, D., Rizzuto, R., and Pozzan, T. (2016). Enjoy the trip: calcium in mitochondria back and forth. *Annu. Rev. Biochem.* 85, 161–192. doi: 10.1146/annurev-biochem-060614-034216

De Villiers, M., and Lochner, A. (1986). Mitochondrial Ca2+ fluxes: role of free fatty acids, acyl-CoA and acylcarnitine. *Biochim. Biophys. Acta* 876, 309–317. doi: 10.1016/0005-2760(86)90289-4

Den Boer, M. E. J., Dionisi-Vici, C., Chakrapani, A., Van Thuijl, A. O. J., Wanders, R. J. A., and Wijburg, F. A. (2003). Mitochondrial trifunctional protein deficiency: a severe fatty acid oxidation disorder with cardiac and neurologic involvement. *J. Pediatr.* 142, 684–689. doi: 10.1067/mpd.2003.231

Den Boer, M. E. J., Wanders, R. J. A., Morris, A. A. M., Ijlst, L., Heymans, H. S. A., and Wijburg, F. A. (2002). Long-chain 3-hydroxyacyl-CoA dehydrogenase deficiency: clinical presentation and follow-up of 50 patients. *Pediatrics* 109, 99–104. doi: 10.1542/peds.109.1.99

Derks, T. G. J., Touw, C. M. L., Ribas, G. S., Biancini, G. B., Vanzin, C. S., Negretto, G., et al. (2014). Experimental evidence for protein oxidative damage and altered antioxidant defense in patients with medium-chain acyl-CoA dehydrogenase deficiency. *J. Inherit. Metab. Dis.* 37, 783–789. doi: 10.1007/s10545-014-9700-0

Diekman, E. F., Van Der Pol, W. L., Nievelstein, R. A. J., Houten, S. M., Wijburg, F. A., and Visser, G. (2014). Muscle MRI in patients with long-chain fatty acid oxidation disorders. *J. Inherit. Metab. Dis.* 37, 405–413. doi: 10.1007/s10545-013-9666-3

Dobrowolski, S. F., Ghaloul-Gonzalez, L., and Vockley, J. (2017). Medium chain acyl-CoA dehydrogenase deficiency in a premature infant. *Pediatr. Rep.* 9, 7045. doi: 10.4081/pr.2017.7045

Drago, I., De Stefani, D., Rizzuto, R., and Pozzan, T. (2012). Mitochondrial Ca2+ uptake contributes to buffering cytoplasmic Ca2+ peaks in cardiomyocytes. *Proc. Natl. Acad. Sci. U. S. A.* 109, 12986–12991. doi: 10.1073/pnas.1210718109

Eisner, D. (2014). Calcium in the heart: from physiology to disease. *Exp. Physiol.* 99, 1273–1282. doi: 10.1113/expphysiol.2013.077305

El-Hattab, A. W., Suleiman, J., Almannai, M., and Scaglia, F. (2018). Mitochondrial dynamics: biological roles, molecular machinery, and related diseases. *Mol. Genet. Metab.* 125, 315–321. doi: 10.1016/j.ymgme.2018.10.003

Engbers, H. M., Dorland, L., De Sain, M. G. M., Eskes, P. F., and Visser, G. (2005). Rhabdomyolysis in early-onset very long-chain acyl-CoA dehydrogenase deficiency despite normal glucose after fasting. *J. Inherit. Metab. Dis.* 28, 1151–1152. doi: 10.1007/s10545-005-0190-y

Enns, G. M., Bennett, M. J., Hoppel, C. L., Goodman, S. I., Weisiger, K., Ohnstad, C., et al. (2000). Mitochondrial respiratory chain complex I deficiency with clinical and biochemical features of long-chain 3-hydroxyacyl-coenzyme A dehydrogenase deficiency. *J. Pediatr.* 136, 251–254. doi: 10.1016/S0022-3476(00)70111-9

Exil, V. J., Gardner, C. D., Rottman, J. N., Sims, H., Bartelds, B., Khuchua, Z., et al. (2006). Abnormal mitochondrial bioenergetics and heart rate dysfunction in mice lacking very-long-chain acyl-CoA dehydrogenase. *Am. J. Physiol. Hear. Circ. Physiol.* 290, H1289-H1297. doi: 10.1152/ajpheart.00811.2005

Feillet, F., Steinmann, G., Vianey-Saban, C., De Chillou, C., Sadoul, N., Lefebvre, E., et al. (2003). Adult presentation of MCAD deficiency revealed by coma and severe arrythmias. *Intensive Care Med.* 29, 1594–1597. doi: 10.1007/s00134-003-1871-3

Ferreira, F. M., Seiça, R., Oliveira, P. J., Coxito, P. M., Moreno, A. J., Palmeira, C. M., et al. (2003). Diabetes induces metabolic adaptations in rat liver mitochondria: role of coenzyme Q and cardiolipin contents. *Biochim. Biophys. Acta* 1639, 113–120. doi: 10.1016/j.bbadis.2003.08.001

Gallis, J. L., Tissier, P., Gin, H., and Beauvieux, M. C. (2007). Decrease in oxidative phosphorylation yield in presence of butyrate in perfused liver isolated from fed rats. *BMC Physiol.* 7, 8. doi: 10.1186/1472-6793-7-8

Gaston, G., Gangoiti, J. A., Winn, S., Chan, B., Barshop, B. A., Harding, C. O., et al. (2020). Cardiac tissue citric acid cycle intermediates in exercised very long-chain acyl-CoA dehydrogenase-deficient mice fed triheptanoin or medium-chain triglyceride. *J. Inherit. Metab. Dis.* 2020:12284. doi: 10.1002/jimd.12284

Gillingham, M. B., Heitner, S. B., Martin, J., Rose, S., Goldstein, A., El-Gharbawy, A. H., et al. (2017). Triheptanoin versus trioctanoin for long-chain fatty acid oxidation disorders: a double blinded, randomized controlled trial. *J. Inherit. Metab. Dis.* 40, 831–843. doi: 10.1007/s10545-017-0085-8

Giorgio, V., Guo, L., Bassot, C., Petronilli, V., and Bernardi, P. (2018). Calcium and regulation of the mitochondrial permeability transition. *Cell Calcium* 70, 56–63. doi: 10.1016/j.ceca.2017.05.004

Go, K. L., Lee, S., Zendejas, I., Behrns, K. E., and Kim, J. S. (2015). Mitochondrial Dysfunction and Autophagy in Hepatic Ischemia/Reperfusion Injury. *Biomed Res. Int.* 2015, 1–14. doi: 10.1155/2015/183469

Gordan, R., Fefelova, N., Gwathmey, J. K., and Xie, L. H. (2016). Involvement of mitochondrial permeability transition pore (mPTP) in cardiac arrhythmias: evidence from cyclophilin D knockout mice. *Cell Calcium* 60, 363–372. doi: 10.1016/j.ceca.2016.09.001

Granatiero, V., De Stefani, D., and Rizzuto, R. (2017). "Mitochondrial calcium handling in physiology and disease." *Adv Exp Med Biol.* 982, 25–47. doi: 10.1007/978-3-319-55330-6_2

Gregersen, N., and Olsen, R. K. J. (2010). Disease mechanisms and protein structures in fatty acid oxidation defects. *J. Inherit. Metab. Dis.* 33, 547–553. doi: 10.1007/s10545-010-9046-1

Grosse, S. D., Khoury, M. J., Greene, C. L., Crider, K. S., and Pollitt, R. J. (2006). The epidemiology of medium chain acyl-CoA dehydrogenase deficiency: an update. *Genet. Med.* 8, 205–212. doi: 10.1097/01.gim.0000204472.25153.8d

Hagenbuchner, J., Scholl-Buergi, S., Karall, D., and Ausserlechner, M. J. (2018). very long-/and long chain-3-Hydroxy Acyl CoA Dehydrogenase eficiency correlates with deregulation of the mitochondrial fusion/fission machinery. *Sci. Rep.* 8:3254. doi: 10.1038/s41598-018-21519-2

Hagenfeldt, L., von Döbeln, U., Holme, E., Alm, J., Brandberg, G., Enocksson, E., et al. (1990). 3-hydroxydicarboxylic aciduria-a fatty acid oxidation defect with severe prognosis. *J. Pediatr.* 116, 387–392. doi: 10.1016/S0022-3476(05)82826-4

Hamel, Y., Mamoune, A., Mauvais, F. X., Habarou, F., Lallement, L., Romero, N. B., et al. (2015). Acute rhabdomyolysis and inflammation. *J. Inherit. Metab. Dis.* 38, 621–628. doi: 10.1007/s10545-015-9827-7

Hickmann, F. H., Cecatto, C., Kleemann, D., Monteiro, W. O., Castilho, R. F., Amaral, A. U., et al. (2015). Uncoupling, metabolic inhibition and induction of mitochondrial permeability transition in rat liver mitochondria caused by the major long-chain hydroxyl monocarboxylic fatty acids accumulating in LCHAD deficiency. *Biochim. Biophys. Acta* 1847, 620–628. doi: 10.1016/j.bbabio.2015.04.003

Hintz, S. R., Matern, D., Strauss, A., Bennett, M. J., Hoyme, H. E., Schelley, S., et al. (2002). Early neonatal diagnosis of long-chain 3-hydroxyacyl coenzyme a dehydrogenase and mitochondrial trifunctional protein deficiencies. *Mol. Genet. Metab.* 75, 120–127. doi: 10.1006/mgme.2001.3282

Hoffmann, L., Seibt, A., Herebian, D., and Spiekerkoetter, U. (2014). Monounsaturated 14:1n-9 and 16:1n-9 fatty acids but not 18:1n-9 induce apoptosis and necrosis in murine HL-1 cardiomyocytes. *Lipids* 49, 25–37. doi: 10.1007/s11745-013-3865-4

Ibdah, J. A., Paul, H., Zhao, Y., Binford, S., Salleng, K., Cline, M., et al. (2001). Lack of mitochondrial trifunctional protein in mice causes neonatal hypoglycemia and sudden death. *J. Clin. Invest.* 107, 1403–1409. doi: 10.1172/JCI12590

Ibdah, J. A., Perlegas, P., Zhao, Y., Angdisen, J., Borgerink, H., Shadoan, M. K., et al. (2005). Mice heterozygous for a defect in mitochondrial trifunctional protein develop hepatic steatosis and insulin resistance. *Gastroenterology* 128, 1381–1390. doi: 10.1053/j.gastro.2005.02.001

Ji, L. L., and Yeo, D. (2019). Mitochondrial dysregulation and muscle disuse atrophy. *F1000 Res.* 8:1621. doi: 10.12688/f1000research.19139.1

Jones, P. M., Moffitt, M., Joseph, D., Harthcock, P. A., Boriack, R. L., Ibdah, J. A., et al. (2001). Accumulation of free 3-hydroxy fatty acids in the culture media of fibroblasts from patients deficient in long-chain L-3-hydroxyacyl-CoA dehydrogenase: a useful diagnostic aid. *Clin. Chem.* 47, 1190–1194. doi: 10.1093/clinchem/47.7.1190

Karall, D., Brunner-Krainz, M., Kogelnig, K., Konstantopoulou, V., Maier, E. M., Möslinger, D., et al. (2015). Clinical outcome, biochemical and therapeutic follow-up in 14 austrian patients with long-chain 3-hydroxy acyl CoA dehydrogenase deficiency (LCHADD). *Orphanet J. Rare Dis.* 10:21. doi: 10.1186/s13023-015-0236-7

Katz, S., Landau, Y., Pode-Shakked, B., Pessach, I. M., Rubinshtein, M., Anikster, Y., et al. (2017). Cardiac failure in very long chain acyl-CoA dehydrogenase deficiency requiring extracorporeal membrane oxygenation (ECMO) treatment: a case report and review of the literature. *Mol. Genet. Metab. Reports* 10, 5–7. doi: 10.1016/j.ymgmr.2016.11.008

Kerr, D. S. (1991). Lactic acidosis and mitochondrial disorders. *Clin. Biochem.* 24, 331–336. doi: 10.1016/0009-9120(91)80007-P

Knottnerus, S. J. G., Bleeker, J. C., Wüst, R. C. I., Ferdinandusse, S., IJlst, L., Wijburg, F. A., et al. (2018). Disorders of mitochondrial long-chain fatty acid oxidation and the carnitine shuttle. *Rev. Endocr. Metab. Disord.* 19, 93–106. doi: 10.1007/s11154-018-9448-1

Knottnerus, S. J. G., Mengarelli, I., Wüst, R. C. I., Baartscheer, A., Bleeker, J. C., Coronel, R., et al. (2020). Electrophysiological abnormalities in VLCAD deficient hiPSC-cardiomyocytes can be improved by lowering accumulation of fatty acid oxidation intermediates. *Int. J. Mol. Sci.* 21:2589. doi: 10.3390/ijms21072589

Kohlhaas, M., Nickel, A. G., and Maack, C. (2017). Mitochondrial energetics and calcium coupling in the heart. *J. Physiol.* 595, 3753–3763. doi: 10.1113/JP273609

Kompare, M., and Rizzo, W. B. (2008). Mitochondrial fatty-acid oxidation disorders. *Semin. Pediatr. Neurol.* 15, 140–149. doi: 10.1016/j.spen.2008.05.008

Kowaltowski, A. J., Menezes-Filho, S. L., Assali, E. A., Gonçalves, I. G., Cabral-Costa, J. V., Abreu, P., et al. (2019). Mitochondrial morphology regulates organellar Ca2+ uptake and changes cellular Ca2+ homeostasis. *FASEB J.* 33, 13176–13188. doi: 10.1096/fj.201901136R

Kudryavtseva, A. V., Krasnov, G. S., Dmitriev, A. A., Alekseev, B. Y., Kardymon, O. L., Sadritdinova, A. F., et al. (2016). Mitochondrial dysfunction and oxidative stress in aging and cancer. *Oncotarget* 7, 44879–44905. doi: 10.18632/oncotarget.9821

Lambert, A. J., and Brand, M. D. (2009). Reactive oxygen species production by mitochondria. *Methods Mol. Biol.* 554, 165–181. doi: 10.1007/978-1-59745-521-3_11

Lefort, B., Gouache, E., Acquaviva, C., Tardieu, M., Benoist, J. F., Dumas, J. F., et al. (2017). Pharmacological inhibition of carnitine palmitoyltransferase 1 restores mitochondrial oxidative phosphorylation in human trifunctional protein deficient fibroblasts. *Biochim. Biophys. Acta* 1863, 1292–1299. doi: 10.1016/j.bbadis.2017.04.005

Leslie, N. D., Valencia, C. A., Strauss, A. W., Connor, J., and Zhang, K. (2019). "Very Long-Chain Acyl-Coenzyme A Dehydrogenase Deficiency," in *GeneReviews®* eds M. P. Adam, H. H. Ardinger, R. A. Pagon, S. E. Wallace, L. J. Bean, K. Stephens, et al. (Seattle (WA): University of Washington), 1993–2020.

Liepinsh, E., Makrecka-Kuka, M., Volska, K., Kuka, J., Makarova, E., Antone, U., et al. (2016). Long-chain acylcarnitines determine ischaemia/reperfusion-induced damage in heart mitochondria. *Biochem. J.* 473, 1191–1202. doi: 10.1042/BCJ20160164

Lim, S. C., Tajika, M., Shimura, M., Carey, K. T., Stroud, D. A., Murayama, K., et al. (2018). Loss of the mitochondrial fatty acid β-oxidation protein medium-chain Acyl-Coenzyme a dehydrogenase disrupts oxidative phosphorylation protein complex stability and function. *Sci. Rep.* 8:153. doi: 10.1038/s41598-017-18530-4

Lotz-Havla, A. S., Röschinger, W., Schiergens, K., Singer, K., Karall, D., Konstantopoulou, V., et al. (2018). Fatal pitfalls in newborn screening for mitochondrial trifunctional protein (MTP)/long-chain 3-hydroxyacyl-CoA dehydrogenase (LCHAD) deficiency. *Orphanet J. Rare Dis.* 13:122. doi: 10.1186/s13023-018-0875-6

Maguolo, A., Rodella, G., Dianin, A., Nurti, R., Monge, I., Rigotti, E., et al. (2020). Diagnosis, genetic characterization and clinical follow up of mitochondrial fatty acid oxidation disorders in the new era of expanded newborn screening: a single centre experience. *Mol. Genet. Metab. Reports* 24;100632. doi: 10.1016/j.ymgmr.2020.100632

Maier, E. M. (2015). Neonatal screening for medium-chain acyl-CoA deficiency—insights and unexpected challenges. *Int. J. Neonatal Screen.* 1, 79–88. doi: 10.3390/ijns1030079

Mansouri, A., Gattolliat, C. H., and Asselah, T. (2018). Mitochondrial dysfunction and signaling in chronic liver diseases. *Gastroenterology* 155, 629–647. doi: 10.1053/j.gastro.2018.06.083

McCoin, C. S., Gillingham, M. B., Knotts, T. A., Vockley, J., Ono-Moore, K. D., Blackburn, M. L., et al. (2019). Blood cytokine patterns suggest a modest inflammation phenotype in subjects with long-chain fatty acid oxidation disorders. *Physiol. Rep.* 7:e14037. doi: 10.14814/phy2.14037

McCoin, C. S., Knotts, T. A., and Adams, S. H. (2015a). Acylcarnitines-old actors auditioning for new roles in metabolic physiology. *Nat. Rev. Endocrinol.* 11, 617–625. doi: 10.1038/nrendo.2015.129

McCoin, C. S., Knotts, T. A., Ono-Moore, K. D., Oort, P. J., and Adams, S. H. (2015b). Long-chain acylcarnitines activate cell stress and myokine release in C2C12 myotubes: calcium-dependent and -independent effects. *Am. J. Physiol. Endocrinol. Metab.* 308, E990-E1000. doi: 10.1152/ajpendo.00602.2014

McCoin, C. S., Piccolo, B. D., Knotts, T. A., Matern, D., Vockley, J., Gillingham, M. B., et al. (2016). Unique plasma metabolomic signatures of individuals with inherited disorders of long-chain fatty acid oxidation. *J. Inherit. Metab. Dis.* 39, 399–408. doi: 10.1007/s10545-016-9915-3

McHugh, D. M. S., Cameron, C. A., Abdenur, J. E., Abdulrahman, M., Adair, O., Al Nuaimi, S. A., et al. (2011). Clinical validation of cutoff target ranges in newborn screening of metabolic disorders by tandem mass spectrometry: a worldwide collaborative project. *Genet. Med.* 13, 230–254. doi: 10.1097/GIM.0b013e31820d5e67

Merritt, J. L. 2nd, and Chang, I. J. (2019). "Medium-Chain Acyl-Coenzyme A Dehydrogenase Deficiency," in *GeneReviews®* eds M. P. Adam, H. H. Ardinger, R. A. Pagon, S. E. Wallace, L. J. Bean, K. Stephens, et al. (Seattle: (WA): University of Washington), 1993–2020.

Moczulski, D., Majak, I., and Mamczur, D. (2009). An overview of beta-oxidation disorders. *Postepy Hig. Med. Dosw.* 63, 266–277.

Najdekr, L., Gardlo, A., Mádrová, L., Friedecký, D., Janečková, H., Correa, E. S., et al. (2015). Oxidized phosphatidylcholines suggest oxidative stress in patients with medium-chain acyl-CoA dehydrogenase deficiency. *Talanta* 139, 62–66. doi: 10.1016/j.talanta.2015.02.041

Nance, J. R., and Mammen, A. L. (2015). Diagnostic evaluation of rhabdomyolysis. *Muscle and Nerve* 51, 793–810. doi: 10.1002/mus.24606

Nguyen, T. B., Louie, S. M., Daniele, J. R., Tran, Q., Dillin, A., Zoncu, R., et al. (2017). DGAT1-dependent lipid droplet biogenesis protects mitochondrial function during starvation-induced autophagy. *Dev. Cell* 42, 9-21. doi: 10.1016/j.devcel.2017.06.003

Nicholls, D. G. (2017). Brain mitochondrial calcium transport: origins of the set-point concept and its application to physiology and pathology. *Neurochem. Int.* 109, 5–12. doi: 10.1016/j.neuint.2016.12.018

Nicholls, D. G., and Ferguson, S. J. (2013). *Bioenergetics*. 4th ed. London: Academic Press.

Nickel, A., Kohlhaas, M., and Maack, C. (2014). Mitochondrial reactive oxygen species production and elimination. *J. Mol. Cell. Cardiol.* 73, 26–33. doi: 10.1016/j.yjmcc.2014.03.011

Olpin, S. E. (2005). Fatty acid oxidation defects as a cause of neuromyopathic disease in infants and adults. *Clin. Lab.* 51, 289–306. doi:

Olpin, S. E. (2013). Pathophysiology of fatty acid oxidation disorders and resultant phenotypic variability. *J. Inherit. Metab. Dis.* 36, 645–658. doi: 10.1007/s10545-013-9611-5

Ørngreen, M. C., Madsen, K. L., Preisler, N., Andersen, G., Vissing, J., and Laforêt, P. (2014). Bezafibrate in skeletal muscle fatty acid oxidation disorders: a randomized clinical trial. *Neurology* 82, 607–613. doi: 10.1212/WNL.0000000000000118

Ørngreen, M. C., Vissing, J., and Laforét, P. (2015). No effect of bezafibrate in patients with CPTII and VLCAD deficiencies. *J. Inherit. Metab. Dis.* 38, 373–374. doi: 10.1007/s10545-014-9779-3

Pernas, L., and Scorrano, L. (2016). Mito-Morphosis: mitochondrial fusion, fission, and cristae remodeling as key mediators of cellular function. *Annu. Rev. Physiol.* 78, 505–531. doi: 10.1146/annurev-physiol-021115-105011

Ploumi, C., Daskalaki, I., and Tavernarakis, N. (2017). Mitochondrial biogenesis and clearance: a balancing act. *FEBS J.* 284, 183–195. doi: 10.1111/febs.13820

Rasola, A., and Bernardi, P. (2011). Mitochondrial permeability transition in Ca2+-dependent apoptosis and necrosis. *Cell Calcium* 50, 222–233. doi: 10.1016/j.ceca.2011.04.007

Rial, S., Ravaut, G., Malaret, T., Bergeron, K.-F., and Mounier, C. (2018). Hexanoic, octanoic and decanoic acids promote basal and insulin-induced phosphorylation of the Akt-mTOR axis and a balanced lipid metabolism in the HepG2 hepatoma cell line. *Molecules* 23:2315. doi: 10.3390/molecules23092315

Rinaldo, P., Matern, D., and Bennett, M. J. (2002). Fatty acid oxidation disorders. *Annu. Rev. Physiol.* 64, 477–502. doi: 10.1146/annurev.physiol.64.082201.154705

Rizzuto, R., De Stefani, D., Raffaello, A., and Mammucari, C. (2012). Mitochondria as sensors and regulators of calcium signalling. *Nat. Rev. Mol. Cell Biol.* 13, 566–578. doi: 10.1038/nrm3412

Rocchiccioli, F., Wanders, R. J. A., Aubourg, P., Vianey-Liaud, C., Ijlst, L., Fabre, M., et al. (1990). Deficiency of long-chain 3-hydroxyacyl-CoA dehydrogenase: a cause of lethal myopathy and cardiomyopathy in early childhood. *Pediatr. Res.* 28, 657–662. doi: 10.1203/00006450-199012000-00023

Roe, C. R., Sweetman, L., Roe, D. S., David, F., and Brunengraber, H. (2002). Treatment of cardiomyopathy and rhabdomyolysis in long-chain fat oxidation disorders using an anaplerotic odd-chain triglyceride. *J. Clin. Invest.* 110, 259–269. doi: 10.1172/JCI0215311

Rose, S., Niyazov, D. M., Rossignol, D. A., Goldenthal, M., Kahler, S. G., and Frye, R. E. (2018). Clinical and molecular characteristics of mitochondrial dysfunction in autism spectrum disorder. *Mol. Diagnosis Ther.* 22, 571–593. doi: 10.1007/s40291-018-0352-x

Rovelli, V., Manzoni, F., Viau, K., Pasquali, M., and Longo, N. (2019). Clinical and biochemical outcome of patients with very long-chain acyl-CoA dehydrogenase deficiency. *Mol. Genet. Metab.* 127, 64–73. doi: 10.1016/j.ymgme.2019.04.001

Ruitenbeek, W., Poels, P. J. E., Turnbull, D. M., Garavaglia, B., Chalmers, R. A., Taylor, R. W., et al. (1995). Rhabdomyolysis and acute encephalopathy in late onset medium chain acyl-CoA dehydrogenase deficiency. *J. Neurol. Neurosurg. Psychiatry* 58, 209–214. doi: 10.1136/jnnp.58.2.209

Sander, J., Sander, S., Steuerwald, U., Janzen, N., Peter, M., Wanders, R. J. A., et al. (2005). Neonatal screening for defects of the mitochondrial trifunctional protein. *Mol. Genet. Metab.* 85, 108–114. doi: 10.1016/j.ymgme.2005.02.002

Scaini, G., Simon, K. R., Tonin, A. M., Busanello, E. N. B., Moura, A. P., Ferreira, G. C., et al. (2012). Toxicity of octanoate and decanoate in rat peripheral tissues: evidence of bioenergetic dysfunction and oxidative damage induction in liver and skeletal muscle. *Mol. Cell. Biochem.* 361, 329–335. doi: 10.1007/s11010-011-1119-4

Schatz, U. A., and Ensenauer, R. (2010). The clinical manifestation of MCAD deficiency: challenges towards adulthood in the screened population. *J. Inherit. Metab. Dis.* 33, 513–520. doi: 10.1007/s10545-010-9115-5

Seminotti, B., Leipnitz, G., Karunanidhi, A., Kochersperger, C., Roginskaya, V. Y., Basu, S., et al. (2019). Mitochondrial energetics is impaired in very long-chain acyl-CoA dehydrogenase deficiency and can be rescued by treatment with mitochondria-targeted electron scavengers. *Hum. Mol. Genet.* 28, 928–941. doi: 10.1093/hmg/ddy403

Shiraishi, H., Yamada, K., Oki, E., Ishige, M., Fukao, T., Hamada, Y., et al. (2019). Open-label clinical trial of bezafibrate treatment in patients with fatty acid oxidation disorders in Japan; 2nd report QOL survey. *Mol. Genet. Metab. Reports* 20:100496. doi: 10.1016/j.ymgmr.2019.100496

Spiekerkoetter, U. (2010). Mitochondrial fatty acid oxidation disorders: clinical presentation of long-chain fatty acid oxidation defects before and after newborn screening. *J. Inherit. Metab. Dis.* 33, 527–532. doi: 10.1007/s10545-010-9090-x

Spiekerkoetter, U., Bastin, J., Gillingham, M., Morris, A., Wijburg, F., and Wilcken, B. (2010). Current issues regarding treatment of mitochondrial fatty acid oxidation disorders. *J. Inherit. Metab. Dis.* 33, 555–561. doi: 10.1007/s10545-010-9188-1

Spiekerkoetter, U., Lindner, M., Santer, R., Grotzke, M., Baumgartner, M. R., Boehles, H., et al. (2009). Treatment recommendations in long-chain fatty acid oxidation defects: consensus from a workshop. *J. Inherit. Metab. Dis.* 32, 498–505. doi: 10.1007/s10545-009-1126-8

Spiekerkoetter, U., and Wood, P. A. (2010). Mitochondrial fatty acid oxidation disorders: pathophysiological studies in mouse models. *J. Inherit. Metab. Dis.* 33, 539–546. doi: 10.1007/s10545-010-9121-7

Suyama, T., Shimura, M., Fushimi, T., Kuranobu, N., Ichimoto, K., Matsunaga, A., et al. (2020). Efficacy of bezafibrate in two patients with mitochondrial trifunctional protein deficiency. *Mol. Genet. Metab. Reports* 24:100610. doi: 10.1016/j.ymgmr.2020.100610

Sykut-Cegielska, J., Gradowska, W., Piekutowska-Abramczuk, D., Andresen, B. S., Olsen, R. K. J., Ołtarzewski, M., et al. (2011). Urgent metabolic service improves survival in long-chain 3-hydroxyacyl-CoA dehydrogenase (LCHAD) deficiency detected by symptomatic identification and pilot newborn screening. *J. Inherit. Metab. Dis.* 34, 185–195. doi: 10.1007/s10545-010-9244-x

Tein, I. (2013). Disorders of fatty acid oxidation. *Handb. Clin. Neurol.* 113, 1675–1688. doi: 10.1016/B978-0-444-59565-2.00035-6

Tucci, S., Flögel, U., Hermann, S., Sturm, M., Schäfers, M., and Spiekerkoetter, U. (2014). Development and pathomechanisms of cardiomyopathy in very long-chain acyl-CoA dehydrogenase deficient (VLCAD-/-) mice. *Biochim. Biophys. Acta* 1842, 677–685. doi: 10.1016/j.bbadis.2014.02.001

Tyni, T., Majander, A., Kalimo, H., Rapola, J., and Pihko, H. (1996). Pathology of skeletal muscle and impaired respiratory chain function in long-chain 3-hydroxyacyl-CoA dehydrogenase deficiency with the G1528C mutation. *Neuromuscul. Disord.* 6, 327–337. doi: 10.1016/0960-8966(96)00352-5

Tyni, T., Rapola, J., Paetau, A., Palotie, A., and Pihko, H. (1997). Pathology of long-chain 3-hydroxyacyl-coa dehydrogenase deficiency caused by the G1528C mutation. *Pediatr. Pathol. Lab. Med.* 17, 427–447. doi: 10.1080/15513819709168585

Vásquez-Trincado, C., García-Carvajal, I., Pennanen, C., Parra, V., Hill, J. A., Rothermel, B. A., et al. (2016). Mitochondrial dynamics, mitophagy and cardiovascular disease. *J. Physiol.* 594, 509–525. doi: 10.1113/JP271301

Ventura, F. V., Ruiter, J. P. N., IJlst, L., Tavares De Almeida, I., and Wanders, R. J. A. (1998). Lactic acidosis in long-chain fatty acid β-oxidation disorders. *J. Inherit. Metab. Dis.* 21, 645–654. doi: 10.1023/A:1005480516801

Vockley, J., Burton, B., Berry, G. T., Longo, N., Phillips, J., Sanchez-Valle, A., et al. (2017). UX007 for the treatment of long chain-fatty acid oxidation disorders: safety and efficacy in children and adults following 24 weeks of treatment. *Mol. Genet. Metab.* 120, 370–377. doi: 10.1016/j.ymgme.2017.02.005

Vockley, J., Burton, B., Berry, G. T., Longo, N., Phillips, J., Sanchez-Valle, A., et al. (2019). Results from a 78-week, single-arm, open-label phase 2 study to

evaluate UX007 in pediatric and adult patients with severe long-chain fatty acid oxidation disorders (LC-FAOD). *J. Inherit. Metab. Dis.* 42, 169–177. doi: 10.1002/jimd.12038

Wang, X., Wang, W., Li, L., Perry, G., Lee, H-g., and Zhu, X. (2014). Oxidative stress and mitochondrial dysfunction in Alzheimer's disease. *Biochim. Biophys. Acta* 1842, 1240–1247. doi: 10.1016/j.bbadis.2013.10.015

Wieckowski, M. R., and Wojtczak, L. (1998). Fatty acid-induced uncoupling of oxidative phosphorylation is partly due to opening of the mitochondrial permeability transition pore. *FEBS Lett.* 423, 339–342. doi: 10.1016/S0014-5793(98)00118-5

Wilcken, B., Haas, M., Joy, P., Wiley, V., Chaplin, M., Black, C., et al. (2007). Outcome of neonatal screening for medium-chain acyl-CoA dehydrogenase deficiency in Australia: a cohort study. *Lancet* 369, 37–42. doi: 10.1016/S0140-6736(07)60029-4

Williams, G. S. B., Boyman, L., Chikando, A. C., Khairallah, R. J., and Lederer, W. J. (2013). Mitochondrial calcium uptake. *Proc. Natl. Acad. Sci. U. S. A.* 110, 10479–10486. doi: 10.1073/pnas.1300410110

Xiong, D., He, H., James, J., Tokunaga, C., Powers, C., Huang, Y., et al. (2014). Cardiac-specific VLCAD deficiency induces dilated cardiomyopathy and cold intolerance. *Am. J. Physiol. Hear. Circ. Physiol.* 306, H326–H338. doi: 10.1152/ajpheart.00931.2012

Yamada, K. A., Kanter, E. M., and Newatia, A. (2000). Long-chain acylcarnitine induces Ca2+ efflux from the sarcoplasmic reticulum. *J. Cardiovasc. Pharmacol.* 36, 14–21. doi: 10.1097/00005344-200007000-00002

Yamada, K., Shiraishi, H., Oki, E., Ishige, M., Fukao, T., Hamada, Y., et al. (2018). Open-label clinical trial of bezafibrate treatment in patients with fatty acid oxidation disorders in Japan. *Mol. Genet. Metab. Reports* 15, 55–63. doi: 10.1016/j.ymgmr.2018.02.003

Yang, J.-Y., Rayalam, S., Della-Fera, M. A., Ambati, S., and Baile, C. A. (2009). Octanoate and Decanoate Induce Apoptosis in 3T3-L1 Adipocytes. *J. Med. Food* 12, 959–966. doi: 10.1089/jmf.2008.0262

Yi, J., Ma, C., Li, Y., Weisleder, N., Ríos, E., Ma, J., et al. (2011). Mitochondrial calcium uptake regulates rapid calcium transients in skeletal muscle during excitation-contraction (E-C) coupling. *J. Biol. Chem.* 286, 32436–32443. doi: 10.1074/jbc.M110.217711

Zeviani, M., and Di Donato, S. (2004). Mitochondrial disorders. *Brain* 127, 2153–2172. doi: 10.1093/brain/awh259

Conflict of Interest: The authors declare that the research was conducted in the absence of any commercial or financial relationships that could be construed as a potential conflict of interest.

frontiers in Genetics

ORIGINAL RESEARCH
published: 07 January 2021
doi: 10.3389/fgene.2020.594828

Sulfite Alters the Mitochondrial Network in Molybdenum Cofactor Deficiency

*Anna-Theresa Mellis[1], Juliane Roeper[1], Albert L. Misko[2], Joshua Kohl[1] and Guenter Schwarz[1,3]**

[1] Department of Chemistry, Institute for Biochemistry, University of Cologne, Cologne, Germany, [2] Department of Neurology, Massachusetts General Hospital, Harvard Medical School, Boston, MA, United States, [3] Center for Molecular Medicine, University of Cologne, Cologne, Germany

Molybdenum cofactor deficiency (MoCD) is an autosomal recessive disorder belonging to the large family of inborn errors in metabolism. Patients typically present with encephalopathy and seizures early after birth and develop severe neurodegeneration within the first few weeks of life. The main pathomechanism underlying MoCD is the loss of function of sulfite oxidase (SO), a molybdenum cofactor (Moco) dependent enzyme located in mitochondrial intermembrane space. SO catalyzes the oxidation of sulfite (SO_3^{2-}) to sulfate (SO_4^{2-}) in the terminal reaction of cysteine catabolism, and in the absence of its activity, sulfurous compounds such as SO_3^{2-}, S-sulfocysteine, and thiosulfate accumulate in patients. Despite growing evidence that these compounds affect neuronal and mitochondrial function, the molecular basis of neuronal dysfunction and cell death in MoCD is still poorly understood. Here we show that mitochondria are severely affected by the loss of SO activity. SO-deficient mouse embryonic fibroblasts display reduced growth rates and impaired ATP production when cultured in galactose, which is an indicator of mitochondrial dysfunction. We also found that mitochondria in SO-deficient cells form a highly interconnected network compared to controls while displaying a slight decrease in motility and unchanged mitochondrial mass. Moreover, we show that the mitochondrial network is directly influenced by SO_3^{2-}, as a moderate elevation of SO_3^{2-} lead to the formation of an interconnected mitochondrial network, while high SO_3^{2-} levels induced fragmentation. Finally, we found a highly interconnected mitochondrial network in MoCD patient-derived fibroblasts, similar to our findings in mouse-derived fibroblasts. We therefore conclude that altered mitochondrial dynamics are an important contributor to the disease phenotype and suggest that MoCD should be included among the mitochondrial disorders.

Keywords: sulfite, sulfite oxidase, mitochondria, molybdenum cofactor deficiency, fission and fusion

OPEN ACCESS

Edited by:
Guilhian Leipnitz, Federal University of Rio Grande do Sul, Brazil

Reviewed by:
Johan Palmfeldt, Aarhus University, Denmark
Lina Ghaloul Gonzalez, University of Pittsburgh, United States

***Correspondence:**
Guenter Schwarz
gschwarz@uni-koeln.de

Specialty section:
This article was submitted to Genetics of Common and Rare Diseases, a section of the journal Frontiers in Genetics

Received: *14 August 2020*
Accepted: *30 November 2020*
Published: *07 January 2021*

Citation:
Mellis A-T, Roeper J, Misko AL, Kohl J and Schwarz G (2021) Sulfite Alters the Mitochondrial Network in Molybdenum Cofactor Deficiency. Front. Genet. 11:594828. doi: 10.3389/fgene.2020.594828

INTRODUCTION

Mitochondrial sulfite oxidase (SO) catalyzes the terminal step in the catabolism of cysteine and methionine, the oxidation of toxic sulfite (SO_3^{2-}) to sulfate (SO_4^{2-}), thereby passing two electrons to cytochrome *c* (Johnson and Rajagopalan, 1979). The cellular concentration of cysteine is tightly controlled by its synthesis and degradation (Stipanuk and Ueki, 2011), the latter proceeding

through two distinct pathways. The first, often referred to as the oxidative pathway, yields taurine, and SO_4^{2-} as the main end products (Kohl et al., 2018). The second pathway involves enzymatic reactions that regulate the formation and clearance of H_2S, an important signaling molecule in mammals, and terminates in the production of thiosulfate and SO_4^{2-}. SO_3^{2-} is a common metabolic intermediate in both catabolic pathways, that, if not removed by SO, can lead to various toxic effects (Vincent et al., 2004; Zhang et al., 2004; de Moura Alvorcem et al., 2017).

In man, the inherited loss of SO activity is caused by two different genetic mechanisms. First, SO may be impaired by mutations in the *SUOX* gene, thus leading to isolated sulfite oxidase deficiency (ISOD). Second, SO may be compromised by mutations in the molybdenum cofactor (Moco) biosynthetic genes (*MOCS1, MOCS2, MOCS3, GPHN*), thereby leading to Moco deficiency (MoCD) and loss of the Moco dependent SO activity (Kohl et al., 2018). Typically, MoCD and ISOD patients present in the neonatal period with identical clinical phenotypes, including encephalopathy, intractable seizures, feeding difficulties, and movement abnormalities. Disease progression involves psychomotor retardation due to progressive cerebral atrophy and ventricular dilatation, often resulting in fatal outcome within their first years of life (Schwarz, 2016). The most prominent biochemical hallmark of MoCD and ISOD is the accumulation of SO_3^{2-} and the sulfite-cysteine adduct S-sulfocysteine in patient urine or plasma (Mudd et al., 1967). However, the disorders are distinguishable on the biochemical level due to the accumulation of xanthine and hypoxanthine, substrates of xanthine oxidase, another Moco enzyme, and diminished levels of uric acid in MoCD, but not ISOD (Schwarz et al., 2009; Schwahn et al., 2015).

Recently, we discovered a new mechanism underlying the neurodegeneration in SO deficiencies as we found that S-sulfocysteine can act as an NMDA receptor agonist and therefore leads to excitotoxic neuronal cell death (Kumar et al., 2017). SO_3^{2-} toxicity has also been investigated in multiple studies, which indicate a disturbance of mitochondrial functions in neurons and kidney cells (Vincent et al., 2004; Zhang et al., 2004; Grings et al., 2014). In particular, exogenous SO_3^{2-} decreased intracellular ATP levels, impaired cellular respiration and inhibited the mitochondrial enzymes glutamate dehydrogenase and malate dehydrogenase. Recently, impairment of mitochondrial respiration has also been shown in various patient cell lines with defects in cysteine catabolism (Grings et al., 2019).

Mitochondria are dynamic organelles constantly undergoing the processes of fusion and fission (Wai and Langer, 2016). The balance of fusion and fission can be influenced in either direction by a multitude of different factors including cellular respiration, ROS formation or the metabolic state of the cell, causing mitochondria to become hypertubular or fragmented. While the effect of SO_3^{2-} on cellular bioenergetics and mitochondrial enzymes has been investigated before, the influence of SO_3^{2-} on mitochondrial dynamics and morphology remains to be determined. In this study, we used SO deficient ($Suox^{-/-}$) mouse embryonic fibroblast (MEF) cells to characterize mitochondrial morphology and function in SO deficiencies to shed light on the role of mitochondria in the disease pathology of ISOD and MoCD.

MATERIALS AND METHODS

Cell Culture

Mouse embryonic fibroblast cells were harvested from heterozygous breedings of $Suox^{\pm}$ mice (Kohl et al., unpublished) as described previously (Xu, 2005). In brief, embryos were removed at E13.5 after timed matings and dissected from the uterus. Fetuses were then minced into fine pieces and incubated in 0.25% trypsin-EDTA at 4°C overnight. On the next day, the suspension was heated for 30 min in a 37°C water bath. The digested tissue was then further broken down into a cell suspension by vigorous pipetting in culture medium. MEF cells were cultivated in Dulbecco's Modified Eagle Medium (DMEM) (Pan Biotech), supplemented with 2 mM glutamine (Gibco by Life Technologies) and 10% Fetal Bovine Serum (FBS) (Pan Biotech; Origin: South Africa). For galactose treatment, cells were cultured in glucose-free DMEM (Pan Biotech, P04-01548S1) supplemented with 10 mM galactose or equal amounts of glucose as control.

Human fibroblasts were extracted from juvenile foreskin. Control fibroblasts were purchased from PromoCell (C-12300). Patient fibroblasts were kindly provided by J. Reiss (Institute for Human Genetics, University of Göttingen, Germany). *GPHN* deficient fibroblasts were first described in Reiss et al. (2001). *MOCS1*-deficient fibroblast were part of an earlier study (Reiss and Hahnewald, 2011). *MOCS2* deficient fibroblasts were characterized in Hahnewald et al. (2006). Fibroblasts were kept in RPMI 1640 medium (Pan Biotech) supplemented with 2 mM glutamine (Gibco by Life Technologies) and 10% FBS (Pan Biotech; Origin: South Africa). All cells were cultured at 37°C and 5% CO_2.

Mouse Keeping

All animals were kept and bred in accordance with European, national and institutional guidelines and protocols were approved by local government authorities (Landesamt für Natur, Umwelt und Verbraucherschutz Nordrhein-Westfalen, Germany; reference 84-02.04.2014.A372). Mice were kept under a 12 h light cycle and provided with regular chow diet and water *ad libitum*. For the generation of homozygous $Suox^{-/-}$ mice, heterozygous mice of at least 2 months of age were kept in 1:1 (male:female) breedings.

Mitochondrial Morphology Analysis

Mitochondrial morphology in MEF cells and patient fibroblasts was visualized using MitoTracker™ Red CMXRos (Invitrogen, United States). The cells were seeded onto sterile cover slips the day prior to the experiment. Cells were incubated in 200 nM MitoTracker™ Red CMXRos diluted in fresh DMEM for 30 min at 37°C. For SO_3^{2-} treatments, the respective SO_3^{2-} concentration was added to the medium 30 min prior to the MitoTracker and incubated at 37°C. Afterward, the cells were washed carefully with PBS before fixation in 4% PFA for 15 min

at 4°C. Remaining PFA was removed by three washing steps with PBS (3 × 5 min). Finally, cover slips were mounted on slides with Mowiol/DABCO (Carl Roth). Images were acquired using a Nikon A1 confocal laser scanning microscope. Images were processed using ImageJ software.

Mitochondrial Membrane Potential

Mitochondrial membrane potential was assessed as described previously with minor modifications (Verburg and Hollenbeck, 2008). In short, a 5 μM stock of tetramethylrhodamine methyl ester (TMRM, Invitrogen) in DMSO was diluted into DMEM medium to a final concentration of 20 nM. Cells were incubated in 20 nM TMRM for 20 min at 37°C. As a control, cells were co-stained with 200 nM MitoTracker™ Deep Red (which accumulates in mitochondria independent of their membrane potential) for 20 min at 37°C. Images were acquired with a Nikon A1R confocal microscope. Pixel intensity for the TMRM was subsequently quantified using ImageJ (ImageJ, RRID:SCR_003070) and normalized by the respective intensity of the MitoTracker™ Deep Red staining.

Mitochondrial Motility and Content

The day prior to the experiment, cells were seeded onto a Nunc™ glass-bottom dish (Thermo Scientific, United States). Mitochondria were visualized via incubation with 200 nM MitoTracker™ Deep Red (diluted in DMEM) for 20 min at 37°C. Mitochondrial motility was analyzed via life cell imaging using a Nikon A1R confocal microscope with environmental chamber. Time-lapse videos were taken over 5 min at 37°C and 5% CO_2. Mitochondrial motility and content were quantified after creating binary images with the software ImageJ (ImageJ, RRID:SCR_003070) as described in Koopman et al. (2006). In brief, maximum intensity projections of image stacks were converted to 8-bit formats and then subjected to a white top-hat filter (MorphoLibJ plugin) before a final thresholding step. Finally, the amount of moved pixels of selected mitochondria between the first and last timepoint (always 5 min apart) were assessed using the XOR function of the Image Calculator.

Transmission Electron Microscopy

For Transmission electron microscopy (TEM), MEF cells were cultured on aclar foil and fixed with pre-warmed fixative solution (2% glutaraldehyde, 2.5% sucrose, 3 mM $CaCl_2$, 100 Mm HEPES, pH 7.3) at RT for 30 min and 4°C for another 30 min. Afterward, fixed cells were washed with 0.1 M sodium cacodylate buffer, incubated with 1% OsO_4, 1.25% Sucrose, 10 mg/ml Potassium ferrocyanide in 0.1 M Cacodylate buffer for 1 h on ice, and washed three times with 0.1 M Cacodylate buffer. Subsequently, cells were dehydrated using ascending ethanol series (50, 70, 90, 3 × 100) for 7 min each at 4°C. After that, cells were incubated with ascending EPON series at 4°C: EPON with ethanol (1 + 1) for 1 h, EPON with ethanol (3 + 1) for 2 h, EPON alone ON, 2 × 2 h with fresh EPON at RT and finally embedded for 48–72 h at 62°C. Ultrathin sections of 70 nm were cut with a diamond knife using an ultramicrotome (Leica, UC7) and stained with uranyl acetate for 15 min at 37°C and lead nitrate solution for 4 min. Electron micrographs were taken with a JEM-2100 Plus Electron Microscope (JEOL). Camera OneView 4K 16 bit (Gatan), and software DigitalMicrograph (Gatan).

ATP Measurement

Intracellular ATP levels in MEF cells were quantified using the CellTiter-Glo® Luminescent Cell Viability Assay (Promega, United States). In short, 8×10^4 cells per well were seeded in 6-well plates the day prior to the experiment. The cells were incubated in glucose- or galactose containing medium for 1 h. They were then lysed in 150 μl RIPA buffer (Sigma). After centrifugation for 20 min at 4°C and 13,000 *g*, 50 μl of the lysate was added to 50 μl CellTiter-Glo® Reagent in a 96-well. The plate was placed on an orbital shaker for 2 min to mix the contents before a 10 min incubation at room temperature. Luminescence was recorded using an EnVision Multimode Plate Reader (PerkinElmer, United States). ATP levels were quantified by comparison to a standard curve and normalized to the protein concentration in the respective sample.

Cell Viability Assay

Cell viability after incubation in glucose- or galactose containing medium was assessed by the MTT assay as described previously (Kumar et al., 2017). In brief, 1×10^4 cells/well were seeded onto a 96-well and grown for 24 h. The next day, the medium was exchanged for DMEM containing either 10 mM glucose or galactose as a carbon source. After 24 h, the old medium was exchanged with fresh phenol red- free DMEM containing 100 μM (3-(4,5-dimethylthiazol-2-yl)-2,5-diphyenyltetrazolium bromide) (MTT). After a 4 h incubation at 37°C in the dark, the MTT solution was exchanged for 100% DMSO. The plate was then placed in a shaker for 10–30 min at 37°C until all cells were solubilized. Finally, the absorption was measured at 570 nm (reference 650 nm) in well plate reader (Tecan Spark).

Determination of Protein Concentration

The concentration of proteins from cell extracts was determined by means of the Bradford assay. Therefore, 190 μl diluted Bradford solution (1/5 dilution) was incubated with 10 μl of protein solution (respective dilution) for 20 min and the absorption change at 595 nm was measured using a well plate reader (BioTek, Germany). The determined absorption change was then compared to that of standard proteins with known concentration in order to determine the protein concentration of unknown solutions.

Western Blot Analysis

Western blotting was performed on crude protein extracts from MEF cells lysed in 100 mM Tris/Ac, pH 8.0. Protein concentration was adjusted accordingly after determination with the Bradford assay. Unless otherwise indicated, 30 μg of protein lysate were separated by SDS-PAGE and immunoblotted using a standard semi-dry blotting protocol onto PVDF membranes. SO protein levels were visualized using a monoclonal anti-SUOX antibody (Sigma-Aldrich Cat# WH0006821M1, RRID:AB_1843810) in conjunction with a HRP-coupled anti-mouse secondary antibody (Santa Cruz

Biotechnology, United States Cat# sc-2055, RRID:AB_631738). Vinculin was detected as loading control using a polyclonal anti-vinculin (H-300) antibody (Santa Cruz Biotechnology, United States Cat# sc-5573, RRID:AB_2214507) together with a HRP-coupled anti-rabbit secondary antibody (Santa Cruz Biotechnology, United States Cat# sc-2054, RRID:AB_631748). Signals were detected using chemiluminescent substrates (Thermo Fisher Scientific, United States, #34580) and a Bio-Rad ChemiDoc XRS + system.

RESULTS

Suox$^{-/-}$ MEFs Show Mitochondrial Impairment

Since previous studies indicate that SO_3^{2-} impacts mitochondrial function (Vincent et al., 2004; Zhang et al., 2004; Grings et al., 2014), we first tested whether SO-deficient MEF cells (**Figure 1A**) generated from *Suox*$^{-/-}$ mice (Kohl et al. unpublished results) exhibited signs of mitochondrial damage. We cultured WT and *Suox*$^{-/-}$ MEFs in either glucose- or galactose-containing medium, thereby forcing the cells to rely on oxidative phosphorylation (OXPHOS) as the main energy source in absence of glucose (galactose-containing medium). After growing the cells for 24 h, we analyzed cell survival using the MTT assay (**Figure 1B**). While the absence of glucose had no effect on the viability of WT cells, survival of *Suox*$^{-/-}$ cells was reduced to less than 50% in galactose, which indicates mitochondrial damage. We then measured intracellular ATP levels under the same conditions and again found no effect on WT MEFs, while *Suox*$^{-/-}$ cells exhibited a severe reduction of ATP levels in galactose-containing medium (∼20% of control), thus showing that *Suox*$^{-/-}$ MEFs are impaired in their ability to produce ATP via OXPHOS (**Figure 1C**). An essential component of OXPHOS is the generation of a proton gradient by different complexes of the respiratory chain (I, III, and IV). We therefore analyzed the mitochondrial membrane potential in WT and *Suox*$^{-/-}$ cells via TMRM staining and found that *Suox*$^{-/-}$ cells have a mild, but significant reduction in their membrane potential relative to WT (**Figure 1D**).

Mitochondrial Morphology Is Altered in *Suox*$^{-/-}$ MEFs

Next, we visualized mitochondrial morphology in WT and *Suox*$^{-/-}$cells after staining with MitoTracker Red CMXRos (**Figure 2A**). We observed that mitochondria in *Suox*$^{-/-}$ MEFs formed a tightly interconnected and hypertubular network distinct from WT MEF cells. We quantified 100 cells per genotype and categorized the mitochondrial network as either fragmented (disturbed, dot-like network, almost no tubules

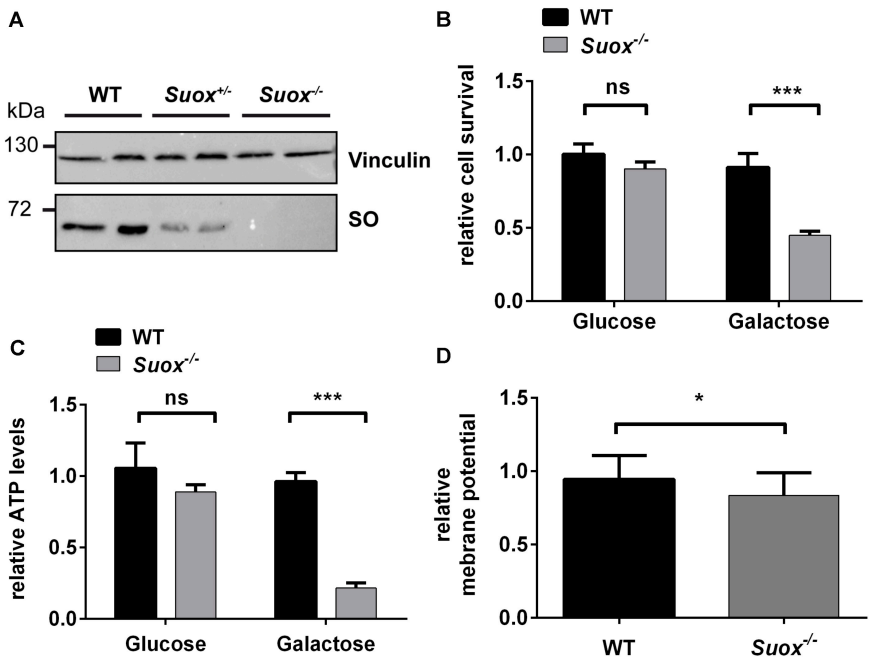

FIGURE 1 | Mitochondrial deficiency in *Suox*$^{-/-}$ MEFs. **(A)** Sulfite oxidase (SO) protein expression in WT, *Suox*$^{\pm}$ and *Suox*$^{-/-}$ MEFs. Vinculin was used as a loading control. **(B)** Determination of cell survival of WT and *Suox*$^{-/-}$ MEFs after a 24 h incubation in glucose- or galactose containing DMEM medium (n = 6). Cell viability was assessed using the MTT assay (Promega). Values were normalized to WT grown in glucose medium. **(C)** Measurement of cellular ATP levels of WT and *Suox*$^{-/-}$ MEFs after a 24 h incubation in glucose- or galactose containing DMEM (n = 3). Intracellular ATP levels were quantified using the CellTiter-Glo Luminescent Cell Viability Assay (Promega). Values were normalized to WT grown in glucose medium. **(D)** Determination of mitochondrial membrane potential in WT and *Suox*$^{-/-}$ MEFs (n = 3). Mitochondrial membrane potential was assessed by staining with 20 nM TMRM (membrane potential-dependent). The pixel intensity was quantified relative to 200 nM MitoTracker Deep Red staining (membrane potential independent). Values were normalized to WT measurement. **(B–D)**: Error bars indicate standard deviation. Student's t test was performed as indicated. p value: *** <0.001; ** <0.01; * <0.05; ns > 0.05.

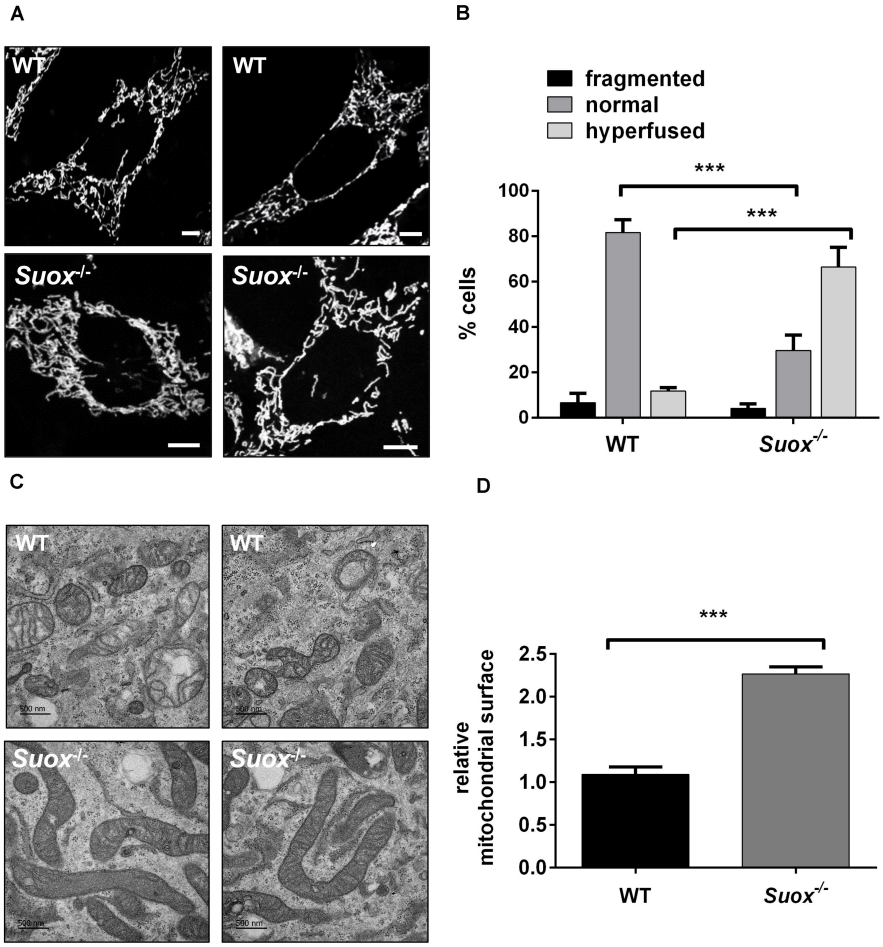

FIGURE 2 | Mitochondrial morphology in *Suox*$^{-/-}$ MEFs. **(A)** Visualization of the mitochondrial network in WT and *Suox*$^{-/-}$ MEFs. Mitochondrial networks in WT and *Suox*$^{-/-}$ MEFs were visualized by incubation in 200 nM MitoTracker Red CMXRos (Invitrogen) for 30 min at 37°C. *Suox*$^{-/-}$ MEFs show a more interconnected and elongated mitochondrial network than WT cells. Scale-bar represents 10 μm. **(B)** Quantification of mitochondrial network phenotypes in WT and *Suox*$^{-/-}$ MEFs presented in panel **(A)**. 100 cells per genotype were categorized according to their mitochondrial network as either fragmented (disturbed, dot-like network, almost no tubules present), normal (both tubules and dot-like mitochondria present) or hyperfused (highly interconnected tubules, no dot-like mitochondria present) (n = 3). Error bars indicate standard deviation. Ordinary two-way ANOVA with Tukey's *post hoc* test for pairwise comparisons was performed as indicated. p value: *** <0.001; ** <0.01; * <0.05; ns > 0.05. **(C)** Mitochondria captured from WT and *Suox*$^{-/-}$ MEFs via TEM. *Suox*$^{-/-}$ MEFs show highly elongated mitochondria compared to WT cells. Scale bar represents 500 nm. **(D)** Quantification of the mitochondrial surface area in WT and *Suox*$^{-/-}$ MEFs based on TEM pictures presented in **(C)**. The surfaces of 50 individual mitochondria were measured with ImageJ and normalized to WT values (n = 3). Error bars indicate standard deviation. Student's t test was performed as indicated. p value: *** <0.001; ** <0.01; * <0.05; ns > 0.05.

present) normal (both tubules and dot-like mitochondria present) or hyperfused (highly interconnected tubules, no dot-like mitochondria present). We found that for WT cells 81% had a normal mitochondrial network, while 6% displayed fragmented mitochondria, and 13% were hyperfused (**Figure 2B**). In contrast, only 30% of the *Suox*$^{-/-}$ cells had a normal mitochondrial network, while 4% had a fragmented network, and 66% had a hyperfused network. To complement these light microscopic studies, we performed TEM and again found the mitochondria in the KO cells to be abnormally elongated compared to WT (**Figure 2C**). Quantification of the cross-sectional area of 50 individual mitochondria confirmed that mitochondria from *Suox*$^{-/-}$ MEFs were on average more than twice as large than WT mitochondria (**Figure 2D**). Finally, TEM revealed that the elongated mitochondria also showed a much more electron dense matrix structure than WT mitochondria.

Suox$^{-/-}$ Mitochondria Are Less Motile Than WT

Mitochondria have a high degree of motility, which enables them to distribute throughout the cytoplasm and facilitates both fusion and fission processes. To measure mitochondrial mobility, we acquired time-lapse videos of mitochondrial movements in an environmental chamber at 37°C over a period of 5 min. The first and last image of each video were colored red or green and overlaid. Yellow pixels represented mitochondria that remained stationary over the 5 min period, while red and green

pixels were quantified as a proxy measure of mitochondrial motility (Yi et al., 2004; **Figure 3A**). Our quantification showed that *Suox*$^{-/-}$ mitochondria moved less than WT mitochondria (**Figure 3B**). We also measured the total amount of mitochondria per cell and found no statistically significant difference, although *Suox*$^{-/-}$ cells tend to have less mitochondrial content than WT cells (**Figure 3C**).

Sulfite Treatment Leads to Abnormal Mitochondrial Morphology

We reasoned that the alterations in mitochondrial morphology observed in *Suox*$^{-/-}$ cells could be a direct result of intracellular SO_3^{2-} accumulation. To test whether SO_3^{2-} affects mitochondrial morphology, we treated human WT fibroblasts with escalating doses of SO_3^{2-} concentrations and assessed for changes in mitochondrial morphology after 1 h of treatment (**Figure 4A**). Addition of 10 or 50 μM SO_3^{2-} led to an increase in the percentage of cells with hyperfused mitochondria (**Figure 4B**). While we found that ∼11% of untreated WT cells were hyperfused, addition of 10 or 50 μM SO_3^{2-} resulted in ∼32% and 23% hyperfused cells, respectively. We also observed that treatment with higher SO_3^{2-} concentrations lead to a higher percentage of fragmented mitochondria. Around 50% of the cells displayed fragmented mitochondria after treatment with 500 μM SO_3^{2-}, whereas untreated cells showed fragmented mitochondria in ∼4% of all analyzed cells. In turn, the number of cells categorized to harbor a normal mitochondrial network were significantly reduced in all SO_3^{2-}-treated cells, regardless of the respective concentration. While 84% of untreated cells had a normal mitochondrial network, this percentage was reduced to ∼57% for SO_3^{2-} concentrations up to 100 μM and ∼50% for 250 and 500 μM SO_3^{2-} treatments. These data show that SO_3^{2-} directly influences mitochondrial morphology in a dose-dependent manner.

MoCD Patient Derived Fibroblasts Recapitulate the Mitochondrial Phenotype of *Suox*$^{-/-}$ MEF Cells

Finally, we analyzed mitochondrial morphology in fibroblasts derived from various MoCD patients that are impaired in

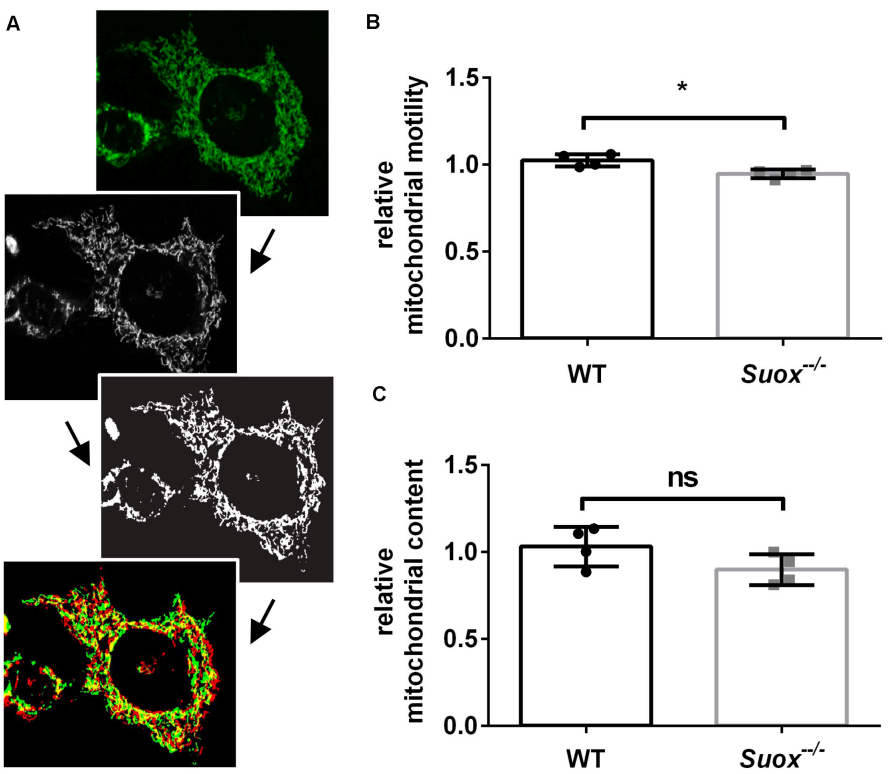

FIGURE 3 | Mitochondrial motility and content in *Suox*$^{-/-}$ MEFs. **(A)** Workflow of mitochondrial motility analysis using ImageJ. Starting from the left, maximum intensity projections of image stacks **(first picture)** were converted to 8-bit formats **(second picture)** and then subjected to a white top-hat filter (MorphoLibJ plugin), before a final thresholding step **(third picture)**. Finally, the amount of moved pixels of selected mitochondria **(last picture)** between the first (green) and last (red) timepoint (always 5 min apart) were assessed using the XOR function of the Image Calculator with yellow pixel indicate overlapping pixels. **(B)** Quantification of mitochondrial motility as shown in **(A)**. Mitochondrial motility was analyzed via life cell imaging following incubation with 200 nM MitoTracker Deep Red (diluted in DMEM) for 20 min at 37°C. Values were normalized to WT. Error bars indicate standard deviation. Student's *t* test was performed as indicated. *p* value: *** <0.001; ** <0.01; * <0.05; ns > 0.05. **(C)** Quantification of mitochondrial content. Mitochondria were visualized via incubation with 200 nM MitoTracker Deep Red (diluted in DMEM) for 20 min at 37°C. Total amount of pixels per cell was quantified using ImageJ. Values were normalized to WT. Error bars indicate standard deviation. Student's *t* test was performed as indicated. *p* value: *** <0.001; ** <0.01; * <0.05; ns > 0.05.

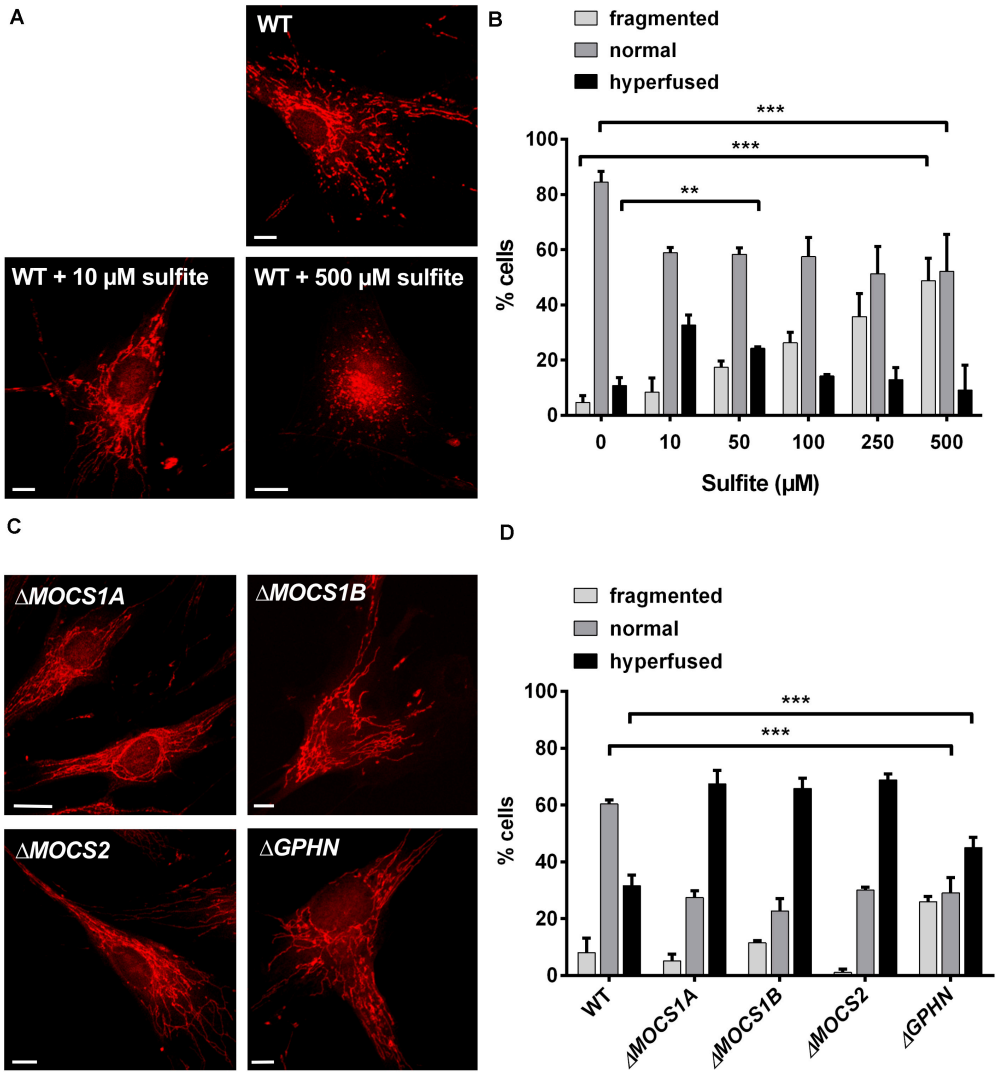

FIGURE 4 | Influence of sulfite (SO_3^{2-}) on mitochondrial morphology. **(A)** Imaging of the mitochondrial network in human WT fibroblasts with and without SO_3^{2-}. Mitochondria in fibroblasts were visualized using 200 nM MitoTracker Red CMXRos (Invitrogen) for 30 min at 37°C. For SO_3^{2-} treatments, the respective SO_3^{2-} concentration was added to the medium 30 min prior to the MitoTracker and incubated at 37°C. While untreated WT cells show a normal mitochondrial network **(upper left)**, treatment with lower SO_3^{2-} concentrations (10 µM) leads to a hypertubular network **(upper right picture)**. Higher SO_3^{2-} concentrations (<500 µM) result in mitochondrial fragmentation **(lower left picture)**. Scale-bar represents 10 µm. **(B)** Quantification of mitochondrial network phenotypes in WT fibroblasts after treatment with different SO_3^{2-} concentrations as presented in **(A)**. 100 cells per genotype were categorized according to their mitochondrial network as either fragmented (disturbed, dot-like network, almost no tubules present), normal (both tubules and dot-like mitochondria present) or hyperfused (highly interconnected tubules, no dot-like mitochondria present, length) (n = 3). Error bars indicate standard deviation. Ordinary two-way ANOVA with Tukey's *post hoc* test for pairwise comparisons was performed as indicated. p value: *** <0.001; ** <0.01; * <0.05; ns > 0.05. **(C)** Imaging of the mitochondrial network in fibroblasts from different MoCD patients. Mitochondria in different patient fibroblasts were visualized using 200 nM MitoTracker Red CMXRos (Invitrogen) for 30 min at 37°C. All cell lines presented strongly interconnected and hyperfused mitochondria. Scale-bar represents 10 µm. **(D)** Quantification of mitochondrial network phenotypes in fibroblasts from different MoCD patients presented in **(C)**. 100 cells per genotype were categorized according to their mitochondrial network as either fragmented (disturbed, dot-like network, almost no tubules present), normal (both tubules and dot-like mitochondria present) or hyperfused (highly interconnected tubules, no dot-like mitochondria present) (n = 3). Error bars indicate standard deviation. Ordinary two-way ANOVA with Tukey's *post hoc* test for pairwise comparisons was performed as indicated. p value: *** <0.001; ** <0.01; * <0.05; ns > 0.05.

different genes important for Moco biosynthesis, namely *MOCS1A*, *MOCS1B*, *MOCS2,* and *GPHN* (**Figure 4C**). We found that cell lines derived from patients with disease causing mutations in *MOCS1* or *MOCS2*∼70% contained a hyperfused mitochondrial network, whereas this was only the case for 30% of the cells for WT fibroblasts (**Figure 4D**). In cells derived from patients with disease causing mutations in the *GPHN* gene, 45% were characterized as hyperfused. In turn, ∼60% of WT cells displayed a normal mitochondrial network, while this phenotype could only be found in ∼25–30% of all patient cells

regardless of the affected gene. The percentage of cells with a fragmented mitochondrial network varied between 1% and 10% for the *MOCS1/2* and WT cell lines. Remarkably, only 1% of the cells deficient in *MOCS2* were fragmented, whereas 25% of the cells affected in *GPHN* showed fragmented mitochondria. In summary, these data confirm a disturbed mitochondrial network in different patient cell lines of MoCD that can collectively be traced back to SO_3^{2-} accumulation.

DISCUSSION

Sulfite oxidase is a mitochondrial enzyme that is vital for the detoxification of SO_3^{2-}. Inactivation of SO, in either ISOD or MoCD, leads to severe neurodegeneration, often with lethal outcome. While mitochondrial impairment has been observed following SO_3^{2-} treatment of different model systems (Vincent et al., 2004; Zhang et al., 2004; Grings et al., 2013), the underlying mechanism and role of mitochondrial damage within the context of SO deficiency remains poorly understood. In this study, we show that mitochondria in *Suox*$^{-/-}$ and patient fibroblasts are abnormally elongated and interconnected. Application of exogenous SO_3^{2-} on WT fibroblasts induced similar morphological changes in the mitochondrial network, suggesting that SO_3^{2-} accumulation in SO-deficient cells directly mediates alterations in mitochondrial function. This pathomechanism provides a new concept underlying SO_3^{2-} toxicity in the SO deficiencies.

We found that cellular viability and ATP production under galactose treatment was markedly reduced in *Suox*$^{-/-}$ MEFs, indicating that the mitochondria in those cells are dysfunctional and thus unable to produce sufficient ATP via OXPHOS. In line with this, one of the earliest identified toxic effects of SO_3^{2-} was a dose-dependent reduction of total cellular ATP levels (Zhang et al., 2004). Moreover, direct treatment of SO_3^{2-} also decreased ATP production from mitochondria isolated from rat renal epithelial cells (Vincent et al., 2004). Therefore, it is likely that elevated SO_3^{2-} levels, due to the lack of SO, lead to the inhibition of mitochondrial ATP production and reduced viability upon longer cultivation in galactose.

In a recent study, Grings et al. (2019) reported that *MOCS1* patient fibroblasts display altered protein levels of mitofusins 1 and 2, indicating a disturbance of mitochondrial dynamics. We analyzed the mitochondrial network in different cell culture models of SO deficiency and found that the mitochondria were hyperfused in the vast majority of SO-deficient cells. Furthermore, treatment of WT cells with low SO_3^{2-} concentrations (up to 40 μM) resulted in similar morphological changes, suggesting that the observed abnormalities are directly mediated by SO_3^{2-}. Hyperfusion is known as a typical response to mild mitochondrial stress, for example nutrient starvation, as it allows to separate mitochondria within one cell to exchange their contents and thereby help to "recover" individual damaged mitochondria (Rugarli et al., 2012). However, treatment of WT cells with high SO_3^{2-} concentrations (more than 50 μM) lead to increased mitochondrial fragmentation, indicating that at this point, the mitochondrial damage becomes too severe to be repaired. Mitochondrial fragmentation can be induced by various different forms of stress and allows the removal of terminally damaged mitochondria by mitophagy (Rugarli et al., 2012). In particular, inhibition of the mitochondrial enzymes malate dehydrogenase and glutamate dehydrogenase has been shown for SO_3^{2-} concentrations of 100 μM and higher (Zhang et al., 2004). Inhibition of the central metabolic enzyme glutamate dehydrogenase could lead to a decreased metabolic flux through the TCA cycle, which might further contribute to the reduced ATP production, thereby inducing fragmentation.

Hyperfusion of mitochondria may be induced by an increase in fusion or a decrease in fission processes. We detected a decrease in mitochondrial motility in *Suox*$^{-/-}$ cells, which might suggest a decrease in fission. Correct function of Drp1, a GTPase that mediates mitochondrial fission, is regulated by a number of different mechanisms, such as recruitment to the outer mitochondrial membrane by recruiting factors as well as post-translational modifications such as phosphorylation or nitrosylation (Suárez-Rivero et al., 2016). Following our initial findings, further studies are needed to elucidate the exact mechanism of how SO_3^{2-} alters mitochondrial dynamics.

The most affected organ in the SO deficiencies is the nervous system. Interestingly, this is also the case in many other disorders of disrupted mitochondrial dynamics. Both Drp1 and mitofusin-2 are required for neuronal development and dysregulation of either protein is associated with a neurological disorder (Suárez-Rivero et al., 2016). For example, mitofusin-2 is necessary for cerebellar development in mice (Chen et al., 2007), and dominant negative variants of mitofusin-2 are associated with Charcot–Marie–Tooth disease type 2A, a length dependent peripheral neuropathy in man (Kijima et al., 2005). Drp1 on the other hand has been associated with multiple disorders, including Huntington's disease, amyotrophic lateral sclerosis, and Parkinson's disease (Song et al., 2011, 2013; Wang et al., 2011).

Among the group of mitochondrial disorders, there is another disease of sulfur metabolism, called ethylmalonic encephalopathy or ETHE1 deficiency (Tiranti et al., 2004). Similar to SO deficiencies, patients present with early onset progressive neurological degeneration, psychomotor retardation and excretion of ethylmalonic acid in urine, resulting in death in the first few years of life (Tiranti et al., 2004). ETHE1 patients accumulate high levels of H_2S and thiosulfate in biological fluids and tissues, the latter also being elevated in ISOD and MoCD. Intriguingly, H_2S has been reported to interfere with cellular respiration via inhibition of cytochrome c oxidase (Tiranti et al., 2009). First attempts have recently been made to improve mitochondrial respiratory function in fibroblasts from ETHE1 and MOCS1 patients by treating cells with the mitochondria-targeted antioxidant JP4-039 (Grings et al., 2019). While these results are promising, future studies should aim for further dissection of the underlying molecular mechanisms that primarily drive mitochondrial pathology in neuronal tissues of SO deficiency models in order to provide new therapy options. In summary, we show here that mitochondrial dynamics are impaired by SO_3^{2-} and dysregulated in SO deficiencies, thereby providing further evidence that SO deficiencies join the large and diverse family of mitochondrial disorders.

DATA AVAILABILITY STATEMENT

The raw data supporting the conclusions of this article will be made available by the authors, without undue reservation.

ETHICS STATEMENT

All animals were kept and bred in accordance with European, national and institutional guidelines and protocols were approved by local government authorities (Landesamt für Natur, Umwelt und Verbraucherschutz Nordrhein-Westfalen, Germany; reference 84-02.04.2014.A372).

AUTHOR CONTRIBUTIONS

A-TM, JR, and GS: study design. JK: providing of study materials. A-TM, JR, AM, and GS: data generation, analysis, and interpretation. A-TM, AM, and GS: manuscript writing. All authors contributed to the article and approved the submitted version.

FUNDING

This work was supported by the German Research Foundation (Deutsche Forschungsgemeinschaft, DFG) SFB1218 project number 269925409 and SFB1403 project number 414786233.

ACKNOWLEDGMENTS

We acknowledge Simona Jansen, Monika Laurien, and Joana Stegemann (University of Cologne) for technical assistance. We thank Dr. Jochen Reiss (University of Göttingen) for providing the patient fibroblasts. We also thank the CECAD Imaging Facility, University of Cologne (Head: Dr. Astrid Schauss) for their support.

REFERENCES

Chen, H., McCaffery, J. M., and Chan, D. C. (2007). Mitochondrial fusion protects against neurodegeneration in the cerebellum. *Cell* 130, 548–562. doi: 10.1016/J.CELL.2007.06.026

de Moura Alvorcem, L., da Rosa, M. S., Glänzel, N. M., Parmeggiani, B., Grings, M., Schmitz, F., et al. (2017). Disruption of energy transfer and redox status by sulfite in hippocampus, striatum, and cerebellum of developing rats. *Neurotox. Res.* 32, 264–275. doi: 10.1007/s12640-017-9732-y

Grings, M., Moura, A. P., Amaral, A. U., Parmeggiani, B., Gasparotto, J., Moreira, J. C. F., et al. (2014). Sulfite disrupts brain mitochondrial energy homeostasis and induces mitochondrial permeability transition pore opening via thiol group modification. *Biochim. Biophys. Acta* 1842, 1413–1422. doi: 10.1016/j.bbadis.2014.04.022

Grings, M., Moura, A. P., Parmeggiani, B., Marcowich, G. F., Amaral, A. U., de Souza Wyse, A. T., et al. (2013). Disturbance of brain energy and redox homeostasis provoked by sulfite and thiosulfate: potential pathomechanisms involved in the neuropathology of sulfite oxidase deficiency. *Gene* 531, 191–198. doi: 10.1016/j.gene.2013.09.018

Grings, M., Seminotti, B., Karunanidhi, A., Ghaloul-Gonzalez, L., Mohsen, A.-W., Wipf, P., et al. (2019). ETHE1 and MOCS1 deficiencies: disruption of mitochondrial bioenergetics, dynamics, redox homeostasis and endoplasmic reticulum-mitochondria crosstalk in patient fibroblasts. *Sci. Rep.* 9:12651. doi: 10.1038/s41598-019-49014-2

Hahnewald, R., Leimkühler, S., Vilaseca, A., Acquaviva-Bourdain, C., Lenz, U., and Reiss, J. (2006). A novel MOCS2 mutation reveals coordinated expression of the small and large subunit of molybdopterin synthase. *Mol. Genet. Metab.* 89, 210–213. doi: 10.1016/j.ymgme.2006.04.008

Johnson, J. L., and Rajagopalan, K. V. (1979). The oxidation of sulphite in animals systems. *Ciba Found. Symp.* 1979, 119–133. doi: 10.1002/9780470720554.CH8

Kijima, K., Numakura, C., Izumino, H., Umetsu, K., Nezu, A., Shiiki, T., et al. (2005). Mitochondrial GTPase mitofusin 2 mutation in charcot-marie-tooth neuropathy type 2A. *Hum. Genet.* 116, 23–27. doi: 10.1007/s00439-004-1199-2

Kohl, J. B., Mellis, A.-T., and Schwarz, G. (2018). Homeostatic impact of sulfite and hydrogen sulfide on cysteine catabolism. *Br. J. Pharmacol.* 176, 554–570. doi: 10.1111/bph.14464

Koopman, W. J. H., Visch, H.-J., Smeitink, J. A. M., and Willems, P. H. G. M. (2006). Simultaneous quantitative measurement and automated analysis of mitochondrial morphology, mass, potential, and motility in living human skin fibroblasts. *Cytom. Part A* 69A, 1–12. doi: 10.1002/cyto.a.20198

Kumar, A., Dejanovic, B., Hetsch, F., Semtner, M., Fusca, D., Arjune, S., et al. (2017). S-sulfocysteine/NMDA receptor–dependent signaling underlies neurodegeneration in molybdenum cofactor deficiency. *J. Clin. Invest.* 127, 4365–4378. doi: 10.1172/JCI89885

Mudd, S. H., Irreverre, F., and Laster, L. (1967). Sulfite oxidase deficiency in man: demonstration of the enzymatic defect. *Science* 156, 1599–1602. doi: 10.1126/science.156.3782.1599

Reiss, J., Gross-Hardt, S., Christensen, E., Schmidt, P., Mendel, R. R., and Schwarz, G. (2001). A mutation in the gene for the neurotransmitter receptor–clustering protein gephyrin causes a novel form of molybdenum cofactor deficiency. *Am. J. Hum. Genet.* 68, 208–213. doi: 10.1086/316941

Reiss, J., and Hahnewald, R. (2011). Molybdenum cofactor deficiency: mutations in GPHN, MOCS1, and MOCS2. *Hum. Mutat.* 32, 10–18. doi: 10.1002/humu.21390

Rugarli, E. I., Langer, T., Akepati, V., Muller, E., Otto, A., Strauss, H., et al. (2012). Mitochondrial quality control: a matter of life and death for neurons. *EMBO J.* 31, 1336–1349. doi: 10.1038/emboj.2012.38

Schwahn, B. C., Van Spronsen, F. J., Belaidi, A. A., Bowhay, S., Christodoulou, J., Derks, T. G., et al. (2015). Efficacy and safety of cyclic pyranopterin monophosphate substitution in severe molybdenum cofactor deficiency type A: a prospective cohort study. *Lancet* 386, 1955–1963. doi: 10.1016/S0140-6736(15)00124-5

Schwarz, G. (2016). Molybdenum cofactor and human disease. *Curr. Opin. Chem. Biol.* 31, 179–187. doi: 10.1016/j.cbpa.2016.03.016

Schwarz, G., Mendel, R. R., and Ribbe, M. W. (2009). Molybdenum cofactors, enzymes and pathways. *Nature* 460, 839–847. doi: 10.1038/nature08302

Song, W., Chen, J., Petrilli, A., Liot, G., Klinglmayr, E., Zhou, Y., et al. (2011). Mutant huntingtin binds the mitochondrial fission GTPase dynamin-related protein-1 and increases its enzymatic activity. *Nat. Med.* 17, 377–382. doi: 10.1038/nm.2313

Song, W., Song, Y., Kincaid, B., Bossy, B., and Bossy-Wetzel, E. (2013). Mutant SOD1G93A triggers mitochondrial fragmentation in spinal cord motor neurons: neuroprotection by SIRT3 and PGC-1α. *Neurobiol. Dis.* 51, 72–81. doi: 10.1016/J.NBD.2012.07.004

Stipanuk, M. H., and Ueki, I. (2011). Dealing with methionine/homocysteine sulfur: cysteine metabolism to taurine and inorganic sulfur. *J. Inherit. Metab. Dis.* 34, 17–32. doi: 10.1007/s10545-009-9006-9

Suárez-Rivero, J., Villanueva-Paz, M., de la Cruz-Ojeda, P., de la Mata, M., Cotán, D., Oropesa-Ávila, M., et al. (2016). Mitochondrial dynamics in mitochondrial diseases. *Diseases* 5:1. doi: 10.3390/diseases5010001

Tiranti, V., D'Adamo, P., Briem, E., Ferrari, G., Mineri, R., Lamantea, E., et al. (2004). Ethylmalonic encephalopathy is caused by mutations in ETHE1, a gene encoding a mitochondrial matrix protein. *Am. J. Hum. Genet.* 74, 239–252. doi: 10.1086/381653

Tiranti, V., Viscomi, C., Hildebrandt, T., Di Meo, I., Mineri, R., Tiveron, C., et al. (2009). Loss of ETHE1, a mitochondrial dioxygenase, causes fatal sulfide toxicity in ethylmalonic encephalopathy. *Nat. Med.* 15, 200–205. doi: 10.1038/nm.1907

Verburg, J., and Hollenbeck, P. (2008). Mitochondrial membrane potential in axons increases with local nerve growth factor or semaphorin signaling. *J. Neurosci.* 28, 8306–8315. doi: 10.1523/JNEUROSCI.2614-08.2008

Vincent, A. S., Lim, B. G., Tan, J., Whiteman, M., Cheung, N. S., Halliwell, B., et al. (2004). Sulfite-mediated oxidative stress in kidney cells. *Kidney Int.* 65, 393–402. doi: 10.1111/J.1523-1755.2004.00391.X

Wai, T., and Langer, T. (2016). Mitochondrial dynamics and metabolic regulation. *Trends Endocrinol. Metab.* 27, 105–117. doi: 10.1016/J.TEM.2015.12.001

Wang, H., Song, P., Du, L., Tian, W., Yue, W., Liu, M., et al. (2011). Parkin ubiquitinates Drp1 for proteasome-dependent degradation: implication of dysregulated mitochondrial dynamics in Parkinson disease. *J. Biol. Chem.* 286, 11649–11658. doi: 10.1074/jbc.M110.144238

Xu, J. (2005). Preparation, culture, and immortalization of mouse embryonic fibroblasts. *Curr. Protoc. Mol. Biol.* Chapter 28:Unit28.1. doi: 10.1002/0471142727.mb2801s70

Yi, M., Weaver, D., and Hajnóczky, G. (2004). Control of mitochondrial motility and distribution by the calcium signal. *J. Cell Biol.* 167, 661–672. doi: 10.1083/jcb.200406038

Zhang, X., Vincent, A. S., Halliwell, B., and Wong, K. P. (2004). A mechanism of sulfite neurotoxicity: direct inhibition of glutamate dehydrogenase. *J. Biol. Chem.* 279, 43035–43045. doi: 10.1074/jbc.M402759200

Conflict of Interest: The authors declare that the research was conducted in the absence of any commercial or financial relationships that could be construed as a potential conflict of interest.

frontiers in Genetics

REVIEW
published: 12 January 2021
doi: 10.3389/fgene.2020.610764

Advances in mt-tRNA Mutation-Caused Mitochondrial Disease Modeling: Patients' Brain in a Dish

*Suleva Povea-Cabello[1], Marina Villanueva-Paz[2], Juan M. Suárez-Rivero[1], Mónica Álvarez-Córdoba[1], Irene Villalón-García[1], Marta Talaverón-Rey[1], Alejandra Suárez-Carrillo[1], Manuel Munuera-Cabeza[1] and José A. Sánchez-Alcázar[1]**

[1] Centro Andaluz de Biología del Desarrollo, Universidad Pablo de Olavide and Centro de Investigación Biomédica en Red: Enfermedades Raras, Instituto de Salud Carlos III, Seville, Spain, [2] Instituto de Investigación Biomédica de Málaga, Departamento de Farmacología y Pediatría, Facultad de Medicina, Universidad de Málaga, Málaga, Spain

OPEN ACCESS

Edited by:
Guilhian Leipnitz, Federal University of Rio Grande do Sul, Brazil

Reviewed by:
Josef Finsterer, K.A. Rasmussen, Norway
Ayman W. El Hattab, Tawam Hospital, United Arab Emirates
Alessandra Maresca, IRCCS Institute of Neurological Sciences of Bologna (ISNB), Italy

***Correspondence:**
José A. Sánchez-Alcázar
jasanalc@upo.es

Specialty section:
This article was submitted to Genetics of Common and Rare Diseases, a section of the journal Frontiers in Genetics

Received: 27 September 2020
Accepted: 26 November 2020
Published: 12 January 2021

Citation:
Povea-Cabello S, Villanueva-Paz M, Suárez-Rivero JM, Álvarez-Córdoba M, Villalón-García I, Talaverón-Rey M, Suárez-Carrillo A, Munuera-Cabeza M and Sánchez-Alcázar JA (2021) Advances in mt-tRNA Mutation-Caused Mitochondrial Disease Modeling: Patients' Brain in a Dish. Front. Genet. 11:610764. doi: 10.3389/fgene.2020.610764

Mitochondrial diseases are a heterogeneous group of rare genetic disorders that can be caused by mutations in nuclear (nDNA) or mitochondrial DNA (mtDNA). Mutations in mtDNA are associated with several maternally inherited genetic diseases, with mitochondrial dysfunction as a main pathological feature. These diseases, although frequently multisystemic, mainly affect organs that require large amounts of energy such as the brain and the skeletal muscle. In contrast to the difficulty of obtaining neuronal and muscle cell models, the development of induced pluripotent stem cells (iPSCs) has shed light on the study of mitochondrial diseases. However, it is still a challenge to obtain an appropriate cellular model in order to find new therapeutic options for people suffering from these diseases. In this review, we deepen the knowledge in the current models for the most studied mt-tRNA mutation-caused mitochondrial diseases, MELAS (mitochondrial encephalomyopathy, lactic acidosis, and stroke-like episodes) and MERRF (myoclonic epilepsy with ragged red fibers) syndromes, and their therapeutic management. In particular, we will discuss the development of a novel model for mitochondrial disease research that consists of induced neurons (iNs) generated by direct reprogramming of fibroblasts derived from patients suffering from MERRF syndrome. We hypothesize that iNs will be helpful for mitochondrial disease modeling, since they could mimic patient's neuron pathophysiology and give us the opportunity to correct the alterations in one of the most affected cellular types in these disorders.

Keywords: mitochondrial diseases, mtDNA, disease modeling, direct reprogramming, induced neurons

Abbreviations: $\Delta\Psi m$, mitochondrial membrane potential; 3D, 3-dimensional; CM, cristae membrane; CoQ_{10}, coenzyme Q_{10}; DPI, days post-infection; EMA, European Medicines Agency; IBM, inner boundary membrane; IMM, inner mitochondrial membrane; iNs, induced neurons; iPSCs, induced pluripotent stem cells; LCLs, lymphoblastoid cell lines; LHON, Leber's hereditary optic neuropathy; MELAS, mitochondrial encephalomyopathy, lactic acidosis, and stroke-like episodes; MERRF, myoclonic epilepsy with ragged red fibers; miRNAs, micro RNAs; MNGIE, mitochondrial neurogastrointestinal encephalomyopathy; MRC, mitochondrial respiratory chain; mtDNA, mitochondrial DNA; NDM, neural differentiation medium; nDNA, nuclear DNA; NPCs, neural progenitor cells; OMM, outer mitochondrial membrane; OXPHOS, oxidative phosphorylation; PGD, preimplantation genetic diagnosis; REST, RE-1 silencing transcription factor; ROS, reactive oxygen species; SCs, supercomplexes; TALENs, transcription activator-like effector nucleases; tRNA, transfer RNA; UPR, unfolding protein response; ZFNs, zinc-finger nucleases.

INTRODUCTION: MITOCHONDRIA, THE POWERHOUSES OF THE CELL

Mitochondria are small, mobile, and plastic organelles located in the cytoplasm of most eukaryotic cells. These organelles are responsible for important cellular processes, such as regulation of apoptosis, calcium homeostasis, and reactive oxygen species (ROS) production. However, the main function of mitochondria is energy production through oxidative phosphorylation (OXPHOS), which takes place in the mitochondrial respiratory chain (MRC) (Russell and Turnbull, 2014). Mitochondria contain their own DNA, the mitochondrial DNA (mtDNA), which is circular and double stranded. The mitochondrial genome consists of 16,569 nucleotide pairs that encode 13 proteins, two ribosomal RNA components, and 22 transfer RNAs (tRNAs) (Alberts et al., 2002). Regarding mitochondrial structure, these organelles are composed by two membranes, the inner and the outer mitochondrial membranes (IMMs and OMMs, respectively) that delimit two main compartments: the internal matrix and the intermembrane space. The IMM contains many folds named cristae that protrude into the matrix and enlarge the IMM surface. This membrane can be subdivided into two compartments, the inner boundary membrane (IBM) and the cristae membrane (CM), that are connected *via* cristae junctions. Albeit IMM is considered a continuous membrane, lateral diffusion of membrane proteins is restricted and IBM and CM exhibit an asymmetric protein distribution. This heterogeneity is important for efficient OXPHOS, mitochondrial biogenesis, and remodeling (Wollweber et al., 2017; Busch, 2020). Although mainly separated, the inner and outer mitochondrial membranes are partially connected *via* contact sites that are involved in cristae organization (Bulthuis et al., 2019). Since the OMM is more permeable than the IMM, containing many copies of the transport protein porin, the intermembrane space composition is equivalent to the cytosolic one. However, due to the presence of cardiolipin, the IMM is specially impermeable to ions and it is selectively permeable to small molecules required by matrix enzymes, thanks to the presence of several transport proteins (Alberts et al., 2002).

For producing energy, mitochondria rely on the MRC components that are five multiprotein complexes whose polypeptides are encoded by mtDNA and nuclear DNA (nDNA), the latter contributing the most. For that reason, mitochondrial function relies on both genomes (Alberts et al., 2002). Four of these components (Complexes I–IV) are involved in electron transfer and proton pumping across the IMM, which generate an electrochemical proton gradient responsible for the mitochondrial membrane potential ($\Delta\Psi m$), a marker of mitochondrial health. The flux of protons into the matrix through the ATP synthase (Complex V) drives ATP synthesis (Alberts et al., 2002). There is a current consensus about a higher level of organization of these components that are arranged in supercomplexes (SCs) (Brzezinski, 2020) that exist in a wide variety of stoichiometries (Cogliati et al., 2016). SC assembly and stability are determined by mitochondrial cristae shape since knockdown of OPA1, a protein that plays a key role in mitochondrial fusion, impairs SC formation (Cogliati et al., 2013; Jang and Javadov, 2020). In addition, cellular pathways such as the unfolding protein response (UPR) are involved in cristae density and SC assembly, improving mitochondrial respiratory function under nutrient stress conditions (Balsa et al., 2019). Thus, this higher level of organization is dynamic and adapts to the energetic status of the cell. Structural and modeling studies indicate that SC assembly facilitates electron transfer, prevents protein aggregation, and preserves the structural organization of MRC components (Jang and Javadov, 2020). However, despite extensive studies, SC functional relevance remains unknown (Brzezinski, 2020).

Defects in mitochondrial function have been linked not only to genetic mitochondrial diseases but also to cardiovascular diseases (Murphy et al., 2016) and neurodegenerative disorders such as Huntington's and Parkinson's diseases (Zeviani and Carelli, 2003; Martin-Jimenez et al., 2020).

MITOCHONDRIAL DISEASES

Mitochondrial diseases are a heterogeneous group of rare genetic disorders caused by a partial or total dysfunction of mitochondria. These illnesses can be caused by mutations in nDNA or mtDNA. These mutations affect not only genes encoding for MRC components but also those that are involved in protein translation and assembly, mtDNA stability, as well as mutations in those nDNA-encoded proteins involved in the maintenance of mitochondrial nucleotide pools, nucleotide transport, mtDNA replication, RNA transcription, and mitochondrial dynamics (Schon et al., 2012; Chapman et al., 2020). Mitochondrial diseases are clinically heterogeneous; they may occur at any age, and patients manifest a wide variety of symptoms (Gorman et al., 2016). However, all of them share morphological and biochemical features. As a consequence of the MRC deficiency, cells manifest a reduced enzymatic function of MRC components, a reduction in oxygen consumption and ATP synthesis, and a ROS overproduction. In the case of patients, they suffer from lactic acidosis and elevated pyruvate levels in serum at rest and, specially, after moderate exercise. Additionally, patients' muscle biopsies usually show ragged red fibers that reflect the proliferation of OXPHOS-defective mitochondria (Schon et al., 2012).

Mitochondrial Diseases Caused by Mutations in Mitochondrial Transfer RNAs

Mutations in mtDNA are associated with a wide variety of maternally inherited genetic disorders that provoke mitochondrial dysfunction (Kirino and Suzuki, 2005). Since 1988, when the first mtDNA mutations were identified (Holt et al., 1988; Wallace et al., 1988; Zeviani et al., 1988), more than 400 pathogenic mutations related to specific and non-specific diseases have been characterized (Lott et al., 2013). Among them, some frequent mitochondrial disorders caused by a point mutation in mtDNA are MELAS and MERRF

syndromes. In most of the cases, MELAS syndrome is caused by a transition from adenine to guanine in the position 3243 in the mt-tRNA$^{Leu(UUR)}$ (MT-TL1) gene (Schon et al., 2012). In the case of MERRF syndrome, the m.8344A > G mutation in the mt-tRNA^{Lys} (MT-TK) gene is the most frequently associated with the disease (Shoffner et al., 1990; Yoneda et al., 1990; Kirino and Suzuki, 2005).

Pathogenic mutations in mt-tRNA affect mtDNA translation, causing a defect in protein synthesis and decreasing MRC complex function (Brisca et al., 2015). In the case of MELAS syndrome, the m.3243A > G mutation affects mt-tRNA structure stabilization, methylation, aminoacylation, and triplet recognition (Finsterer, 2007). This mutation causes a specific defect of UUG-rich gene translation such as ND6 gene that encodes a subunit of the NADH-coenzyme Q reductase complex, also known as Complex I. This translation defect results in specific Complex I deficiency due to a reduction in the synthesis of ND6 subunit that is characteristic of the MELAS syndrome (Kirino and Suzuki, 2005). On the other hand, m.8344A > G mutation, which accounts for the MERRF syndrome, affects both AAA and AAG codon translation, causing a defect of whole mitochondrial protein synthesis. This fact could explain some of the different symptoms that are associated with these two different diseases (Kirino and Suzuki, 2005).

Due to the multicopy nature of mtDNA, these mutations can be homoplasmic or heteroplasmic. Thus, MELAS and MERRF syndromes are heteroplasmic, which means that mutant and wild-type mtDNA copies coexist within the same cell. This feature is associated with the severity of the symptoms and hinders disease prognosis. In fact, it is thought that there is a threshold from which biochemical alterations are apparent (Zeviani and Carelli, 2007). This genetic heterogeneity gives rise to a wide variety of symptoms of diverse severity among patients. Both MELAS and MERRF syndromes are associated with neurological symptoms. MELAS syndrome affects several organs, and some of its manifestations include stroke-like episodes, dementia, epilepsy, lactic acidemia, myopathy, recurrent headaches, hearing impairment, diabetes, and short stature (El-Hattab et al., 2015). Stroke-like episodes are one of the main features of this syndrome, and patients' brain MRIs usually show multiple stroke-like lesions in both occipital and temporoparietal areas (Angelini, 2014; El-Hattab et al., 2015). In the case of MERRF syndrome, the first symptom is usually myoclonus that is followed by generalized epilepsy, ataxia, weakness, and dementia. Other findings are hearing loss, short stature, optic atrophy, and cardiomyopathy (DiMauro, 2015).

Therapeutic Management of Mitochondrial Diseases

The development of useful therapies for mitochondrial diseases is challenging due to the difficulty of correcting the lack or dysfunction of essential mitochondrial proteins, the phenotypical heterogeneity of the diseases, and multisystem alteration. Furthermore, the brain, one of the most affected organs, is difficult to reach by potential therapies because it is protected by the blood–brain barrier. For those reasons, there are no effective treatments available for mitochondrial diseases and management of these diseases is mainly symptomatic. Still, several strategies that are summarized in this review (Viscomi and Zeviani, 2020) have been developed.

Pharmacological treatment options are generally focused on targeting cellular pathways, such as mitochondrial biogenesis or autophagy, or preventing oxidative damage. For these reasons, AMP-activated protein kinase (AMPK) and mammalian target of rapamycin complex 1 (mTORC1) signaling have been the main targets of these strategies. Some of the most known drugs for treating mitochondrial diseases are rapamycin and its analogs (rapalogs) that inhibit mTORC1. Rapamycin and/or rapalogs have been demonstrated to improve the symptoms of some patients (Sage-Schwaede et al., 2019), but individual cases should be evaluated and long-term side effects remain unknown (Viscomi and Zeviani, 2020). Another common compound that is usually used for mitochondrial disease treatment is coenzyme Q_{10} (CoQ_{10}), an essential component in the mitochondrial electron transport and antioxidant in cell membranes (Santa, 2010). However, improvement of symptoms under CoQ_{10} treatment has been variable, and no sustained clinical benefits have been reported (Santa, 2010; Gorman et al., 2016). The activation of mitochondrial biogenesis through AMPK is another common therapeutic option for these diseases. 5-Aminoimidazole-4-carboxamide-1-β-D-ribofuranoside (AICAR), an AMP analog that activates AMPK, has been demonstrated to ameliorate the clinical phenotype in mouse models of mitochondrial diseases (Viscomi and Zeviani, 2020), but it is still not clarified if all tissues will benefit from this treatment in the long term (Suomalainen and Battersby, 2018).

Particularly in mtDNA mutations, several supplements as antioxidants and cofactors are being used. In MELAS syndrome, these treatments are L-arginine, citrulline, CoQ_{10}, creatine monohydrate, and L-carnitine (El-Hattab et al., 2015). In addition, oral taurine supplementation has been demonstrated to reduce the recurrence of stroke-like episodes and increase taurine modification in mt-tRNA$^{Leu(UUR)}$ (Ohsawa et al., 2019). Moreover, idebenone, a CoQ_{10} analog, has shown promising results alone (Ikejiri et al., 1996) or in combination with riboflavin (Napolitano et al., 2000) when used in concrete patients. In Leber's hereditary optic neuropathy (LHON), a mitochondrial disease commonly caused by a primary homoplasmic mutation in mtDNA (Meyerson et al., 2015), orphan designation (EU/3/07/434) was granted by the European Medicines Agency (EMA) for idebenone on 2007, and recently, commercialization of idebenone (Raxone) has been authorized by EMA for the treatment of visual impairment in adolescent and adult patients with this disease (EMA/480039/2015). In the case of MERRF syndrome, CoQ_{10}, idebenone, or L-carnitine is frequently prescribed. Conventional anticonvulsant drugs, such as levetiracetam, are also used to treat seizures (DiMauro and Hirano, 1993; Finsterer, 2019). However, none of these treatments has demonstrated enough effectiveness and only partially ameliorate some symptoms.

Given the diversity of mutations and the different therapeutic options, a personalized therapeutic approach is required in mitochondrial diseases. For this reason, the development of

cellular models derived from patients (discussed below) can be useful for both the evaluation of new drugs and the repositioning of existing ones.

Gene therapy is a promising alternative for treating mitochondrial diseases. Since pathogenic mtDNA mutations are usually heteroplasmic, reducing mutational load can be used as a therapeutic approach. There are several tools that could target mtDNA, but only two of them have been demonstrated to be successful: zinc-finger nucleases (ZFNs) and transcription activator-like effector nucleases (TALENs). Both tools are delivered into mitochondria using a mitochondria localization signal, and they selectively target mtDNA sequences to create double-strand breaks (Reddy et al., 2020).

Zinc-finger nucleases have been demonstrated to reduce mutant mtDNA and consequently restore mitochondrial respiratory function in cytoplasmic hybrid (cybrid) cell models (Minczuk et al., 2008; Gammage et al., 2014). In addition, this tool has been able to specifically eliminate mutant mtDNA in the cardiac tissue of a mitochondrial disease mouse model (Gammage et al., 2018). ZFNs are small and, due to their similarity to mammalian transcription factors, they are thought to have low immunogenic properties. However, they are complex, expensive, and exhibit lower specificity and efficiency than TALENs (Reddy et al., 2020). TALENs have been widely used for genetic manipulation in different organisms. This tool has been demonstrated to reduce mutant mtDNA load and improve the pathophysiology in a cellular model of MERRF syndrome (Hashimoto et al., 2015) as well as to eliminate the m.3243A > G mutation in MELAS iPSCs and porcine oocytes (Yang et al., 2018). In addition, TALENs have been able to reduce mutant mtDNA load in a mouse model harboring a mutation in a mt-tRNA, reverting disease-related phenotypes (Bacman et al., 2018). These gene therapy tools could be used together with other therapies aiming the elimination or prevention of pathogenic mtDNA transfer from mother to child (Nissanka and Moraes, 2020).

Regarding prevention of these diseases, the only option available is transferring embryos below the threshold of clinical expression in order to avoid or at least reduce the risk of transmission of mtDNA mutations. The selection of these embryos is based on preimplantation genetic diagnosis (PGD) (Gorman et al., 2016). In addition, there is a new strategy, the mitochondrial donation, that consists of the substitution of mutant maternal mitochondria using enucleated donor oocytes (Gorman et al., 2016). However, this technique has raised ethical issues and remains controversial (Saxena et al., 2018).

COMMON MODELS FOR MITOCHONDRIAL DISEASE STUDY

Clinical research in mitochondrial diseases has been traditionally carried out in many patients worldwide. There are many articles regarding these disorders that are in fact case reports. These studies have provided valuable information about these diseases such as the clinical hallmarks, the mutations that cause the disease, the onset, and the effects of the available treatments and supplements. In addition, they help to infer the pathophysiological mechanisms underlying these diseases.

However, experimental research has been hindered by the lack of proper biological models. These models are necessary for understanding the pathophysiology of the diseases as well as for finding new therapeutic targets. Despite the difficulties to mimic the repercussions of mtDNA mutations, there are several models to study mitochondrial diseases, such as microorganism, animal, and cellular models (**Figure 1**).

Microorganism Models

Saccharomyces cerevisiae is the most used microorganism model to study mitochondrial diseases. Mitochondrial functions are highly conserved between humans and *S. cerevisiae*, and this microorganism maintains pathogenic mutations that lead to mitochondrial dysfunction in humans. Therefore, yeasts are a good model to study mitochondrial diseases, providing insight into both physiological and pathophysiological processes (Baile and Claypool, 2013). The *S. cerevisiae* strain harboring the A14G mutation is equivalent to the human m.3243A > G mutation that causes MELAS syndrome. This model has been demonstrated to be suitable for compound screening (Garrido-Maraver et al., 2012). In the case of MERRF syndrome, there are no yeast strains with an equivalent mutation. However, the SLM3 gene in yeast is homologous to human TRMU, an enzyme involved in mt-tRNA wobble position thiolation. Mutations in SLM3 gene cause phenotypic features similar to those of m.8344A > G mutation, and consequently, yeasts harboring a defect in that gene have been used to study MERRF syndrome (Umeda et al., 2005). However, they do not maintain these mutations in a heteroplasmic state, so this aspect cannot be assessed using this model (Rinaldi et al., 2010).

Animal Models

To deepen the knowledge in the consequences of mtDNA mutations as well as develop new therapeutic strategies for mitochondrial diseases, animal models are necessary. However, there are only a few animal models for studying mitochondrial diseases, and none of them is specific for MELAS and MERRF syndromes.

The fruit fly *Drosophila melanogaster* is an excellent model organism for studying molecular mechanisms of human diseases and has been used for modeling neurodegenerative diseases such as Alzheimer's and Parkinson's diseases as well as for drug discovery (Pandey and Nichols, 2011). In the case of mitochondrial diseases, there are *Drosophila* mutants of MRC components that show neurodegeneration, motor dysfunction, increased ROS production, and abnormal mitochondrial morphology (Liu et al., 2007; Mast et al., 2008), as well as mutants of mtDNA, such as a model of Leigh syndrome (Celotto et al., 2006). However, currently, it is not possible to generate a *Drosophila* mutant with intermediate heteroplasmy for studying MELAS and MERRF syndromes (Palladino, 2010).

Mitochondrial composition, function, and mtDNA are well conserved between *Caenorhabditis elegans* and humans (Falk et al., 2009). *C. elegans* growth and development are energy-dependent, and the main ATP source for this organism is the

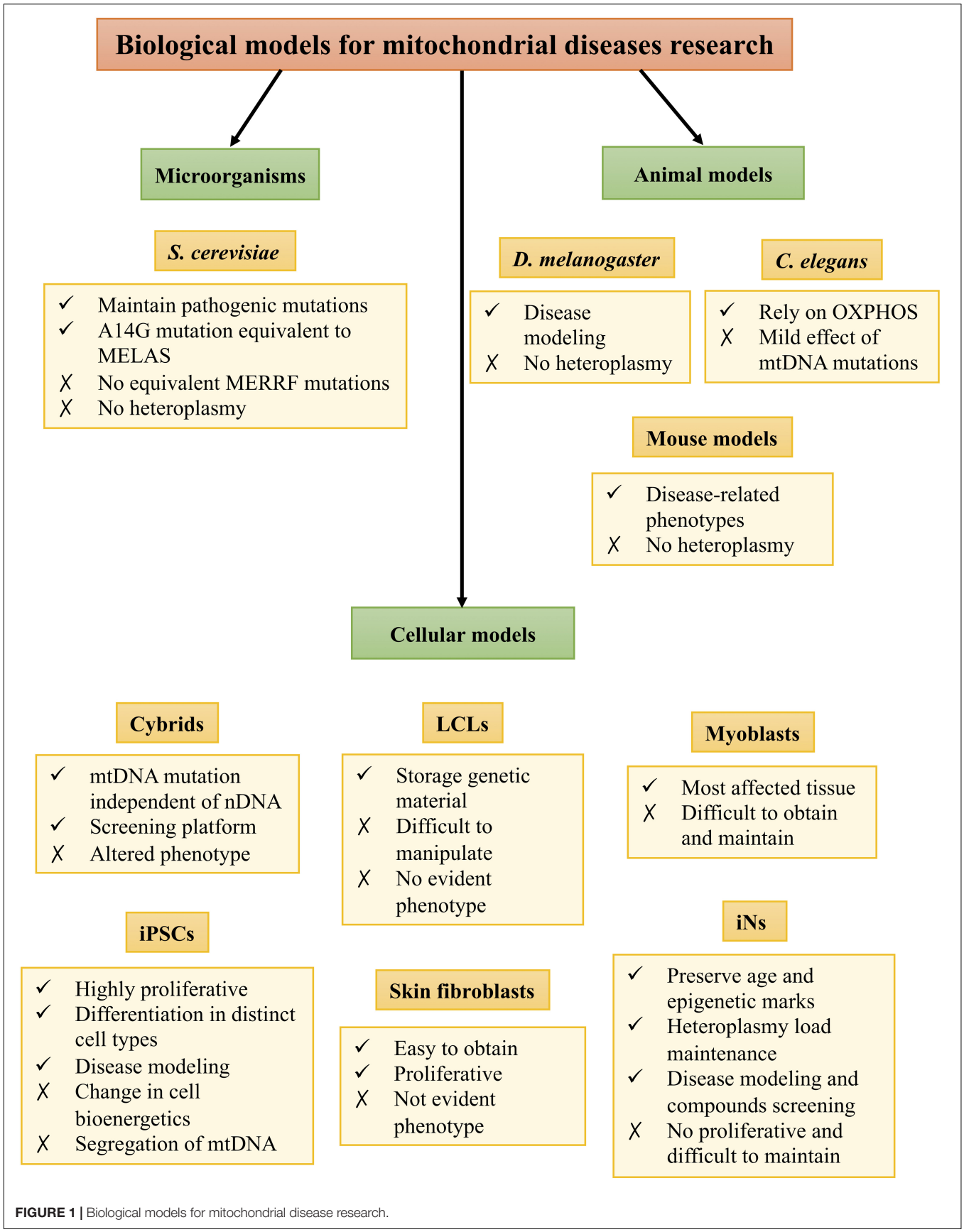

FIGURE 1 | Biological models for mitochondrial disease research.

MRC, which makes it interesting for studying mitochondrial diseases. In fact, there are worm strains that harbor mutations in MRC subunits encoded by nDNA (Ishii et al., 1998; Kayser et al., 2001; Tsang et al., 2001). However, mtDNA mutations have a mild effect in *C. elegans* (Tsang and Lemire, 2003), and they do not mimic the pathophysiological features of mtDNA mutation-caused mitochondrial diseases.

Mammalian models are necessary for studying pathogenesis or tissue-specific alterations that cannot be addressed using other models. Several murine models for OXPHOS deficiencies caused by mutations in nuclear genes encoding for MRC complexes, regulatory factors, and other components required for mitochondrial function have been created by transgenesis (Iommarini et al., 2015; Torraco et al., 2015). However, this is not the case for diseases caused by mutations in mtDNA, whose modeling is technically difficult (Tyynismaa and Suomalainen, 2009). Different mutagenesis methods to generate mutations in mouse mtDNA have been described, and these mutations can be transferred from cultured cells into mice, thereby creating transmitochondrial mice (mito-mice) (Inoue et al., 2000; Nakada et al., 2001; Fan et al., 2008; Kauppila et al., 2016). For example, a mouse model of LHON has been generated by introducing the equivalent of the human ND6 G14600A P25L mutation in homoplasmy into the mouse. Mutant mice showed a reduction in retinal function and neuronal accumulation of abnormal mitochondria among other events probably due to partial Complex I defects and increased ROS production (Lin et al., 2012). However, the generation of a mouse model with pathological heteroplasmic mtDNA mutations has proved challenging due to the multicopy nature of the mitochondrial genome. Furthermore, the transfection of plasmids or modified mtDNA into mouse mitochondria has not been successful (McGregor et al., 2001).

Cellular Models

Due to the lack of proper animal models for studying these diseases, cellular models have been extensively used in order to study MELAS and MERRF syndromes. Among them, we can find transmitochondrial cybrids, human B lymphoblastoid cell lines (LCLs), patient-derived cells such as myoblasts and dermal fibroblasts, and induced pluripotent stem cells (iPSCs) (Hu et al., 2019).

Transmitochondrial cybrids are generated by fusing enucleated cells that harbor wild-type or mutated mtDNA with ρ(0) cells, in which endogenous mtDNA has been depleted. For that reason, they are very useful for studying mtDNA mutations excluding the influence of nDNA variability (Vithayathil et al., 2012; Wilkins et al., 2014), and they have been used for studying MELAS and MERRF syndromes (Cotan et al., 2011; De la Mata et al., 2012; Garrido-Maraver et al., 2012; Villanueva-Paz et al., 2020). However, cybrid models show important limitations such as the need for a high mutational load to observe some pathophysiological features and the alteration in the cell behavior due to the loss of nDNA and mtDNA interactions (Dunbar et al., 1995).

Lymphoblastoid cell lines are generated by transformation of peripheral B lymphocytes and constitute a valuable source of mitochondria to study their function in mitochondrial diseases patients (Bourgeron et al., 1992). This model offers advantages such as the facility to obtain large quantities of lymphocytes and that they can be immortalized efficiently (Hu et al., 2019). For that reason, they have been used to study MERRF syndrome (Chang et al., 2013) and other mitochondrial diseases (Chin et al., 2018). Although this model is still the choice of storage for patients' genetic material due to its low somatic mutation rate and ease of maintenance, LCLs have some limitations such as the presence of two different cellular stages and the different response in comparison with other cell types (Sie et al., 2009). Moreover, they are difficult to manipulate, and the phenotype is often not evident.

Myoblasts derived from patients' biopsies are a very attractive model because they belong to one of the most affected tissues in these diseases. For that reason, they have been used to study the role of antioxidant enzymes and ATP levels in MELAS syndrome (Rusanen et al., 2000) and the distribution and expression of mutant mtDNAs in MERRF syndrome (Boulet et al., 1992). However, using myoblasts as a cellular model for mitochondrial diseases has several drawbacks. First, large quantities of proliferative myoblasts are difficult to isolate from a muscle tissue biopsy at later stages, so it is probable that more than one muscle biopsy is necessary to obtain enough cells for the analysis required. Moreover, primary myoblasts demand special conditions for optimal growth, and myoblast enrichment protocols are needed in order to obtain a pure cell culture.

Cultured fibroblasts are other patient-derived cells that have been a useful tool to study mitochondrial diseases. This model offers numerous advantages, since it is easy to obtain from a little invasive process such as a skin biopsy. In addition, fibroblast cultures are highly proliferative and provide a renewable source of cells (Hu et al., 2019). This model has been and still is widely used for studying cellular pathophysiology and as a screening tool for MELAS and MERRF syndromes (Wu et al., 2010; Cotan et al., 2011; De la Mata et al., 2012; Garrido-Maraver et al., 2015; Hayashi and Cortopassi, 2015; Villanueva-Paz et al., 2020) and other mitochondrial diseases. Nevertheless, it has some drawbacks as a cellular model for these diseases. First, they rely on glycolytic metabolism for energy production; therefore, they are not much vulnerable to energy-dependent defects resulting from mitochondrial dysfunction. In addition, they are difficult to maintain in culture and sometimes it is challenging to observe pathophysiological alterations, especially when the heteroplasmy load is low.

The most affected cell types in these diseases are the brain and the skeletal muscle cells, since they have a huge mitochondrial density due to high energy requirements and, consequently, they are more vulnerable to defects caused by mitochondrial dysfunction (DiMauro, 2007). In fact, neuron alteration is such that MELAS and MERRF syndromes are considered neurodegenerative mitochondriopathies in which there is neuronal cell death. MELAS neurodegeneration usually involves cortical territories in occipital and temporoparietal areas, as well as neurons in the Purkinje layer; meanwhile, in MERRF syndrome, the most affected areas are the Purkinje layer and dentate nucleus (Swerdlow, 2009).

The appearance of iPSCs in 2006 (Takahashi and Yamanaka, 2006) has led to numerous possibilities in the field of disease modeling. In fact, it has been a great step forward in the study of neurodegenerative diseases (Ebert et al., 2009; Lee et al., 2009; Kondo et al., 2013), as well as mitochondrial diseases (Cherry et al., 2013; Kodaira et al., 2015; Chou et al., 2016; Zhang et al., 2016; Inak et al., 2017; Lorenz et al., 2017; Yang et al., 2018). These iPSCs can be differentiated into somatic cell types such as neurons, which allow the study of these diseases in one of the most affected cellular types.

In the case of MERRF syndrome, neural progenitor cells (NPCs) derived from iPSCs have been demonstrated to reproduce pathophysiological features previously observed in other models of the disease, such as an impaired mitochondrial respiration, increased ROS production, altered antioxidant enzyme expression, as well as a fragmented mitochondrial network (Chou et al., 2016). Regarding MELAS syndrome, iPSC-derived neurons have made possible the study of not only common pathophysiological alterations but also neuron-specific alterations in the disease. For instance, in this work (Klein Gunnewiek et al., 2020), MELAS iPSC-derived neurons harboring a high heteroplasmy load showed lower dendrite complexity compared to control and low heteroplasmy neurons. These neurons also exhibited a reduced synaptic density, axonal mitochondrial abundance, and frequency of spontaneous excitatory activity, as well as an impaired neuronal network activity and synchronicity.

In addition, iPSC-derived neurons from mitochondrial disease patients can show different pathophysiological characteristics than parental patient-derived cells. For example, Hämäläinen et al. (2013) observed that parental MELAS fibroblast lines with intermediate heteroplasmy levels showed a combined deficiency of mtDNA-encoded Complexes I, III, and IV subunits; meanwhile, MELAS iPSC-derived neurons manifested a remarkable CI deficiency, which is typical for MELAS patient tissues and commonly reported upon mitochondria-associated neurodegeneration.

Reprogramming into iPSCs offers several advantages, since iPSCs can be cultured and a large quantity of starting material can be obtained. However, the protocol is complex, expensive, and time-consuming (Dolmetsch and Geschwind, 2011; **Figure 2**). Furthermore, this technique results in some disadvantages related to their use in mitochondrial disease research.

Several studies have demonstrated that reprogramming into iPSCs resets cellular age (Hsu et al., 2016), obtaining young neurons that could not show cell pathophysiology and, as a result, might not be useful to study neurodegenerative diseases. Furthermore, another study shows that this approach causes mitochondrial rejuvenation and an improvement in the cellular energy production capacity upon differentiation (Suhr et al., 2010). Another drawback would be that the use of these cells in cell replacement therapies is limited due to uncompleted differentiation and their propension to form tumors (Parmar and Jakobsson, 2011). In addition, analysis of mtDNA variants in

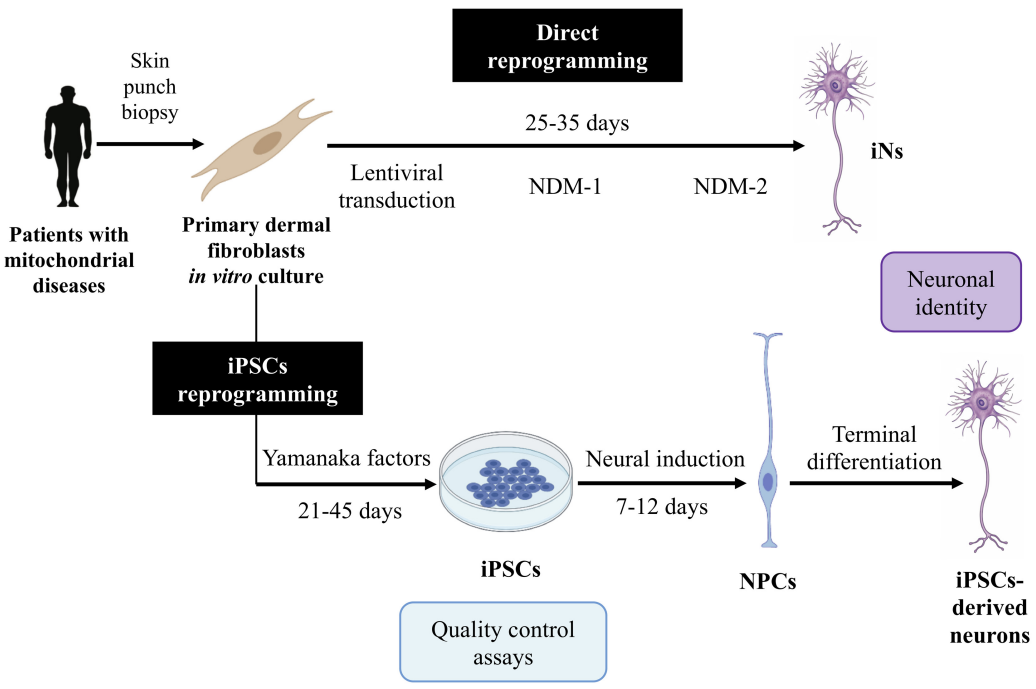

FIGURE 2 | Induced neurons (iNs) and induced pluripotent stem cell (iPSC)-derived neuron generation. This figure summarizes the protocols for the generation of iNs and iPSC-derived neurons. For iN generation, following lentiviral transduction of neural transcription factors, cells are exposed to a neural differentiation medium (NDM) I containing specific small molecules and growth factors and then to an NDM II containing only the growth factors. iNs are obtained at 25–35 days post-infection (DPI). For iPSC-derived neuron generation, fibroblasts are transduced with Yamanaka factors to generate iPSCs. These iPSCs are converted into neural progenitor cells (NPCs) by defined factors, and these are then differentiated into the desired neuron subtype.

iPSCs showed that low levels of potentially pathogenic mutations in the fibroblasts are revealed during reprogramming into iPSCs. Thus, mutant iPSCs are generated, causing a deleterious effect on their differentiated progeny and contributing to intra-person variability. This accumulation of mtDNA mutations can impact metabolic functions in iPSCs, hampering mitochondrial respiration (Kang et al., 2016; Perales-Clemente et al., 2016). These results highlight the need for monitoring mtDNA mutations and examining the metabolic status and quality of iPSCs intended for disease modeling or drug screening. Finally, reprogramming into iPSCs provokes an mtDNA segregation toward homoplasmy. In this way, after reprogramming, mutant and wild-type cells are obtained (Pickrell and Youle, 2013). These wild-type cells might be useful for cell therapy or as a syngeneic control, since they would be identical but will not express pathophysiological features. Therefore, the iPSC approach could be considered an autologous source of material suitable for cell therapy, without the risk of immune rejection (Smith et al., 2015). However, homoplasmic mutant iPSCs would not reflect patients' cell pathophysiology, since they harbor the mutation in a heteroplasmic state. Thus, there are major limitations that we still have to overcome, and currently, iPSCs have no therapeutic use (Crow, 2019). All of the above reasons make necessary the generation of additional models for these diseases.

NEW MODEL FOR MITOCHONDRIAL DISEASE RESEARCH: INDUCED NEURONS GENERATED BY DIRECT REPROGRAMMING

Direct reprogramming of fibroblasts into induced neurons (iNs) was achieved for the first time in 2010 (Vierbuchen et al., 2010). Using a combination of proneural transcription factors such as Ascl1, Brn2, and Myt1l, Vierbuchen et al. (2010) achieved the conversion of embryonic and postnatal murine fibroblasts into functional neurons *in vitro*. One year later, several advances allowed the improvement of the technique and increased the conversion efficiency. One of them was the utilization of microRNAs (miRNAs), in concrete miR-9/9* and miR-124, that leads to the conversion of fibroblasts into neurons even without the overexpression of proneural factors. However, since the reprogramming efficiency was low, these miRNAs were combined with the expression of NeuroD2 factor, Ascl1 and Myt1l (Yoo et al., 2011). Alternatively, using NeuroD1 factor together with the overexpression of Ascl1, Brn2, and Myt1l, direct reprogramming of fibroblasts into iNs was achieved with high efficiency (Pang et al., 2011). Additionally, compound screening has allowed the usage of a combination of small molecules and neural growth factors that increase reprogramming efficiency (Ladewig et al., 2012; Pfisterer et al., 2016).

Later, Drouin-Ouellet et al. (2017a) described a barrier for adult fibroblast reprogramming, the REST (RE-1 silencing transcription factor) complex, and developed one single lentiviral vector for the conversion of human adult fibroblasts into iNs in a very efficient manner. These iNs expressed neuron-specific proteins and exhibited electrophysiological properties. A recent paper from this group describes that the addition of the miRNAs indicated above, together with the overexpression of Ascl1 and Brn2, and the REST complex silencing, support neuronal maturation (Birtele et al., 2019). This technique allows the generation of a pan-neuronal population, but there are other strategies for reprogramming into neuronal subtypes, such as dopaminergic (Caiazzo et al., 2011), motor (Son et al., 2011; Qin et al., 2018), and serotonergic neurons (Xu et al., 2016). These approaches are valuable for some diseases in which there is one specific neuronal subtype affected or even different neuron subtypes may express distinct disease-related phenotypes.

Direct reprogramming brings numerous advantages. First, the procedure is relatively simple and fast (Ladewig et al., 2013; **Figure 2**). In addition, iNs maintain the age (Mertens et al., 2015) and the epigenetic marks of the donor (Horvath, 2013; Huh et al., 2016), which make them excellent models to study neurodegenerative diseases such as mitochondrial disorders. Furthermore, iNs have demonstrated to not cause tumorigenic processes after *in vivo* reprogramming (Torper et al., 2013), so they might be a promising tool for cell therapy. Thus, iN generation from patients' fibroblasts is thought to be a useful approach for studying the pathogenesis of these diseases.

One of the main challenges of direct reprogramming is reaching a high conversion efficiency. It is defined as the percentage of iNs obtained over the number of cells plated for conversion and can be very variable depending on the starting cells and the protocol used. The first approaches using direct reprogramming obtained very poor conversion efficiencies (Yoo et al., 2011; Ladewig et al., 2013), but the single vector-based approach developed by Drouin-Ouellet et al. (2017a; 2017b) and Shrigley et al. (2018) can generate very high yields of iNs. However, it is also necessary to reach a high percentage of purity, which is the number of iNs in the final population over the cells remaining in the plate. These two parameters are crucial since neurons are post-mitotic cells not able to further expand.

In addition, maintaining iNs in long-term cultures is difficult and expensive, since cell death can be observed from 30 days post-infection (DPI). This fact may hinder electrophysiological characterization of iNs, since the earliest time point when spontaneous action potentials have been detected is at 80–100 DPI (Drouin-Ouellet et al., 2017a). Moreover, iNs tend to form clusters during the reprogramming process, hampering isolation of individual cells for further analysis.

To our knowledge, the first work that uses iNs for mitochondrial disease study comes from our group. Following the protocol established for generating iNs using a single lentiviral vector (Shrigley et al., 2018), we successfully generated iNs from two MERRF patient-derived fibroblasts harboring the m.8344A > G mutation (Villanueva-Paz et al., 2019). The proportion of this mutation in the fibroblast cultures was 66% in MERRF 1 and 33% in MERRF 2 fibroblasts, and we demonstrated that iNs maintained these proportions after reprogramming. The maintenance of the heteroplasmy load is crucial if iNs are going to be used for disease modeling or as a screening platform. In addition, this fact makes direct reprogramming a more suitable approach for studying mitochondrial diseases

than iPSC generation because, in the latter case, mtDNA segregation and a tendency to homoplasmy have been observed (Pickrell and Youle, 2013).

In this work (Villanueva-Paz et al., 2019), the presence of bouton-like structures and spine-like protrusions was observed in both control and MERRF iNs, suggesting neuronal maturation. Furthermore, in another paper from our group, we performed electrophysiological recordings, and iNs showed electrophysiological properties at 60–80 DPI (Villanueva-Paz et al., 2020). The presence of neuronal maturation markers and functional properties suggest that iNs are behaving like neurons and make them a good candidate for mimicking the alterations happening in the patients' brain. We also characterized the iN areas, perimeters, neurite features, as well as mitochondrial morphology, and we observed differences between control and MERRF iNs, indicating that the maintenance of the mutational load was affecting these features (Villanueva-Paz et al., 2019).

In this regard, MERRF iNs also showed pathophysiological features that have been described in other models of the disease such as fibroblasts, cybrids (De la Mata et al., 2012; Villanueva-Paz et al., 2020), and NPCs derived from MERRF iPSCs (Chou et al., 2016). For instance, they showed a reduced $\Delta\Psi$m, a ROS overproduction, a disrupted autophagy flux, and an increased mitophagy (Villanueva-Paz et al., 2019). This fact makes them a good model for studying the cellular alterations happening in one of the most affected cell types in the disease. MERRF iNs were also suitable for performing other experiments such as the assessment of cellular bioenergetics using an extracellular flux analyzer. In these experiments, MERRF iNs showed alterations in the bioenergetic status such as reduced basal and maximal respirations, spare respiratory capacity, and ATP production (Villanueva-Paz et al., 2019). Some of these alterations were able to be rescued by Guttaquinon CoQ_{10} (a water-soluble derivative of CoQ_{10}) treatment, demonstrating that iNs are not only suitable for disease modeling but also for compound screening (Villanueva-Paz et al., 2020).

CONCLUSION AND FUTURE PERSPECTIVES

The generation of mitochondrial disease patient-derived iNs is a very promising starting point for the advance in the study of these illnesses and the search for new treatments. This model has been demonstrated to have neuronal identity as well as to reproduce pathophysiological features of the diseases (Villanueva-Paz et al., 2019). Among these characteristics, they have been able to show mitochondrial dysfunction that is a hallmark in mitochondrial disorders and other neurodegenerative illnesses such as Parkinson's or Huntington's diseases (Zeviani and Carelli, 2003). The presence of these features in iNs is even more important due to the fact that they are the most affected cell types in neurodegenerative disorders. This model also brings other advantages for studying this kind of diseases, such as the maintenance of the age and the epigenetic marks of the donor (Horvath, 2013; Mertens et al., 2015; Huh et al., 2016). For those reasons, we think that iNs are very valuable for modeling diseases that are accompanied by mitochondrial dysfunction. An interesting further step in heteroplasmic mitochondrial disease modeling would be the establishment of 3-dimensional (3D) cultures, such as cerebral organoids (Amin and Pasca, 2018), in which iNs as the main cellular component would presumably be maintained in culture for prolonged periods while remaining viable and retaining their specific activities. This 3D model has already been generated using iPSCs derived from mitochondrial neurogastrointestinal encephalomyopathy (MNGIE) patients' cells (Pacitti and Bax, 2018). In addition, iNs have been demonstrated to be suitable for compound screening, since bioenergetic status of MERRF iNs was able to be rescued by Guttaquinon CoQ_{10} treatment (Villanueva-Paz et al., 2020). However, we still have to go deeper into the characterization of these new models and their suitability for finding new therapeutic targets for mitochondrial diseases.

AUTHOR CONTRIBUTIONS

SP-C wrote the manuscript. JS-R, MÁ-C, IV-G, MT-R, AS-C, and MM-C contributed to the literature search. MV-P and JS-A revised the manuscript. All authors contributed to the article and approved the submitted version.

FUNDING

This work was supported by PI19/00377 grant, Instituto de Salud Carlos III, Spain, and Fondo Europeo de Desarrollo Regional (FEDER-Unión Europea), Spanish Ministry of Education, Culture and Sport, "Ayudas para la Formación de Profesorado Universitario" (FPU), and AEPMI (Asociación de Enfermos de Patología Mitocondrial).

REFERENCES

Alberts, B., Johnson, A., Lewis, J., Raff, M., Roberts, K., and Walter, P. (2002). "The mitochondrion," in *Molecular Biology of the Cell*, 4th Edn, (New York, NY: Garland Science).

Amin, N. D., and Pasca, S. P. (2018). Building models of brain disorders with three-dimensional organoids. *Neuron* 100, 389–405. doi: 10.1016/j.neuron.2018.10.007

Angelini, C. (2014). *Genetic Neuromuscular Disorders: A Case-Based Approach*. Switzerland: Springer International Publishing.

Bacman, S. R., Kauppila, J. H. K., Pereira, C. V., Nissanka, N., Miranda, M., Pinto, M., et al. (2018). MitoTALEN reduces mutant mtDNA load and restores tRNA(Ala) levels in a mouse model of heteroplasmic mtDNA mutation. *Nat. Med.* 24, 1696–1700. doi: 10.1038/s41591-018-0166-8

Baile, M. G., and Claypool, S. M. (2013). The power of yeast to model diseases of the powerhouse of the cell. *Front. Biosci.* 18:241–278. doi: 10.2741/4098

Balsa, E., Soustek, M. S., Thomas, A., Cogliati, S., Garcia-Poyatos, C., Martin-Garcia, E., et al. (2019). ER and nutrient stress promote assembly of respiratory chain Supercomplexes through the PERK-eIF2alpha axis. *Mol Cell* 74:877-890.e6. doi: 10.1016/j.molcel.2019.03.031

Birtele, M., Sharma, Y., Kidnapillai, S., Lau, S., Stoker, T. B., Barker, R. A., et al. (2019). Dual modulation of neuron-specific microRNAs and the REST complex promotes functional maturation of human adult induced neurons. *FEBS Lett.* 593, 3370–3380. doi: 10.1002/1873-3468.13612

Boulet, L., Karpati, G., and Shoubridge, E. A. (1992). Distribution and threshold expression of the tRNA(Lys) mutation in skeletal muscle of patients with myoclonic epilepsy and ragged-red fibers (MERRF). *Am. J. Hum. Genet.* 51, 1187–1200.

Bourgeron, T., Chretien, D., Rotig, A., Munnich, A., and Rustin, P. (1992). Isolation and characterization of mitochondria from human B lymphoblastoid cell lines. *Biochem. Biophys. Res. Commun.* 186, 16–23. doi: 10.1016/s0006-291x(05)80769-7

Brisca, G., Fiorillo, C., Nesti, C., Trucco, F., Derchi, M., Andaloro, A., et al. (2015). Early onset cardiomyopathy associated with the mitochondrial tRNALeu((UUR)) 3271T>C MELAS mutation. *Biochem. Biophys. Res. Commun.* 458, 601–604. doi: 10.1016/j.bbrc.2015.01.157

Brzezinski, P. (2020). New structures reveal interaction dynamics in respiratory *Supercomplexes*. *Trends Biochem. Sci.* 45, 3–5. doi: 10.1016/j.tibs.2019.10.011

Bulthuis, E. P., Adjobo-Hermans, M. J. W., Willems, P., and Koopman, W. J. H. (2019). Mitochondrial Morphofunction in mammalian cells. *Antioxid. Redox. Signal.* 30, 2066–2109. doi: 10.1089/ars.2018.7534

Busch, K. B. (2020). Inner mitochondrial membrane compartmentalization: dynamics across scales. *Int. J. Biochem. Cell Biol.* 120:105694. doi: 10.1016/j.biocel.2020.105694

Caiazzo, M., Dell'Anno, M. T., Dvoretskova, E., Lazarevic, D., Taverna, S., Leo, D., et al. (2011). Direct generation of functional dopaminergic neurons from mouse and human fibroblasts. *Nature* 476, 224–227. doi: 10.1038/nature10284

Celotto, A. M., Frank, A. C., McGrath, S. W., Fergestad, T., Van Voorhies, W. A., Buttle, K. F., et al. (2006). Mitochondrial encephalomyopathy in Drosophila. *J. Neurosci.* 26, 810–820. doi: 10.1523/JNEUROSCI.4162-05.2006

Chang, J. C., Liu, K. H., Chuang, C. S., Su, H. L., Wei, Y. H., Kuo, S. J., et al. (2013). Treatment of human cells derived from MERRF syndrome by peptide-mediated mitochondrial delivery. *Cytotherapy* 15, 1580–1596. doi: 10.1016/j.jcyt.2013.06.008

Chapman, J., Ng, Y. S., and Nicholls, T. J. (2020). The maintenance of Mitochondrial DNA integrity and dynamics by Mitochondrial membranes. *Life* 10:164. doi: 10.3390/life10090164

Cherry, A. B., Gagne, K. E., McLoughlin, E. M., Baccei, A., Gorman, B., Hartung, O., et al. (2013). Induced pluripotent stem cells with a mitochondrial DNA deletion. *Stem Cells* 31, 1287–1297. doi: 10.1002/stem.1354

Chin, R. M., Panavas, T., Brown, J. M., and Johnson, K. K. (2018). Patient-derived lymphoblastoid cell lines harboring mitochondrial DNA mutations as tool for small molecule drug discovery. *BMC Res. Notes* 11:205. doi: 10.1186/s13104-018-3297-6

Chou, S. J., Tseng, W. L., Chen, C. T., Lai, Y. F., Chien, C. S., Chang, Y. L., et al. (2016). Impaired ROS scavenging system in human induced Pluripotent stem cells generated from patients with MERRF Syndrome. *Sci. Rep.* 6:23661. doi: 10.1038/srep23661

Cogliati, S., Calvo, E., Loureiro, M., Guaras, A. M., Nieto-Arellano, R., Garcia-Poyatos, C., et al. (2016). Mechanism of super-assembly of respiratory complexes III and IV. *Nature* 539, 579–582. doi: 10.1038/nature20157

Cogliati, S., Frezza, C., Soriano, M. E., Varanita, T., Quintana-Cabrera, R., Corrado, M., et al. (2013). *Mitochondrial cristae* shape determines respiratory chain supercomplexes assembly and respiratory efficiency. *Cell* 155, 160–171. doi: 10.1016/j.cell.2013.08.032

Cotan, D., Cordero, M. D., Garrido-Maraver, J., Oropesa-Avila, M., Rodriguez-Hernandez, A., Gomez Izquierdo, L., et al. (2011). Secondary coenzyme Q10 deficiency triggers mitochondria degradation by mitophagy in MELAS fibroblasts. *FASEB J.* 25, 2669–2687. doi: 10.1096/fj.10-165340

Crow, D. (2019). Could iPSCs Enable "Off-the-Shelf". Cell Therapy?. *Cell* 177, 1667–1669. doi: 10.1016/j.cell.2019.05.043

De la Mata, M., Garrido-Maraver, J., Cotan, D., Cordero, M. D., Oropesa-Avila, M., Izquierdo, L. G., et al. (2012). Recovery of MERRF fibroblasts and cybrids pathophysiology by coenzyme Q10. *Neurotherapeutics* 9, 446–463. doi: 10.1007/s13311-012-0103-3

DiMauro, S. (2007). Mitochondrial DNA medicine. *Biosci. Rep.* 27, 5–9. doi: 10.1007/s10540-007-9032-5

DiMauro, S., and Hirano, M. (1993). "MERRF," in *GeneReviews(®)*, eds M. P. Adam, H. H. Ardinger, R. A. Pagon, S. E. Wallace, L. J. H. Bean, K. Stephens, et al. (Seattle, WA: University of Washington).

DiMauro, S. H. M. (2015). "MERRF," in *GeneReviews*, eds A. H. Adam, H. H Ardinger, R. A. Pagon, and S. E Wallace (Seattle, WA: University of Washington).

Dolmetsch, R., and Geschwind, D. H. (2011). The human brain in a dish: the promise of iPSC-derived neurons. *Cell* 145, 831–834. doi: 10.1016/j.cell.2011.05.034

Drouin-Ouellet, J., Lau, S., Brattas, P. L., Rylander Ottosson, D., Pircs, K., Grassi, D. A., et al. (2017a). REST suppression mediates neural conversion of adult human fibroblasts via microRNA-dependent and -independent pathways. *EMBO Mol. Med.* 9, 1117–1131. doi: 10.15252/emmm.201607471

Drouin-Ouellet, J., Pircs, K., Barker, R. A., Jakobsson, J., and Parmar, M. (2017b). Direct neuronal reprogramming for disease modeling studies using patient-derived neurons: what have we learned? *Front. Neurosci.* 11:530. doi: 10.3389/fnins.2017.00530

Dunbar, D. R., Moonie, P. A., Jacobs, H. T., and Holt, I. J. (1995). Different cellular backgrounds confer a marked advantage to either mutant or wild-type mitochondrial genomes. *Proc. Natl. Acad. Sci. U.S.A.* 92, 6562–6566. doi: 10.1073/pnas.92.14.6562

Ebert, A. D., Yu, J., Rose, F. F. Jr., Mattis, V. B., Lorson, C. L., et al. (2009). Induced pluripotent stem cells from a spinal muscular atrophy patient. *Nature* 457, 277–280. doi: 10.1038/nature07677

El-Hattab, A. W., Adesina, A. M., Jones, J., and Scaglia, F. (2015). MELAS syndrome: clinical manifestations, pathogenesis, and treatment options. *Mol. Genet. Metab.* 116, 4–12. doi: 10.1016/j.ymgme.2015.06.004

Falk, M. J., Rosenjack, J. R., Polyak, E., Suthammarak, W., Chen, Z., Morgan, P. G., et al. (2009). Subcomplex Ilambda specifically controls integrated mitochondrial functions in *Caenorhabditis elegans*. *PLoS One* 4:e6607. doi: 10.1371/journal.pone.0006607

Fan, W., Waymire, K. G., Narula, N., Li, P., Rocher, C., Coskun, P. E., et al. (2008). A mouse model of mitochondrial disease reveals germline selection against severe mtDNA mutations. *Science* 319, 958–962. doi: 10.1126/science.1147786

Finsterer, J. (2007). Genetic, pathogenetic, and phenotypic implications of the mitochondrial A3243G tRNALeu(UUR) mutation. *Acta Neurol. Scand.* 116, 1–14. doi: 10.1111/j.1600-0404.2007.00836.x

Finsterer, J. (2019). Pharmacotherapeutic management of epilepsy in MERRF syndrome. *Exp. Opin. Pharmacother.* 20, 1289–1297. doi: 10.1080/14656566.2019.1609941

Gammage, P. A., Rorbach, J., Vincent, A. I., Rebar, E. J., and Minczuk, M. (2014). Mitochondrially targeted ZFNs for selective degradation of pathogenic mitochondrial genomes bearing large-scale deletions or point mutations. *EMBO Mol. Med.* 6, 458–466. doi: 10.1002/emmm.201303672

Gammage, P. A., Viscomi, C., Simard, M. L., Costa, A. S. H., Gaude, E., Powell, C. A., et al. (2018). Genome editing in mitochondria corrects a pathogenic mtDNA mutation in vivo. *Nat. Med.* 24, 1691–1695. doi: 10.1038/s41591-018-0165-9

Garrido-Maraver, J., Cordero, M. D., Monino, I. D., Pereira-Arenas, S., Lechuga-Vieco, A. V., Cotan, D., et al. (2012). Screening of effective pharmacological treatments for MELAS syndrome using yeasts, fibroblasts and cybrid models of the disease. *Br. J. Pharmacol.* 167, 1311–1328. doi: 10.1111/j.1476-5381.2012.02086.x

Garrido-Maraver, J., Paz, M. V., Cordero, M. D., Bautista-Lorite, J., Oropesa-Avila, M., de la Mata, M., et al. (2015). Critical role of AMP-activated protein kinase in the balance between mitophagy and mitochondrial biogenesis in MELAS disease. *Biochim. Biophys. Acta* 1852, 2535–2553. doi: 10.1016/j.bbadis.2015.08.027

Gorman, G. S., Chinnery, P. F., DiMauro, S., Hirano, M., Koga, Y., McFarland, R., et al. (2016). Mitochondrial diseases. *Nat. Rev. Dis. Primers* 2:16080. doi: 10.1038/nrdp.2016.80

Hämäläinen, R. H., Manninen, T., Koivumaki, H., Kislin, M., Otonkoski, T., and Suomalainen, A. (2013). Tissue- and cell-type-specific manifestations of heteroplasmic mtDNA 3243A>G mutation in human induced pluripotent stem cell-derived disease model. *Proc. Natl. Acad. Sci. U.S.A.* 110, E3622–E3630. doi: 10.1073/pnas.1311660110

Hashimoto, M., Bacman, S. R., Peralta, S., Falk, M. J., Chomyn, A., Chan, D. C., et al. (2015). MitoTALEN: a general approach to reduce Mutant mtDNA loads and restore oxidative Phosphorylation Function in Mitochondrial diseases. *Mol. Ther.* 23, 1592–1599. doi: 10.1038/mt.2015.126

Hayashi, G., and Cortopassi, G. (2015). Oxidative stress in inherited mitochondrial diseases. *Free Radic. Biol. Med.* 88(Pt A), 10–17. doi: 10.1016/j.freeradbiomed.2015.05.039

Holt, I. J., Harding, A. E., and Morgan-Hughes, J. A. (1988). Deletions of muscle mitochondrial DNA in patients with mitochondrial myopathies. *Nature* 331, 717–719. doi: 10.1038/331717a0

Horvath, S. (2013). DNA methylation age of human tissues and cell types. *Genome Biol.* 14:R115. doi: 10.1186/gb-2013-14-10-r115

Hsu, Y. C., Chen, C. T., and Wei, Y. H. (2016). Mitochondrial resetting and metabolic reprogramming in induced pluripotent stem cells and mitochondrial disease modeling. *Biochim. Biophys. Acta* 1860, 686–693. doi: 10.1016/j.bbagen.2016.01.009

Hu, S. Y., Zhuang, Q. Q., Qiu, Y., Zhu, X. F., and Yan, Q. F. (2019). Cell models and drug discovery for mitochondrial diseases. *J. Zhejiang Univ. Sci. B* 20, 449–456. doi: 10.1631/jzus.B1900196

Huh, C. J., Zhang, B., Victor, M. B., Dahiya, S., Batista, L. F., Horvath, S., et al. (2016). Maintenance of age in human neurons generated by microRNA-based neuronal conversion of fibroblasts. *eLife* 5:e18648. doi: 10.7554/eLife.18648

Ikejiri, Y., Mori, E., Ishii, K., Nishimoto, K., Yasuda, M., and Sasaki, M. (1996). Idebenone improves cerebral mitochondrial oxidative metabolism in a patient with MELAS. *Neurology* 47, 583–585. doi: 10.1212/wnl.47.2.583

Inak, G., Lorenz, C., Lisowski, P., Zink, A., Mlody, B., and Prigione, A. (2017). Concise review: induced Pluripotent stem cell-based drug discovery for Mitochondrial disease. *Stem Cells* 35, 1655–1662. doi: 10.1002/stem.2637

Inoue, K., Nakada, K., Ogura, A., Isobe, K., Goto, Y., Nonaka, I., et al. (2000). Generation of mice with mitochondrial dysfunction by introducing mouse mtDNA carrying a deletion into zygotes. *Nat. Genet.* 26, 176–181. doi: 10.1038/82826

Iommarini, L., Peralta, S., Torraco, A., and Diaz, F. (2015). Mitochondrial Diseases Part II: mouse models of OXPHOS deficiencies caused by defects in regulatory factors and other components required for mitochondrial function. *Mitochondrion* 22, 96–118. doi: 10.1016/j.mito.2015.01.008

Ishii, N., Fujii, M., Hartman, P. S., Tsuda, M., Yasuda, K., Senoo-Matsuda, N., et al. (1998). A mutation in succinate dehydrogenase cytochrome b causes oxidative stress and ageing in nematodes. *Nature* 394, 694–697. doi: 10.1038/29331

Jang, S., and Javadov, S. (2020). OPA1 regulates respiratory supercomplexes assembly: the role of mitochondrial swelling. *Mitochondrion* 51, 30–39. doi: 10.1016/j.mito.2019.11.006

Kang, E., Wang, X., Tippner-Hedges, R., Ma, H., Folmes, C. D., Gutierrez, N. M., et al. (2016). Age-related accumulation of somatic Mitochondrial DNA mutations in adult-derived human iPSCs. *Cell Stem Cell* 18, 625–636. doi: 10.1016/j.stem.2016.02.005

Kauppila, J. H. K., Baines, H. L., Bratic, A., Simard, M. L., Freyer, C., Mourier, A., et al. (2016). A Phenotype-Driven approach to generate mouse models with Pathogenic mtDNA mutations causing mitochondrial disease. *Cell Rep.* 16, 2980–2990. doi: 10.1016/j.celrep.2016.08.037

Kayser, E. B., Morgan, P. G., Hoppel, C. L., and Sedensky, M. M. (2001). Mitochondrial expression and function of GAS-1 in *Caenorhabditis elegans*. *J. Biol. Chem.* 276, 20551–20558. doi: 10.1074/jbc.M011066200

Kirino, Y., and Suzuki, T. (2005). Human mitochondrial diseases associated with tRNA wobble modification deficiency. *RNA Biol.* 2, 41–44. doi: 10.4161/rna.2.2.1610

Klein Gunnewiek, T. M., Van Hugte, E. J. H., Frega, M., Guardia, G. S., Foreman, K., Panneman, D., et al. (2020). m.*3243A* > G-Induced Mitochondrial Dysfunction impairs human neuronal development and reduces neuronal network activity and synchronicity. *Cell Rep.* 31:107538. doi: 10.1016/j.celrep.2020.107538

Kodaira, M., Hatakeyama, H., Yuasa, S., Seki, T., Egashira, T., Tohyama, S., et al. (2015). Impaired respiratory function in MELAS-induced pluripotent stem cells with high heteroplasmy levels. *FEBS Open Biol.* 5, 219–225. doi: 10.1016/j.fob.2015.03.008

Kondo, T., Asai, M., Tsukita, K., Kutoku, Y., Ohsawa, Y., Sunada, Y., et al. (2013). Modeling Alzheimer's disease with iPSCs reveals stress phenotypes associated with intracellular Abeta and differential drug responsiveness. *Cell Stem Cell* 12, 487–496. doi: 10.1016/j.stem.2013.01.009

Ladewig, J., Koch, P., and Brustle, O. (2013). Leveling Waddington: the emergence of direct programming and the loss of cell fate hierarchies. *Nat. Rev. Mol. Cell Biol.* 14, 225–236. doi: 10.1038/nrm3543

Ladewig, J., Mertens, J., Kesavan, J., Doerr, J., Poppe, D., Glaue, F., et al. (2012). Small molecules enable highly efficient neuronal conversion of human fibroblasts. *Nat. Methods* 9, 575–578. doi: 10.1038/nmeth.1972

Lee, G., Papapetrou, E. P., Kim, H., Chambers, S. M., Tomishima, M. J., Fasano, C. A., et al. (2009). Modelling pathogenesis and treatment of familial dysautonomia using patient-specific iPSCs. *Nature* 461, 402–406. doi: 10.1038/nature08320

Lin, C. S., Sharpley, M. S., Fan, W., Waymire, K. G., Sadun, A. A., Carelli, V., et al. (2012). Mouse mtDNA mutant model of Leber hereditary optic neuropathy. *Proc. Natl. Acad. Sci. U.S.A.* 109, 20065–20070. doi: 10.1073/pnas.1217113109

Liu, W., Gnanasambandam, R., Benjamin, J., Kaur, G., Getman, P. B., Siegel, A. J., et al. (2007). Mutations in cytochrome c oxidase subunit VIa cause neurodegeneration and motor dysfunction in Drosophila. *Genetics* 176, 937–946. doi: 10.1534/genetics.107.071688

Lorenz, C., Lesimple, P., Bukowiecki, R., Zink, A., Inak, G., Mlody, B., et al. (2017). Human iPSC-derived neural progenitors are an effective drug discovery model for neurological mtDNA disorders. *Cell Stem Cell* 20, 659-674.e9. doi: 10.1016/j.stem.2016.12.013

Lott, M. T., Leipzig, J. N., Derbeneva, O., Xie, H. M., Chalkia, D., Sarmady, M., et al. (2013). mtDNA variation and analysis using Mitomap and Mitomaster. *Curr. Protoc. Bioinform.* 44, 21–26. doi: 10.1002/0471250953.bi0123s44

Martin-Jimenez, R., Lurette, O., and Hebert-Chatelain, E. (2020). Damage in Mitochondrial DNA associated with Parkinson's disease. *DNA Cell Biol.* 39, 1421–1430. doi: 10.1089/dna.2020.5398

Mast, J. D., Tomalty, K. M., Vogel, H., and Clandinin, T. R. (2008). Reactive oxygen species act remotely to cause synapse loss in a Drosophila model of developmental mitochondrial encephalopathy. *Development* 135, 2669–2679. doi: 10.1242/dev.020644

McGregor, A., Temperley, R., Chrzanowska-Lightowlers, Z. M., and Lightowlers, R. N. (2001). Absence of expression from RNA internalised into electroporated mammalian mitochondria. *Mol. Genet. Genomics* 265, 721–729. doi: 10.1007/s004380100469

Mertens, J., Paquola, A. C. M., Ku, M., Hatch, E., Bohnke, L., Ladjevardi, S., et al. (2015). Directly reprogrammed human neurons retain aging-associated Transcriptomic signatures and reveal age-related Nucleocytoplasmic defects. *Cell Stem Cell* 17, 705–718. doi: 10.1016/j.stem.2015.09.001

Meyerson, C., Van Stavern, G., and McClelland, C. (2015). Leber hereditary optic neuropathy: current perspectives. *Clin. Ophthalmol.* 9, 1165–1176. doi: 10.2147/OPTH.S62021

Minczuk, M., Papworth, M. A., Miller, J. C., Murphy, M. P., and Klug, A. (2008). Development of a single-chain, quasi-dimeric zinc-finger nuclease for the selective degradation of mutated human mitochondrial DNA. *Nucleic Acids Res.* 36, 3926–3938. doi: 10.1093/nar/gkn313

Murphy, E., Ardehali, H., Balaban, R. S., DiLisa, F., Dorn, G. W. II, Kitsis, R. N., et al. (2016). Mitochondrial function, biology, and role in disease: a scientific statement from the american heart association. *Circ. Res.* 118, 1960–1991. doi: 10.1161/RES.0000000000000104

Nakada, K., Inoue, K., and Hayashi, J. I. (2001). Mito-mice: animal models for mitochondrial DNA-based diseases. *Semin. Cell Dev. Biol.* 12, 459–465. doi: 10.1006/scdb.2001.0283

Napolitano, A., Salvetti, S., Vista, M., Lombardi, V., Siciliano, G., and Giraldi, C. (2000). Long-term treatment with idebenone and riboflavin in a patient with MELAS. *Neurol Sci.* 21(5 Suppl.), S981–S982. doi: 10.1007/s100720070015

Nissanka, N., and Moraes, C. T. (2020). Mitochondrial DNA heteroplasmy in disease and targeted nuclease-based therapeutic approaches. *EMBO Rep.* 21:e49612. doi: 10.15252/embr.201949612

Ohsawa, Y., Hagiwara, H., Nishimatsu, S. I., Hirakawa, A., Kamimura, N., Ohtsubo, H., et al. (2019). Taurine supplementation for prevention of stroke-like episodes in MELAS: a multicentre, open-label, 52-week phase III trial. *J. Neurol. Neurosurg. Psychiatry* 90, 529–536. doi: 10.1136/jnnp-2018-317964

Pacitti, D., and Bax, B. E. (2018). The development of an in vitro cerebral organoid model for investigating the pathomolecular mechanisms associated with the central nervous system involvement in Mitochondrial Neurogastrointestinal Encephalomyopathy (MNGIE). *Nucleosides Nucleotides Nucleic Acids* 37, 603–617. doi: 10.1080/15257770.2018.1492139

Palladino, M. J. (2010). Modeling mitochondrial encephalomyopathy in Drosophila. *Neurobiol. Dis.* 40, 40–45. doi: 10.1016/j.nbd.2010.05.009

Pandey, U. B., and Nichols, C. D. (2011). Human disease models in Drosophila melanogaster and the role of the fly in therapeutic drug discovery. *Pharmacol. Rev.* 63, 411–436. doi: 10.1124/pr.110.003293

Pang, Z. P., Yang, N., Vierbuchen, T., Ostermeier, A., Fuentes, D. R., Yang, T. Q., et al. (2011). Induction of human neuronal cells by defined transcription factors. *Nature* 476, 220–223. doi: 10.1038/nature10202

Parmar, M., and Jakobsson, J. (2011). Turning skin into dopamine neurons. *Cell Res.* 21, 1386–1387. doi: 10.1038/cr.2011.130

Perales-Clemente, E., Cook, A. N., Evans, J. M., Roellinger, S., Secreto, F., Emmanuele, V., et al. (2016). Natural underlying mtDNA heteroplasmy as a potential source of intra-person hiPSC variability. *EMBO J.* 35, 1979–1990. doi: 10.15252/embj.201694892

Pfisterer, U., Ek, F., Lang, S., Soneji, S., Olsson, R., and Parmar, M. (2016). Small molecules increase direct neural conversion of human fibroblasts. *Sci. Rep.* 6:38290. doi: 10.1038/srep38290

Pickrell, A. M., and Youle, R. J. (2013). Mitochondrial disease: mtDNA and protein segregation mysteries in iPSCs. *Curr. Biol.* 23, R1052–R1054. doi: 10.1016/j.cub.2013.10.048

Qin, H., Zhao, A., Ma, K., and Fu, X. (2018). Chemical conversion of human and mouse fibroblasts into motor neurons. *Sci. China Life Sci.* 61, 1151–1167. doi: 10.1007/s11427-018-9359-8

Reddy, P., Vilella, F., Izpisua Belmonte, J. C., and Simón, C. (2020). Use of customizable nucleases for gene editing and other novel applications. *Genes* 11:976. doi: 10.3390/genes11090976

Rinaldi, T., Dallabona, C., Ferrero, I., Frontali, L., and Bolotin-Fukuhara, M. (2010). Mitochondrial diseases and the role of the yeast models. *FEMS Yeast Res.* 10, 1006–1022. doi: 10.1111/j.1567-1364.2010.00685.x

Rusanen, H., Majamaa, K., and Hassinen, I. E. (2000). Increased activities of antioxidant enzymes and decreased ATP concentration in cultured myoblasts with the 3243A–>G mutation in mitochondrial DNA. *Biochim. Biophys. Acta* 1500, 10–16. doi: 10.1016/s0925-4439(99)00081-2

Russell, O., and Turnbull, D. (2014). Mitochondrial DNA disease-molecular insights and potential routes to a cure. *Exp. Cell Res.* 325, 38–43. doi: 10.1016/j.yexcr.2014.03.012

Sage-Schwaede, A., Engelstad, K., Salazar, R., Curcio, A., Khandji, A., Garvin, J. H., et al. (2019). Exploring mTOR inhibition as treatment for mitochondrial disease. *Ann. Clin. Transl. Neurol* 6, 1877–1881. doi: 10.1002/acn3.50846

Santa, K. M. (2010). Treatment options for mitochondrial myopathy, encephalopathy, lactic acidosis, and stroke-like episodes (MELAS) syndrome. *Pharmacotherapy* 30, 1179–1196. doi: 10.1592/phco.30.11.1179

Saxena, N., Taneja, N., Shome, P., and Mani, S. (2018). Mitochondrial donation: a boon or curse for the treatment of incurable mitochondrial diseases. *J. Hum. Reprod. Sci.* 11, 3–9. doi: 10.4103/jhrs.JHRS_54_17

Schon, E. A., DiMauro, S., and Hirano, M. (2012). Human mitochondrial DNA: roles of inherited and somatic mutations. *Nat. Rev. Genet.* 13, 878–890. doi: 10.1038/nrg3275

Shoffner, J. M., Lott, M. T., Lezza, A. M., Seibel, P., Ballinger, S. W., and Wallace, D. C. (1990). Myoclonic epilepsy and ragged-red fiber disease (MERRF) is associated with a mitochondrial DNA tRNA(Lys) mutation. *Cell* 61, 931–937. doi: 10.1016/0092-8674(90)90059-n

Shrigley, S., Pircs, K., Barker, R. A., Parmar, M., and Drouin-Ouellet, J. (2018). Simple generation of a high yield culture of induced neurons from human adult skin fibroblasts. *J. Vis. Exp.* 132:56904. doi: 10.3791/56904

Sie, L., Loong, S., and Tan, E. K. (2009). Utility of lymphoblastoid cell lines. *J. Neurosci. Res.* 87, 1953–1959. doi: 10.1002/jnr.22000

Smith, C., Abalde-Atristain, L., He, C., Brodsky, B. R., Braunstein, E. M., Chaudhari, P., et al. (2015). Efficient and allele-specific genome editing of disease loci in human iPSCs. *Mol. Ther.* 23, 570–577. doi: 10.1038/mt.2014.226

Son, E. Y., Ichida, J. K., Wainger, B. J., Toma, J. S., Rafuse, V. F., Woolf, C. J., et al. (2011). Conversion of mouse and human fibroblasts into functional spinal motor neurons. *Cell Stem Cell* 9, 205–218. doi: 10.1016/j.stem.2011.07.014

Suhr, S. T., Chang, E. A., Tjong, J., Alcasid, N., Perkins, G. A., Goissis, M. D., et al. (2010). Mitochondrial rejuvenation after induced pluripotency. *PLoS One* 5:e14095. doi: 10.1371/journal.pone.0014095

Suomalainen, A., and Battersby, B. J. (2018). Mitochondrial diseases: the contribution of organelle stress responses to pathology. *Nat. Rev. Mol. Cell Biol.* 19, 77–92. doi: 10.1038/nrm.2017.66

Swerdlow, R. H. (2009). The neurodegenerative mitochondriopathies. *J. Alzheimers Dis.* 17, 737–751. doi: 10.3233/JAD-2009-1095

Takahashi, K., and Yamanaka, S. (2006). Induction of pluripotent stem cells from mouse embryonic and adult fibroblast cultures by defined factors. *Cell* 126, 663–676. doi: 10.1016/j.cell.2006.07.024

Torper, O., Pfisterer, U., Wolf, D. A., Pereira, M., Lau, S., Jakobsson, J., et al. (2013). Generation of induced neurons via direct conversion in vivo. *Proc. Natl. Acad. Sci. U.S.A.* 110, 7038–7043. doi: 10.1073/pnas.1303829110

Torraco, A., Peralta, S., Iommarini, L., and Diaz, F. (2015). Mitochondrial Diseases Part I: mouse models of OXPHOS deficiencies caused by defects in respiratory complex subunits or assembly factors. *Mitochondrion* 21, 76–91. doi: 10.1016/j.mito.2015.01.009

Tsang, W. Y., and Lemire, B. D. (2003). The role of mitochondria in the life of the nematode, *Caenorhabditis elegans*. *Biochim. Biophys. Acta* 1638, 91–105. doi: 10.1016/s0925-4439(03)00079-6

Tsang, W. Y., Sayles, L. C., Grad, L. I., Pilgrim, D. B., and Lemire, B. D. (2001). Mitochondrial respiratory chain deficiency in *Caenorhabditis elegans* results in developmental arrest and increased life span. *J. Biol. Chem.* 276, 32240–32246. doi: 10.1074/jbc.M103999200

Tyynismaa, H., and Suomalainen, A. (2009). Mouse models of mitochondrial DNA defects and their relevance for human disease. *EMBO Rep.* 10, 137–143. doi: 10.1038/embor.2008.242

Umeda, N., Suzuki, T., Yukawa, M., Ohya, Y., Shindo, H., Watanabe, K., et al. (2005). Mitochondria-specific RNA-modifying enzymes responsible for the biosynthesis of the wobble base in mitochondrial tRNAs. Implications for the molecular pathogenesis of human mitochondrial diseases. *J. Biol. Chem.* 280, 1613–1624. doi: 10.1074/jbc.M409306200

Vierbuchen, T., Ostermeier, A., Pang, Z. P., Kokubu, Y., Sudhof, T. C., and Wernig, M. (2010). Direct conversion of fibroblasts to functional neurons by defined factors. *Nature* 463, 1035–1041. doi: 10.1038/nature08797

Villanueva-Paz, M., Povea-Cabello, S., Villalon-Garcia, I., Alvarez-Cordoba, M., Suarez-Rivero, J. M., Talaveron-Rey, M., et al. (2020). Parkin-mediated mitophagy and autophagy flux disruption in cellular models of MERRF syndrome. *Biochim. Biophys. Acta Mol. Basis Dis.* 1866:165726. doi: 10.1016/j.bbadis.2020.165726

Villanueva-Paz, M., Povea-Cabello, S., Villalon-Garcia, I., Suarez-Rivero, J. M., Alvarez-Cordoba, M., de la Mata, M., et al. (2019). Pathophysiological characterization of MERRF patient-specific induced neurons generated by direct reprogramming. *Biochim. Biophys. Acta Mol. Cell Res.* 1866, 861–881. doi: 10.1016/j.bbamcr.2019.02.010

Viscomi, C., and Zeviani, M. (2020). Strategies for fighting mitochondrial diseases. *J. Intern. Med.* 287, 665–684. doi: 10.1111/joim.13046

Vithayathil, S. A., Ma, Y., and Kaipparettu, B. A. (2012). Transmitochondrial cybrids: tools for functional studies of mutant mitochondria. *Methods Mol. Biol.* 837, 219–230. doi: 10.1007/978-1-61779-504-6_15

Wallace, D. C., Singh, G., Lott, M. T., Hodge, J. A., Schurr, T. G., Lezza, A. M., et al. (1988). Mitochondrial DNA mutation associated with Leber's hereditary optic neuropathy. *Science* 242, 1427–1430. doi: 10.1126/science.3201231

Wilkins, H. M., Carl, S. M., and Swerdlow, R. H. (2014). Cytoplasmic hybrid (cybrid) cell lines as a practical model for mitochondriopathies. *Redox Biol.* 2, 619–631. doi: 10.1016/j.redox.2014.03.006

Wollweber, F., von der Malsburg, K., and van der Laan, M. (2017). Mitochondrial contact site and cristae organizing system: a central player in membrane shaping and crosstalk. *Biochim. Biophys. Acta Mol. Cell Res.* 1864, 1481–1489. doi: 10.1016/j.bbamcr.2017.05.004

Wu, S. B., Ma, Y. S., Wu, Y. T., Chen, Y. C., and Wei, Y. H. (2010). Mitochondrial DNA mutation-elicited oxidative stress, oxidative damage, and altered gene expression in cultured cells of patients with MERRF syndrome. *Mol. Neurobiol.* 41, 256–266. doi: 10.1007/s12035-010-8123-7

Xu, Z., Jiang, H., Zhong, P., Yan, Z., Chen, S., and Feng, J. (2016). Direct conversion of human fibroblasts to induced serotonergic neurons. *Mol. Psychiatry* 21, 62–70. doi: 10.1038/mp.2015.101

Yang, Y., Wu, H., Kang, X., Liang, Y., Lan, T., Li, T., et al. (2018). Targeted elimination of mutant mitochondrial DNA in MELAS-iPSCs by mitoTALENs. *Protein Cell* 9, 283–297. doi: 10.1007/s13238-017-0499-y

Yoneda, M., Tanno, Y., Horai, S., Ozawa, T., Miyatake, T., and Tsuji, S. (1990). A common mitochondrial DNA mutation in the t-RNA(Lys) of patients with myoclonus epilepsy associated with ragged-red fibers. *Biochem. Int.* 21, 789–796.

Yoo, A. S., Sun, A. X., Li, L., Shcheglovitov, A., Portmann, T., Li, Y., et al. (2011). MicroRNA-mediated conversion of human fibroblasts to neurons. *Nature* 476, 228–231. doi: 10.1038/nature10323

Zeviani, M., and Carelli, V. (2003). Mitochondrial disorders. *Curr. Opin. Neurol.* 16, 585–594. doi: 10.1097/01.wco.0000093101.34793.c8

Zeviani, M., and Carelli, V. (2007). Mitochondrial disorders. *Curr. Opin. Neurol.* 20, 564–571. doi: 10.1097/WCO.0b013e3282ef58cd

Zeviani, M., Moraes, C. T., DiMauro, S., Nakase, H., Bonilla, E., Schon, E. A., et al. (1988). Deletions of mitochondrial DNA in Kearns-Sayre syndrome. *Neurology* 38, 1339–1346. doi: 10.1212/wnl.38.9.1339

Zhang, X., Li, S., Yang, W., Pan, H., Qin, D., Zhu, X., et al. (2016). Mitochondrial disease-specific induced Pluripotent stem cell models: generation and characterization. *Methods Mol. Biol.* 1353, 323–342. doi: 10.1007/7651_2014_195

Conflict of Interest: The authors declare that the research was conducted in the absence of any commercial or financial relationships that could be construed as a potential conflict of interest.

frontiers in Genetics

PERSPECTIVE
published: 15 January 2021
doi: 10.3389/fgene.2020.598760

Physiological Perspectives on the Use of Triheptanoin as Anaplerotic Therapy for Long Chain Fatty Acid Oxidation Disorders

*Evgenia Sklirou[1], Ahmad N. Alodaib[1,2], Steven F. Dobrowolski[3], Al-Walid A. Mohsen[1,4] and Jerry Vockley[1,4,5]**

[1] Department of Pediatrics, School of Medicine, University of Pittsburgh, Pittsburgh, PA, United States, [2] Newborn Screening and Biochemical Genetics Lab, Department of Genetics, King Faisal Specialist Hospital & Research Centre, Riyadh, Saudi Arabia, [3] Department of Pathology, School of Medicine, University of Pittsburgh, Pittsburgh, PA, United States, [4] Department of Human Genetics, Graduate School of Public Health, University of Pittsburgh, Pittsburgh, PA, United States, [5] Center for Rare Disease Therapy, UPMC Children's Hospital of Pittsburgh, Pittsburgh, PA, United States

OPEN ACCESS

Edited by:
Enrico Baruffini,
University of Parma, Italy

Reviewed by:
Gerarda Cappuccio,
University of Naples Federico II, Italy
Theresa V. Strong,
Foundation for Prader-Willi Research, United States

***Correspondence:**
Jerry Vockley
gerard.vockley@chp.edu

Specialty section:
This article was submitted to Genetics of Common and Rare Diseases, a section of the journal Frontiers in Genetics

Received: 25 August 2020
Accepted: 27 November 2020
Published: 15 January 2021

Citation:
Sklirou E, Alodaib AN, Dobrowolski SF, Mohsen A-WA and Vockley J (2021) Physiological Perspectives on the Use of Triheptanoin as Anaplerotic Therapy for Long Chain Fatty Acid Oxidation Disorders. Front. Genet. 11:598760. doi: 10.3389/fgene.2020.598760

Inborn errors of mitochondrial fatty acid oxidation (FAO) comprise the most common group of disorders identified through expanded newborn screening mandated in all 50 states in the United States, affecting 1:10,000 newborns. While some of the morbidity in FAO disorders (FAODs) can be reduced if identified through screening, a significant gap remains between the ability to diagnose these disorders and the ability to treat them. At least 25 enzymes and specific transport proteins are responsible for carrying out the steps of mitochondrial fatty acid metabolism, with at least 22 associated genetic disorders. Common symptoms in long chain FAODs (LC-FAODs) in the first week of life include cardiac arrhythmias, hypoglycemia, and sudden death. Symptoms later in infancy and early childhood may relate to the liver or cardiac or skeletal muscle dysfunction, and include fasting or stress-related hypoketotic hypoglycemia or Reye-like syndrome, conduction abnormalities, arrhythmias, dilated or hypertrophic cardiomyopathy, and muscle weakness or fasting- and exercise-induced rhabdomyolysis. In adolescent or adult-onset disease, muscular symptoms, including rhabdomyolysis, and cardiomyopathy predominate. Unfortunately, progress in developing better therapeutic strategies has been slow and incremental. Supplementation with medium chain triglyceride (MCT; most often a mixture of C8–12 fatty acids containing triglycerides) oil provides a fat source that can be utilized by patients with long chain defects, but does not eliminate symptoms. Three mitochondrial metabolic pathways are required for efficient energy production in eukaryotic cells: oxidative phosphorylation (OXPHOS), FAO, and the tricarboxylic (TCA) cycle, also called the Krebs cycle. Cell and mouse studies have identified a deficiency in TCA cycle intermediates in LC-FAODs, thought to be due to a depletion of odd chain carbon compounds in patients treated with a predominantly MCT fat source. Triheptanoin (triheptanoyl glycerol; UX007, Ultragenyx Pharmaceuticals) is chemically composed of three heptanoate (seven carbon fatty acid) molecules linked to glycerol through ester

bonds that has the potential to replete TCA cycle intermediates through production of both acetyl-CoA and propionyl-CoA through medium chain FAO. Compassionate use, retrospective, and recently completed prospective studies demonstrate significant reduction of hypoglycemic events and improved cardiac function in LC-FAOD patients, but a less dramatic effect on muscle symptoms.

Keywords: metabolomics, very long chain acyl-CoA dehydrogenase, fatty acid oxidation disorders, energy metabolism, tricarboxylic acid cycle, anaplerosis, inborn errors of metabolism, fatty acid oxidation

INTRODUCTION

Long-chain fatty acid oxidation disorders (LC-FAODs) are a rare group of inborn errors of metabolism that affect several enzymes involved in the pathway of mitochondrial β-oxidation, including both the transportation of long-chain fatty acids into the mitochondria through the carnitine shuttle, as well as the process of chain shortening of acyl-CoA substrates (Knottnerus et al., 2018). Fatty acid oxidation (FAO) ultimately leads to the production of energy during times of fasting and physiologic stress. In addition to an energy deficit that impacts multiple organ systems, the incomplete oxidation of fatty acids also causes accumulation of toxic long-chain acyl-CoA intermediates. The disorders of the LC-FAODs are autosomal recessive and include carnitine palmitoyl transferase 1 (CPTI), carnitine palmitoyl transferase 2 (CPTII), carnitine-acylcarnitine translocase (CACT), very long-chain acyl-CoA dehydrogenase (VLCAD), long-chain 3-hydroxyacyl-CoA dehydrogenase (LCHAD), and mitochondrial trifunctional protein (TFP) deficiencies (Knottnerus et al., 2018).

Epidemiologic studies of NBS populations indicate that the combined incidence of all FAODs ranges from 0.9–15.2 per 100,000 (Marsden et al., 2020). Very long-chain acyl-CoA dehydrogenase (VLCAD) deficiency is the most prevalent LC-FAOD in most populations, with incidences ranging from 0.07–1.9 per 100,000, whereas other LC-FAODs have a low incidence (<1.0 per 100,000) (Marsden et al., 2020).

LC-FAODs present with variable clinical manifestations and severity ranging from early neonatal presentations with hypoketotic hypoglycemia, metabolic acidosis, cardiomyopathy, severe hepatopathy, multiorgan failure and death, to later onset disease presentations with recurrent episodes of rhabdomyolysis, exercise intolerance, myopathy, peripheral neuropathy and retinopathy. Cardiomyopathy and cardiac arrhythmias can occur at any age (Baruteau et al., 2013). Patients are at constant risk for a metabolic decompensation during periods of increased energy requirements such as prolonged fasting or illness. LC-FAODs are currently included in the newborn screening programs in many countries including the US, allowing early intervention to prevent the devastating early manifestations as well as the chronic disease-related complications. However, despite early diagnosis and appropriate treatment, most patients still experience disease-related complications and long-term disabilities (Spiekerkoetter et al., 2009a).

Medical treatment for LC-FAODs is consensus and experience driven rather than evidence based (Vockley et al., 2002; Spiekerkoetter et al., 2009b; Knottnerus et al., 2018). The cornerstone of management is avoidance of fasting in order to reduce the need of fatty acid oxidation. Treatment often includes a diet that is rich in carbohydrates and low in long-chain fats and is usually supplemented with medium even chain triglycerides (MCT oil), as well as essential fatty acids to prevent possible deficiencies secondary to dietary fat restriction (Spiekerkoetter et al., 2009b; Spiekerkoetter and Mayatepek, 2010; Knottnerus et al., 2018). The use of L-carnitine is controversial due to the concern about the potential arrhythmogenic potential of long-chain acylcarnitines, but it is sometimes prescribed if blood free carnitine levels are felt to be too low. Emergency protocols with intravenous glucose supplementation must be promptly initiated in acute clinical presentations with sickness and inability to maintain adequate oral intake. However, progress in treating LC-FAODs has been achieved with the introduction of trihepatnoin, an odd medium chain fatty acid in a triglyceride form (triheptanoyl glycerol).

MITOCHONDRIAL FATTY ACID OXIDATION

Mitochondrial fatty acid oxidation (FAO) is the process by which fatty acids from endogenous stores (usually 16 or 18 carbons in chain length) or, in some situations, from the diet are metabolized for energy (Vockley et al., 2016a). Typically during times of metabolic stress or physiologic fasting, endogenous fatty acids, typically stored in the body as long-chain triglycerides, are mobilized through the action of lipases, transported through the blood stream to cells by carrier proteins, then taken up by peripheral cells through specific membrane receptors/transporters where they are activated to acyl-CoAs by a set of acyltransferases. Medium and short chain acyl-CoAs can enter mitochondria directly, but substrates longer than 10 carbons use a series of reactions known as the carnitine cycle for transport across the mitochondrial membrane (**Figure 1**) (Longo, 2016). Here, the acyl-CoA is first conjugated to carnitine by carnitinepalmitoyl transferase 1 (CPTI), shuttled across the intermembrane space by carnitine-acylcarnitine translocase (CACT) in exchange for carnitine, then the acyl-CoA is released in the mitochondrial matrix along with free carnitine by carnitinepalmitoyl transferase 2 (CPTII). In the mitochondrial matrix, a series of four enzymatic reactions cleaves the two carbon moiety acetyl-CoA and leaves an acyl-CoA with a primary carbon backbone that is two carbons shorter

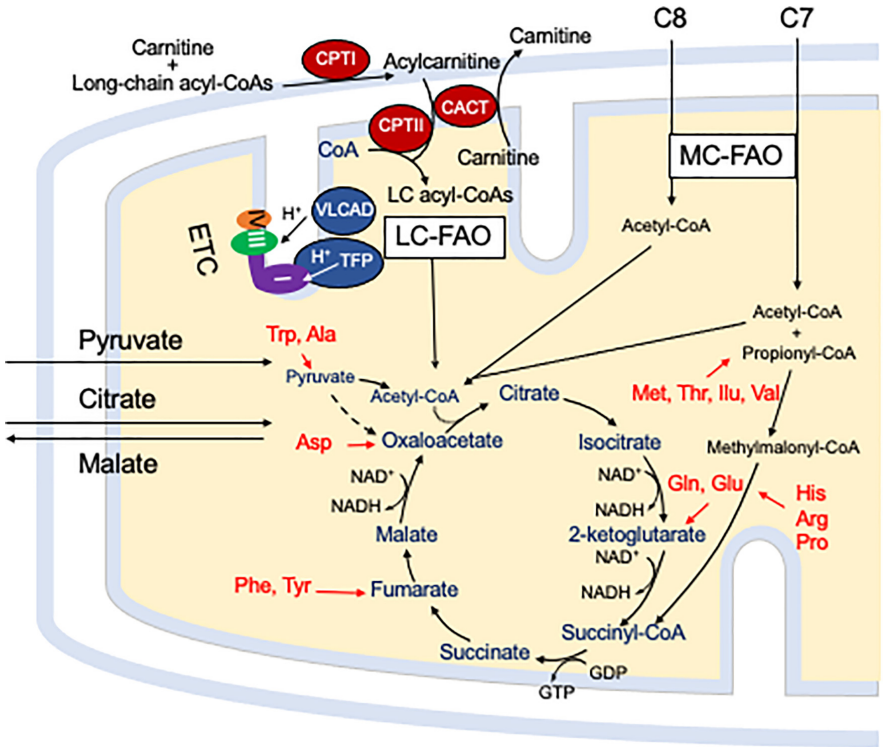

FIGURE 1 | The carnitine cycle involves generation of a long chain acylcarnitine from activated fatty acids by CPT I, transport across the mitochondrial membranes by CACT, and release of the activated acyl-CoA substrate for FAO into the mitochondrial matrix by CPT II. Carnitine itself is transported into cells by a high affinity transporter (OCTN2). All abbreviations are as defined in the text. Interactions of mitochondrial energy metabolism pathways. The carnitine cycle transport long-chain CoAs into the mitochondrial matrix with carnitine ultimately being restored to the cytoplasm in exchange for release of an acyl-CoA in the mitochondrial matrix. Medium chain fats directly diffuse into mitochondria. ETC and the enzymes of LC-FAO functionally and physically interact. Mitochondrial TFP interacts with and passes its reducing equivalents to the matrix arm of ETC complex I. VLCAD interacts with TFP, but its reducing equivalents are transferred to ETC complex III via electron transfer flavoprotein (ETF, not shown) and ETF dehydrogenase (not shown). The acetyl-CoA product of one cycle of FAO enters the TCA cycle to produce citrate. While standard medium chain trioctanoylglycerol (C8) provides double the amount of acetyl-CoA compared to triheptanoin (C7), the latter provides a propionyl-CoA that enters the TCA cycle through succinyl-CoA. Anaplerotic amino acids are listed in red. Pyruvate and citrate enter the mitochondria through specific carriers (the latter with counter transport of malate to the cytoplasm). All abbreviations are as defined in the text.

(**Figure 2**) (Vockley et al., 2016a). These reactions are catalyzed by families of chain length optimized enzymes. In the first, the acyl-CoA is oxidized to an enoyl-CoA by the acyl-CoA dehydrogenases (ACADs), including enzymes with substrate optima of 16, 8, and 4 carbons in chain length (very long-, medium- and short chain ACADs; VLCAD, MCAD, and SCAD, respectively) (Swigonova et al., 2009). The next three steps for long-chain acyl-CoAs [enoyl-CoA hydratase (ECDH), long-chain 3-hydroxyacyl-CoA dehydrogenase (LCHAD), and 3-ketoacyl-CoA thiolase (KAT)] are catalyzed by a single multimeric enzyme known as the mitochondrial trifunctional protein (TFP), while individual enzymes specific to each reaction exist for medium and short chain substrates (Liang et al., 2018; Xia et al., 2019). Additional enzymes are required to completely metabolize unsaturated fats. The acetyl-CoA final product of FAO is available to participate in other mitochondrial process [most often the tricarboxylic acid (TCA) or Krebs cycle] or in liver can enter in the ketone synthesis pathway to make 3-hydroxybutyrate and acetoacetate, alternative fuels that can be used by many tissues.

INTERACTION OF MITOCHONDRIAL ENERGY PATHWAYS

Energy generation in the mitochondria occurs through the intersection of three major enzyme pathway, oxidative phosphorylation (OXPHOS), FAO and the TCA cycle (**Figure 1**) (Vockley et al., 2019b). Reducing equivalents are generated at two steps in FAO, by ACADs with production of a reduced FAD cofactors, and by 3-hydroxyacyl-CoA dehydrogenase, utilizing nicotin adenine dinucleotide (NAD) as the electron acceptor. The ACADs are re-oxidized by electron transfer flavoprotein (ETF), which in turn is re-oxidized by the ETF dehydrogenase (ETFDH, also known as ETF-Coenzyme Q oxidoreductase). Finally, reducing equivalents are passed from ETFDH to complex III of the electron transfer chain (ETC). Electrons from reduced NADH (NADH) are direct substrates for complex I of the ETC. The enzymes of long-chain FAO and the ETC are both functionally and physically associated in a macromolecular energy complex. The LCHAD subunit of TFP interacts with the matrix arm of complex I, while ETFDH interacts with the cor2

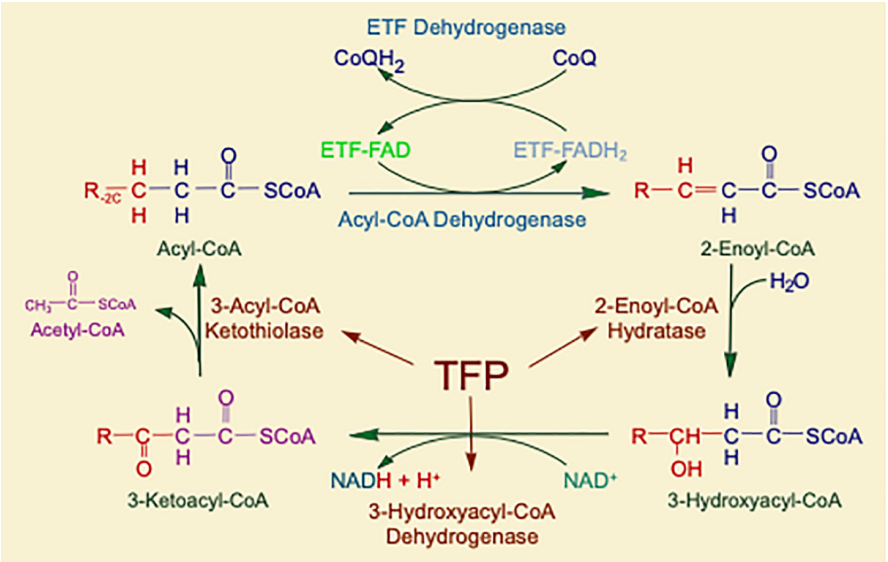

FIGURE 2 | The matrix reactions of FAO consist of four steps that result in one molecule of acetyl-CoA and an acyl-CoA that is shortened by two-carbon units. For long-chain substrates, VLCAD, which catalyzes the first step is long-chain fatty acid β-oxidation, is the most important acyl-CoA dehydrogenase for energy generation. The next three steps are performed by a single multifunctional enzyme with three active sites, the mitochondrial TFP. All abbreviations are as defined in the text.

subunit of complex III. VLCAD binds with the ECDH subunit of TFP, thus creating a metabolon that optimizes enzymatic efficiency of the linked enzymatic processes.

DISORDERS OF FATTY ACID OXIDATION

Inborn errors of LC-FAOD are among the most common in humans, affecting ∼1:10,000 babies born. At least 25 enzymes and specific transport proteins are responsible for carrying out the steps of mitochondrial fatty acid metabolism, with at least 22 associated genetic disorders (Wilcken et al., 2009; Lindner et al., 2010). Most patients with LC-FAODs in the US are now identified pre-symptomatically through newborn screening. Common symptoms in the first week of life include cardiac arrhythmias, hypoglycemia, and sudden death (Knottnerus et al., 2018). Symptoms later in infancy and early childhood may relate to liver, cardiac, or skeletal muscle dysfunction, and include fasting or stress-related hypoketotic hypoglycemia or Reye-like syndrome, cardiomyopathy, and recurrent rhabdomyolysis. In adolescents or adults, muscular symptoms, including rhabdomyolysis and cardiomyopathy predominate. Progressive peripheral neuropathy and retinopathy are unique to TFP/LCHAD deficiency (Spiekerkoetter et al., 2004; Rector et al., 2008). Current therapies do not address the basic pathologies of LC-FAODs (Spiekerkoetter and Mayatepek, 2010). MCT oil provides a medium chain fat source (octanoate in its most purified form) that can be utilized by patients with long-chain FAO defects, but does not eliminate symptoms. Mutations have been described in numerous patients with LC-FAODs, but genotype-phenotype correlations are imperfect (Nahabet et al., 2016).

TCA Cycle Depletion and the Role of Anaplerosis in Treating FAODs

In the early years after the discovery of the LC-FAODs, especially VLCAD and TFP/LCHAD deficiencies, the expectation of most metabolic specialists was that MCT oil should completely rescue patients from the effects of these disorders because of an ample supply of acetyl-CoA groups to the TCA cycle. While it was at least partially effective, some symptoms persisted and, in many cases, worsened again with time. This observation led to the novel suggestion that loss of some TCA cycle intermediates through either cellular damage or use in other metabolic pathways led to a depletion of those substrates generated from odd chain carbon sources (i.e., succinate from propionyl-CoA) that led to energy impairment regardless of continued delivery of acetyl-CoA from octanoate. Triheptanoin, the triglyceride of heptanoate, was proposed as an alternative treatment that could directly address both TCA cycle substrate needs in LC-FAODs since it still bypassed the need for long-chain fat transport and catabolism and was metabolized to two molecules of acetyl-CoA and one of propionyl-CoA. Indeed, the first patient treated with this compound, a 5 years old with VLCAD deficiency and persistent cardiomyopathy, responded to the medication with dramatic improvement of heart function (see below) (Roe et al., 2002). Subsequent metabolic flux experiments in rats demonstrated that intra-duodenal infusion of heptanoate led to nearly complete uptake in the liver and stimulated production of C5 ketone bodies presumed to be synthesized from propionyl-CoA (Deng et al., 2009). However, it was subsequently demonstrated that nearly all of the liver generated propionyl-CoA was channeled to the TCA cycle, indicating that the C5-ketone bodies were being derived instead from the partial heptanoate degradation

to produce valeryl-CoA that was then used for odd chain ketone body synthesis (Kinman et al., 2006). In addition, the incorporation of label from heptanoate into C5-ketone bodies was lower than that from labeled octanoate into C4-ketone bodes. Thus, the anaplerotic potential of heptanoate is greater than that of octanoate. Original concern that stimulation of lipolysis of long-chain lipids by intravenous infusion of heptanoate might be limited in this setting were negated by additional studies showing that they were in fact efficiently re-esterified with no effect on delivery of long-chain fats into FA (Kinman et al., 2006; Gu et al., 2010). Induction of ketosis through a ketogenic diet for 60 days with or without triheptanoin showed that hexadecanoic, 9-hexadecenoic, and 9-octadecenoic were elevated in the livers of the triheptanoin fed animals (Vieira de Melo et al., 2015). The physiologic implications of these findings are unclear as both sets of animals appeared well. An MCT arm was not included in the study.

Additional information on the disposition of ingested triheptanoin has been obtained in long term studies on mice. After 1 year of supplementation with either C8 MCT oil or triheptanoin, both wild type and VLCAD deficient mice demonstrated a significant accumulation of a variety of even and odd chain complex lipids, respectively, in liver including heptadecenoic acid (C17:1n9), eicosanoic acid (C20:1n9), erucicacid (C22:1n9), and mead acid (C20:3n9) (Tucci et al., 2015). Peroxisomal fatty acid oxidation was also increased in these animals compared to normal diet, consistent with increased flux through complex lipid metabolic pathways. However, only animals fed C8 had upregulation of the peroxisomal L-bifunctional fatty acid oxidase protein, a finding associated with increased toxicity presumed to be related to increased production of reactive oxygen species. Heart lipid composition was also altered with an increase in monounsaturated fats in C8 and C7 fed mice and a corresponding decrease in polyunsaturated fats. Elongation of the medium chain fats in this model was supported by an upregulation of the sterol element binding transcription factor 1 that regulates many of the genes involved in lipid synthesis as well as increased expression of several genes in lipid chain length elongation. Finally, VLCAD deficient mice show an age dependent shift in muscle fibers from oxidative to the glycolytic type. This shift is inhibited when mice are treated with MCT oil, but not with triheptanoin. In total, these studies indicate that both MCT (C8) and triheptanoin induce changes in the lipidome with an increase in long-chain fats due to elongation of the octanoyl- and heptanoyl-CoA substrates. However, the former seems to have more potential for toxicity than the latter.

Metabolomic Abnormalities in VLCAD Deficient Patients

Given these animal findings, we sought to explore changes that might be occurring in patients with VLCAD deficiency. Because of participation in clinical trials for FDA approval of triheptanoin, we had a large biobank of samples from patients on standard of care (MCT oil) and triheptanoin. We selected plasma samples from 8 patients each on MCT oil or on triheptanoin and sent them to Metabolon[1] for evaluation of small molecule metabolomics using their clinically validated MetaGA platform (Dobrowolski et al., 2020). Briefly, this test applies three platforms for analysis: liquid chromatography/tandem mass spectrometry (LC-MS/MS) optimized for basic species, LC-MS/MS optimized for acidic species, and gas chromatography/mass spectrometry (Evans et al., 2009; Dehaven et al., 2010). Sample preparation for gas chromatography/mass spectrometry utilized bistrimethyl-silyl-trifluoroacetamide derivatization in a acetonitrile:dichloromethane:cyclohexane (5:4:1) solvent. LC-MS/MS utilized a Waters Acquity UPLC (Waters, Millford, MA, United States) and an LTQ mass spectrometer (Thermo Fisher Scientific, Inc., Waltham, MA, United States) assessing masses of 99–1,000 m/z as described. Gas chromatography/mass spectrometry applied a 5% phenyldimethyl silicone column (60–340°C) with a Thermo-Finnigan Trace DSQ MS (Thermo Fisher Scientific, Inc.) to assess masses of 50–750 atomic mass units as described. Data analysis was performed with company proprietary software as previously described (Quell et al., 2017). Briefly, automated and visual comparison of ion features to reference standards (i.e., retention time, mass-to-charge ratio, fragmentation mass spectra) was determined. Statistical analysis was performed using "R" version 2.14. Welch's *t*-tests compared data from patient blood to a validated age and sex match normal control database. The calculated *z*-scores show deviation from the mean of age matched controls measured and curated by the clinical testing lab. Analyte differences were considered significantly with $p \leq 0.05$. Thus, all patient samples are compared to normal population controls rather than each other.

Results are shown in **Table 1** and **Figures 3**, **4**. With the exception of α-ketoglutarate, representation of Krebs' cycle intermediates trend lower in VLCAD deficient patients (**Figure 3**). However, citrate, aconitate, fumarate and malate are higher in those treated with C7. Reduced succinate is common to both treatment groups suggesting rapid utilization of this metabolite. These findings support the anaplerotic role of C7 in supplementation of the Krebs' cycle via combined propionyl-CoA and acetyl-CoA production. Analysis of patients revealed enrichment of very long-chain carnitine esters including arachidoylcarnitine (C20), behenoylcarnitine (C22), and nervonoylcarnitine (C24:1) regardless of treatment (**Table 1** and **Figure 4**). Patients treated with C7 also showed an increase of unique odd chain sphingomyelins, phosphatidylcholines, and phosphatidylethanolamines compared to control and patients treated with MCT. While the mechanism for the increase and pattern of these metabolites remains to be proven, studies in VLCAD deficient mice suggest that that they are due to excess substrate of the supplemented medium chain oil (C7 or C8) that is then chain elongated and participates in increased complex lipid synthesis (Tucci et al., 2015; Tucci, 2017; Tucci et al., 2017). Regardless of mechanism, these results demonstrate that long-chain complex lipids with significant signaling potential to induce inflammation accumulate in VLCAD deficient patients,

[1]https://www.metabolon.com

TABLE 1 | Complex lipids significantly increased in VLCAD patients.

Pathway	Metabolite
Lipid synthesis	
	Arachidoylcarnitine (C20)
	Margaroylcarnitine (C17)
	Nervonoylcarnitine (C24:1)
Lysophospholipid	
	1-margaroyl-glycerophosphoethanolamine (C17)
	1-pentadecanoyl- glycerylphosphorylcholine (C15)
Phosphatidylcholine	
	1-margaroyl-2-arachidonoyl-glycerylphosphorylcholine (17:0/20:4)
	1-margaroyl-2-docosahexaenoyl-glycerylphosphorylcholine (17:0/22:6)
	1-margaroyl-2-linoleoyl- glycerylphosphorylcholine (17:0/18:2)
	1-pentadecanoyl-2-arachidonoyl-glycerylphosphorylcholine (15:0/20:4)
	1-pentadecanoyl-2-docosahexaenoyl-glycerylphosphorylcholine (15:0/22:6)
	Phosphatidylcholine (15:0/18:1, 17:0/16:1, 16:0/17:1)
Sphingolipid	
	Sphingomyelin (d18:2/23:1)
	Sphingomyelin (d17:2/16:0, d18:2/15:0)
Amino acid	
	Gamma-glutamylglycine

regardless of treatment with C7 and C8. These findings raise the possibility that while a bioenergetic deficit plays a major role in the development of hypoglycemia and cardiomyopathy, the accumulation of abnormal long-chain fats serve as a signal for inflammation and subsequent rhabdomyolysis.

TREATMENT OF LC-FAODS WITH TRIHEPTANOIN

Until recently, no medications had been approved for treatment of long-chain fatty acid oxidation disorders. However, the U.S. Food and Drug Administration (FDA) approved Dojolvi (generic name triheptanoin, also known as UX007 when in clinical trials), in June 2020, for the treatment of pediatric and adult patients with LC-FAODs. The use of triheptanoin in treatment of LC-FAODs is based on its action as an anaplerotic molecule that can correct secondary depletion of TCA cycle intermediates that occurs in these disorders (Roe et al., 2002). **Table 2** summarizes published studies on the use of triheptanoin in LC-FAODs. The first report was three VLCAD deficient patients with early presentation including neonatal hypoglycemia, cardiomyopathy in infancy, muscle weakness, and subsequent recurrent episodes of rhabdomyolysis. At enrollment, one patient had persistent cardiomyopathy at 5 years old, and two had hepatomegaly prior to triheptanoin initiation at 2 and 9 years old, respectively. Following triheptanoin, all patients showed marked improvement of strength, endurance and activity, the cardiomyopathy improved in the 5 years old, and the hepatomegaly resolved in the other two patients. The family of the 2 years old patient elected to discontinue the triheptanoin diet and returned to previously administered MCT diet, with subsequent recurrence of rhabdomyolysis episodes. Both four-carbon ketone bodies (acetoacetate, β-hydroxybutyrate) and five-carbon ketones (β-hydroxypentanoate, β-ketopentanoate) were substantially increased in triheptanoin treated patients, while disease specific markers (C14:1) were reduced and C3 was increased.

Triheptanoin was also studied in 7 patients with CPTII deficiency with an age range 10–55 years' old for 7–61 months (Roe et al., 2008). All patients but one, had been hospitalized at least once for episodes of rhabdomyolysis and had been restricting exercise due to muscle pain on exertion. Their previous diet management consisted of low fat and increased carbohydrates, while patients younger than 14 years also received MCT oil comprising 6–10% of their daily caloric intake. By the end of the first week, most patients experienced some improvement in daily activities and within 1–2 months, their exercise tolerance was enhanced. While on triheptanoin, none was admitted due to rhabdomyolysis and two experienced mild muscle pain with exercise. All participants were able to compete in sports, a previously restricted activity. Two patients presented with rhabdomyolysis following strenuous exercise requiring admission after discontinuing triheptanoin use for 1–2 weeks.

A large retrospective review of 52 patients treated with triheptanoin included 8 infants, 28 children, 7 adolescents, and 9 adults with CPT-I, CACT, CPT II, VLCAD, TFP, and LCHAD deficiency (Roe and Brunengraber, 2015). Forty-one of the participants, had been using MCT prior to the study. All infants and children also received a daily L-carnitine supplement of 100 mg/kg divided four times daily with a maximum dose of a 1,000 mg. The average frequency of serious clinical complications was reduced from ∼60% on conventional diet therapy to ∼10% with triheptanoin and carnitine treatment, and mortality decreased from ∼65% on conventional diet therapy to 3.8%. Specifically, episodes of rhabdomyolysis that required admission reduced from 85 to 31%. Reported weakness decreased from 92 to 12%. Hepatomegaly and elevated liver enzymes were present in 46% of patients prior to treatment compared to 6% while on triheptanoin. Liver abnormalities were seen during intercurrent illness but resolved rapidly with treatment. Hypoglycemia was frequent with patients on conventional diets (42%) but was not reported after initiation of triheptanoin treatment. Cardiomyopathy was identified during the first year of life in 18 of the 52 patients prior to treatment with triheptanoin, while only one patient with VLCAD deficiency developed cardiomyopathy while on triheptanoin.

Case histories of several patients reported in this publication are noteworthy. Following the neonatal death of two affected siblings, one neonate with CACT was treated with triheptanoin at

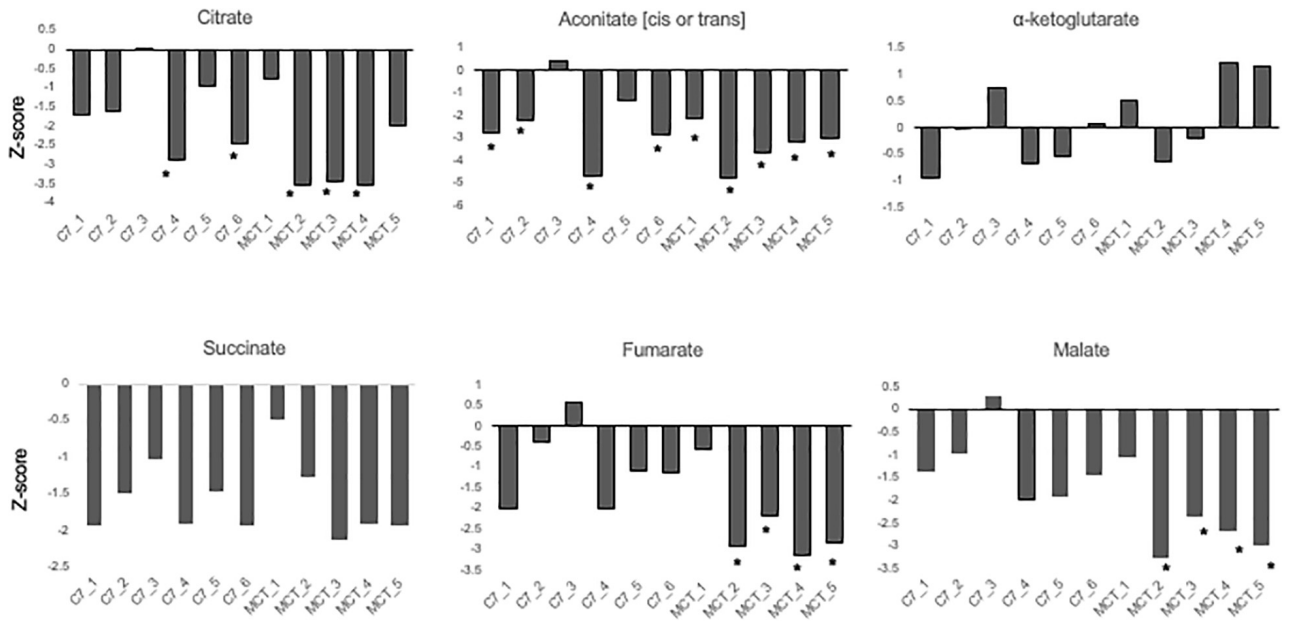

FIGURE 3 | Concentrations of TCA cycle intermediates in the blood from VLCAD deficiency patients treated with standard MCT oil (MCT1–5) or triheptanoin (C1–6). The values are given as *Z*-score, defined as the number of standard deviations from age and sex matched control means.

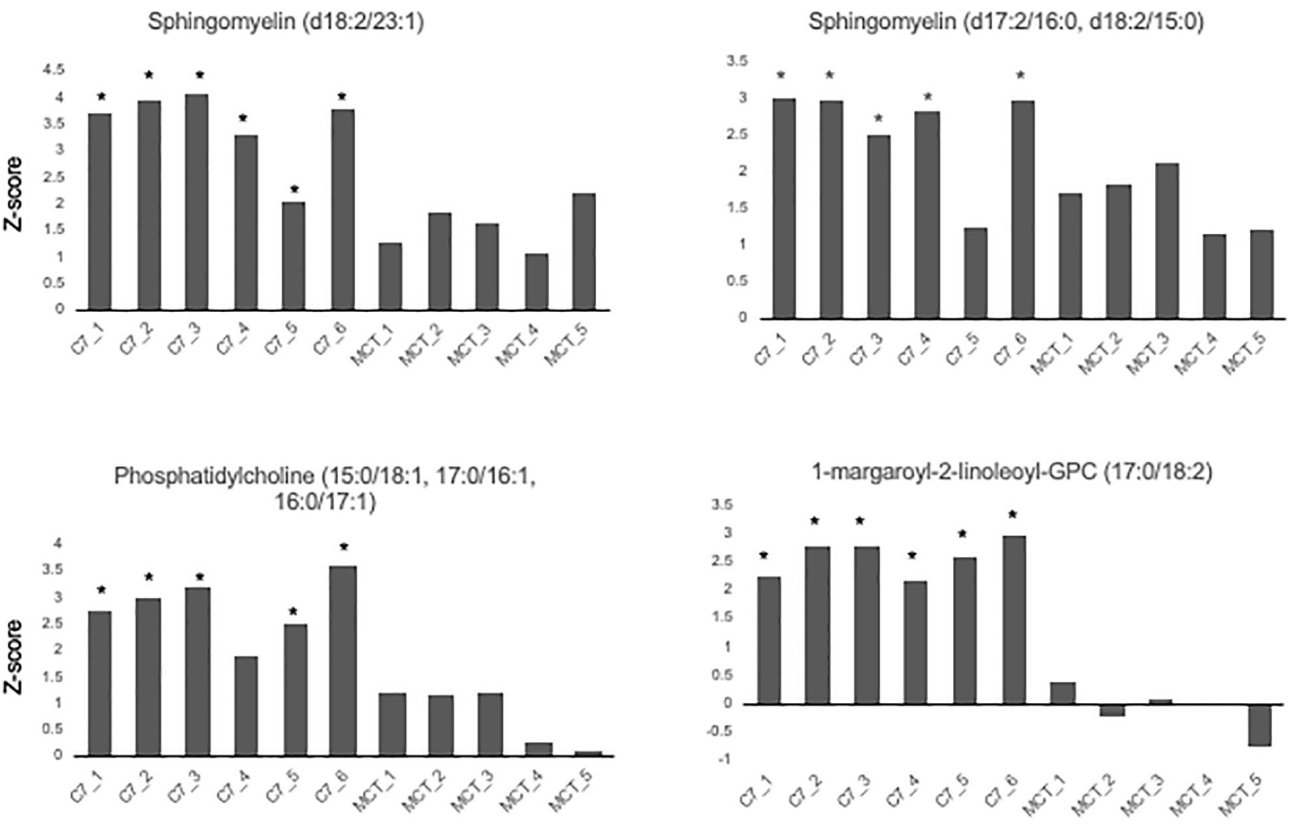

FIGURE 4 | Concentrations of odd chain long-chain complex lipids in VLCAD patients treated with MCG oil (MCT 1–5) or triheptanoin (C7 1–6). The values are given as *Z*-score, defined as the number of standard deviations from age and sex matched control means. Compound abbreviation are as defined in **Table 1**.

TABLE 2 | Triheptanoin studies for LC-FAODs.

Study (References)	Design	Sample size	Disease	Clinical presentation	Intervention	Outcomes
Roe et al., 2002; Mochel et al., 2005	Case series	3 (age 2,6 9 y)	VLCAD	Neonatal hypoglycemia (3 pt), cardiomyopathy (1 pt), muscle weakness (3 pt), hepatomegaly (2 pt), recurrent rhabdomyolysis episodes (2 pt).	Triheptanoin 2.6–4 gr/kg/day	Cardiomyopathy improved, hepatomegaly resolved, improved muscle strength, improved endurance and activity. One pt discontinued C7 and rhabdo episodes recurred.
Roe et al., 2008; Breen et al., 2014	Case series	7 (10–55 y)	CPTII	6 pts hospitalized at least once for rhabdo episodes. Hx of exercise restriction due to muscle pain	Triheptanoin 1-2 gr/kg/day (adolescents, adults). Triheptanoin 3–4 gr/kg/day (for pts <12 y), div QID. Prior to C7, 41 pts on MCT	Improvement in daily activities. None hospitalized for rhabdo while on C7. All pts able to compete in team sports. 2 pts had mild muscle pain w exercise. 2 pts admitted with rhabdo with strenuous exercise after discontinuing C7 × 1–2 weeks.
Pascual et al., 2014; Roe and Brunengraber, 2015	Case series	52 (birth-51 y)	CACT (2) CPTI (2) CPTII (11) LCHAD (10) TFP (6) VLCAD (21)	3 pts started C7 < 1 m old (1 at birth). 1 infant with CACT with ventricular arrhythmia, cardiomyopathy, hyperammonemia, hepatomegaly, hypotonia. 2 pregnant pts with VLCAD/rhabdo during previous pregnancies, muscle pain, weakness.	C7 at 30–35% of total dailt calories; 1 gr/kg/day (adolescents, adults), 3–4 gr/kg/day (<12 y)	SCC reduced (∼60% > ∼10%). Mortality decreased (∼65% > ∼3.8%). Rhabdo reduced (85% > 31%). Weakness decreased (92% > 12%). Hypoglycemia not reported (42% on previous conventional diet). Hepatomegaly, elev LFTs reduced (46% > 6%) Cardiomyopathy: 1 pt with VLCAD on C7, 18/52 pts before C7
Vockley et al., 2015; Mochel et al., 2016	Chart review, Retrospective	20	CACT (1) CPTII (3) LCHAD (5) TFP (2) VLCAD (9)	Cardiomyopathy Rhabdomyolysis Muscle pain Hypoglycemia	Analyzed pts' clinical course for the 2 years before and after the start of C7. 85% pt on MCT before.	35% reduction in mean hospitalizations/year. 67% decrease in mean total hospital days/year. Hypoglycemia event rate: 96% decrease. Cardiomyopathy improved (3/6), stable (1/6). Rhabdo event rate not change substantially (however, 60% decrease in mean hospital days/year)
Vockley et al., 2016b; Hainque et al., 2019	Case series	10 (2.5 m–20 y) 8pts < 1 y	CACT (2) LCHAD (2) TFP (2) VLCAD (4)	Cardiomyopathy. 9/10pts presented in infancy and most required ECMO and/or vasopressors	C7 at 25–35% of total calories	EF improvement between 2 and 21 ds. Mean EF increased to 60% (range 33–71) ECMO and/or pressors discontinued in 2–10 days 2 deaths: 3.5 m with VLCAD died of sepsis. 3.5 m old with TFP died of refractory cardiogenic shock.
Gillingham et al., 2017; Hainque et al., 2020	Double blind, randomized controlled trial	32	CPTII (11) LCHAD/TFP (12) VLCAD (9)	Recurrent episodes of rhabdomyolysis 1 pt with VLCAD with abnormal cardiac function. 1 pt with LCHAD had cardiac arrest with resuscitation.	Pts received diet with C7 vs. C8 at 20% of their total daily calories × 4 m	C7 pts: increased LVEF by 7.4%. C7 pts: exercise at lower max heart rate. Muscle symptoms: no difference between C7, C8 groups. Rhabdo admissions: Same in both groups. Admission length: Same in both groups.
Roe et al., 2010; Vockley et al., 2017	Single arm Open label	29 (10 m–58 y)	CPTII (4) LCHAD (10) VLCAD (12) TFP (3)	Skeletal myopathy[a] Hypoglycemia Cardiac disease. Hepatic disease.	C7 at 25–35% of total daily caloric intake × 24 weeks	12-MWT: 28% increase from baseline. ETT: 60% increase in generated watts. HR-QoL: significant improvement in 5/6 adults. No change from baseline in children.

(Continued)

TABLE 2 | Continued

Study (References)	Design	Sample size	Disease	Clinical presentation	Intervention	Outcomes
Calvert et al., 2018; Vockley et al., 2019a	Single arm. Open label.	29 (10 m–58 y)	CPTII (4) LCHAD (10) VLCAD (12) TFP (3)	Skeletal myopathy[a]. Hypoglycemia Cardiac disease. Hepatic disease.	C7 at 25–35% of total daily caloric intake × 78 weeks	MAMER: 48% decrease. MAMEDR: 50.3% decrease. MAHR: 53.1% decrease. MAHDR: 51.5% decrease. MARR: 36.1% decrease. MARDR: 29.3% decrease. Mean annualized hypoglycemia event rate: 92.8% decrease.

abn, abnormal; CACT, carnitine-acylcarnitine translocase; CPTI, carnitine palmitoyltransferase I; CPTII, carnitine palmitoyltransferase II; EF, ejection fraction; ETT, exercise tolerance test; HR-QoL, health related quality of life; LCHAD, long-chain 3-hydroxyacyl-CoA dehydrogenase; LFTs, liver function tests; LVEF, left ventricular ejection fraction; m, month(s); max, maximum; MAHDR, mean annualized hospitalization duration rate; MAHR, mean annualized hospitalization rate; MAMEDR, mean annualized major event duration rate; MAMER, mean annualized major event rate; MARDR, mean annualized rhabdomyolysis duration rate; MARR, mean annualized rhabdomyolysis rate; SCC, serious clinical complications; TFP, trifunctional protein; w, with; wk, week(s); y, year; 12MWT, 12-min walk test.[a]*Rhabdomyolysis, muscle pain, exercise intolerance, muscle weakness.*

18 h of life and remained asymptomatic for the first 7 months of life. Another patient with VLCAD deficiency and a family history of an affected sibling who died of hypertrophic cardiomyopathy was enrolled at 22 days of age and remained asymptomatic at 14 years of age. A neonate with LCHAD deficiency was treated at 15 days of age and remained well for 15 years on triheptanoin and carnitine, with occasionally illness-induced episodes of rhabdomyolysis. Two pregnant females with VLCAD deficiency were included in this review. One had history of multiple episodes of rhabdomyolysis during the third trimester with her 2 previous pregnancies. She was enrolled in the study at 26 weeks of gestational age with mild hepatomegaly, muscle weakness, and decreased endurance for day to day activities. After starting triheptanoin, her muscle strength and endurance increased, while her hepatomegaly resolved. She had no episode of rhabdomyolysis and her CPK levels remained normal until the delivery of a healthy baby. The second was a 34 years old treated at 20 weeks of gestation for weakness and a history of multiple episodes of rhabdomyolysis that required hospitalization after puberty. On triheptanoin her weakness resolved, and she had no muscle pain, weakness, or episodes of rhabdomyolysis for the remainder of the pregnancy.

A retrospective, comprehensive medical record review study reviewed data from 20 (9 VLCAD, 5 LCHAD, 3 CPT II, 2 TFP, and 1 CACT deficient) of a total 24 patients with LC-FAOD who were treated for up to 12.5 years (median 8.7 years) with triheptanoin as part of a compassionate use protocol (Vockley et al., 2015). Major medical events were collected from primary medical records, including hospitalizations and emergency room admissions and home treatment of rhabdomyolysis (CPK >5,000U/L), hypoglycemia and cardiomyopathy (Vockley et al., 2015). Analyses of data of an additional 4 infants that received triheptanoin at ≤6 m old were conducted separately for events of interest, because the time period prior to initiation of triheptanoin treatment was not sufficient to allow an accurate comparison of pre and post treatment events. About 85% of the patients received MCT oil and almost all were on a low-fat high carbohydrate diet. Total hospitalizations and hospital days per year were reduced by 35 and 67%, respectively, following initiation of triheptanoin treatment. Nine patients were experiencing hypoglycemia events prior to triheptanoin treatment., and these were essentially eliminated post treatment. Although the hospitalization rate due to rhabdomyolysis did not change substantially in eleven patients, their mean hospital days/year decreased by 60% on triheptanoin treatment. Six patients with cardiomyopathy participated in the study. The cardiomyopathy resolved prior to treatment in one patient with VLCAD deficiency, the cardiac function improved in three patients (CACT, LCHAD, and VLCAD deficiencies), and one patient (VLCAD deficient) remained stable while on treatment. One patient with neonatal CPTII deficiency had extremely poor pretreatment function with cardiac fibrosis, and eventually required a heart transplant. However, this patient experienced a dramatic improvement in muscle tone and glucose control. In the four infants who began treatment with triheptanoin before 6 months of age, the median post-treatment follow up was 9.5 years, and the mean number of hospital days/year was reduced by 91%. The overall hospitalization event rate was 13.01 annualized events/year pretreatment vs. 1.36 events/year post treatment, though the number of patients was small and there was high variability in the pretreatment period.

A case series of 10 patients with LC-FAOD who presented with cardiomyopathy in infancy and childhood and received triheptanoin on a compassionate basis included 4 patients with VLCAD, two with CACT, two with TFP, and two with LCHAD deficiency (Vockley et al., 2016b). One of the patients with VLCAD deficiency was also included in the previous retrospective study (Vockley et al., 2015). Nine patients had cardiomyopathy diagnosed within the first year of life and most of the patients required ECMO and/or vasopressors during their episode of decompensation with cardiomyopathy. Ejection fraction was available for 9 patients prior to triheptanoin treatment and its mean value was 28% (range 12–45%). Following initiation of triheptanoin, patients started showing improvements in their EF between days 2–21 and their mean EF increased to 60% (range 33–71%). Eight of the patients ultimately achieved an EF within the normal range. Two patients were weaned from ECMO within 2–3 days of initiating triheptanoin. In others, ECMO and/or vasopressors was discontinued within 8–10 days following initiation of

treatment. Two infants died, both at 3.5 months of age; one with VLCADD died of sepsis and one with TFP had refractory cardiogenic shock.

In a double blind randomized controlled trial, 32 subjects with LC-FAODs (11 with CPTII, 9 with VLCAD, 12 with LCHAD/TFP deficiency) older than 7 years old, received a diet containing 20% of their total energy intake from either triheptanoin (C7) or trioctanoin (C8) for 4 months (Gillingham et al., 2017). Primary outcomes included changes in total energy expenditure, cardiac function by echocardiogram, exercise tolerance, and phosphocreatine recovery following acute exercise. Secondary outcomes included body composition, blood biomarkers, and adverse events, including incidence of rhabdomyolysis. A 3-day diet record analysis during the 4-month treatment period showed that participants consumed approximately 16 and 14% of total reported energy intake from C7 and C8, respectively. All patients had a prior history of recurrent episodes of rhabdomyolysis requiring hospitalization. All patients except for one with VLCADD had normal cardiac function. A young adult with LCHAD had recently experienced sudden cardiac arrest with resuscitation. Echocardiographic data was only available for 10 subjects in the C7 and 11 subjects in the C8 group due a change in data collection part way through the study. After 4 months, patients on C7 had increased left ventricular ejection fraction (LVEF) by 7.4%, with an 8.0% decrease in LV wall mass on their resting echocardiogram. They were able to accomplish the same level of aerobic exercise at a significantly lower maximal heart rate, suggesting reverse cardiac remodeling and improved cardiorespiratory fitness. There was no significant difference in musculoskeletal symptoms between patients treated with C7 and C8; there were 7 hospitalizations for acute rhabdomyolysis in both groups, with no difference in the hospitalization length or peak CPK elevations during admissions. The other primary and secondary parameters were not different between the two groups. The main limitation of this study was the relatively short 4 months follow-up period. Thus, the clinical significance of cardiac function improvement in patients with normal ejection function could not be determined.

A single-arm, open-label, multi-center phase 2 study evaluated 29 patients (10 months–58 years old) with history of severe LC-FAOD for a total study duration of 78 weeks (Vockley et al., 2017, 2019a). Enrolled patients had history of severe LC-FAOD evidenced by ongoing musculoskeletal disease (86%), cardiomyopathy (∼7%), and hypoglycemia (10%). They received triheptanoin (UX007) in a titrating dose to 25–35% (mean 27.5%) of their total daily caloric intake, following a 4-week run in on their current treatment. All patients followed a low-fat high-carbohydrate diet prior to entering the study, 76% received carnitine supplementation, and 93% were on MCT. The objectives of the study were to evaluate changes in muscle function, exercise tolerance, and health-related quality of life following 24 weeks of treatment on triheptanoin (Vockley et al., 2017), as well as its impact on major clinical events associated with LC-FAOD over 78 weeks of treatment (Vockley et al., 2019a). An external control was employed with each patient's results on treatment compared to the year prior to starting the study. Patients were additionally evaluated on age/condition-eligible endpoints, including 12-min walk test (12MWT), cycle ergometry and age appropriate questionnaires to assess their health-related quality of life (HR-QoL). At week 18, eight eligible patients showed a 28% increase from baseline in 12MWT distance. At week 24, seven eligible patients showed a 60% increase over baseline in watts generated through cycle ergometry, and 5 adults reported significant improvements in physical and mental component scores on the HR-QoL scale compared to baseline. There was no difference in the physical health and psychosocial summary score in 5 pediatric patients compared to baseline. Eighty six percent of participants (25/29) elected to continue treatment in the 78 weeks extension period and pediatric patients now showed a significant increase in the physical health summary scores. Overall, there was a 48% reduction in the mean annualized major event rate and a 50.3% decrease in the mean annualized duration rate on triheptanoin. The mean annualized hospitalization rate and hospitalization duration was reduced by 53.1 and 51.5%, respectively. Rhabdomyolysis was the most common major event, and the mean annualized rhabdomyolysis rate decreased by 36.1%, while the mean annualized duration rate for rhabdomyolysis was reduced by 29.3%. The mean annualized hypoglycemia event rate decreased by 92.8%. The single hypoglycemia event that occurred during UX007 treatment, did not result in hospitalization, and occurred early during the UX007 treatment. Eleven hospitalizations due to hypoglycemia were recorded prior to UX007, with 2 episodes requiring ICU admission. There was a 69.7% decrease in annualized mean cardiomyopathy events (3 events in the pretreatment period, 1 event after UX007). While the study was a small size and unblinded, the objective nature of major events was well standardized in the historic control and treatment analyses.

Adverse events in all of the clinical trials were similar with C7 compared to C8 treatment with domination by gastrointestinal symptoms and/or those related to the underlying disease. Very few patients elected to discontinue C7 treatment during the trials, and those that did, did so because of gastrointestinal symptoms.

USE OF TRIHEPTANOIN IN OTHER DISORDERS

Triheptanoin has been studied as a potential therapy for several other disorders (**Table 3**). Most of these have significant neurologic phenotypes including seizures. Pyruvate carboxylase deficiency that results in depletion oxaloacetate, another cycle intermediate is probably the most attractive of this group. This enzyme is responsible for ensuring proper balance of oxaloacetate, the TCA cycle intermediate that together acetyl-CoA form citrate, for the TCA cycle to function normally. The anaplerotic effect of triheptanoin could in theory directly compensate for this defect; however, studies to date have reported conflicting results (Mochel et al., 2005; Breen et al., 2014). A clinical trial for treatment of seizures in GLUT1 deficiency failed to show improvement in a cohort of patients who had failed to respond to MCT oil, but a direct comparison was not performed (Mochel, 2017; Hainque et al., 2019; Hainque et al., 2020).

TABLE 3 | Use of triheptanoin in other disorders.

Study (References)	Design	Sample size	Disease	Clinical presentation	Intervention	Outcomes
Mochel et al., 2005	Case report	1	PCD	At birth w lactic acidosis (L 17 mmol/L), ketoacidosis, elevated LFTs, hypotonia, hyperammonemia, mild hepatomegaly, bilateral periventricular pseudocysts	Triheptanoin on d7, 35% of total calories. Loading dose 2 mg/kg, then 0.5 mg/kg q3h	Lactic acidosis decreased, NH3 normalized, liver failure reversed in <48 h, resolution of pseudocysts at 3 m. At 4 m: increased lactate and ketones. Died at 6 m from metabolic decompensation due to infection
Breen et al., 2014	Case report	2	PCD	Pt 1: presented at birth with lactic acidosis (L19.5 mmol/L), ketonuria, hyperammonemia, mild liver dysfunction, brain anomalies. Pt 2: presented at birth w severe lactic acidosis (L: 32 mmol/L), hyperammonemia, brain cysts.	Triheptanoin at 11 d (up to 36.5% total calories) Triheptanoin at 3 w (32% of total calories).	No improvement in clinical and biochemical parameters. Persistent lactic acidosis. Pt 1 died at 7 m of pneumonia. Pt 2 died at 8 m of L lung collapse, severe acidosis.
Pascual et al., 2014	Open label	14 (age 2—28 y)	GLUT1-DS	Varying degrees of disease severity, not receiving KD	Triheptanoin ∼1 gr/kg/d administered for 3 m. 12/14 pts completed the study. 5/14 had MRI imaging and 9/14 completed neuropsychological testing.	All patients had decreased spike-wave seizures. Most pts showed increase in cerebral metabolic rate and improved neuropsychological performance.
Mochel et al., 2016	Open label	8 (age 7–47 y)	GLUT1-DS	Pts with chronic history of non-epileptic paroxysmal motor disorders, limb weakness, headache, drowsiness, and dysphoria. Three pts had mild cognitive deficit. None received KD	Triheptanoin 1 gr/kg/d, div TID-QID for 2 m. Two pts were non-compliant	90% reduction of non-epileptic paroxysmal manifestations that recurred w treatment withdrawal. Brain bio-energetic profile (f-MRS) normalized but returned to abnormal with treatment withdrawal
Hainque et al., 2019	Open label, extended protocol of Mochel et al. (2016)	5	GLUT1-DS	Pts with history of non-epileptic paroxysmal motor disorders, limb weakness, headache, drowsiness, and dysphoria. Three pts had mild cognitive deficit. None received KD.	Triheptanoin 1 gr/kg/d, div TID-QID for 3 years. One pt withdrew.	Triheptanoin led to dramatic (97%) and sustained reduction of paroxysmal events
Hainque et al., 2020	Open label	4	GLUT1-DS	Pts with persistent paroxysmal manifestations previously on KD	Triheptanoin was gradually introduced in about 30% of pt's daily caloric intake. Pts were followed for 3 y	During transition from KD to triheptanoin, 3 pts had increased paroxysmal episodes. One pt quit after transition due to symptoms' worsening. At 3 y, 2 pts had sustained reduction of total events, 1 pt had stable events.
Roe et al., 2010	Open label	5 adults	APBD	Pts with variable APBD manifestations including difficulty walking, peripheral neuropathy, poor balance, weakness, neurogenic bladder, ptosis.	Triheptanoin at 1.0–1.5 gr/kg/d div QID for 30–35% daily caloric intake for 6–8 m.	All pts perceived stabilization of disease progression, and strength increase. Most patients had 6-min walk improvement, ptosis elimination and decreased leg burning. After 6–8 m on therapy, pts sensed plateau in rate of improvement.
Calvert et al., 2018	Open-label, non-randomized, uncontrolled phase I	12 (3—18 y)	Medically refractory epilepsy	Pts with epilepsy with at least 2 motor seizures per 2-wk period over 2 m before enrollment, despite treatment with at least one AED.	Triheptanoin titrated for 3–6 w up to a max dose of 35% caloric intake or 100 ml/d, div over 3–5 doses w meals. Duration of treatment on maintenance was 12 w.	8 pts completed the study; 5/8 had >50% reduction in seizure frequency. 2/8 had initial improvement but then relapsed although seizure control was better compared to pretreatment period. 1 pt had no changes. 4 pts exited the study due to GI side effects (diarrhea, abdominal pain). Seizures returned in 3 pts that went on extension.

(Continued)

TABLE 3 | Continued

Study (References)	Design	Sample size	Disease	Clinical presentation	Intervention	Outcomes
Borges et al., 2019	Double blind, randomized controlled trial	34 adults	Medicall y refractory epilepsy	Adult pts	Pts randomized to receive triheptanoin or MCT (17 pts to each arm) add-on treatment. Dose titrated over 3 w and maintained for another 12 w. Max dose 100 ml/d div TID	Number and type of adverse effects were similar between arms. Study not designed to compare anti-seizure effects. However, 5/11 pts on MCT showed >50% reduction of focal unaware seizures, 1/9 pts on triheptanoin showed seizure reduction.
Borges et al., 2020	Open label, extension trial	10	Medically refractory epilepsy	Adult pts with drug resistant epilepsy who had previously completed a 12 w randomized controlled trial of add-on MCT vs. triheptanoi, received add-on triheptanoin for 48 w.	Dose titrated over 3 w to a maximum tolerated dose of 100 ml/d or 35% caloric intake, then maintenance dose ×48 w	5/10 pts showed >50% reduction in seizure frequency. 2/10 completed 48 w trial. 8 pts withdrew due to lack of efficacy (3), seizure increase (1), other reasons excluding adverse effects (4).
Mochel et al., 2010	Open label, short-term	6	HD	Mild-to-moderate HD, measured by the UHDRS clinical scale.	Triheptanoin at 1 gr/kg/d for 4 d.	2 pts had end-exercise muscle acidosis that corrected 4 d post triheptanoin treatment. All pts had increased serum IGF1 after treatment. There was no significant change in UHDRS scores before and after triheptanoin.

AED, anti-epileptic drug; APBD, adult polyglucosan body disease; d, day(s); div, divided; f-MRS, functional^{31} P-NMR spectroscopy; GLUT1-DS, glucose transporter type 1 deficiency syndrome; h, hour(s); HD, Huntington's disease; KD, ketogenic diet; L, lactate; LFTs, liver function tests; m, month(s); MCT, medium−chain triglycerides; NH3, ammonia; PCD, pyruvate carboxylase deficiency; pt, patient; UHDRS, unified Huntington Disease Rating Scale; w, week(s); y, year(s).

FAO and Cardiolipin Metabolism

Cardiolipin (CL) is the main phospholipid in the inner mitochondrial membrane (IMM) (Mejia et al., 2014; Ren et al., 2014). Unlike other phospholipids, it has 4 fatty acyl chains. In the heart and muscle, its predominant form is tetralinoleoylcardiolipin (L4CL); which has 4 symmetrical linoleoyl chains giving it a coned shape. This unique molecular structure and location is critical to maintain the integrity of the cristae of the IMM, cristae, and respiratory chain complexes (OXPHOS) to optimize energy production capacity as demonstrated by the severe cardiac manifestations seen in Barth syndrome due to *TAZ* gene mutations. This defect alters the composition and distribution of cardiolipin species leading to a major reduction in L4CL species, and accumulation of an asymmetrical form of monolysocardiolipin, leading to disorganization and destabilization of the IMM and OXPHOS supercomplexes, reduced ATP production and cardiac dysfunction (Ikon and Ryan, 2017). Recently, it has been demonstrated that the MTPα/HADHA subunit also encompasses a monolysocardiolipin acetyltransferase (MLCLAT) activity critical to cardiolipin remodeling (Taylor et al., 2012; Miklas et al., 2019). MLCLAT is a portion of the C-terminus (59 kDa) of MTPα/HADHA (75 kDa) minus the final 227 amino acids. MLCLAT has *in vitro* specificity for linoleoyl-CoA > oleoyl-CoA > palmitoyl-CoA, and specificity for acylation of monolysocardiolipin. Pluripotential stem cells made from an HADAH deficient patient differentiated to a cardiomyocyte phenotype show impaired calcium metabolism and repolarization kinetics and mitochondrial bioenergetics with abnormal mitochondrial structure and maturation of cardiolipin (Miklas et al., 2019). The mitochondrial proton leak improved with treatment with SS-31, a cardiolipin binding peptide that improves mitochondrial stability, emphasizing the role of LCHAD in cardiolipin metabolism. Some symptoms seen in LCHAD/TFP deficient patients are unique among the LC-FAODs (retinopathy and peripheral neuropathy) and are more in keeping with those seen in mitochondrial myopathies. Thus the role of CL abnormalities related to the development of these symptoms in LCHAD/TFP deficiency remains to be determined.

SUMMARY

In summary, patients with LC-FAODs have a secondary deficit of TCA cycle intermediates that further impairs the primary energy deficit due to defective FAD. Triheptanoin is an anaplerotic medium chain triglyceride that provides both even and odd chain substrates to the TCA cycle, restoring its balance and improving ATP generation in experimental systems. LC-FAOD Patients treated with triheptanoin show significant improvement compared to pretreatment, with the greatest improvements in glucose homeostasis and cardiomyopathy. While episodes of rhabdomyolysis decreased significantly with triheptanoin treatment, the effect was less than with the other symptoms, suggesting a role for other pathophysiologic mechanisms and demonstrating the need for additional therapies. The

use of triheptanoin in a variety of other disorders remains under investigation.

AUTHOR CONTRIBUTIONS

ES performed the literature review and wrote the first draft of the manuscript. AA performed metabolomic experiments. SD and A-WM helped supervise metabolomic experiments and edited manuscript. JV supervised entire project, edited manuscript, and made figures. All authors contributed to the article and approved the submitted version.

FUNDING

JV was funded in part by NIH Grants R01-DK78755 and FD-R03895-01, and was the lead investigator in clinical trials of triheptanoin for long chain fatty acid oxidation disorders sponsored by Ultragenyx.

REFERENCES

Baruteau, J., Sachs, P., Broué, P., Brivet, M., Abdoul, H., Vianey-Saban, C., et al. (2013). Clinical and biological features at diagnosis in mitochondrial fatty acid beta-oxidation defects: a French pediatric study of 187 patients. *J. Inherit. Metab. Dis.* 36, 795–803. doi: 10.1007/s10545-012-9542-6

Borges, K., Kaul, N., Germaine, J., Carrasco-Pozo, C., Kwan, P., and O'Brien, T. J. (2020). Open-label long-term treatment of add-on triheptanoin in adults with drug-resistant epilepsy. *Epilepsia Open* 5, 230–239. doi: 10.1002/epi4.12391

Borges, K., Kaul, N., Germaine, J., Kwan, P., and O'Brien, T. J. (2019). Randomized trial of add-on triheptanoin vs medium chain triglycerides in adults with refractory epilepsy. *Epilepsia Open* 4, 153–163. doi: 10.1002/epi4.12308

Breen, C., White, F. J., Scott, C. A., Heptinstall, L., Walter, J. H., Jones, S. A., et al. (2014). Unsuccessful treatment of severe pyruvate carboxylase deficiency with triheptanoin. *Eur. J. Pediatr.* 173, 361–366. doi: 10.1007/s00431-013-2166-5

Calvert, S., Barwick, K., Par, M., Ni Tan, K., and Borges, K. (2018). A pilot study of add-on oral triheptanoin treatment for children with medically refractory epilepsy. *Eur. J. Paediatr. Neurol.* 22, 1074–1080. doi: 10.1016/j.ejpn.2018.07.014

Dehaven, C. D., Evans, A. M., Dai, H., and Lawton, K. A. (2010). Organization of GC/MS and LC/MS metabolomics data into chemical libraries. *J. Cheminform.* 2:9.

Deng, S., Zhang, G. F., Kasumov, T., Roe, C. R., and Brunengraber, H. (2009). Interrelations between C4 ketogenesis, C5 ketogenesis, and anaplerosis in the perfused rat liver. *J. Biol. Chem.* 284, 27799–27807. doi: 10.1074/jbc.m109.048744

Dobrowolski, S. F., Alodaib, A., Karunanidhi, A., Basu, S., Holecko, M., Lichter-Konecki, U., et al. (2020). Clinical, biochemical, mitochondrial, and metabolomic aspects of methylmalonate semialdehyde dehydrogenase deficiency: report of a fifth case. *Mol. Genet. Metab.* 129, 272–277. doi: 10.1016/j.ymgme.2020.01.005

Evans, A. M., DeHaven, C. D., Barrett, T., Mitchell, M., and Milgram, E. (2009). Integrated, nontargeted ultrahigh performance liquid chromatography/electrospray ionization tandem mass spectrometry platform for the identification and relative quantification of the small-molecule complement of biological systems. *Anal. Chem.* 81, 6656–6667. doi: 10.1021/ac901536h

Gillingham, M. B., Heitner, S. B., Martin, J., Rose, S., Goldstein, A., El-Gharbawy, A. H., et al. (2017). Triheptanoin versus trioctanoin for long-chain fatty acid oxidation disorders: a double blinded, randomized controlled trial. *J. Inherit. Metab. Dis.* 40, 831–843. doi: 10.1007/s10545-017-0085-8

Gu, L., Zhang, G. F., Kombu, R. S., Allen, F., Kutz, G., Brewer, W. U., et al. (2010). Parenteral and enteral metabolism of anaplerotic triheptanoin in normal rats. II. Effects on lipolysis, glucose production, and liver acyl-CoA profile. *Am. J. Physiol. Endocrinol. Metab.* 298, E362–E371.

Hainque, E., Gras, D., Meneret, A., Atencio, M., Luton, M. P., Barbier, M., et al. (2019). Long-term follow-up in an open-label trial of triheptanoin in GLUT1 deficiency syndrome: a sustained dramatic effect. *J. Neurol. Neurosurg. Psychiatry* 90, 1291–1293. doi: 10.1136/jnnp-2018-320283

Hainque, E., Meneret, A., Gras, D., Atencio, M., Luton, M. P., Barbier, M., et al. (2020). Transition from ketogenic diet to triheptanoin in patients with GLUT1 deficiency syndrome. *J. Neurol. Neurosurg. Psychiatry* 91, 444–445. doi: 10.1136/jnnp-2019-321694

Ikon, N., and Ryan, R. O. (2017). Barth syndrome: connecting cardiolipin to cardiomyopathy. *Lipids* 52, 99–108. doi: 10.1007/s11745-016-4229-7

Kinman, R. P., Kasumov, T., Jobbins, K. A., Thomas, K. R., Adams, J. E., Brunengraber, L. N., et al. (2006). Parenteral and enteral metabolism of anaplerotic triheptanoin in normal rats. *Am. J. Physiol. Endocrinol. Metab.* 291, E860–E866.

Knottnerus, S. J. G., Bleeker, J. C., Wüst, R. C. I., Ferdinandusse, S., IJlst, L., Wijburg, F. A., et al. (2018). Disorders of mitochondrial long-chain fatty acid oxidation and the carnitine shuttle. *Rev. Endocr. Metab. Disord.* 19, 93–106. doi: 10.1007/s11154-018-9448-1

Liang, K., Li, N., Wang, X., Dai, J., Liu, P., Wang, C., et al. (2018). Cryo-EM structure of human mitochondrial trifunctional protein. *Proc. Natl. Acad. Sci. U.S.A.* 115, 7039–7044. doi: 10.1073/pnas.1801252115

Lindner, M., Hoffmann, G. F., and Matern, D. (2010). Newborn screening for disorders of fatty-acid oxidation: experience and recommendations from an expert meeting. *J. Inherit. Metab. Dis.* 33, 521–526. doi: 10.1007/s10545-010-9076-8

Longo, N. (2016). Primary carnitine deficiency and newborn screening for disorders of the carnitine cycle. *Ann. Nutr. Metab.* 68(Suppl. 3), 5–9. doi: 10.1159/000448321

Marsden, D., Bedrosian, C., and Vockley, J. (2020). Impact of newborn screening on the reported incidence and clinical outcomes associated with medium- and long-chain fatty acid oxidation disorders. *Genet. Med.*

Mejia, E. M., Nguyen, H., and Hatch, G. M. (2014). Mammalian cardiolipin biosynthesis. *Chem. Phys. Lipids* 179, 11–16. doi: 10.1016/j.chemphyslip.2013.10.001

Miklas, J. W., Clark, E., Levy, S., Detraux, D., Leonard, A., Beussman, K., et al. (2019). TFPa/HADHA is required for fatty acid beta-oxidation and cardiolipin re-modeling in human cardiomyocytes. *Nat. Commun.* 10:4671.

Mochel, F. (2017). Triheptanoin for the treatment of brain energy deficit: a 14-year experience. *J. Neurosci. Res.* 95, 2236–2243. doi: 10.1002/jnr.24111

Mochel, F., DeLonlay, P., Touati, G., Brunengraber, H., Kinman, R. P., Rabier, D., et al. (2005). Pyruvate carboxylase deficiency: clinical and biochemical response to anaplerotic diet therapy. *Mol. Genet. Metab.* 84, 305–312. doi: 10.1016/j.ymgme.2004.09.007

Mochel, F., Duteil, S., Marelli, C., Jauffret, C., Barles, A., Holm, J., et al. (2010). Dietary anaplerotic therapy improves peripheral tissue energy metabolism in patients with Huntington's disease. *Eur. J. Hum. Genet.* 18, 1057–1060. doi: 10.1038/ejhg.2010.72

Mochel, F., Hainque, E., Gras, D., Adanyeguh, I. M., Caillet, S., Héron, B., et al. (2016). Triheptanoin dramatically reduces paroxysmal motor disorder in patients with GLUT1 deficiency. *J. Neurol. Neurosurg. Psychiatry* 87, 550–553. doi: 10.1136/jnnp-2015-311475

Nahabet, E. H., Gatherwright, J., Vockley, J., Henderson, N., Tomei, K. L., Grigorian, A. P., et al. (2016). Postnatal pancraniosynostosis in a patient with infantile hypophosphatasia. *Cleft Palate Craniofac. J.* 53, 741–744. doi: 10.1597/15-027

Pascual, J. M., Liu, P., Mao, D., Kelly, D. I., Hernandez, A., Sheng, M., et al. (2014). Triheptanoin for glucose transporter type I deficiency (G1D): modulation of human ictogenesis, cerebral metabolic rate, and cognitive indices by a food supplement. *JAMA Neurol.* 71, 1255–1265. doi: 10.1001/jamaneurol.2014.1584

Quell, J. D., Römisch-Margl, W., Colombo, M., Krumsiek, J., Evans, A. M., Mohney, R., et al. (2017). Automated pathway and reaction prediction facilitates in silico identification of unknown metabolites in human cohort studies.

J. Chromatogr. B Analyt. Technol. Biomed. Life Sci. 1071, 58–67. doi: 10.1016/j.jchromb.2017.04.002

Rector, R. S., Payne, R. M., and Ibdah, J. A. (2008). Mitochondrial trifunctional protein defects: clinical implications and therapeutic approaches. *Adv. Drug. Deliv. Rev.* 60, 1488–1496. doi: 10.1016/j.addr.2008.04.014

Ren, M., Phoon, C. K., and Schlame, M. (2014). Metabolism and function of mitochondrial cardiolipin. *Prog. Lipids Res.* 55, 1–16. doi: 10.1016/j.plipres.2014.04.001

Roe, C. R., Bottiglieri, T., Wallace, M., Arning, E., and Martin, A. (2010). Adult polyglucosan body disease (APBD): anaplerotic diet therapy (Triheptanoin) and demonstration of defective methylation pathways. *Mol. Genet. Metab.* 101, 246–252. doi: 10.1016/j.ymgme.2010.06.017

Roe, C. R., and Brunengraber, H. (2015). Anaplerotic treatment of long-chain fat oxidation disorders with triheptanoin: review of 15 years experience. *Mol. Genet. Metab.* 116, 260–268. doi: 10.1016/j.ymgme.2015.10.005

Roe, C. R., Sweetman, L., Roe, D. S., David, F., and Brunengraber, H. (2002). Treatment of cardiomyopathy and rhabdomyolysis in long-chain fat oxidation disorders using an anaplerotic odd-chain triglyceride. *J. Clin. Invest.* 110, 259–269. doi: 10.1172/jci0215311

Roe, C. R., Yang, B. Z., Brunengraber, H., Roe, D. S., Wallace, M., and Garritson, B. K. (2008). Carnitine palmitoyltransferase II deficiency: successful anaplerotic diet therapy. *Neurology* 71, 260–264. doi: 10.1212/01.wnl.0000318283.42961.e9

Spiekerkoetter, U., Bennett, M. J., Ben-Zeev, B., Strauss, A. W., and Tein, I. (2004). Peripheral neuropathy, episodic myoglobinuria, and respiratory failure in deficiency of the mitochondrial trifunctional protein. *Muscle Nerve* 29, 66–72. doi: 10.1002/mus.10500

Spiekerkoetter, U., Lindner, M., Santer, R., Grotzke, M., Baumgartner, M. R., Boehles, H., et al. (2009b). Treatment recommendations in long-chain fatty acid oxidation defects: consensus from a workshop. *J. Inherit. Metab. Dis.* 32, 498–505. doi: 10.1007/s10545-009-1126-8

Spiekerkoetter, U., Lindner, M., Santer, R., Grotzke, M., Baumgartner, M. R., Boehles, H., et al. (2009a). Management and outcome in 75 individuals with long-chain fatty acid oxidation defects: results from a workshop. *J. Inherit. Metab. Dis.* 32, 488–497. doi: 10.1007/s10545-009-1125-9

Spiekerkoetter, U., and Mayatepek, E. (2010). Update on mitochondrial fatty acid oxidation disorders. *J. Inherit. Metab. Dis.* 33, 467–468. doi: 10.1007/s10545-010-9208-1

Swigonova, Z., Mohsen, A. W., and Vockley, J. (2009). Acyl-CoA dehydrogenases: dynamic history of protein family evolution. *J. Mol. Evol.* 69, 176–193. doi: 10.1007/s00239-009-9263-0

Taylor, W. A., Mejia, E. M., Mitchell, R. W., Choy, PC., Sparagna, GC., and Hatch, GM. (2012). Human trifunctional protein alpha links cardiolipin remodeling to beta-oxidation. *PLoS One* 7:e48628. doi: 10.1371/journal.pone.0048628

Tucci, S. (2017). Very long-chain acyl-CoA dehydrogenase (VLCAD-) deficiency-studies on treatment effects and long-term outcomes in mouse models. *J. Inherit. Metab. Dis.* 40, 317–323. doi: 10.1007/s10545-017-0016-8

Tucci, S., Behringer, S., and Spiekerkoetter, U. (2015). De novo fatty acid biosynthesis and elongation in very long-chain acyl-CoA dehydrogenase-deficient mice supplemented with odd or even medium-chain fatty acids. *FEBS J.* 282, 4242–4253. doi: 10.1111/febs.13418

Tucci, S., Floegel, U., Beermann, F., Behringer, S., and Spiekerkoetter, U. (2017). Triheptanoin: long-term effects in the very long-chain acyl-CoA dehydrogenase-deficient mouse. *J. Lipid Res.* 58, 196–207. doi: 10.1194/jlr.m072033

Vieira de Melo, I. S., Da Rocha Ataide, T., Lima de Oliveira, S., Bezerra Bueno, N., Duarte de Freitas, J., and Goulart Sant'Ana, A. E. (2015). Hepatic fatty acid profile of rats fed a triheptanoin-based ketogenic diet. *Nutr. Hosp.* 32, 265–269.

Vockley, J., Bennett, M. J., and Gillingham, M. B. (2016a). "Mitochondrial fatty acid oxidation disorders," in *The Online Metabolic and Molecular Bases of Inherited Disease*, eds A. L. Beaudet, B. Vogelstein, K. W. Kinzler, S. E. Antonarakis, A. Ballabio, K. M. Gibson, and G. Mitchell (New York, NY: The McGraw-Hill Companies, Inc).

Vockley, J., Burton, B., Berry, G. T., Longo, N., Phillips, J., Sanchez-Valle, A., et al. (2017). UX007 for the treatment of long chain-fatty acid oxidation disorders: safety and efficacy in children and adults following 24weeks of treatment. *Mol. Genet. Metab.* 120, 370–377. doi: 10.1016/j.ymgme.2017.02.005

Vockley, J., Burton, B., Berry, G. T., Longo, N., Phillips, J., Sanchez-Valle, A., et al. (2019a). Results from a 78-week, single-arm, open-label phase 2 study to evaluate UX007 in pediatric and adult patients with severe long-chain fatty acid oxidation disorders (LC-FAOD). *J. Inherit. Metab. Dis.* 42, 169–177. doi: 10.1002/jimd.12038

Vockley, J., Charrow, J., Ganesh, J., Eswara, M., Diaz, G. A., McCracken, E., et al. (2016b). Triheptanoin treatment in patients with pediatric cardiomyopathy associated with long chain-fatty acid oxidation disorders. *Mol. Genet. Metab.* 119, 223–231. doi: 10.1016/j.ymgme.2016.08.008

Vockley, J., Dobrowolski, S. F., Arnold, G. L., Guerrero, R. B., Derks, T. G. J., Weinstein, D. A., et al. (2019b). Complex patterns of inheritance, including synergistic heterozygosity, in inborn errors of metabolism: Implications for precision medicine driven diagnosis and treatment. *Mol. Genet. Metab.* 128, 1–9. doi: 10.1016/j.ymgme.2019.07.011

Vockley, J., Marsden, D., McCracken, E., DeWard, S., Barone, A., Hsu, K., et al. (2015). Long-term major clinical outcomes in patients with long chain fatty acid oxidation disorders before and after transition to triheptanoin treatment–A retrospective chart review. *Mol. Genet. Metab.* 116, 53–60. doi: 10.1016/j.ymgme.2015.06.006

Vockley, J., Singh, R. H., and Whiteman, D. A. (2002). Diagnosis and management of defects of mitochondrial beta-oxidation. *Curr. Opin. Clin. Nutr. Metab. Care* 5, 601–609. doi: 10.1097/00075197-200211000-00002

Wilcken, B., Haas, M., Joy, P., Wiley, V., Bowling, F., Carpenter, K., et al. (2009). Expanded newborn screening: outcome in screened and unscreened patients at age 6 years. *Pediatrics* 124, e241–e248.

Xia, C., Fu, Z., Battaile, K. P., and Kim, J. P. (2019). Crystal structure of human mitochondrial trifunctional protein, a fatty acid beta-oxidation metabolon. *Proc. Natl. Acad. Sci. U.S.A.* 116, 6069–6074. doi: 10.1073/pnas.1816317116

Conflict of Interest: The authors declare that the research was conducted in the absence of any commercial or financial relationships that could be construed as a potential conflict of interest.

frontiers in Genetics

ORIGINAL RESEARCH
published: 25 January 2021
doi: 10.3389/fgene.2021.625120

Glycine Cleavage System H Protein Is Essential for Embryonic Viability, Implying Additional Function Beyond the Glycine Cleavage System

Kit-Yi Leung, Sandra C. P. De Castro, Gabriel L. Galea, Andrew J. Copp and Nicholas D. E. Greene†*

Great Ormond Street Institute of Child Health, University College London, London, United Kingdom

Glycine cleavage system H protein (GCSH) is a component of the glycine cleavage system (GCS), a conserved protein complex that acts to decarboxylate glycine. Mutation of *AMT* or *GLDC*, encoding the GCS components aminomethyltransferase and glycine decarboxylase, can cause malformations of the developing CNS (neural tube defects (NTDs) and ventriculomegaly) as well as a post-natal life-limiting neurometabolic disorder, Non-Ketotic Hyperglycinemia. In contrast, it is unclear whether mutation of *GCSH* contributes to these conditions and we therefore investigated GCSH loss of function in mice. Mice that were heterozygous for a *Gcsh* null allele were viable and did not exhibit elevated plasma glycine. Moreover, heterozygous mutation of *Gcsh* did not increase the frequency of NTDs in *Gldc* mutant embryos. Homozygous *Gcsh* null mice were not recovered at post-natal stages. Analysis of litters at E8.5-10.5, revealed the presence of homozygous null embryos which were much smaller than littermates and had failed to develop beyond early post-implantation stages with no visible somites or head-folds. Hence, unlike null mutations of *Gldc* or *Amt*, which are compatible with embryonic survival despite the presence of NTDs, loss of *Gcsh* causes embryonic death prior to mid-gestation. Maternal supplementation with formate did not restore embryonic development beyond E7.5, suggesting that the primary cause of lethality was not loss of glycine cleavage activity or suppression of folate one-carbon metabolism. These findings suggest that GCSH has additional roles beyond function in the glycine cleavage system. We hypothesize that GCSH potentially acts in lipoylation of 2-oxoacid dehydrogenase proteins, as reported in bacteria.

Keywords: glycine cleavage system, glycine cleavage system H protein, embryonic lethality, lipoylation, mouse models

OPEN ACCESS

Edited by:
Guilhian Leipnitz, Federal University of Rio Grande do Sul, Brazil

Reviewed by:
Dean Appling, University of Texas at Austin, United States
Nelson L. S. Tang, The Chinese University of Hong Kong, China

***Correspondence:**
Nicholas D. E. Greene
n.greene@ucl.ac.uk
orcid.org/0000-0002-4170-5248

Specialty section:
This article was submitted to Genetics of Common and Rare Diseases, a section of the journal Frontiers in Genetics

Received: *02 November 2020*
Accepted: *04 January 2021*
Published: *25 January 2021*

Citation:
Leung K-Y, De Castro SCP, Galea GL, Copp AJ and Greene NDE (2021) Glycine Cleavage System H Protein Is Essential for Embryonic Viability, Implying Additional Function Beyond the Glycine Cleavage System. Front. Genet. 12:625120. doi: 10.3389/fgene.2021.625120

INTRODUCTION

Glycine cleavage system H-protein (GCSH) is one of four enzymes which, together with glycine decarboxylase (GLDC), aminomethyltransferase (AMT), and dehydrolipamide dehydrogenase (DLD), make up the glycine cleavage system (GCS). This highly conserved protein complex is located at the mitochondrial membrane in eukaryotes and is the major route of glycine catabolism.

GCS action involves oxidative cleavage of glycine with release of carbon dioxide (CO_2) and ammonia (NH_3) and transfer of a methylene group ($-CH_2-$) to tetrahydrofolate, with concomitant reduction of NAD^+ to NADH (**Figure 1A**; Kikuchi et al., 2008).

Based on analysis in the leaf of pea plants (*Pisum sativum*), the stoichiometry of the GCS is estimated at 4 GLDC :27 GCSH: 9 AMT :2 DLD (Oliver et al., 1990). GCSH plays a central role in the catalytic process, forming an amino-methyl intermediate with GLDC and acting as the acceptor of the methylamine group which is then transferred as the substrate for AMT (**Figure 1A**). This function of GCSH depends on modification by covalent addition of lipoic acid, as a cofactor, to form the active lipoyl-enzyme. The lipoyl moiety is believed to assembled on GCSH in a multi-step process, with addition of the octanoyl group followed by insertion of the sulphydryl groups (**Figure 1B**; Christensen et al., 2011; Cao et al., 2018b; Cronan, 2020). DLD mediates reduction of NAD^+ and oxidation of the lipoyl group of GCSH (**Figure 1A**).

Loss of function of the GCS is predicted to cause accumulation of glycine and suppression of folate one-carbon metabolism (FOCM) and this is associated with post-natal neurometabolic disease and structural malformations of the developing brain including neural tube defects (NTDs) and ventriculomegaly. Accumulation of glycine in tissue and body fluids is a hallmark of Non-Ketotic Hyperglycinemia (NKH), a life-limiting inborn error of metabolism which presents in the neonatal period with hypotonia, apnea, and seizures. Subsequently, affected babies and children suffer complex epilepsy and profound developmental delay (Hoover-Fong et al., 2004; Swanson et al., 2015). Enlarged brain ventricles and/or hydrocephalus are also associated with NKH in a proportion of patients (Van Hove et al., 2000; Hennermann et al., 2012). Classic NKH, caused by mutation of GCS-encoding genes, is inherited as an autosomal recessive condition with the majority of patients carrying mutations in *GLDC* and around 20% carrying mutations in *AMT* (Kure et al., 2006; Kanno et al., 2007; Coughlin et al., 2017).

In addition to NKH, mutations in *GLDC* and *AMT* contribute to susceptibility to NTDs (Narisawa et al., 2012; Shah et al., 2016), severe birth defects which result from failed closure of the neural tube during embryonic development. To date, GCS mutations reported in NTDs are in heterozygous form suggesting that mutations in other genes and/or environmental factors also contribute to these cases, consistent with the multifactorial etiology of NTDs (Greene and Copp, 2014).

The potential role of *GLDC* and *AMT* mutations in some NTDs is supported by the occurrence of NTDs in mouse knockouts of the orthologous genes (Narisawa et al., 2012; Pai et al., 2015; Leung et al., 2017). Among *Gldc*-deficient mice that are not affected by NTDs, the occurrence of ventriculomegaly and hydrocephalus (resulting from stenosis of the aqueduct of Sylvius) similarly confirm that these are specific effects of GCS-encoding mutations in NKH patients (Autuori et al., 2017; Santos et al., 2020).

The loss of GCS activity in *Gldc*-deficient mice results in elevated glycine and a number of glycine derivatives in plasma and tissues, including liver and brain (Pai et al., 2015; Leung et al., 2020). In parallel, metabolic labeling shows that the contribution of glycine-derived one-carbon units to folate one-carbon metabolism is ablated (Leung et al., 2017) and the folate profile is perturbed, with a deficit of folates that carry one-carbon groups (Pai et al., 2015).

Whereas DLD acts in at least three other mitochondrial enzyme complexes, GLDC, AMT, and GCSH have been described as specific to the glycine cleavage system. However, unlike *GLDC* and *AMT*, mutations in *GCSH* have not been reported in patients with NTDs or NKH (Kure et al., 2006; Coughlin et al., 2017). However, a putative heterozygous mutation was identified in an individual with transient neonatal hyperglycinemia (Kure et al., 2002). In addition, patients have been identified in which elevated plasma glycine is associated with reduced GCSH activity and defects in addition of the lipoic acid moiety (Hiraga et al., 1981), with mutations identified in lipoic acid synthase, *LIAS* (Baker et al., 2014). In the current study, we investigated the effect of *Gcsh* loss of function in mice, in order to ask whether this revealed a potential role in NTDs and/or features of NKH.

MATERIALS AND METHODS

Mice

Animal studies were carried out under regulations of the Animals (Scientific Procedures) Act 1986 of the United Kingdom Government, and in accordance with the guidance issued by the Medical Research Council, United Kingdom in *Responsibility in the Use of Animals for Medical Research* (July 1993). The $Gcsh^{em1(IMPC)H}$ (previously denoted H-GCSH-DEL653-EM1-B6N) mouse line was generated by CRISPR/Cas9 targeting at MRC Harwell, Mary Lyon Centre (Oxfordshire) on a C57BL/6N Tac background (Mianne et al., 2017). The *Gcsh* mutant allele (hereafter denoted $Gcsh^-$) carried a deletion of 653 nucleotides (nucleotides 116,987,776–116,987,124) encompassing exon 3 of *Gcsh* (ENSMUSG00000034424).

Genotyping

Genotyping of mice and embryos was carried out by PCR amplification of genomic DNA. Use of primers which flank the deletion (*Gcsh*_F2;5′-GCACGTAGTAGGGTTGACAAGT-3′ and Gcsh_R2; 5′-CGCGGATGGAGAACTGTAAGG-3′) produces a PCR product of 1,033 bp from wild-type DNA whereas the deletion allele generates a smaller product of 380 bp. A confirmatory reaction (Gcsh_F2 primer and Gsch_R1; 5′-CAGGAAGCGTTGGGAGATGTTG-3′) used a reverse primer which binds in the deleted region and therefore generated PCR product from wild-type but not *Gcsh* deleted DNA.

Generation of $Gldc^{-/-}$; $Gcsh^{+/-}$ Mice

Gldc-deficient mice, denoted $Gldc^{GT1}$, carry a gene-trap construct in intron 2 of *Gldc* (Pai et al., 2015) and are maintained on a C57Bl/6J background. $Gldc^{GT1/+}$; $Gcsh^{+/-}$ males were generated by intercross of $Gcsh^{+/-}$ males with $Gldc^{GT1/+}$ females. The double heterozygotes were used in timed matings

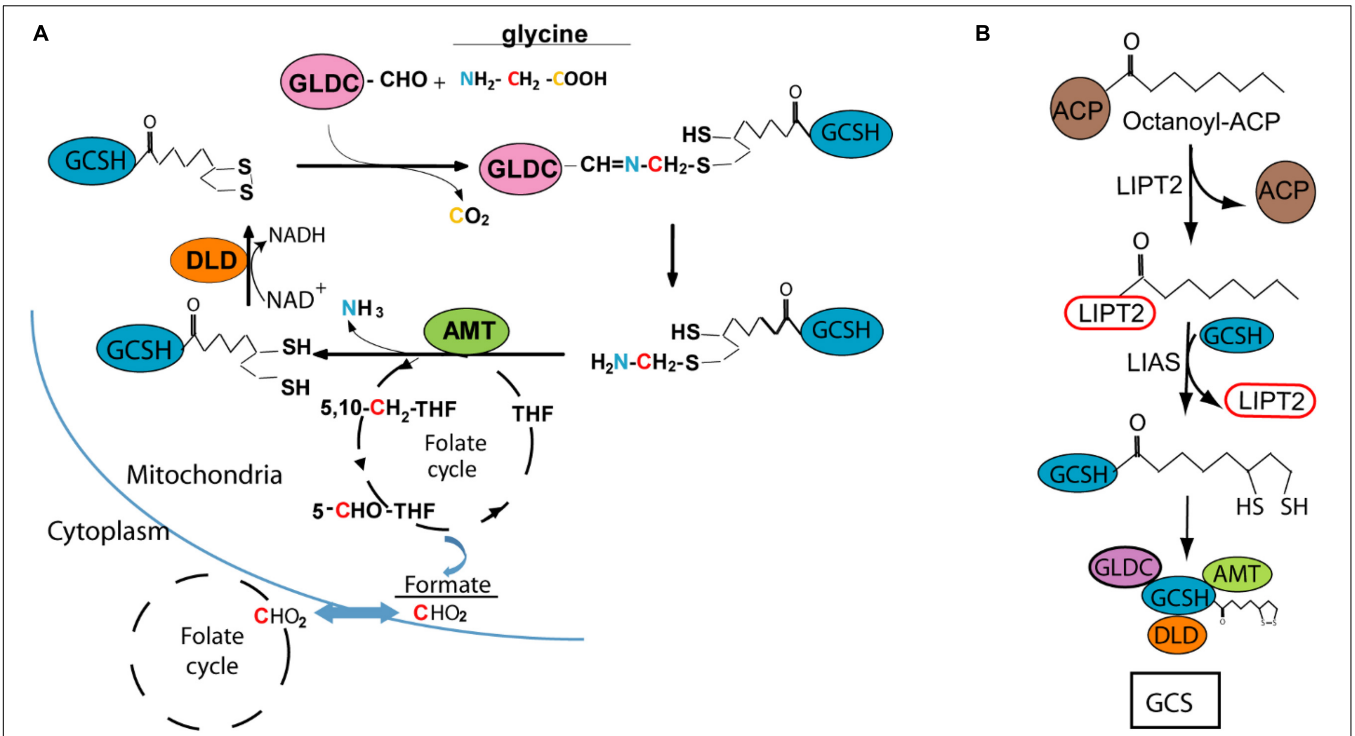

FIGURE 1 | Glycine cleavage system H protein (GCSH) function and lipoylation. **(A)** Diagram of the glycine cleavage system showing decarboxylation of glycine by GLDC with transfer of the methylamine group to GCSH, followed by AMT mediated release of ammonia and transfer of the methylene group to tetrahydrofolate (THF), which enters the mitochondrial folate cycle that generates formate for transfer to the cytoplasm. **(B)** Lipoyl-GCSH is generated via LIPT2 (lipoyltransferase 2) acyl enzyme intermediate generated from octanoyl-ACP (acyl carrier protein), with subsequent transfer to GCSH and sulfur insertion by lipoic acid synthase (LIAS).

with *Gldc*$^{GT1/+}$ females in order to generate embryos of genotype, *Gldc*$^{GT1/GT1}$; *Gcsh*$^{+/-}$.

Collection of Embryos and Formate Supplementation

Timed matings were set up overnight and the day of finding a copulation plug was designated embryonic day 0.5 (E0.5). For embryo collection, the dam was killed by cervical dislocation and the uterus explanted into Dulbecco's Modified Eagles Medium (DMEM) containing 10% fetal bovine serum, prior to dissection of embryos from the extra-embryonic membranes. In formate supplementation studies, the drinking water of pregnant dams was replaced on E0.5 with water containing 30 mg/ml sodium formate (Sigma) and mice were maintained on this water until litters were collected at E8.5 or E10.5 as in previous studies (Pai et al., 2015; Leung et al., 2017).

Plasma Glycine Assay

Blood was collected by terminal cardiac exsanguination under isofluorane anesthetic, transferred to lithium-heparin tubes (BD Microtainer), immediately centrifuged at 3,000*g* for isolation of plasma and stored at −20°C. Glycine was labeled using the Kairos AccQ-tag derivation kit and analyzed on a Xevo ACQUITY UPLC I-Class PLUS System with Xevo TQ-S micro (Waters, United Kingdom). Derivatisation of glycine and UPLC-MS/MS conditions were in accordance with the manufacturer's protocol.

Confocal Microscopy Imaging of E7.5 Embryos

Confocal images of micro-dissected E7.5 DAPI-stained embryos were captured on a Zeiss Examiner LSM880 confocal microscope using a 20×/NA1.0 Plan Apochromat dipping objective. Images were also captured in reflection mode as previously described (Galea et al., 2017) and visualized as maximum projections or as 3D reconstructions in Fiji (Schindelin et al., 2012). For 3D reconstructions, reflection signal was enhanced using the local contrast enhancement tool (CLAHE) in-built in Fiji as previously described (Galea et al., 2018).

RESULTS

The Deleted *Gcsh* Allele Results in Embryonic Lethality

The *Gcsh* gene consists of 5 exons which generate a 1,192 nucleotide transcript encoding a polypeptide of 173 amino acids that is processed to give a mature protein of 125 amino acids. We analyzed mice carrying a 643 base pair deletion that encompassed the entire exon 3 of *Gcsh*, creating a frame-shift after exon 2 (amino acid 73) and a predicted null allele (here denoted *Gcsh*$^{-}$). *Gcsh*$^{+/-}$ mice were viable and fertile and were indistinguishable from wild-type littermates. It has been reported that the electrocardiogram shows an abnormally long RR interval

(time between R waves) in heterozygotes (n = 8 female, 7 male) compared with wild-type controls[1].

No *Gcsh* homozygous mutant pups were recovered among the offspring of heterozygous matings, resulting in a clear distortion of the expected Mendelian ratio (n = 18 $Gcsh^{+/+}$, 41 $Gcsh^{+/-}$ and 0 $Gcsh^{-/-}$). This was consistent with data subsequently reported from the MRC Harwell preweaning lethality screen and indicates lethality of homozygous *Gcsh* null mice at neonatal or pre-natal stage.

Loss of function of the GCS components *Gldc* and *Amt* also results in lethal phenotypes, but null embryos survive to late-fetal stages and exhibit neural tube defects (NTDs) with varying penetrance (Narisawa et al., 2012; Pai et al., 2015; Leung et al., 2017). Therefore, we asked whether $Gcsh^{-/-}$ embryos were detected at pre-natal stages and if so whether NTDs were present. Experimental litters were generated by timed matings of $Gcsh^{+/-}$ heterozygotes and litters collected at mid-gestation. Among an initial three litters collected at E10.5, a total of twenty embryos included only two conceptuses (10%) that genotyped as $Gcsh^{-/-}$ (**Table 1A**). Moreover, in both cases the embryonic material consisted of only a small tissue fragment within the yolk sac without typical morphology of littermates. Hence, embryonic lethality occurs prior to E10.5, as further supported by the high rate of resorption in these litters which likely corresponds to $Gcsh^{-/-}$ implantations (**Table 1A**).

Additional litters were collected at E8.5 (**Table 1A**) and among five litters (n = 48 embryos), seven implantations (15%) contained tissue masses within the yolk sac that genotyped as $Gcsh^{-/-}$, but which had not developed recognizable embryonic features such as head-folds or somites (**Figure 2**). Small size and abnormal embryonic structures, presumably corresponding to homozygous null embryos, was also noted by E7.5 (**Figure 2**).

Heterozygous $Gcsh^{+/-}$ Mice Do Not Exhibit Elevated Plasma Glycine

A hallmark of loss of function of the GCS in humans and mice is the presence of elevated glycine concentration in tissue and body fluids. Although this could not be assessed in homozygous mutants, we compared plasma glycine concentration in wild-type and $Gcsh^{+/-}$ adult mice (n = 3 per genotype). The plasma glycine concentration in $Gcsh^{+/-}$ (391 ± 72 μM; mean ± *SD*) did not significantly differ from that in wild-type mice (347 ± 16 μM), suggesting that loss of one Gcsh allele did not cause appreciable suppression of glycine cleavage system activity.

Early Lethality of *Gcsh* Null Embryos Cannot Be Rescued by Formate Supplementation

In addition to regulation of glycine abundance, a key activity of the GCS is the provision of glycine-derived one carbon units to folate one-carbon metabolism (FOCM), with downstream flux into nucleotide biosynthesis and methylation reactions. Suppression of FOCM is implicated in the causation of structural malformations in *Gldc*-deficient embryos, including NTDs and ventriculomegaly (Leung et al., 2017; Santos et al., 2020). Hence, these abnormalities can be rescued by provision of additional one-carbon groups to the folate cycle, for example via maternal supplementation with formate (Pai et al., 2015; Leung et al., 2017; Santos et al., 2020).

In order to test whether formate treatment would enhance development of $Gcsh^{-/-}$ embryos, heterozygous timed

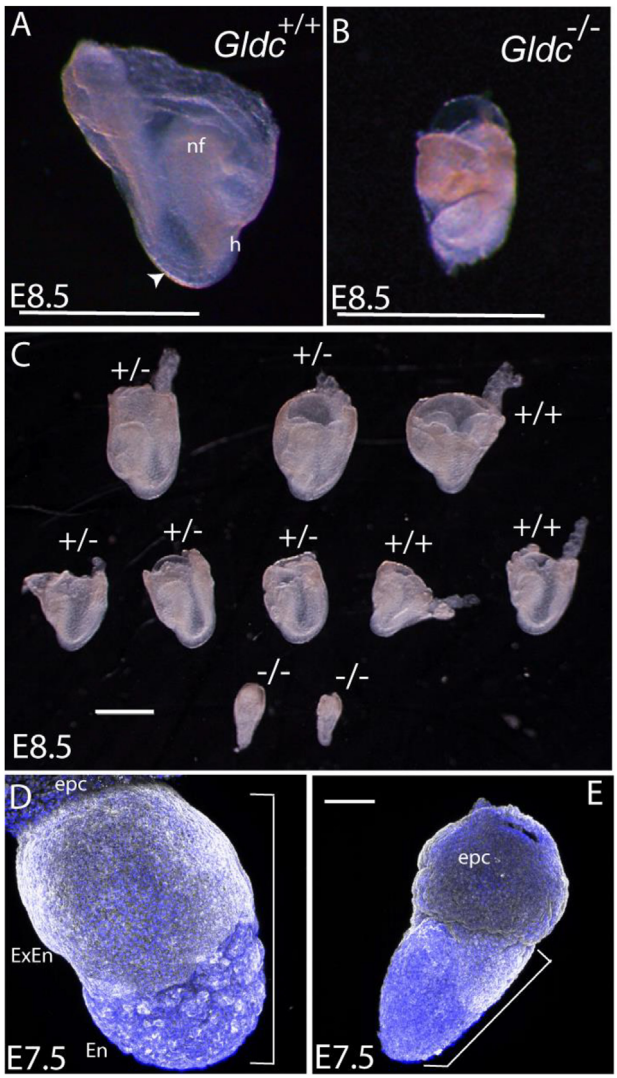

FIGURE 2 | Morphological appearance of *Gcsh* null embryos. **(A,B)** Images at 8.5 show the typical appearance of **(A)** a wild-type embryo (inside the yolk sac), with visible somites (arrowhead), cranial neural folds (nf), and heart loop (h), whereas **(B)** a typical $Gcsh^{-/-}$ littermate is smaller and under-developed. **(C)** A representative litter of embryos (contained within the yolk sac) at E8.5, in which wild-type and $Gldc^{+/-}$ embryos had developed to the 4–5 somite stage, with clearly visible neural folds and heart structure. In contrast, $Gldc^{-/-}$ littermates were much smaller, with no detectable somites or age-appropriate morphological structures. **(D,E)** A subset of embryos were already significantly smaller than littermates at E7.5 (example in **E**); for comparison the region encompassing extra-embryonic/embryonic tissue is indicated by brackets (epc, ectoplacental cone; extra-embryonic endoderm; En, embryonic endoderm). Scale bar represents 1 mm **(A–C)** or 0.1 mm **(D,E)**.

[1]www.mousephenotype.org

TABLE 1 | Frequency of embryo genotypes among litters from *Gcsh*$^{+/-}$ intercrosses.

A. *Gcsh*$^{+/-}$ × *Gcsh*$^{+/-}$ litters								
	Litters	**Embryos (n)**	**Resorption (n)**	**Implantations litter**	**"Embryos" litter**	**Genotype**		
						***Gcsh*$^{+/+}$**	***Gcsh*$^{+/-}$**	***Gcsh*$^{-/-}$**
E8.5	5	48	1	9.8	9.6	18	23	7*
						38%	48%	15%
E10.5	3	20	7	9.0	6.7	6	12	2*
						30%	60%	10%
B. *Gcsh*$^{+/-}$ × *Gcsh*$^{+/-}$ litters with formate supplementation								
	Litters	**Embryos (n)**	**Resorption (n)**	**Implantations litter**	**"Embryos" litter**	**Genotype**		
						***Gcsh*$^{+/+}$**	***Gcsh*$^{+/-}$**	***Gcsh*$^{-/-}$**
E8.5-9.5	4	36	1	9.3	9.6	10	19	7#
						28%	53%	19%
E10.5	4	20	7	6.8	6.7	6	11	3#
						30%	55%	15%

(A,B) Implantations were dissected and "embryos" (classified on the basis that some tissue was present inside an intact yolk sac) were genotyped. (A) Among untreated litters, the material that genotyped as Gcsh$^{-/-}$ *(*) consisted of morphologically undefined tissue masses with no visible somites. (B) This was the case for the majority of Gcsh*$^{-/-}$ *embryos exposed to maternal formate supplementation (#), except 1/7 embryos at E9.5 had 2 somites (compared with 15 somites in littermates) while 1/7 embryos had headfolds but no somites. Similarly, 1/3 embryos at E10.5 was slightly more developed with 1 visible somite (in contrast to littermates that had 29 or more somites).*

matings were performed and pregnant *Gcsh*$^{+/-}$ females were supplemented with 30 mg/ml formate in the drinking water from E0.5 as in previous studies (Pai et al., 2015). Among litters collected at E8.5-10.5, the frequency of resorption was similar to that observed among non-supplemented embryos suggesting that lethality had not been prevented (**Table 1B**). The majority of *Gcsh*$^{-/-}$ embryos among formate-supplemented litters resembled untreated mutants, being considerably smaller than littermates with apparent cessation of morphological development. However, a few *Gcsh*$^{-/-}$ embryos (3 of 10) showed progression to a slightly later stage, with evidence of head-folds and segmentation of 1–2 somites. Nevertheless, at E9.5 these embryos exhibited developmental retardation of least 24–30 h (resembling wild-type embryos at E8.0 or younger) and showed no further developmental progression at E10.5 (**Table 1B**).

Heterozygosity for *Gcsh*$^{+/-}$ Did Not Increase the Frequency of NTDs Among *Gldc*-Deficient Embryos

Analysis of loss of function models of *Gldc* in mice shows that frequency of NTDs correlates with the degree of suppression of *Gldc* expression, defects occurring among around 25% of *Gldc*$^{GT1/GT1}$ embryos and 60% of *Gldc*$^{-/-}$ embryos, which exhibit 90% and 100% reduction in *Gldc* mRNA abundance, respectively (Pai et al., 2015; Leung et al., 2017). The frequency of NTDs is also modified by genetic interaction with a null allele of *Mthfr* (Leung et al., 2017). We therefore tested the hypothesis that the presence of a *Gcsh* null allele may have an additive effect with *Gldc*-deficiency leading to exacerbation of NTDs in *Gldc*$^{GT1/GT1}$ embryos.

The frequency of NTDs was assessed at E10.5 or 13.5 among litters generated by intercross of *Gsch*$^{+/-}$; *Gldc*$^{GT1/+}$ males and *Gldc*$^{GT1/+}$ females (**Table 2**). Surprisingly, we observed NTDs among 67% (n = 8 of 12) of *Gldc*$^{GT1/GT1}$ embryos, which is higher than previously observed with this allele of *Gldc* (Pai et al., 2015). It is possible that the penetrance is influenced by alteration of the genetic background, *Gcsh* being on a C57BL/6N background compared with the C57BL/6J background of the *Gldc*^{GT1} line. Nevertheless, the finding that NTDs were present among only 50% of *Gcsh*$^{+/-}$; *Gldc*$^{GT1/GT1}$ embryos compared with 83% of *Gcsh*$^{+/+}$; *Gldc*$^{GT1/GT1}$ embryos (non-significant difference between genotypes) suggests that the introduction of the *Gcsh* null allele did not exacerbate the NTDs in *Gldc*$^{GT1/GT1}$ embryos (**Table 2**).

DISCUSSION

Loss of function of Gcsh in mice results in early lethality, prior to E8.5, such that a requirement for Gcsh function in neural tube closure or later brain development and function could not be evaluated. This phenotype of *Gcsh* null embryos differed from that of *Amt* and *Gldc* in which embryos survive to at least perinatal stages, with death at or shortly after birth resulting from NTDs in affected pups (Narisawa et al., 2012; Leung et al., 2017). Overall, these findings indicate that the lethal effect of Gsch mutation at pre-neurulation stages is unlikely to result solely from loss of function of the GCS. However, a few formate supplemented *Gcsh* null embryos appeared to show a slight improvement in development compared with untreated embryos, suggesting that the suppression of FOCM may contribute in part to early lethality. The prevention of NTDs in *Gldc* mutant

TABLE 2 | Frequency of genotypes and NTDs among litters from *Gcsh*$^{+/-}$; *Gldc*$^{GT1/GT1}$ × *Gcsh*$^{+/+}$; *Gldc*$^{GT1/GT1}$ intercrosses.

		Genotype	*Gcsh*$^{+/+}$			*Gcsh*$^{+/-}$		
			Gldc$^{+/+}$	*Gldc*$^{+/GT1}$	*Gldc*$^{GT1/GT1}$	*Gldc*$^{+/+}$	*Gldc*$^{+/GT1}$	*Gldc*$^{GT1/GT1}$
	Litters	Embryos	No. embryos (NTDs)			No. embryos (NTDs)		
E10.5	3	16	1 (0)	5 (0)	4 (4)	2 (0)	2 (0)	2 (1)
E13.5	3	20	1 (0)	5 (0)	2 (1)	1 (0)	7 (0)	4 (2)
Total	7	36	2 (0)	10 (0)	6 (5) = 83%	3	9	6 (3) = 50%

NTDs only arose among Gldc$^{GT1/GT1}$ *embryos and there was no significant effect of Gcsh genotype (Fisher Exact test).*

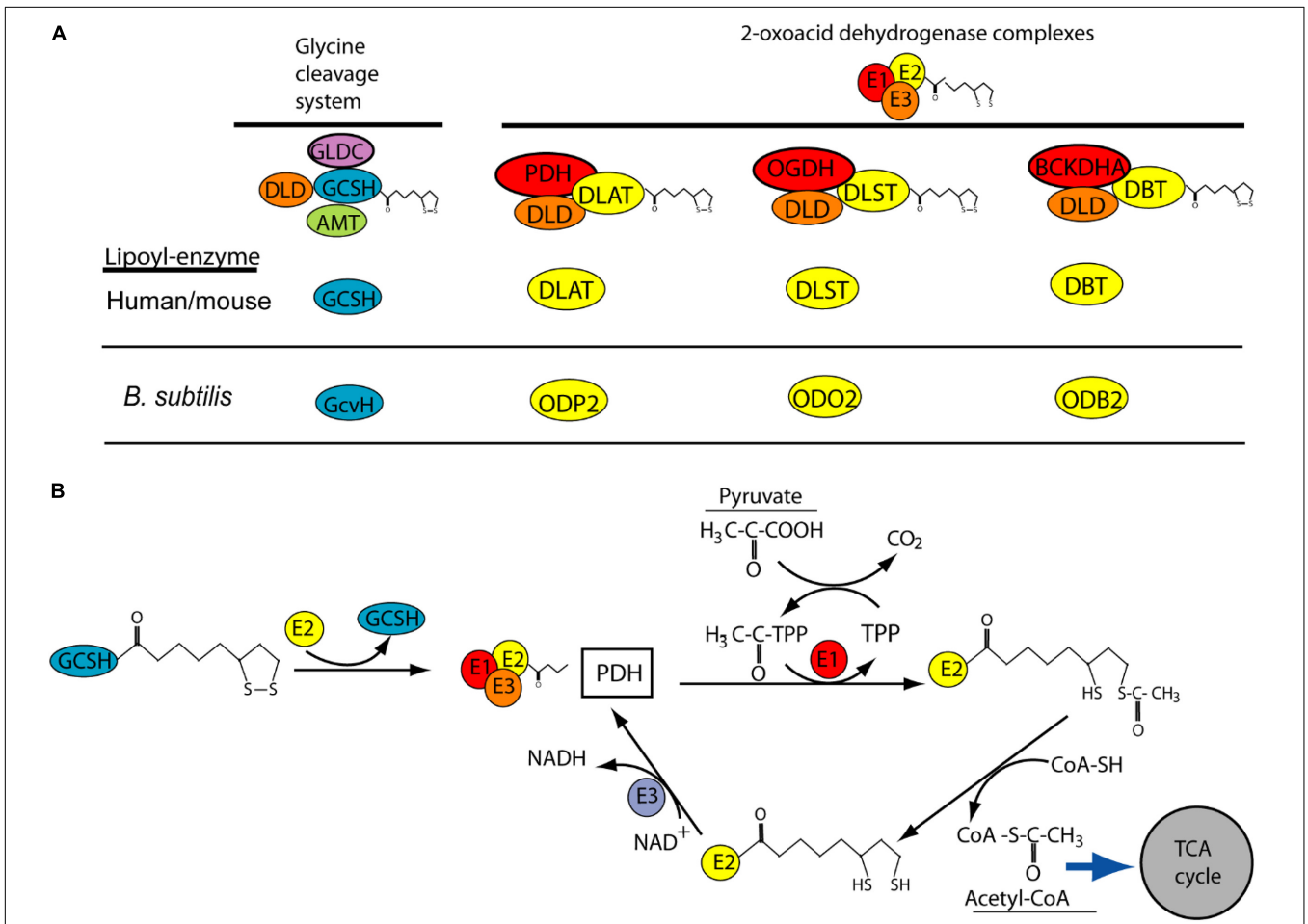

FIGURE 3 | Potential role of GCSH as a donor of lipoic acid to multiple lipoylated-proteins. **(A)** Lipoylation is required for function of GCSH in the glycine cleavage system, and for transfer or lipoyl groups to subunits of 2-oxoacid dehydrogenase complexes including pyruvate dehydrogenase (PDH), 2-oxyglutarate dehydrogenase (OGDH) and branched-chain alpha keto-dehydrogenase (BCKDHA). These complexes are highly conserved (orthologs in *B. subtilis* are shown). **(B)** Possible mechanism by which GSCH acts as lipoyl-donor to the E2 subunit of pyruvate dehydrogenase, whose action leads to production of acetyl-CoA. This activity has been demonstrated in *B. subtilis* but not yet in human or mouse.

embryos is associated with increase in cell proliferation, perhaps via enhanced nucleotide biosynthesis, so it is possible that such an effect also supports earlier development in *Gcsh* mutants.

The requirement for GCSH function during early development may explain why homozygous or compound heterozygous mutations have not been reported in NKH patients. Similarly, NKH patients have not been found to carry *DLD* mutations, while knockout of *Dld* in mice results in embryonic lethality prior to E9.5, with developmental delay apparent by E7.5 (Johnson et al., 1997). This early lethality of *Dld* null embryos is thought to be due to the requirement for DLD function for multiple enzymes, rather than specifically the GCS. DLD acts as the so called E3 component (as dihydrolipoamide dehydrogenase) of the GCS and three other

mitochondrial multienzyme complexes, known as 2-oxoacid dehydrogenase complexes (**Figure 3A**). These complexes, pyruvate dehydrogenase, α-ketogutarate dehydrogenase and branched-chain α-ketoacid dehydrogenase, are required for aerobic metabolism and branched-chain fatty acid synthesis. In these complexes, DLD or E3 is tightly bound to the E1 and E2 subunits where E1 is a thiamine pyrophosphate-dependent 2-oxoacid dehydrogenase. Interestingly, E2 subunits of the complexes are highly conserved and like GCSH they require covalent attachment of lipoic acid, as a cofactor, to form the active lipoyl-enzyme (**Figure 3A**).

Like DLD, GCSH may have functions in addition to the requirement in the GCS. This concept is supported by recent studies of the *GCSH* ortholog, *GcvH*, in *B. subtilis* (Cao et al., 2018a). Unlike in other bacteria, such as *E. coli*, where GcvH functions only in the GCS, *B. subtilis* GcvH can act as lipoyl-moiety donor in the biosynthetic modification of other lipoic acid requiring 2-oxoacid dehydrogenase proteins. Moreover, human GCSH can substitute for loss of *GcvH* in *B. subtilis* (Cao et al., 2018a). GSCH may act as a master donor of the lipoyl group to E2 subunit of other 2-oxoacid dehydrogenase complexes such as pyruvate dehydrogenase where its function is crucial for the tricarboxylic acid (TCA) cycle (**Figure 3B**).

Interestingly, the transcriptional regulation of *GcvH* is also separate from other GCS components in *B. subtilis*, unlike in *E. coli* where it is co-regulated with *GcvP* and *GcvT* in response to glycine (Cao et al., 2018a). Tissue expression of *GCSH* in higher vertebrates may also occur in sites that do not express the specific GCS components (*GLDC* and *AMT*), suggesting a possible requirement beyond that in the GCS. For example, the expression level of *GCSH* in chick correlated with that of *GLDC* in liver, kidney, and brain but mRNA was also detected in other sites including heart, spleen and skeletal muscle where *GLDC* was absent (Kure et al., 1991). In mouse embryos *Gldc* is abundantly expressed throughout the neuroepithelium during neural tube closure (Pai et al., 2015) but becomes more restricted at later stages, with post-natal expression being highest in liver, kidney and brain, whereas *Gcsh* also is expressed in *Gldc*-negative tissue such as skeletal muscle (Gene expression database (GXD)[2], October 2020). Similarly, human mRNA and protein databases reveal a more widespread tissue distribution of GCSH than GLDC, which is primarily expressed in liver, kidney and brain (Human Protein Atlas)[3] (Uhlen et al., 2015).

[2] http://www.informatics.jax.org

[3] http://www.proteinatlas.org

CONCLUSION

In conclusion, Gcsh activity is required for embryonic survival in mice. We hypothesize that Gcsh has GCS-independent activity as a lipoate relay that is required for post-implantation development in mice and humans.

DATA AVAILABILITY STATEMENT

The original contributions presented in the study are included in the article/supplementary material, further inquiries can be directed to the corresponding author/s.

ETHICS STATEMENT

The animal study was reviewed and approved by the University College London Animal Welfare Review Board.

AUTHOR CONTRIBUTIONS

NG, K-YL, and AC conceived the study. NG, K-YL, SDC, and GG carried out the experimental work. NG and K-YL drafted the manuscript. All authors analyzed the data and edited the manuscript.

FUNDING

This work was funded by Medical Research Council (N003713) and Action Medical Research (GN2403). Research was supported by Joseph's Goal, the UCL Biological Mass Spectrometry Centre and the National Institute for Health Research Biomedical Research Centre at Great Ormond Street Hospital for Children NHS Foundation Trust and University College London.

ACKNOWLEDGMENTS

We are grateful to Chloe Santos and Diana Gold-Diaz for technical assistance and helpful discussion. The C57BL/6NTac-Gcsh$^{em1(IMPC)H}$/H mice were obtained from the MRC Harwell Institute which distributes these mice on behalf of the European Mouse Mutant Archive (www.infrafrontier.eu). The MRC Harwell Institute is also a member of the International Mouse Phenotyping Consortium (IMPC) and has received funding from the Medical Research Council for generating and/or phenotyping the C57BL/6NTac-Gcsh$^{em1(IMPC)H}$/H mice. The research reported in this publication is solely the responsibility of the authors and does not necessarily represent the official views of the Medical Research Council. Funding and associated primary phenotypic information may be found at www.mousephenotype.org.

REFERENCES

Autuori, M. C., Pai, Y. J., Stuckey, D. J., Savery, D., Marconi, A. M., Massa, V., et al. (2017). Use of high frequency ultrasound to study the prenatal development of cranial neural tube defects and hydrocephalus in Gldc-deficient mice. *Prenat. Diag.* 37, 273–281. doi: 10.1002/pd.5004

Baker, P. R. II, Friederich, M. W., Swanson, M. A., Shaikh, T., Bhattacharya, K., and Scharer, G. H. (2014). Variant non ketotic hyperglycinemia is caused by

mutations in LIAS. BOLA3 and the novel gene GLRX5. *Brain* 137, 366–379. doi: 10.1093/brain/awt328

Cao, X., Hong, Y., Zhu, L., Hu, Y., and Cronan, J. E. (2018a). Development and retention of a primordial moonlighting pathway of protein modification in the absence of selection presents a puzzle. *Proc. Natl. Acad. Sci. U S A.* 115, 647–655. doi: 10.1073/pnas.1718653115

Cao, X., Koch, T., Steffens, L., Finkensieper, J., Zigann, R., Cronan, J. E., et al. (2018b). Lipoate-binding proteins and specific lipoate-protein ligases in microbial sulfur oxidation reveal an atpyical role for an old cofactor. *eLife* 7:e37439. doi: 10.7554/eLife.37439

Christensen, Q. H., Martin, N., Mansilla, M. C., de Mendoza, D., and Cronan, J. E. (2011). A novel amidotransferase required for lipoic acid cofactor assembly in *Bacillus subtilis*. *Mol. Microbiol.* 80, 350–363. doi: 10.1111/j.1365-2958.2011.07598.x

Coughlin, C. R., Swanson, M. A., Kronquist, K., Acquaviva, C., Hutchin, T., Rodriguez-Pombo, P., et al. (2017). The genetic basis of classic nonketotic hyperglycinemia due to mutations in GLDC and AMT. *Genet. Med.* 19, 104–111. doi: 10.1038/gim.2016.74

Cronan, J. E. (2020). Progress in the enzymology of the mitochondrial diseases of lipoic acid requiring enzymes. *Front. Genet.* 11:510. doi: 10.3389/fgene.2020.00510

Galea, G. L., Cho, Y. J., Galea, G., Mole, M. A., Rolo, A., Savery, D., et al. (2017). Biomechanical coupling facilitates spinal neural tube closure in mouse embryos. *Proc. Natl. Acad. Sci. U S A.* 114, E5177–E5186.

Galea, G. L., Nychyk, O., Mole, M. A., Moulding, D., Savery, D., Nikolopoulou, E., et al. (2018). Vangl2 disruption alters the biomechanics of late spinal neurulation leading to spina bifida in mouse embryos. *Dis. Model. Mech.* 11:dmm032219. doi: 10.1242/dmm.032219

Greene, N. D., and Copp, A. J. (2014). Neural tube defects. *Annu. Rev. Neurosci.* 37, 221–242.

Hennermann, J. B., Berger, J. M., Grieben, U., Scharer, G., and Van Hove, J. L. (2012). Prediction of long-term outcome in glycine encephalopathy: a clinical survey. *J. Inherit. Metab. Dis.* 35, 253–261. doi: 10.1007/s10545-011-9398-1

Hiraga, K., Kochi, H., Hayasaka, K., Kikuchi, G., and Nyhan, W. L. (1981). Defective glycine cleavage system in nonketotic hyperglycinemia. occurrence of a less active glycine decarboxylase and an abnormal aminomethyl carrier protein. *J. Clin. Invest.* 68, 525–534. doi: 10.1172/jci110284

Hoover-Fong, J. E., Shah, S., Van Hove, J. L., Applegarth, D., Toone, J., and Hamosh, A. (2004). Natural history of nonketotic hyperglycinemia in 65 patients. *Neurology* 63, 1847–1853. doi: 10.1212/01.wnl.0000144270.83080.29

Johnson, M. T., Yang, H. S., Magnuson, T., and Patel, M. S. (1997). Targeted disruption of the murine dihydrolipoamide dehydrogenase gene (Dld) results in perigastrulation lethality. *Proc. Natl. Acad. Sci. U S A.* 94, 14512–14517. doi: 10.1073/pnas.94.26.14512

Kanno, J., Hutchin, T., Kamada, F., Narisawa, A., Aoki, Y., Matsubara, Y., et al. (2007). Genomic deletion within GLDC is a major cause of non-ketotic hyperglycinaemia. *J. Med. Genet.* 44:e69. doi: 10.1136/jmg.2006.043448

Kikuchi, G., Motokawa, Y., Yoshida, T., and Hiraga, K. (2008). Glycine cleavage system: reaction mechanism, physiological significance, and hyperglycinemia. *Proc. Jpn. Acad. Ser. B Phys. Biol. Sci.* 84, 246–263. doi: 10.2183/pjab.84.246

Kure, S., Kato, K., Dinopoulos, A., Gail, C., DeGrauw, T. J., Christodoulou, J., et al. (2006). Comprehensive mutation analysis of GLDC. AMT, and GCSH in nonketotic hyperglycinemia. *Hum. Mutat.* 27, 343–352. doi: 10.1002/humu.20293

Kure, S., Kojima, K., Ichinohe, A., Maeda, T., Kalmanchey, R., Fekete, G., et al. (2002). Heterozygous GLDC and GCSH gene mutations in transient neonatal hyperglycinemia. *Ann. Neurol.* 52, 643–646.

Kure, S., Koyata, H., Kume, A., Ishiguro, Y., and Hiraga, K. (1991). The glycine cleavage system. The coupled expression of the glycine decarboxylase gene and the H-protein gene in the chicken. *J. Biol. Chem.* 266, 3330–3334. doi: 10.1016/s0021-9258(18)49992-9

Leung, K. Y., De Castro, S. C. P., Santos, C., Savery, D., Prunty, H., Gold-Diaz, D., et al. (2020). Regulation of glycine metabolism by the glycine cleavage system and conjugation pathway in mouse models of non-ketotic hyperglycinemia. *J. Inherit. Metab. Dis.* 43, 1186–1198. doi: 10.1002/jimd.12295

Leung, K. Y., Pai, Y. J., Chen, Q., Santos, C., Calvani, E., Sudiwala, S., et al. (2017). Partitioning of one-carbon units in folate and methionine metabolism is essential for neural tube closure. *Cell Rep.* 21, 1795–1808. doi: 10.1016/j.celrep.2017.10.072

Mianne, J., Codner, G. F., Caulder, A., Fell, R., Hutchison, M., King, R., et al. (2017). Analysing the outcome of CRISPR-aided genome editing in embryos: screening, genotyping and quality control. *Methods* 12, 68–76. doi: 10.1016/j.ymeth.2017.03.016

Narisawa, A., Komatsuzaki, S., Kikuchi, A., Niihori, T., Aoki, Y., Fujiwara, K., et al. (2012). Mutations in genes encoding the glycine cleavage system predispose to neural tube defects in mice and humans. *Hum. Mol. Genet.* 21, 1496–1503. doi: 10.1093/hmg/ddr585

Oliver, D. J., Neuburger, M., Bourguignon, J., and Douce, R. (1990). Interaction between the component enzymes of the glycine decarboxylase multienzyme complex. *Plant Physiol.* 94, 833–839. doi: 10.1104/pp.94.2.833

Pai, Y. J., Leung, K. Y., Savery, D., Hutchin, T., Prunty, H., Heales, S., et al. (2015). Glycine decarboxylase deficiency causes neural tube defects and features of non-ketotic hyperglycinemia in mice. *Nat. Commun.* 6:6388.

Santos, C., Pai, Y. J., Mahmood, M. R., Leung, K. Y., Savery, D., Waddington, S. N., et al. (2020). Impaired folate 1-carbon metabolism causes formate-preventable hydrocephalus in glycine decarboxylase-deficient mice. *J. Clin. Invest.* 130, 1446–1452. doi: 10.1172/jci132360

Schindelin, J., Arganda-Carreras, I., Frise, E., Kaynig, V., Longair, M., Pietzsch, T., et al. (2012). Fiji: an open-source platform for biological-image analysis. *Nat. Methods* 9, 676–682. doi: 10.1038/nmeth.2019

Shah, R. H., Northrup, H., Hixson, J. E., Morrison, A. C., and Au, K. S. (2016). Genetic association of the glycine cleavage system genes and myelomeningocele. *Birth Defects Res. A Clin. Mol. Teratol.* 106, 847–853. doi: 10.1002/bdra.23552

Swanson, M. A., Coughlin, C. R. Jr., Scharer, G. H., Szerlong, H. J., Bjoraker, K. J., et al. (2015). Biochemical and molecular predictors for prognosis in nonketotic hyperglycinemia. *Ann. Neurol.* 78, 606–618.

Uhlen, M., Fagerberg, L., Hallstrom, B. M., Lindskog, C., Oksvold, P., Mardinoglu, A., et al. (2015). Proteomics. tissue-based map of the human proteome. *Science* 347:1260419.

Van Hove, J. L., Kishnani, P. S., Demaerel, P., Kahler, S. G., Miller, C., Jaeken, J., et al. (2000). Acute hydrocephalus in nonketotic hyperglycemia. *Neurology* 54, 754–756. doi: 10.1212/wnl.54.3.754

Conflict of Interest: The authors declare that the research was conducted in the absence of any commercial or financial relationships that could be construed as a potential conflict of interest.

frontiers in Pediatrics

CASE REPORT
published: 16 April 2021
doi: 10.3389/fped.2021.660076

Case Report and Review of the Literature: A New and a Recurrent Variant in the *VARS2* Gene Are Associated With Isolated Lethal Hypertrophic Cardiomyopathy, Hyperlactatemia, and Pulmonary Hypertension in Early Infancy

Katarína Kušíková[1], *René Günther Feichtinger*[2], *Bernhard Csillag*[3], *Ognian Kostadinov Kalev*[4], *Serge Weis*[4], *Hans-Christoph Duba*[5], *Johannes Adalbert Mayr*[2†] *and Denisa Weis*[5*†]

[1] *Department of Pediatric Neurology, Medical School, Comenius University and National Institute of Children's Diseases, Bratislava, Slovakia,* [2] *Department of Pediatrics, University Hospital Salzburg, Paracelsus Medical University Salzburg, Salzburg, Austria,* [3] *Department of Neonatology, Kepler University Hospital Med Campus IV, Johannes Kepler University Linz, Linz, Austria,* [4] *Division of Neuropathology, Department of Pathology and Molecular Pathology, Kepler University Hospital Neuromed Campus, Johannes Kepler University Linz, Linz, Austria,* [5] *Department of Medical Genetics, Kepler University Hospital Med Campus IV, Johannes Kepler University Linz, Linz, Austria*

OPEN ACCESS

Edited by:
Ronald Wanders, University of Amsterdam, Netherlands

Reviewed by:
Ann Saada, Hebrew University of Jerusalem, Israel
Emanuela Bottani, University of Verona, Italy

***Correspondence:**
Denisa Weis
denisa.weis@kepleruniklinikum.at

[†] *These authors have contributed equally to this work*

Specialty section:
This article was submitted to Genetics of Common and Rare Diseases, a section of the journal Frontiers in Pediatrics

Received: *28 January 2021*
Accepted: *22 March 2021*
Published: *16 April 2021*

Citation:
Kušíková K, Feichtinger RG, Csillag B, Kalev OK, Weis S, Duba H-C, Mayr JA and Weis D (2021) Case Report and Review of the Literature: A New and a Recurrent Variant in the VARS2 Gene Are Associated With Isolated Lethal Hypertrophic Cardiomyopathy, Hyperlactatemia, and Pulmonary Hypertension in Early Infancy. Front. Pediatr. 9:660076. doi: 10.3389/fped.2021.660076

Mitochondriopathies represent a wide spectrum of miscellaneous disorders with multisystem involvement, which are caused by various genetic changes. The establishment of the diagnosis of mitochondriopathy is often challenging. Recently, several mutations of the *VARS2* gene encoding the mitochondrial valyl-tRNA synthetase were associated with early onset encephalomyopathies or encephalocardiomyopathies with major clinical features such as hypotonia, developmental delay, brain MRI changes, epilepsy, hypertrophic cardiomyopathy, and plasma lactate elevation. However, the correlation between genotype and phenotype still remains unclear. In this paper we present a male Caucasian patient with a recurrent c.1168G>A (p.Ala390Thr) and a new missense biallelic variant c.2758T>C (p.Tyr920His) in the *VARS2* gene which were detected by whole exome sequencing (WES). VARS2 protein was reduced in the patient's muscle. A resulting defect of oxidative phosphorylation (OXPHOS) was proven by enzymatic assay, western blotting and immunohistochemistry from a homogenate of skeletal muscle tissue. Clinical signs of our patient included hyperlactatemia, hypertrophic cardiomyopathy (HCM) and pulmonary hypertension, which led to early death at the age of 47 days without any other known accompanying signs. The finding of novel variants in the *VARS2* gene expands the spectrum of known mutations and phenotype presentation. Based on our findings we recommend to consider possible mitochondriopathy and to include the analysis of the *VARS2* gene in the genetic diagnostic algorithm in cases with early manifesting and rapidly progressing HCM with hyperlactatemia.

Keywords: *VARS2* gene, oxidative phosphorylation, mitochondriopathy, hyperlactatemia, lethal hypertrophic cardiomyopathy, pulmonary hypertension

INTRODUCTION

Mitochondria are organelles responsible for energy production in the form of adenosine triphosphate (ATP) through the oxidative phosphorylation system (OXPHOS). The process of energy production is performed by the mitochondrial respiratory chain and ATP synthase located in the inner membrane of mitochondria (1). Mitochondrial disorders represent a wide spectrum of heterogeneous syndromes predominantly presenting with symptoms as lactic acidosis, hypotonia, developmental delay, failure to thrive, and encephalopathy due to cell energy depletion. Mitochondrial disorders are associated with many causative genes (2–4), which are encoded by mitochondrial DNA (mtDNA) or nuclear DNA (5). Valyl-tRNA synthetase (Val-tRNA) involved in mitochondrial translation (the process of protein synthesis from the information contained in a molecule of messenger RNA – mRNA) is encoded by the *VARS2* gene (6) and catalyzes the amino acid valine's attachment to its tRNA (7). Dysfunction of the protein product is responsible for combined oxidative phosphorylation deficiency 20 (OMIM: # 615917) inherited in an autosomal recessive manner. Rare biallelic variants in the *VARS2* gene have been associated with severe clinical features as mitochondrial encephalomyopathy or encephalocardiomyopathy in 23 affected individuals from 19 families worldwide (1, 4, 6–15). In the present paper we describe a compound heterozygous case with a recurrent c.1168G>A (p.Ala390Thr) and a novel missense variant c.2758T>C (p.Tyr920His) in the *VARS2* gene causing isolated hypertrophic cardiomyopathy, hyperlactatemia, and pulmonary hypertension leading to early death. The pathogenicity of the detected variants is supported by immunohistochemistry, enzymatic analysis, and western blot in a muscle sample of the affected individual. Finally, we compare our findings with the case reports published so far.

METHODS

Clinical Description

All clinical information about our patient was obtained from medical records retrospectively with the patient's parents' informed consent and was correlated with potential causative mutations detected by whole-exome sequencing (WES).

Genetic Investigation

Genetic testing was performed from the peripheral blood of the patient. Karyotyping was performed according to a standard cytogenetic protocol. SNP array was performed with Illumina Cyto 850Kv1.1 Bead Chip. In addition, DNA isolated from the patient's peripheral blood lymphocytes was analyzed by whole-exome sequencing. The library was prepared by SureSelect60Mbv6 (Agilent) and paired-end sequenced on a HiSeq 4000 platform (Illumina) with a read-length of 100 bases. In order to align reads to the human genome assembly hg19 Burrows-Wheeler Aligner (BWA, v.0.5.87.5) was applied and detection of genetic variation was performed using SAMtools (v 0.1.18), PINDEL (v 0.2.4t), and ExomeDepth (v 1.0.0). The cut-off for biallelic inheritance was set to <1% allele frequency, for monoallelic inheritance to <0.1%. The size of reference entries was >20,000 exomes in the database at the time of analysis (16). With this approach, 97.3% of the target sequences were covered >20-fold. The detected mutations were verified by Sanger sequencing, followed by examining the DNA from peripheral blood of the patient's parents.

Muscle Biopsy

The biopsy of the vastus lateralis muscle was performed under general anesthesia according to standard procedures. Muscle tissue was cut into several pieces for formalin fixation, glutaraldehyde fixation, and rapid freezing in isopentane cooled in liquid nitrogen for subsequent analyses.

Histopathology

The histopathology and the enzyme histochemical stain analysis encompassed the following stains: Haematoxylin and Eosin (H&E), Elastica van Gieson (EvG), Congored, ATPase at pH 9,4, pH 4,3 and 4,2, reduced nicotinamide adenine dinucleotide-tetrazolium reductase (NADH), Gomori trichrome, cytochrome c oxidase (COX), succinate dehydrogenase (SDH), acid phosphatase, periodic acid-Schiff (PAS), Sudan black, myoadenylate deaminase (MAD), phosphofructokinase (PFK), phosphorylase, and acetylcholinesterase (ACE). The immunohistochemical analyses included the following antibodies: CD3, CD20, CD8, CD4, CD45, CD79a, CD68, HLA-DRII, beta-spectrin, alpha-sarcoglycan, beta-sarcoglycan, gamma-sarcoglycan, delta-sarcoglycan, dystrophin (N-terminus), dystrophin (C-terminus), dystrophin (rod domain), dysferlin, titin, emerin, telethonin, POMT1, myotilin, lamin A/C, caveolin-3, actinin, laminin2, collagen VI, desmin, myosin fast, myosin slow, myosin neonatal, membrane attack complex, vimentin, and utrophin at appropriate dilutions.

Enzymatic Analysis

Muscle 600 × g homogenates were used for determination of enzymatic activities of the OXPHOS complexes. Enzyme activities of the OXPHOS complexes were determined as previously described (17). The rotenone-sensitive complex I activity was measured spectrophotometrically as NADH/decylubiquinoneoxidoreductase at 340 nm. The enzyme activities of citrate synthase, complex IV (ferrocytochrome c/oxygenoxidoreductase), and oligomycin-sensitive ATPase activity of the F_1F_O ATP synthase (complex V) were determined as previously described (18). The whole reaction mixture for the ATPase activity measurement was treated for 10 s with an ultra-sonifier (Bio cell disruptor 250, Branson, Vienna, Austria). The reaction mixture for the measurement of the complex III activity contained 50 mM potassium phosphate buffer pH 7.8, 2 mM EDTA, 0.3 mM KCN, 100 μM cytochrome c, 200 μM reduced decyl-ubiquinol. The reaction was started by addition of the 600 g homogenate. After 3–4 min the reaction was inhibited with 1 μM antimycin A. All spectrophotometric measurements (Uvicon 922, Kontron, Milan, Italy) were performed at 37°C.

TABLE 1 | OXPHOS enzymes activity measurements and substrate oxidation in muscle of the reported patient with *VARS2* deficiency.

Enzyme	**mUnit/mg/ protein**	***N***	**mUnit/mUnit CS**	***N***	**mUnit/mUnit Complex II**	***N***
Citrate synthase (CS)	198	150–338			3,02↓	3,06–5,47
Complex I	**12↓**	28–76	**0,06↓**	0,14–0,35	**0,18↓**	0,46–1,07
Complex I + III	80	49–218	0,41	0,24–0,81	1,22	0,93–2,84
Complex II (CII)	66	33–102	0,33	0,18–0,41		
Complex II + III	171	65–180	**0,86↑**	0,3–0,67	2,61↑	1,36–2,49
Complex III	611	304–896	3,09	1,45–3,76	9,32	5,94–12,91
Cytochrome c oxidase	193	181–593	0,97	0,91–2,24	**2,94↓**	4,19–12,05
Complex V	248	86–257	1,25	0,42–1,25	3,78	1,68–3,96
Pyruvate dehydrogenase	20,6	5,3–19,8	**0,104↑**	0,026–0,079	0,314	0,107–0,315
Substrate oxidation	**nmol/h/mUnit CS**	***N***	**mUnit/mUnit CS**	***N***	**nmol/h/mUnit Complex II**	***N***
[1-14C]Pyruvate+Malate	600	263–900	3,03	1,54–3,55	9,15	3,57–11,97
[1-14C]Pyruvate+Carnitine	**948↑**	302–856	**4,79↑**	1,65–3,66	14,45↑	4,48–14,24
[1-14C]Pyruvate+Malate-ADP	**119↑**	32–102	**0,60↑**	0,21–0,41	1,82	0,69–1,88
[1-14C]Pyruvate+Malate+ CCCP	803	304–889	**4,05↑**	1,31–3,11	12,24	3,55–12,35
[1-14C]Pyruvate+Malate+Atracyloside	**134↑**	19–90	**0,68↑**	0,16–0,55	3,24	1,17–3,61
[U-14C]Malate+Pyruvate+Malonate	509	282–874	2,57	1,56–3,87	7,75	3,69–12,53
[U-14C]Malate+Acetylcarn.+Malonate	517	273–678	2,61	1,16–2,82	7,89	3,8–11,44
[U-14C]Malate+ Acetylcarn.+Arsenite	301	156–378	1,52	0,57–1,52	4,58	2,17–6,14
[U-14C]Glutamate+Acetylcarnitine	162	86–209	0,82	0,35–1,06	2,48	1,4–5,11

N, normal range; CS, citrate synthase, protein concentration of the patient muscle 600 × g homogenate: ***1.64*** *mg/ml. Values in bold show abnormal values. Arrow down: reduced values compared to healthy controls. Arrow up: increased values compared to healthy controls.*

Substrate Oxidation Analysis

Muscle 600 × g homogenate was incubated with different ^{14}C-labeled substrates (**Table 1**) for 20 min at 37°C according to Bookelman et al. (19) in a reaction volume of 50 µl. The reactions were stopped by the addition of 20 µl of 15% $HClO_4$ and the $^{14}CO_2$ was collected in 1M NaOH-wetted filter paper snippets (Whatman) placed in the screw cap of 2 ml reaction tubes (Sarstedt). After incubation for 15 min on ice, the filter papers were transferred to new 2 ml reaction tubes containing 1 ml of scintillation buffer Ultima Gold (Perkin Elmer) and counted in a scintillation counter (Packard 1600 TR). The scintillation counts of the different substrate combinations were related to the total activities per reaction and calculated as nmol/h/mg protein activity oxidation.

Western Blot

Muscle tissue homogenates from the patient and controls (centrifuged at 600 × g) were analyzed on 10% acrylamide/bisacrylamide gels and transferred to nitrocellulose membranes. The membranes were washed in Tris-buffered saline (TBS) for 5 min, air-dried for 30 min, washed 10 min in TBS, and blocked 1 h at room temperature in 1x western blocking solution in TBS-T (Roche, Mannheim, Germany). After washing with TBS-Tween 20 (0.5%; TBS-T), the membranes were incubated with the primary antibody diluted in 1x western blocking solution in TBS-T. The indicated primary antibody dilutions and incubation times were used for western blot analysis: polyclonal rabbit VARS2 (1:1,000, o/n, 4°C; Proteintech), monoclonal mouse NDUFS4 (1:1,000, 1 h, room temperature; Abcam), SDHA (1:2,000, 1 h, room temperature; Abcam), UQCRC2 (1:1,500, 1 h, room temperature; Abcam); MT-CO2 (1:1,000, 1 h, room temperature; Abcam), ATP5F1A (1:2,000, 1 h, room temperature; Abcam), VDAC1 (1:2,000, 1 h, room temperature; Abcam), CS (1:3,000, 1 h, room temperature; THP), GPI (1:800, 1 h, room temperature; Santa Cruz). Membranes were incubated with secondary antibodies labeled polymer horseradish peroxidase-(HRP) 1:100 (EnVisionkit, Dako) at room temperature. Detection was carried out with Lumi-Light PLUSPOD substrate (Roche).

Immunohistochemistry

Muscle tissue was stained as previously described (20–23). For IHC, the following antibodies were used: complex I subunit NDUFB8 (rabbit polyclonal, 1:500; Abcam, Cambridge, UK), complex II subunit SDHA (mouse monoclonal, 1:2,000; Abcam, Cambridge, UK), complex III subunit UQCRC2 (mouse monoclonal, 1:1,500; Abcam, Cambridge, UK), complex IV subunit MT-CO1 (mouse monoclonal, 1:1,000; Abcam, Cambridge, UK), complex V subunit ATP5F1A (mouse monoclonal, 1:2,000; Abcam, Cambridge, UK), and VDAC1 (mouse monoclonal, 1:3,000; Abcam, Cambridge, UK). All antibodies were diluted in Dako antibody diluent with background-reducing components (Dako, Glostrup, Denmark). For antigen retrieval, the sections were immersed for 45 min in 1 mM EDTA, 0.05% Tween-20, pH 8, at 95°C. Muscle tissue sections were incubated for 60 min with the above-mentioned primary antibodies. Staining was done with the DAKO envision kit.

RESULTS

Case Report – Clinical Features of the Patient

The male patient was born at term (at 39+3 weeks of gestation) by vaginal delivery using vacuum extraction, as the first child of non-consanguineous Caucasian parents. Due to the prenatally suspected aortic stenosis, the patient was immediately transferred to the Neonatal Intensive Care Unit. Birth weight (3140 g; 21st percentile), birth length (51 cm; 48th percentile), head circumference (33.5 cm; 17th percentile), Apgar scores 9/10/10, and pH from the umbilical artery were normal (pH: 7.27). The newborn had marks after vacuum extraction over the parietal region (cephalohematoma); muscle tone was normal, and no dysmorphic features were present. Postnatal echocardiography showed borderline width of the isthmus and aortic arch (but still within normal range), bicuspid aortic valve, and an open ductus arteriosus Botalli. No surgery or prostaglandin treatment was necessary, but the patient developed a need for oxygen therapy. On the third day after birth blood gas analysis showed an uncompensated metabolic acidosis with hyperlactatemia: plasma lactate: 6.7 mmol/l (normal range < 2.1 mmol/l), pH: 7.28 (N: 7.35–7.45), pCO_2: 42.1 mmHg (N: 35–45 mmHg), HCO_3^-: 18.2 mmol/l (N: 21–28), Base excess: −7.3 (N: 0 ± 3 mmol/l) with normoglycemia (Blood glucose: 59 mg/dl, N: 50–114). Anion gap was slightly elevated (AG: 16.9, N: 7–16). Since an inherited disorder of metabolism was suspected, metabolic screening was performed, which showed repeatedly lactate elevation: preprandial lactate: 6 mmol/l (N: 0.5–1.6), 3-OH-butyrate: 0.1 mmol/l (N: 0.03–0.3) glucose: 57 mg/dl (N: 50–114); postprandial lactate: 4 mmol/l, 3-OH-butyrate: 0.3 mmol/l, glucose: 84 mg/dl; plasmatic alanine elevation: 539.8 μmol/l (N: 116–376) and normal level of lactate in urine (19 mmol/mol creatinine, N 51 (1–156) mmol/mol creatinine). Other parameters (acylcarnitine profile, creatine kinase, aminotransferases, ammonemia, electrolytes, blood count) were normal. Glucose infusion (5 mg/kg/min.) was administered. The patient could have oral intake (suction) and neurological status was normal, with no signs of lethargy or hypotonia. Sonography of the abdomen did not show any

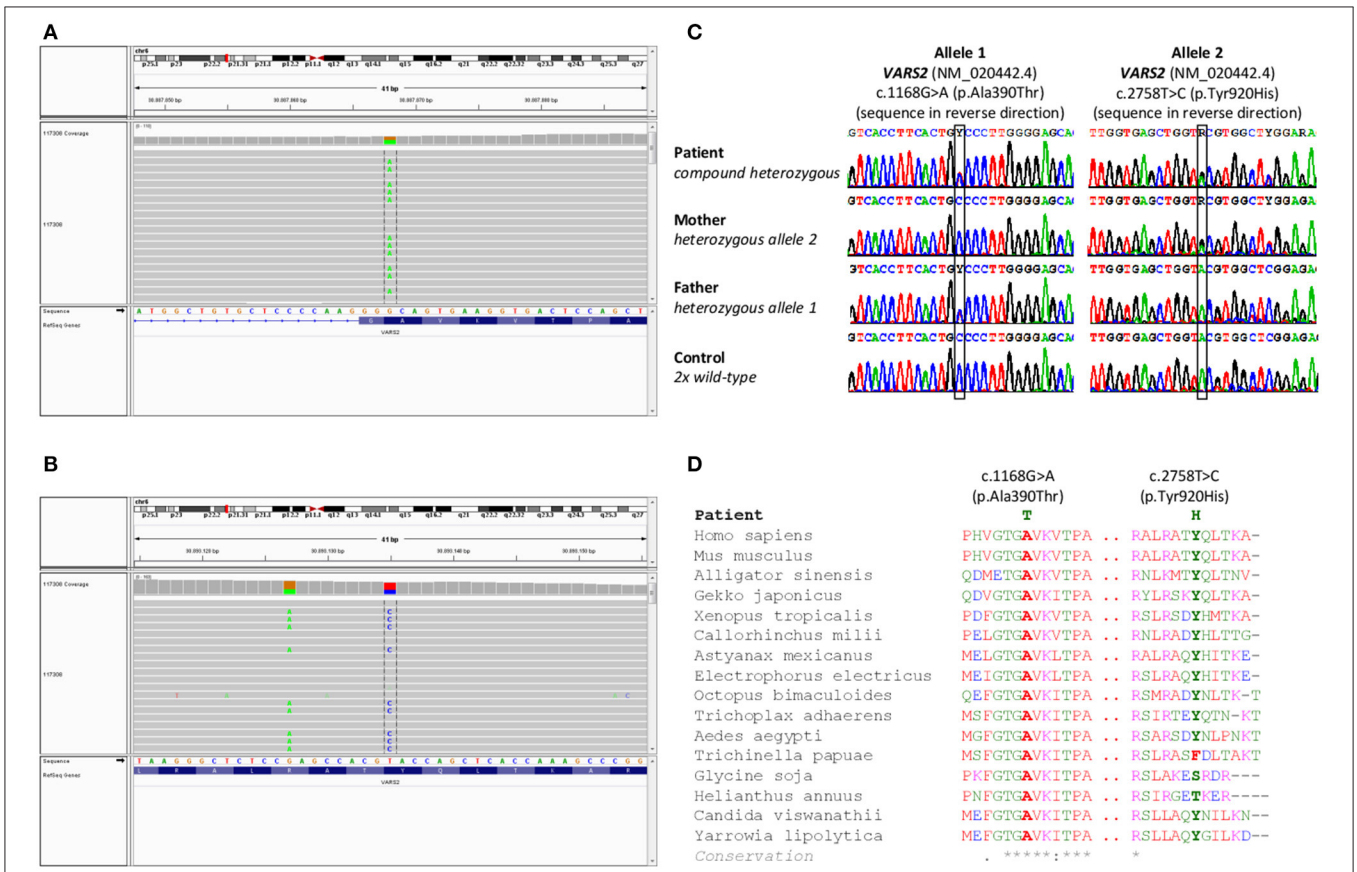

FIGURE 1 | Results of genetic testing. **(A,B)** Whole exome sequencing results in a patient with a finding of biallelic variants in the *VARS2* gene, heterozygous variant c.2758T>C (p.Tyr920His) and heterozygous variant c.1168G>A (p.Ala390Thr)**. (C)** Sanger sequencing confirmed both variants in the patient. Heterozygous variant c.2758T>C (p.Tyr920His) was found in patient's mother and heterozygous variant c.1168G>A (p.Ala390Thr) was found in patient's father. These findings confirmed biallelic position of variants in the patient, **(D)** shows phylogenetic conservation of VARS2 protein (NP 065175.4) in various organisms. Multiple sequence alignment was performed with Clustal Omega (https://www.ebi.ac.uk/Tools/msa/clustalo/).

pathology, especially no hepatosplenomegaly. Ophthalmologic examination showed normal findings without signs of cataract. The patient developed progressive symptoms of heart failure over the next few days. Echocardiography on the 16th day of life revealed primary pulmonary hypertension and hypertrophic cardiomyopathy of the left heart. Investigation of alpha-glucosidase excluded Pompe disease (19 nmol/mg–normal value). Cardiac catheterization showed pulmonary hypertension (PHT) and hemodynamic failure of the right heart. The myocardial biopsy was contraindicated due to the patient's severe clinical condition. Dobutamine, nitric oxide therapy, sildenafil, and oxygen therapy, with 60% FiO2 was administered. Based on suspicion of a mitochondrial disorder, muscle biopsy from the vastus lateralis muscle was performed for histopathological purposes. No changes for a primary muscle disorder were found. Based on specific enzyme histochemical staining (e.g., combined COX-SDH), no evidence for the presence of a mitochondrial myopathy could be demonstrated. Genetic testing of the *ACAD9* gene associated with mitochondrial complex I deficiency, nuclear type 20 (OMIM: # 611126) did not reveal any pathogenic mutation, and therefore whole-exome sequencing was indicated. Because of lasting suspicion of a mitochondrial disorder, treatment with riboflavin (20 mg/kg/d), coenzyme Q10 (30 mg/kg/d), and continuous intravenous glucose was administered. Under this treatment, lactate levels declined but still were above normal values. Levels were elevated during PHT crises (values during PHT crises were 11–13.3 mmol/l). On day 22, cardiac insufficiency worsened, and a first cardiopulmonary resuscitation was necessary. MRI of the brain and thorax performed on day 23 showed a focal hemorrhage in the right frontal subcortical region. The degree of myelination was appropriate for age. Cardiomegaly was evident. Low pleural effusions on both sides of the thorax and dystelectasia/atelectasia in both lungs were seen. On day 31, because of recurrent PHT crisis, dilatation and stent treatment of the foramen ovale was performed but was not successful. The patient was intubated and sedated with ketamine, midazolam, sufentanil, and myorelaxed. Cardiomyopathy progressed despite intensive care and the patient died on day 47 due to cardiopulmonary failure. A few days after the patient's death, the result of the WES analysis

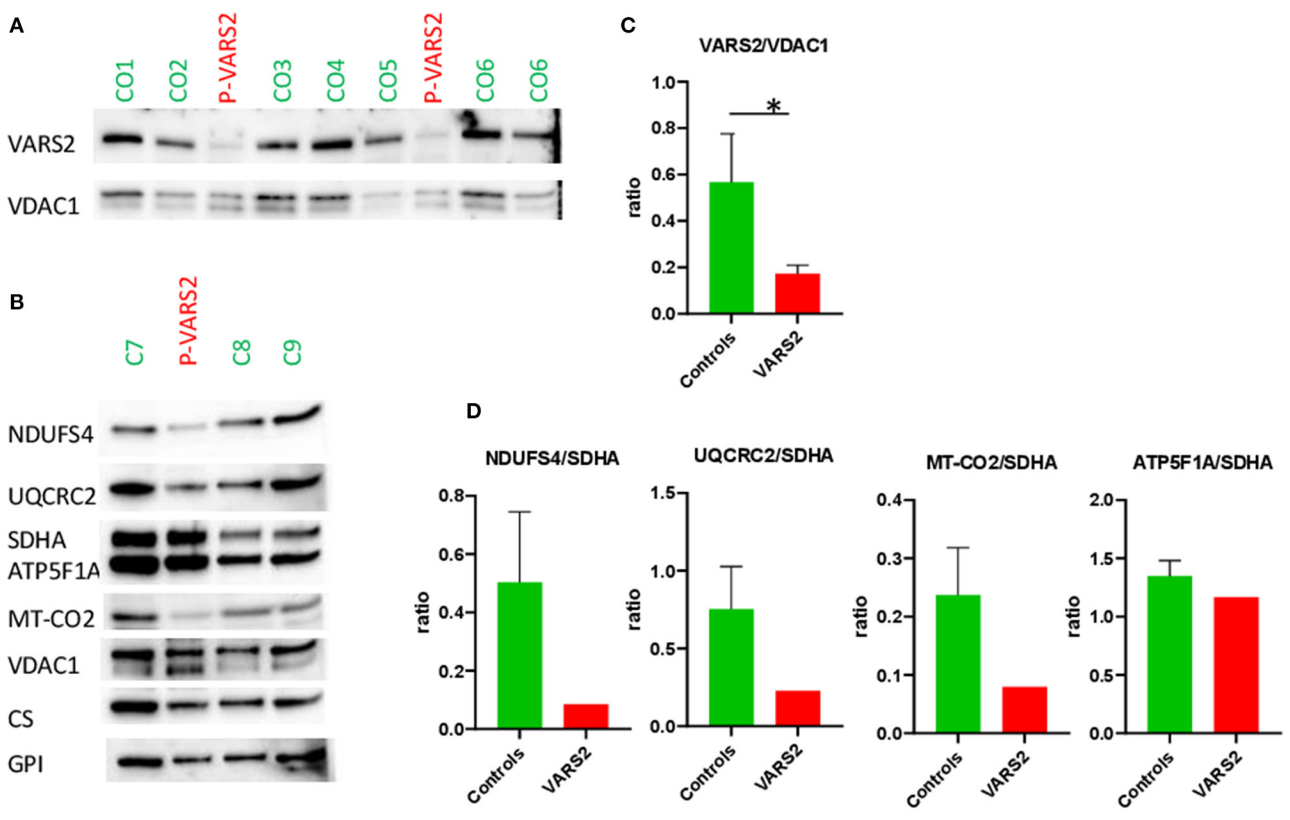

FIGURE 2 | (A,B) Western blot analysis of the muscle sample of the patient compared to healthy controls, using antibodies against VARS2, NADH dehydrogenase [ubiquinone] iron-sulfur protein 4 (NDUFS4), ubiquinol-cytochrome c reductase core protein 2 (UQCRC2), succinate dehydrogenase complex flavoprotein subunit A (SDHA), ATP synthase F1 subunit alpha (ATP5F1A), mitochondrially encoded cytochrome c oxidase II (MT-CO2), voltage-dependent anion-selective channel 1 (VDAC1, in outer mitochondrial membrane), citrate synthase (CS), glucosephosphate isomerase (GPI). **(C,D)** Bar graphs show the densitometry of the western blot bands. The intensity of the bands was determined using evaluation software (Imagelab, Biorad). The subunits of the OXPHOS complexes were evaluated in relation to VDAC1, CS, and GPI as loading controls. The results showed reduction of complex I in comparison to SDHA; moderate reduction of complex III and IV in comparison to SDHA and compensatory up-regulation/increase of complexes II and V. The ratios to VDAC1, CS, and GPI are shown in **Supplementary Table 1**. $^*p < 0.05$.

confirmed the state of compound heterozygosity for variants in the *VARS2* gene, supporting the assumption of a mitochondrial disorder in the child. Following the wish of the parents, no autopsy was performed.

Molecular Genetics Findings

Cytogenetic examination showed a normal male karyotype 46, XY. Genomic imbalances were ruled out by the SNP array. The whole-exome sequencing revealed the following biallelic variants in *VARS2* gene: allele 1 [NM_020442.6:exon13: c.1168G>A (p.Ala390Thr)] (https://www.ncbi.nlm.nih.gov/clinvar/variation/522814/); allele 2 [NM_020442.6:exon27: c.2758T>C (p.Tyr920His)] (https://www.ncbi.nlm.nih.gov/clinvar/variation/997679/) (**Figures 1A,B**). The finding was verified by Sanger sequencing. Examination of the parents showed the paternal *VARS2* variant c.1168G>A (p.Ala390Thr) in a heterozygous form and the maternal *VARS2* variant c.2758T>C (p.Tyr920His) in a heterozygous form (**Figure 1C**). Both variants involve residues that are highly conserved among phylogenetically distant organisms. At position 920, tyrosine is most frequently found in some organisms, also the amino acid phenylalanine, both with a phenyl group. In plants, this position is not conserved with serine or threonine in the alignment. Position 390 is highly conserved (**Figure 1D**). Position 390 corresponds to the tRNA-synthetase domain and position 920 corresponds to the anticodon binding domain of the protein VARS2 (1, 12). These findings support the pathogenicity of the variants found in our patient.

Histopathology, Immunohistochemistry, Enzymatic Analysis, Substrate Oxidation, and Western Blot

Western blot analysis revealed a reduction of VARS2 protein amount in muscle homogenates of the affected patient compared to seven controls (**Figures 2A,C**; **Supplementary Table 1**). VARS2 was normalized to four loading proteins namely VDAC1, CS, GPI, and SDHA. Residual VARS2 protein levels were between 16 and 34% of the control levels. No obvious histopathological findings pointing toward a mitochondrial disorder were found. The enzymatic analysis showed values in or above the normal range for the mitochondrial marker enzyme citrate synthase (summary of the results is shown in **Table 1**). Absolute complex I activity was significantly reduced in patient muscle compared to controls. Consistently, the complex I activities normalized to the citrate synthase and complex II were significantly lower in patients muscle (**Table 1**). Normalized to complex II which is not dependent on mitochondrial translation a downregulation of complex IV was found. An increase in combined normalized complex II-III activity was present. A compensatory upregulation of unaffected complexes is a well-known phenomenon in mitochondrial disorders. In substrate oxidation analysis some activities were in relation to the protein content in the normal range, others were elevated. Also in relation to citrate synthase similar activities were high. In relation to complex II the oxidation rate of pyruvate + carnitine was slightly elevated. These elevated activities are likely due to compensatory upregulation of mitochondria. In contrast, the ratio of the long oxidation path via pyruvate + malate compared to pyruvate + carnitine was somewhat reduced with a value of 0.63 (normal 0.68–1.09). This is consistent with a defect in the respiratory chain, while the reaction from pyruvate to acetyl-carnitine works better. This shortcut of the full oxidation route forms only one NADH, while the whole path creates 4 NADH and 1 $FADH_2$. Consistently, western blot analysis revealed a reduction of complexes I, III and IV in patient homogenate compared to controls (**Figure 2**). The reduction was present compared to several normalization proteins VDAC1 (outer mitochondrial membrane), CS (mitochondrial matrix), GPI (cytosol) and SDHA (inner mitochondrial membrane and independent from mitochondrial translation) (**Figure 2**; **Supplementary Figure 1**; **Supplementary Table 1**). Also in immunohistochemical staining of VDAC1 (Voltage-dependent anion-selective channel 1) and subunits of the OXPHOS complexes in skeletal muscle showed a slight reduction of NDUFB8 (complex I subunit) and UQCRC2 (complex III subunit) in the affected individual compared to controls (**Supplementary Figure 2**). A compensatory upregulation of complex II was also present in immunohistochemical staining.

DISCUSSION

Mitochondriopathies associated with mutations in mitochondrial aminoacyl-tRNA synthetases present a wide spectrum of miscellaneous disorders based on various genetic changes. Recently, several mutations in *VARS2* gene were associated with clinical features such as hypotonia, psychomotor delay, encephalopathy, cardiomyopathy, hyperlactatemia, but the correlation between genotype and phenotype remains unclear (1, 15). To date, 19 families with more than 23 affected individuals have been described in the literature worldwide (1, 4, 6–15) whereby c.1100C>T (p.Thr367Ile) is the most common variant in the *VARS2* gene present in 60.8% (14/23) of the published cases (see **Table 2**). Common features of homozygous carriers for variant c.1100C>T (p.Thr367Ile) include microcephaly, global psychomotor delay, and hypotonia, less often nystagmus, limb spasticity, and difficulties with feeding. In the first 12 months of life, ataxia, dystonic movements, and seizures can occur, which later (from 2 to 4 years) almost always lead to refractory epilepsy and status epilepticus based on mitochondrial encephalopathy (1, 6, 13). Nevertheless, hypertrophic cardiomyopathy (HCM) has never been observed in these patients (eight patients of which five had no HCM, in three cases the results of cardiologic examination are not available) (1, 6, 13, 15). However, in compound heterozygotes (for variant c.1100C>T (p.Thr367Ile) and another, or two other pathogenic variants, hypertrophic cardiomyopathy was present in 14/15 cases (1, 4, 7–12, 14). These additional findings support Bruni et al. (1) assumption that "*c.1100C>T variant could have a lesser effect to the heart.*" In the present paper we describe a compound heterozygous case with a recurrent c.1168G>A

TABLE 2 | Review of published cases and new patient with *VARS2* deficiency – clinical characteristics, laboratory and molecular genetics findings [modified after (1)].

Patient/ family	References	Sex	Mutation	Ethnicity	Current age/death	Onset	Hearth	Neurological signs	MRI + spectroscopy/other features	Lab tests/ Lactate	OXPHOS muscle
Our case P24/F20	**Kušíková et al., this study**	**M**	**c.1168G>A c.2758T>C**	**Caucasian (Austrian)**	**Death 47 d.**	**From birth**	**HCM**	**Normal**	**Normal MRI of the brain + PPHN**	**Plasma (4–13 mmol/l)**	**↓↓ CI ↓ CIII+CIV ↑CII+CV**
P1/F1	Bruni et al. (1)	F	Homozygous c.1100C>T	Caucasian (Polish)	Alive at 5 y.	From birth	No HCM	Hypotonia, poor coordination, develompmental delay, seizures	Hyperintensity in the periventricular white matter bilaterally, cerebral atrophy; small lactate peak at MRS	N/A	N/A
P2/F2	Bruni et al. (1)	F	c.2557-2A>G c.1100C>T	Caucasian	Death at 3,5 m.	From birth	HCM	Hypotonia, hyporeflexia, exag. startle, staring episodes, vocal cord paralysis	Diffuse cerebral and cerebellar atrophy, focal gliosis around the Sylvian fissures bilaterally, cerebellum, scattered areas of cortical restricted diffusion, subtle thalamic restricted diffusion bilaterally, large lactate peak at MRS	Plasma (1.7–8.9 mmol/l) and urinary elevation	Normal
P3/F3	Bruni et al. (1)	M	c.1546G>T c.2239G>A	Jewish comunity	Death at 19 m.	From birth	HCM	Hypotonia, severe stridor, poor sucking, hypertonia of the lower limbs	N/A	Plasma (3.5–4 mmol/l) and urinary elevation	↓ CIV
P4/F4	Bruni et al. 2018 (1)	F	c.1100C>T c.1150G>A	Italian	Death at 5 m.	From birth	HCM	Hypotonia, feeding difficulties and psychomotor delay	Cerebellar atrophy, corpus callosum hypotrophy	Plasma (4.2 mmol/l) and CSF (3 mmol/l; Nv<2.3 mmol/l)	Normal activities
P5/F5	Bruni et al. (1) and Taylor et al. (4)	M	c.1135G>A c.1877C>A	British	Alive at 18 y.	First few months	mild concentric ventricular hypertrophy	Developmental delay, ptosis and ophtalmoparesis, generalized epilepsy, fatigue, proximal weakness, dyspraxia	Symmetrical bilateral basal ganglia calcification, symmetrical increased T2 signal in the peri-trigonal white matter	N/A	↓ CI+CIV
P6/F6	Bruni et al. (1) and Pronicka et al. (9)	M	c.1100C>T c.1490G>A	Polish	Death at 3 m.	Birth	HCM	Hypotonia, stridor and respiratory failure, limbs spasticity	N/A	Plasma (4.4–8.7 mmol/l)	↓CIV
P7/F6	Bruni et al. (1) and Pronicka et al. (9)	M	c.1100C>T c.1490G>A	Polish	Death at 9 y.	From birth	HCM	Hypotonia, stridor and respiratory failure, limbs spasticity, epilepsy	Hypoplasia of vermis, mild cerebral atrophy, small symmetric hyperintense changes in thalamus and septum pellucidum	Plasma (2.9–10.6 mmol/l)	N/A
P8/F7	Bruni et al. (1)	M	Homozygous c.1258G>A	Mexican	Death at 9 d.	From birth	HCM	Hypotonia, feeding difficulty	N/A	Plasma elevation	N/A

(Continued)

TABLE 2 | Continued

Patient/ family	References	Sex	Mutation	Ethnicity	Current age/death	Onset	Hearth	Neurological signs	MRI + spectroscopy/other features	Lab tests/ Lactate	OXPHOS muscle
Our case P24/F20	**Kušíková et al., this study**	**M**	**c.1168G>A c.2758T>C**	**Caucasian (Austrian)**	**Death 47 d.**	**From birth**	**HCM**	**Normal**	**Normal MRI of the brain + PPHN**	**Plasma (4–13 mmol/l)**	**↓↓ CI ↓ CIII+CIV ↑CII+CV**
P9/F7	Bruni et al. (1)	F	Homozygous c.1258G>A	Mexican	Death at 3 m.	From birth	HCM	Hypotonia, feeding difficulty	N/A	Plasma elevation	N/A
P10/F8	Bruni et al. (1)	M	Homozygous c.1258G>A	Mexican	Alive at 3 m.	From birth	HCM	Hypotonia, feeding difficulty, respiratory distress, developmental delay, epilepsy	N/A	Plasma elevation	N/A
P11/F9	Bruni et al. (1)	F	Homozygous c.1100C>T	Afganistan	Death at 7 y.	From 1st month	N/A	Severe hypotonia, feeding difficulty, psychomotor retardation, nystagmus, intractable epilepsy	Cerebellar atrophy (cerebellar hemispheres + vermis), signal intensity in dentate nuclei, signal intensity and mild atrophy in thalami, corpus callosum slightly thin	Plasma normal (2.3 mmol/l)	N/A
P12/F9	Bruni et al. (1)	F	Homozygous c.1100C>T	Afganistan	Death at 8 y.	From 1st month	N/A	Hypotonia, feeding difficulty (gastrostomy), psychomotor retardation, limb spasticity, intractable epilepsy	Cerebellar atrophy, signal intensity in dentatenuclei and thalami, thin corpus callosum, no lactatepeak in MRS	Plasma (2.8 mmol/l)	N/A
P13/F9	Bruni et al. (1)	M	Homozygous c.1100C>T	Afganistan	Alive at 5 m.	From birth	No HCM	Hypotonia	Unilateral mild cerebellar hemispheric hypoplasia	Plasma (4.4 mmol/l), CSF (3.08 mmol/l)	N/A
P14/F10	Diodato et al. (6)	M	Homozygous c.1100C>T	Italian	Alive at 8 y.	From birth	N/A	Psychomotor delay, microcephaly, epilepsy, status epilepticus	Hyperintense lesions in the periventricular regions, the insulae, and the frontotemporal right cortex, MRS: lactate peak in the frontal white matter + facial dysmorphy	N/A	↓ CI
P15/F11	San Millan et al. (8)	N/A	c.1010C>T stop codon	N/A	Death 4 m.	From birth	HCM	Floppy infant, tongue fasciculation	N/A	N/A	↓ CIV
P16/F12	Baertling et al. (11)	M	c.601C>T c.1100C>T	Greek	Alive at 5 m.	From birth	HCM	Epilepsy, burst suppression, spasticity, microcephaly, exotrophy	Hypoplasia of the corpus callosum and the cerebellum, edema of the brain stem and the frontal white matter, hyperintensities in basal ganglia displayed, MRS lactate peak	Plasma (>28 mmol/l)	N/A
P17/F13	Alsemari et al. (10)	M	Homozygous c.3650G>A	Saudi Arabia	23 y.	4 m.	N/A	Severe mental retardation, ataxia, speech impairment, epilepsy	Cerebellar atrophy + short stature, microcephaly, dysmorphia, excitable personality, excessive chewing mouth behaviors, severe growth hormone deficiency, hypogonadism, severe osteomalacia, Angelman-like syndrome	N/A	N/A

(Continued)

TABLE 2 | Continued

Patient/ family	References	Sex	Mutation	Ethnicity	Current age/death	Onset	Hearth	Neurological signs	MRI + spectroscopy/other features	Lab tests/ Lactate	OXPHOS muscle
Our case P24/F20	**Kušíková et al., this study**	**M**	**c.1168G>A c.2758T>C**	**Caucasian (Austrian)**	**Death 47 d.**	**From birth**	**HCM**	**Normal**	**Normal MRI of the brain + PPHN**	**Plasma (4–13 mmol/l)**	**↓↓ CI ↓ CIII+CIV ↑CII+CV**
P18/F14	Ma et al. (12)	F	c.643C>T c.1354A>G	Chinese	Death at 16 d.	From birth	HCM	Poor sucking, hypertonia	The brain ultrasonic examination: mild echo enhancement on the side of the bilateral paraventricular parenchyma, a left-ependymal cyst and a right-choroid plexus cyst + PPHN	Plasma (3-15.6 mmol/l)	N/A
P19/F15	Pereira et al. (13)	F	Homozygous c.1100C>T	Portuguese	Death at 28 m.	From birth	No HCM	Microcephaly, severe global hypotonia, severe epileptic encephalopathy	Global atrophy and a small glioepithelial cyst associated with left hippocampal molding + progressive feedings difficulties, and failure to thrive	Plasma (5.35 mmol/l)	Normal
P20/F16	Ruzman et al. (14)	F	c.1100C>T c.603_606dupGATG	N/A	Death at 10 m.	1 month	HCM	Microcephaly, infantile spasms with hypsarrhytmia on EEG, later burstsuppression pattern, severe global hypotonia	Diffuse cerebral atrophy, hypoplasia of the cerebellum (vermis), brainstem, and corpus callosum, MRS high lactate peak	Plasma (2.0–5.4 mmol/l), CSF (3 mmol/l), Alanin plasma and CSF (537 and 36.1 umol/l)	N/A
P21/F17	Begliuomini et al. (15)	F	Homozygous c.1100C>T	Sardinian	Alive at 6 years	From 11 months	No HCM	Motor and language delays, hypotonia, brisk tendon reflexes	Atrophic progression of the cerebellum with T2-FLAIR hyperintensities of cerebellar white matter and dentate nuclei, MRS increased lactate and decreased N-acetyl aspartate peaks	N/A	↓ CI + CIII
P22/F18	Begliuomini et al. (15)	F	Homozygous c.1100C>T	Sardinian	Alive at 5 years	From 12 months	No HCM	Nystagmus with alternating strabismus, brisk tendon reflexes, global hypotonia and impaired coordination, swallowing difficulties	Cerebellar atrophy and vermis hypoplasia with normal MRS	increased	N/A
P23/F19	Chin et al. (7)	M	c.1940C>T c.2318G>A	Chinese	Alive at 14 months	From 1 month	No HCM	Developmental delay	Normal MRI of the brain + PPHN, moderate hypertrophy of RV and dilat. RA and RV, growth failure, gastroesophageal reflux	Plasma (9.2 mmol/l)	N/A

P/F, patient/family; F, female; M, male; d., day; m., month; y., year; HCM, hypertrophic cardiomyopathy; RV, right ventricle; RA, right atrium; PPHN, persistent pulmonary hypertension of the newborn; MRI, magnetic resonance imaging; MRS, magnetic resonance spectroscopy; CSF, cerebrospinal fluid; N/A, not available information; CI-CV, OXPHOS complex I–V. Arrow down: reduced values compared to healthy controls. Arrow up: increased values compared to healthy controls.

(p.Ala390Thr) and a novel missense variant c.2758T>C (p.Tyr920His) in the *VARS2* gene. Position 390 corresponds to the tRNA-synthetase domain and position 920 corresponds to the anticodon binding domain of the protein VARS2 (1, 12). Both variants show a relatively high level of phylogenetic conservation (**Figure 1D**). The p.Ala390Thr was reported in ClinVar four times (Accession number: VCV000522814.3). Bruni et al. (1) published a case with a homozygous p.Ala390Thr underlining its pathologic relevance. However, we for the first time proved pathogenicity of this obviously recurrent variant with biochemical and immunohistochemical methods. Here we show that the recurrent p.Ala390Thr in combination with a novel missense variant causes a severe reduction of VARS2 protein amount. In contrast with published data, in our case, HCM was a leading feature accompanied by hyperlactatemia and pulmonary hypertension, which led to early death (on 47th day of life) without any other accompanying signs. We see a certain similarity in the case of a patient with pathogenic *VARS2* mutations c.643C>T (p.His215Tyr) and c.1354A>G (p.Met452Val) who presented with poor sucking at birth, poor motor activity, hyporeflexia, hypertonia, persistent pulmonary hypertension of the newborn (PPHN), metabolic acidosis, severe lactic acidosis, and hypertrophic cardiomyopathy (12). The patient died on the 16th day of life due to cardiac arrest due to pulmonary hypertension and hypertrophic cardiomyopathy. Our patient had a normal neurological assessment with no hypotonia and no signs of encephalopathy, neither clinically nor on brain MRI on the 23rd day of life; this finding contrasts with published data (1, 15). Finally, we correlated published histopathological findings of skeletal muscle tissue with negative findings in our patient. Five of 13 patients reported by Bruni et al. (1) underwent muscle biopsy (quadriceps muscle). Two patients showed normal histopathologic findings, one case had mild unspecific myopathic changes with COX-deficient/SDH-positive fibers, and one patient showed signs of neurogenic atrophy. The fifth patient showed at the electron microscopy level mitochondria that were relatively decreased in number and size, with mostly unremarkable morphology, although some were distorted or atypical (with atypical cristae). The data from San Millan et al. (8) demonstrate an uneven involvement of muscles with predominant involvement of myocardium and diaphragm. Our patient had no obvious histopathological findings pointing toward a mitochondrial disorder in vastus lateralis muscle. Unfortunately, a myocardial biopsy was contraindicated in our patient due to the patient's serious clinical condition and an autopsy was not done following the wish of the patient's parents. It would be interesting to evaluate the lactate peak by MR spectroscopy and determine lactate and alanine in cerebrospinal fluid (1, 6, 11, 14), but these were unfortunately not performed during the patient's life. OXPHOS activity was evaluated in eight patients from Bruni et al. (1), Diodato et al. (6) San Millan et al. (8), and Begliuomini et al. (15). However, OXPHOS activity was decreased only in six of them (the first patient had low complex IV activity, the second patient had combined complex I + complex IV deficiencies, the third patient had low complex IV activity, the fourth had low complex I activity, the fifth had low complex IV activity, and the sixth showed reduced complex I and III activity). In our case the results showed a strong reduction of complex I, a moderate reduction of complex III and IV, and compensatory upregulation in complex II and V. A review of all published patients so far is shown in **Table 2**. Clinical manifestations, disease severity, and life expectancy vary significantly between published cases. We assume that the different phenotypic manifestations in the reported cases could result from the variable expression of valyl-tRNA synthetase in different tissues at different time points after birth, and/or due to unknown epigenetic effects, but further investigations in this field are needed.

CONCLUSION

The data and finding of a novel variants in the *VARS2* gene of our case expands the spectrum of known mutations in humans and the spectrum of associated clinical features. Nowadays, thanks to increasing number of publish data we can assume a reduced impact of the homozygous c.1100C>T (p.Thr367Ile) mutation on the myocardium, but we cannot postulate that specific OXPHOS complexes or organ systems are impaired due to specific mutations in the *VARS2* gene. Further investigations to find specific genotype-phenotype correlations are needed in this field. It is known that biallelic mutations in the *VARS2* gene cause systemic impairment. Structural cardiac abnormalities and hypertrophic cardiomyopathy (HCM) could be the first manifestation of the disease leading to early death in the newborn period or in early infancy before developing other clinical features. That is why we think that it is of utmost importance to consider the presence of a possible mitochondriopathy in these patients and to include the analysis of the *VARS2* gene in the genetic diagnostic algorithm in cases with early manifesting and rapidly progressing HCM with hyperlactatemia.

DATA AVAILABILITY STATEMENT

Publication of the complete exome data is not included in the consent for clinical exome sequencing. The VARS2 variants have been made publicly available via ClinVar. Requests to access the datasets in more detail can be directed to the corresponding author.

The ClinVar registration numbers are: SUB9123334, SUB9123465 and they are publicly available:

Variant 1: https://www.ncbi.nlm.nih.gov/clinvar/variation/522814/

Variant 2: https://www.ncbi.nlm.nih.gov/clinvar/variation/997679/.

ETHICS STATEMENT

The studies involving human participants were reviewed and approved by Ethics Committee of the Land Salzburg (number 415-E/2552/10-2019). Written informed consent to participate in

this study was provided by the participants' legal guardian/next of kin.

AUTHOR CONTRIBUTIONS

This manuscript was written by KK under the guidance of DW. RF, SW, and JM conceptualized figures, revised, and edited the manuscript. H-CD performed sample collection. BC provided clinical data. OK performed muscle biopsy. All authors contributed to the article and approved the submitted version.

FUNDING

This work was supported by the Austrian Science Fund (FWF) [I 4695-B, GENOMIT] to JM.

ACKNOWLEDGMENTS

The authors would like to thank the patient's family. The patient's parents signed informed consent for publication.

SUPPLEMENTARY MATERIAL

The Supplementary Material for this article can be found online at: https://www.frontiersin.org/articles/10.3389/fped.2021.660076/full#supplementary-material

Supplementary Table 1 | Densitometric analysis of the western blotting experiments shown in **Figure 2** and **Supplementary Figure 1**.

Supplementary Figure 1 | Western blot analysis of the muscle sample of the patient compared to healthy controls, using antibodies against VARS2, NADH dehydrogenase [ubiquinone] iron-sulfur protein 4 (NDUFS4), ubiquinol-cytochrome c reductase core protein 2 (UQCRC2), succinate dehydrogenase complex flavoprotein subunit A (SDHA), ATP synthase F1 subunit alpha (ATP5F1A), voltage-dependent anion-selective channel 1 (VDAC1), citrate synthase (CS), glucosephosphate isomerase (GPI). Because of a low gel resolution ATP5F1A and UQCRC2 cannot be visually separated in the technical replicate 1 of the western blot.

Supplementary Figure 2 | Immunohistochemical staining of VDAC1 and subunits of the OXPHOS complexes in skeletal muscle of affected individual and controls. **(A–C)** VDAC1 staining; **(D–F)** NDUFB8 staining; **(G–I)** SDHA staining; **(J–L)** UQCRC2 staining; **(M–O)** MT-CO1 staining; **(P–R)** ATP5F1A staining; **(A,D,G,J,M,P)** control 1; **(B,E,H,K,N,Q)** control 2; **(C,F,I,L,O,R)** affected individual. Images were taken with a 400x magnification. A slight reduction of NDUFB8 and UQCRC2 was present in muscle of the affected individual compared to controls.

REFERENCES

1. Bruni F, Meo Di I, Bellacchio E, Webb BD, McFarland R, Chrzanowska-Lightowlers ZMA, et al. Clinical, biochemical, and genetic features associated with VARS2-related mitochondrial disease. *Hum Mutat*. (2018) 39:563–78. doi: 10.1002/humu.23398
2. Ghezzi D, Zeviani M. Assembly factors of human mitochondrial respiratory chain complexes: physiology and pathophysiology. In: Kadenbach B, editor. *Mitochondrial Oxidative Phosphorylation. Advances in Experimental Medicine and Biology, Vol 748*. New York, NY: Springer (2012). p. 65–106. doi: 10.1007/978-1-4614-3573-0_4
3. Rötig A. Human diseases with impaired mitochondrial protein synthesis. *Biochim Biophys Acta*. (2011) 1807:1198–205. doi: 10.1016/j.bbabio.2011.06.010
4. Taylor RW, Pyle A, Griffin H, Blakley EL, Duff J, He L, et al. Use of whole-exome sequencing to determine the genetic basis of multiple mitochondrial respiratory chain complex deficiencies. *JAMA*. (2014) 312:68–77. doi: 10.1001/jama.2014.7184
5. Spinazzola A, Zeviani M. Mitochondrial diseases: a cross-talk between mitochondrial and nuclear genomes. In: Espinós C, Felipo V, Palau F, editors. *Inherited Neuromuscular Diseases. Advances in Experimental Medicine and Biology, Vol 652*. Dordrecht: Springer (2009). p. 69–84. doi: 10.1007/978-90-481-2813-6_6
6. Diodato D, Melchionda L, Haack TB, Dallabona C, Baruffini E, Donnini C., et al. VARS2 and TARS2 mutations in patients with mitochondrial Encephalomyopathies. *Hum Mutat*. (2014) 35:983–9. doi: 10.1002/humu.22590
7. Chin HL, Goh DL, Wang FS, Tay SKH, Heng CK, Donnini C. et al. A combination of two novel VARS2 variants causes a mitochondrial disorder associated with failure to thrive and pulmonary hypertension. *J Mol Med*. (2019) 97:1557–66. doi: 10.1007/s00109-019-01834-5
8. San Millan B, Blazquez A, Delmiro A, Ruffian L, Navarro C, Teijeira S, et al. Variable skeletal muscle involvement in VARS2 mitochondrial encephalomyopathy. *NMD*. (2016) 26:178. doi: 10.1016/j.nmd.2016.06.333
9. Pronicka E, Piekutowska-Abramczuk D, Ciara E, Trubicka J, Rokicki D, Karkucinska-Wieckowska A, et al. New perspective in diagnostics of mitochondrial disorders: two years' experience with whole-exome sequencing at a national paediatric centre. *J Transl Med*. (2014) 14:174. doi: 10.1186/s12967-016-0930-9
10. Alsemari A, Al-Younes B, Goljan E, Jaroudi D, BinHumaid F, Meyer BF, et al. Recessive VARS2 mutation underlies a novel syndrome with epilepsy, mental retardation, short stature, growth hormone deficiency, and hypogonadism. *Human Genomics*. (2017) 11:28. doi: 10.1186/s40246-017-0130-6
11. Baertling F, Alhaddad B, Seibt A, Budaeus S, Meitinger T, Strom TM., et al. Neonatal encephalocardiomyopathy caused by mutations in VARS2. *Metab Brain Dis*. (2017) 32:267–70. doi: 10.1007/s11011-016-9890-2
12. Ma K, Xie M, He X, Liu G, Lu X, Peng Q, et al. A novel compound heterozygous mutation in *VARS2* in a newborn with mitochondrial cardiomyopathy: a case report of a Chinese family. *BMC Med Genet*. (2018) 19:202. doi: 10.1186/s12881-018-0689-3
13. Pereira S, Adrião M, Sampaio M, Basto MA, Rodrigues E, Vilarinho L, et al. Mitochondrial encephalopathy: first Portuguese report of a VARS2 causative variant. *JIMD Rep*. (2018) 42:113–9. doi: 10.1007/8904_2018_89
14. Ruzman L, Kolic L, Radic Nisevic J., Ruzic Barsic A, Skarpa Prpic I, Prpic I, et al. A novel VARS2 gene variant in a patient with epileptic encephalopathy. *Upsala J Med Sci*. (2019) 124:273–7. doi: 10.1080/03009734.2019.1670297
15. Begliuomini C, Magli G, Rocco Di. M, Santorelli FM, Cassandrini D, Nesti C, et al. VARS2-linked mitochondrial encephalopathy: two case reports enlarging the clinical phenotype. *BMC Med Genet*. (2019) 20:77. doi: 10.1186/s12881-019-0798-7
16. Feichtinger RG, Mucha BE, Hengel H, Hengel H, Orfi Z, Makowski CH., et al. Biallelic variants in the transcription factor PAX7 are a new genetic cause of myopathy. *Genet Med*. (2019) 21:2521–31. doi: 10.1038/s41436-019-0532-z
17. Feichtinger RG, Zimmermann F, Mayr JA, Neureiter D, Hauser-Kronberger C, Schillin FH et al. Low aerobic mitochondrial energy metabolism in poorly- or undifferentiated neuroblastoma. *BMC Cancer*. (2010) 10:149. doi: 10.1186/1471-2407-10-149
18. Rustin P, Chretien D, Bourgeron T, Gérard B, Rötig A, Saudubray JM, et al. Biochemical and molecular investigations in respiratory chain deficiencies. *Clin Chim Acta*. (1994) 228:35–51. doi: 10.1016/0009-8981(94)90055-8
19. Bookelman H, Trijbels JM, Sengers RC, Janssen AJ, Veerkamp JH, Stadhouders AM. Pyruvate oxidation in rat and human skeletal muscle mitochondria. *Biochem Med*. (1978) 20:395–403. doi: 10.1016/0006-2944(78)90089-3
20. Feichtinger RG, Neureiter D, Kemmerling R, Mayr JA, Kiesslich T, Kofler B. Low VDAC1 expression is associated with an aggressive phenotype and reduced overall patient survival in cholangiocellular carcinoma. *Cells*. (2019) 8:539. doi: 10.3390/cells8060539

21. Feichtinger RG, Schäfer G, Seifarth C, Mayr JA, Kofler B, Klocker H. Reduced levels of ATP synthase subunit ATP5F1A correlate with earlier-onset prostate cancer. *Oxid Med Cell Longev*. (2018) 2018:1347174. doi: 10.1155/2018/1347174
22. Feichtinger RG, Weis S, Mayr JA, Zimmermann FA, Bogner B, Sperl W, et al. Alterations of oxidative phosphorylation in meningiomas and peripheral nerve sheath tumors. *Neu Onc*. (2016) 18:184–94. doi: 10.1093/neuonc/nov105
23. Feichtinger RG, Weis S, Mayr JA, Zimmermann F, Geilberger R, Sperl W, et al. Alterations of oxidative phosphorylation complexes in astrocytomas. *Glia*. (2014) 62:514–25. doi: 10.1002/glia.22621

Conflict of Interest: The authors declare that the research was conducted in the absence of any commercial or financial relationships that could be construed as a potential conflict of interest.

frontiers in Genetics

ORIGINAL RESEARCH
published: 01 July 2021
doi: 10.3389/fgene.2021.611226

Novel Mutations in the *GTPBP3* Gene for Mitochondrial Disease and Characteristics of Related Phenotypic Spectrum: The First Three Cases From China

Hui-ming Yan[1,2,3†], Zhi-mei Liu[4†], Bei Cao[5], Victor Wei Zhang[6,7], Yi-duo He[7], Zheng-jun Jia[1,2,3], Hui Xi[1,2,3], Jing Liu[1,2,3], Fang Fang[4] and Hua Wang[1,2,3*]*

[1] Department of Genetic Medicine, Hunan Provincial Maternal and Child Health Care Hospital, Changsha, China, [2] National Health Commission Key Laboratory of Birth Defect, Research and Prevention, Changsha, China, [3] Newborn Screening Center of Hunan Province, Changsha, China, [4] Department of Neurology, National Center for Children's Health, Beijing Children's Hospital, Capital Medical University, Beijing, China, [5] Department of Neonatology, Hunan Provincial Maternal and Child Health Care Hospital, Changsha, China, [6] Department of Human and Molecular Genetics, Baylor College of Medicine, Houston, TX, United States, [7] AmCare Genomics Lab, Guangzhou, China

OPEN ACCESS

Edited by:
Ronald Wanders,
University of Amsterdam, Netherlands

Reviewed by:
Rita Horvath,
University of Cambridge,
United Kingdom
Grant M. Hatch,
University of Manitoba, Canada

***Correspondence:**
Fang Fang
13910150389@163.com
Hua Wang
wanghua_213@126.com

[†] These authors have contributed equally to this work

Specialty section:
This article was submitted to Genetics of Common and Rare Diseases, a section of the journal Frontiers in Genetics

Received: 17 October 2020
Accepted: 12 May 2021
Published: 01 July 2021

Citation:
Yan H-m, Liu Z-m, Cao B, Zhang VW, He Y-d, Jia Z-j, Xi H, Liu J, Fang F and Wang H (2021) Novel Mutations in the GTPBP3 Gene for Mitochondrial Disease and Characteristics of Related Phenotypic Spectrum: The First Three Cases From China. Front. Genet. 12:611226. doi: 10.3389/fgene.2021.611226

Combined Oxidative Phosphorylation Deficiency 23 (COXPD23) caused by mutations in *GTPBP3* gene is a rare mitochondrial disease, and this disorder identified from the Chinese population has not been described thus far. Here, we report a case series of three patients with COXPD23 caused by *GTPBP3* mutations, from a severe to a mild phenotype. The main clinical features of these patients include lactic acidosis, myocardial damage, and neurologic symptoms. Whole genome sequencing and targeted panels of candidate human mitochondrial genome revealed that patient 1 was a compound heterozygote with novel mutations c.413C > T (p. A138V) and c.509_510del (p. E170Gfs*42) in *GTPBP3*. Patient 2 was a compound heterozygote with novel mutations c.544G > T (p. G182X) and c.785A > C (p.Q262P), while patient 3 was a compound heterozygote with a previously reported mutation c.424G > A (p.E142K) and novel mutation c.785A > C (p.Q262P). In conclusion, we first describe three Chinese individuals with COXPD23, and discuss the genotype-phenotype correlations of *GTPBP3* mutations. Our findings provide novel information in the diagnosis and genetic counseling of patients with mitochondrial disease.

Keywords: mitochondrial disease, Combined Oxidative Phosphorylation Deficiency 23, *GTPBP3* gene, hyperlactacidemia, hyperalaninemia

INTRODUCTION

Mitochondrial disease is a clinically and genetically heterogeneous group of disorders that result from dysfunction of the mitochondrial respiratory chain and oxidative phosphorylation (OXPHOS) (Craven et al., 2017). It is an unusual clinical entity with an estimated incidence of 5/100,000 in children and most often affects organs with the highest energy demands such as the brain, heart, liver, and skeletal muscle, etc. (Skladal et al., 2003; Craven et al., 2017; Rahman and Wolf, 2017). Mitochondrial function is under the dual genetic control of both

the mitochondrial and nuclear genomes. The human *GTPBP3* gene (MIM #608536) is a nuclear encoded gene and is mapped on chromosome 19p13.11. It encodes the Gtpbp3 protein, a mitochondrial GTP-binding protein involving mitochondrial tRNA (mt-tRNA) post-transcription modification. Defects of *GTPBP3* inhibit taurine modification of mt-tRNA, causing mitochondrial translation defects, leading to Combined Oxidative Phosphorylation Deficiency 23 (OMIM #608536, COXPD23). It is autosomal recessive disease characterized by lactic acidosis, hypertrophic cardiomyopathy and encephalopathy with onset in early childhood (Kopajtich et al., 2014; Murayama et al., 2019). To date, 12 cases of COXPD23 and 15 different mutations in *GTPBP3* have been described (Kopajtich et al., 2014; Murayama et al., 2019), but COXPD23 caused by mutations in GTPBP3 identified from the Chinese population has not been reported. In this report, we describe a case series of COXPD23 cases caused by *GTPBP3* mutations. The mechanism, genotype-phenotype correlations, and diagnosis of this clinical entity are discussed, and the literature is reviewed.

MATERIALS AND METHODS

Next-Generation Sequencing and Bioinformatics Analysis

Blood samples were collected from the probands and family members. According to the manufacturer's instructions, genomic DNA was extracted using the SolPure Blood DNA kit (Magen) followed by DNA fragmentation using Q800R Sonicator (Qsonica). Based on the paired-end libraries, custom designed NimbleGen SeqCap solution-based exome capture reagent (Roche NimbleGen, Madison, WI) was used for fragments enrichment prior to sequencing on a NextSeq500 sequencer (Illumina, San Diego, CA). Multiple computational algorithms were applied to achieve pathogenicity and evolutionary conservative analysis as previously described (Jiang et al., 2017). Sanger sequencing was used to confirm the variants and determine the family co-segregation state. The interpretation of variants was manipulated according to the American College of Medical Genetics (ACMG) guidelines (Richards et al., 2015). Finally, the interpretation of variants was classified according to the ACMG guidelines, combined with the clinical manifestations and pedigree analysis of the proband. This study was performed in accordance with the Declaration of Helsinki and approved by the Ethical Committees of Beijing Children's Hospital and Hunan Provincial Maternal and Child Health Care Hospital. Written informed consent was obtained from the children's parents/guardians.

RESULTS

Patient Series Presentation

Patient 1, a 40-week gestation male baby, with a birth weight of 3,350 g, was delivered by cesarean section to a 32-year-old mother. His mother had a healthy boy aged 4 years old, and she suffered from Thrombocytopenia during this pregnancy. The infant's Apgar scores were 10 at 1 min and 9 at 10 min after delivery. Breastfeeding was initiated within 30 min after birth, but the infant demonstrated poor feeding. At the 17th hour after delivery, the infant experienced a sudden onset of dyspnea, cyanosis, mild stridor, and difficulty in suction. Physical examination revealed a temperature of 36°C, respiratory rate of 25/min, pulse rate of 118/min, BP of 66/29 mmHg, and SpO_2 of 76% (on mechanical ventilation), poor response, severe cyanosis, weak pulse, cool extremities, and low muscle tone. Routine laboratory investigations revealed hyperglycemia (7.3 mmol/L, normal: 3.9–6.1 mmol/L), pronounced hyperlactatemia (26 mmol/L, normal: <12 mmol/L), severe metabolic acidosis (PH 7.098, BE -29 mmol/L). The cerebrospinal fluid (CSF) lactate concentration increased to 20 mmol/L (normal: 0.9–2.7 mmol/L), and blood ketone concentration was 0.6 mmol/L (normal: 0–0.3 mmol/l). Moreover, serum lactate dehydrogenase (LDH) (721.7 U/L, normal: 120–250 U/L), creatine kinase (CK) (3,395.6 U/L, normal: 26–308 U/L), CK-MB (99.7 U/L, normal: 0–24 U/L), and myoglobin (656.2 U/L, normal: 0–90 U/L) levels were markedly elevated, consistent with skeletal muscle damage. The blood count, serum electrolytes, and ammonia level were normal. A chest x-ray showed significant cardiomegaly with a cardiothoracic ratio of 0.7. Urinary organic acid analysis by gas chromatography-mass spectrometry (GC-MS) revealed that urinary lactate concentration was significantly increased. Tandem-mass-spectrometry (MS-MS) showed a grossly increased level of alanine (2,384.51 μmol/L, normal: 100–510 μmol/L). The infant was promptly treated with mechanical ventilation, fluid resuscitation, correct metabolic acidosis, and intravenous supplementation of L-carnitine Coenzyme Q10, vitamin B1, and C. Unfortunately, the infant's condition deteriorated progressively, and he died of congestive heart failure (CHF) on the 4th day of life.

Patient 2, a girl was born to non-consanguineous healthy parents after an uneventful pregnancy. Her mother had one miscarriage at 7 weeks. She had normal developmental milestones before she was 6 months old. At the age of 1 year, she was first noticed to have remarkable developmental delay, with inflexibility of the lower extremities, and inability to stand walk alone, or speak. When she was first admitted to our hospital at the age of 2.5 years, she could not walk for a few steps steadily with wide legs stance and still couldn't speak, run, or jump. Physical examination revealed slight hypotonia of lower extremities. The routine laboratory test showed plasma lactate was markedly elevated (7.74–14 mmol/L, normal: 0–2.2 mmol/L), and CK-MB was slightly elevated (32 U/L, normal: 0–25 U/L). The plasma ammonia, glucose, LDH, aminotransferases, and CK were all within normal limits. GC-MS showed a grossly increased level of urine lactate. MS-MS revealed hyperalanine of 256.75 μmol/L (normal: 51–180 μmol/L) with normal plasma acylcarnitine profiles. Brain magnetic resonance imaging (MRI) demonstrated bilateral lesions in the midbrain, thalamus and dentate body of the cerebellum. The patient was treated with thiamine, riboflavin, Vitamin C, CoQ10, and carnitine. However, there was no significant improvement in her condition at the 6-month follow-up.

Patient 3, was the first child of non-consanguineous healthy parents. She was born at 41 weeks of gestational age after an uneventful pregnancy. At the age of 1 year and 9 months, she was admitted with three episodes of sudden convulsions. She was also found to have mild developmental delay and intellectual disability, fatigability, and hypertrophic cardiomyopathy. At the age of 3 years and 9 months, she could walk and run but easily fell down. She could understand most of the others' expressions and speak a few words but was unable to construct a complete sentence. Plasma lactate was consistently elevated (4.26–16 mmol/L, normal: <2.2 mmol/L). There were no significant abnormalities in other routine laboratory tests, urine organic acid profile, plasma amino acid, and acylcarnitine profiles. The electroencephalogram (EEG) and electrocardiography (ECG) were normal, but echocardiography revealed left ventricular hypertrophy (no data or images were found regarding this description). Brain MRI demonstrated bilateral lesions in the brain stem, thalamus and dentate body

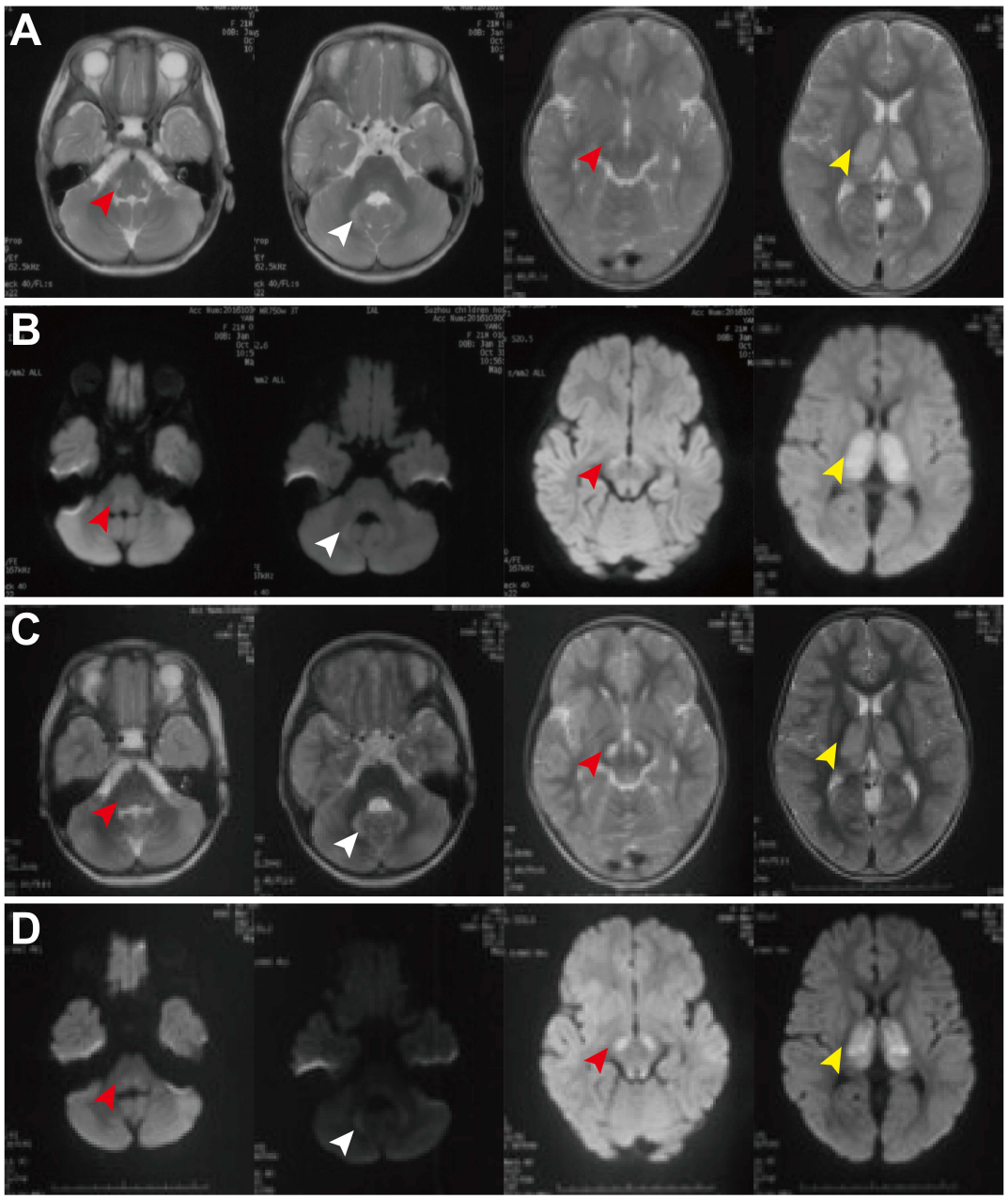

FIGURE 1 | Brain MRI of patient 3 at the ages of 1 year and 9 months old **(A,B)** and 3 years and 8 month old **(C,D)**. MRI demonstrated bilateral lesions in the brain stem (red arrowheads), thalamus (white arrowheads), and dentate body of cerebellum (yellow arrowheads), with diffusion limitation in diffusion weighted image. There is no significant improvement during the follow-up period.

of the cerebellum, with diffusion limitation in diffusion-weighted images (**Figure 1**). She was treated with thiamine, CoQ10, and carnitine. There was no significant improvement in her condition at the 8-month follow-up.

Molecular Genetics Analysis

Whole genome sequencing (WES) and targeted panels of candidate human mitochondrial genome were provided and revealed five variants in the *GTPBP3* gene in these three Chinese families. The mutations c.413C > T (p. A138V), c.509_510del (p. E170Gfs*42), c.544G > T (p. G182X), and c.424G > A (p.E142K) were localized in exon 4 while the mutation c.785A > C (p.Q262P) was localized in exon 5. The encoded amino acid residues of these mutations are all localized between the SH3 domain (101–118) and GTP-binding domain (283–301) of Gtpbp3 protein (**Figure 2A**). Further cross-species conservative analysis indicated that Ala138, Glu142, Glu170, and Gly182 residues are all highly conserved during evolution. Despite the amino acid variation at position 262 (Glu or Gln) among the six investigated species, both Glu and Gln are hydrophilic residues, which present high structure similarities (**Figure 2B**). These mutations cause amino acid alteration at highly conserved residues, which is physiochemically different from how the wild-type residue would impact the spiral structure and the function of the protein.

Patient 1 was a compound heterozygote with novel mutations c.413C > T (p. A138V) and c.509_510del (p. E170Gfs*42) in *GTPBP3*. Sanger sequencing revealed that the c.413C > T (p. A138V) was inherited from the paternal allele while the c.509_510del (p. E170Gfs*42) came from the maternal allele. Additionally, the infant's brother was a carrier of the mutation c.509_510del (p. E170Gfs*42), which was inherited from his mother (**Figure 3A**). The mutation c.413C > T (p. A138V) was not found in ExAc, dbSNP, 1,000 G, or ESP, and mutation c.509_510del (p. E170Gfs*42) is less frequent in our reference population genetic database (**Table 1**, PM2). Furthermore, the mutation c.413C > T (p. A138V) was predicted to be pathogenic by multiple computational analyses (**Table 1**, PP3). For recessive disorders, the frameshift mutation c.509_510del (p. E170Gfs*42) in *GTPBP3* (**Table 1**, PVS1) was detected in trans with a pathogenic variant (**Table 1**, PM4). And the newborn's phenotype (hyperlactacidemia and metabolic acidosis complicated with respiratory acidosis) is highly specific for a disease with a single genetic etiology (**Table 1**, PP4). Given the above analysis, we speculate that compound heterozygote mutations c.413C > T (p. A138V) and c.509_510del (p. E170Gfs*42) mutations in *GTPBP3* are the cause for COXPD23 with recessive inheritance (**Table 1**).

Patient 2 was a compound heterozygote with novel mutations c.544G > T (p. G182X) and c.785A > C (p. Q262P) in *GTPBP3*, and the c.544G > T (p. G182X) was inherited from

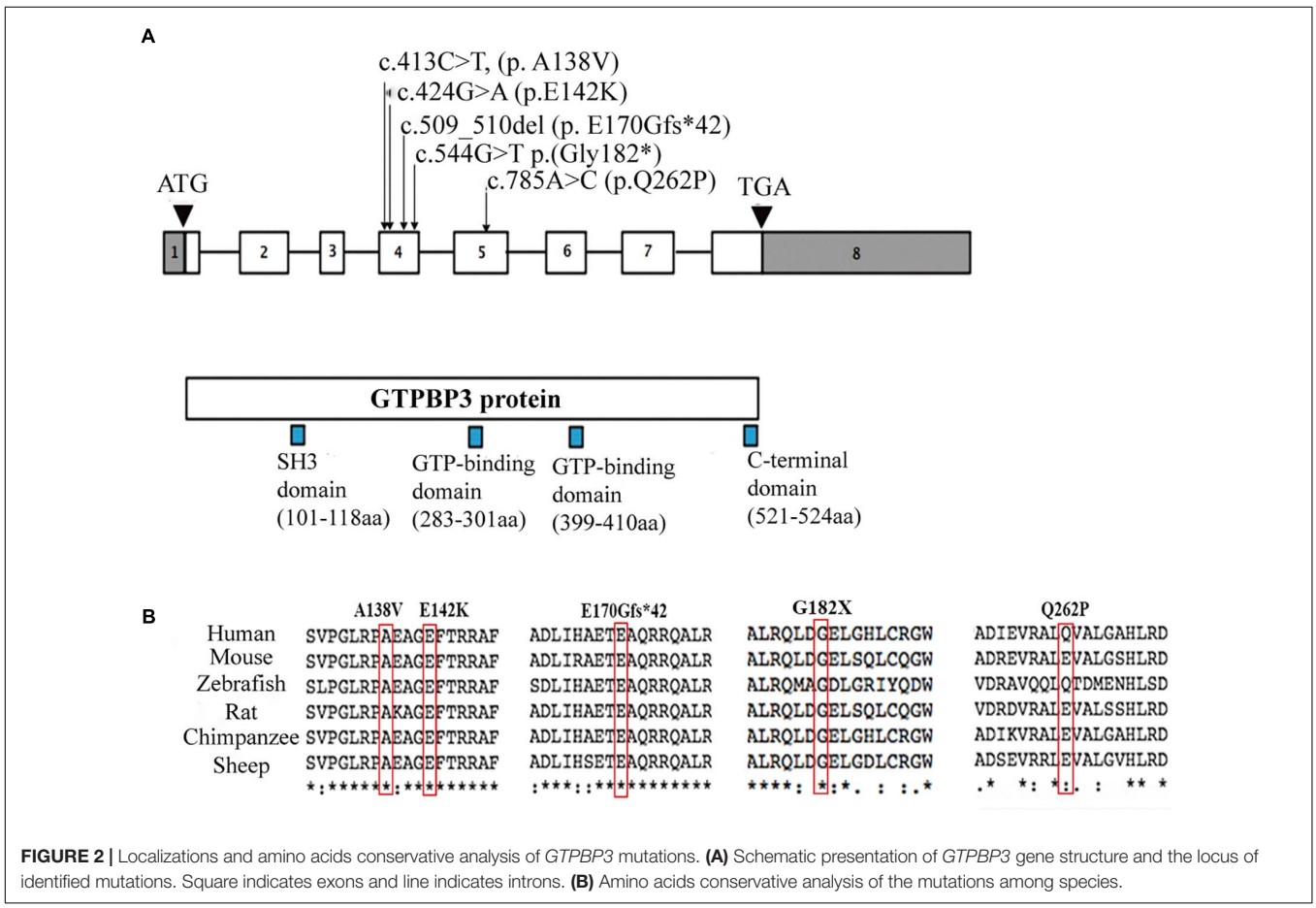

FIGURE 2 | Localizations and amino acids conservative analysis of *GTPBP3* mutations. **(A)** Schematic presentation of *GTPBP3* gene structure and the locus of identified mutations. Square indicates exons and line indicates introns. **(B)** Amino acids conservative analysis of the mutations among species.

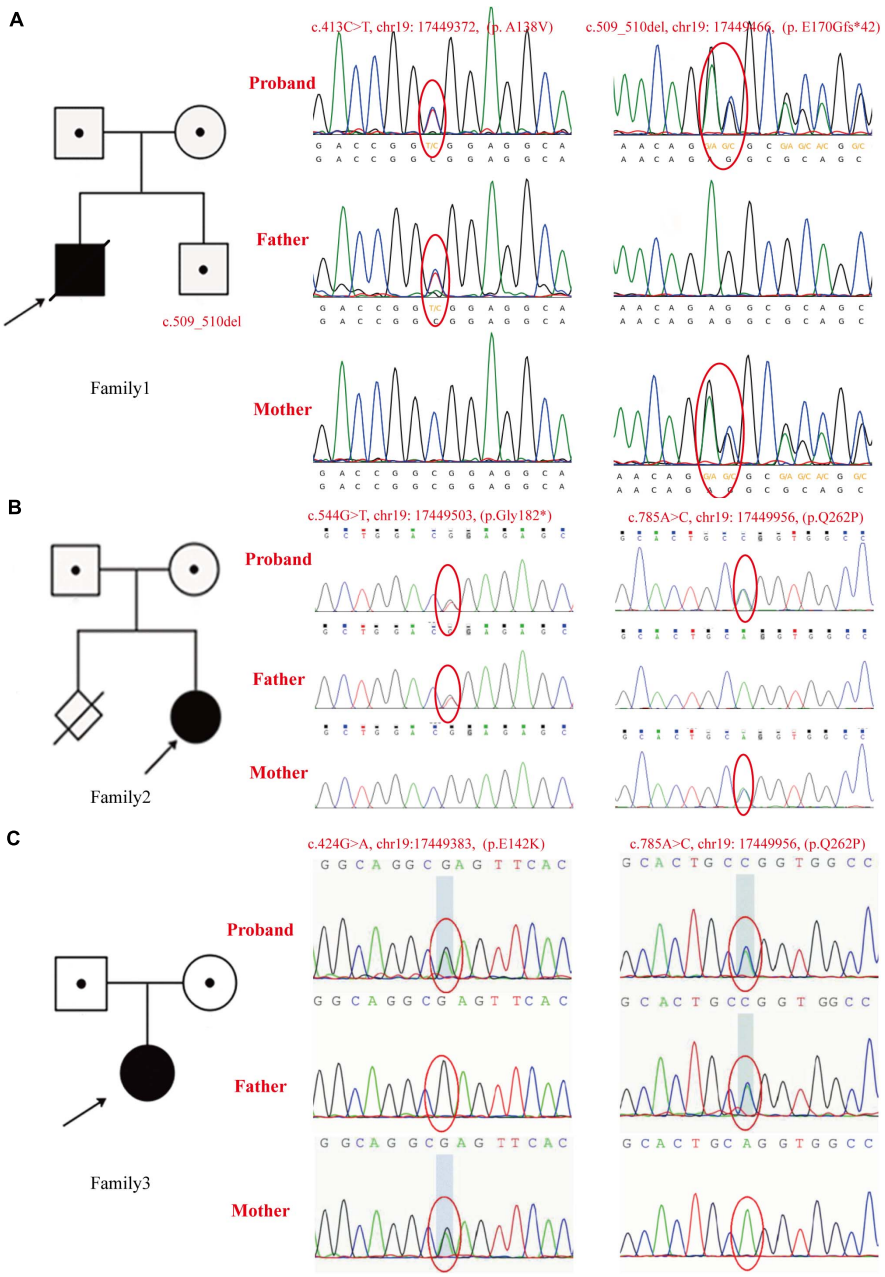

FIGURE 3 | The pedigrees and identified *GTPBP3* mutations. **(A)** In family 1, the c.413C > T (p. A138V) mutation was detected in the proband and his father, c.509_510del (p. E170Gfs*42) was detected in the proband and his mother. As shown in the pedigree of the nuclear family, c.509_510del (p. E170Gfs*42) was found in his brother as validated by Sanger sequencing. **(B)** Mutations identified in family 2 as confirmed by Sanger sequencing. The c.544G > T (p. G182X) mutation was found in the proband and her father, and the c.785A > C (p.Q262P) mutation was found in the proband and her mother. As shown in the pedigree of the nuclear family, there is a history of firstborn spontaneous abortion of the mother at the 7th week of gestation. **(C)** Mutations found in family 3 as confirmed by Sanger sequencing. The c.785A > C (p.Q262P) was found in the proband and her father, mutation c.424G > A (p.E142K) was found in the proband and her mother. The arrow indicates the proband.

the paternal allele, while the c.785A > C (p. Q262P) came from the maternal allele (**Figure 3B**). The frameshift mutation [c.544G > T (p. G182X)] (**Table 1**, PVS1) was not found in ExAc, dbSNP, 1,000 G, or ESP, and missense mutation [c.785A > C (p. Q262P)] is less frequent in our reference population genetic database (**Table 1**, PM2). In addition, the results of bioinformatics analysis of missense mutation [c.785A > C (p. Q262P)] were inconsistent. PolyPhen-2 and SIFT predicted that it was benign, but Mutation-Taster predicted that it was harmful (**Table 1**, BP4). However, the patient's clinical manifestations (developmental delay, fatigability, and hyperlactacidemia) are highly consistent with COXPD23 caused by *GTPBP3* defects. Therefore, we

TABLE 1 | The molecular genetics analysis of three patients.

Patient ID	Variant (paternal)	Variant (maternal)	Evidence of pathogenicity	ACMG classification
#1	c.413C > T, chr19: 17449372, (p. A138V)		PM2 + PM3 + PP3 + PP4	Likely pathogenic
		c.509_510del, chr19: 17449466, (p. E170Gfs*42)	PVS1 + PM2	Likely pathogenic
#2	c.544G > T, chr19: 17449503, (p.Gly182*)		PVS1 + PM2	Likely pathogenic
		c.785A > C, chr19: 17449956, (p.Q262P)	PM2 + BP4	Uncertain significance
#3	c.785A > C, chr19: 17449956, (p.Q262P)		PM2 + BP4	Uncertain significance
		c.424G > A, chr19:17449383, (p.E142K)	PM2 + PP3	Uncertain significance

Trio whole exome sequencing (WES) successfully defined GTPBP3 gene variations in chromosome 19 (GRCh37/hg19, NM_133644). Evidence of Pathogenicity were according to ACMG standards and guidelines doi: 10.1038/gim.2015.30. And the missense prediction is analyzed on the website http://varcards.biols.ac.cn/.

speculate that compound heterozygote mutations c.544G > T (p. G182X) and c.785A > C (p. Q262P) mutations in *GTPBP3* are the cause for COXPD23 with recessive inheritance (**Table 1**).

Patient 3 was a compound heterozygote with c.424G > A (p. E142K) and novel mutation c.785A > C (p.Q262P) in *GTPBP3*, and the c.785A > C (p.Q262P) was inherited from the paternal allele while the c.424G > A (p.E142K) from the maternal allele (**Figure 3C**). The mutation c.424G > A (p. E142K) was not found in ExAc, dbSNP, 1,000 G, or ESP, and missense mutation [c.785A > C (p. Q262P)] is less frequent in our reference population genetic database (**Table 1**, PM2). The region of variation [c.424G > A (p. E142K)] is an important part of the Gtpbp3 protein, and the amino acid sequences of different species are highly conserved. Computer-aided analysis predicts that this variation is more likely to affect the structure and function of proteins (**Table 1**, PP3). Considering the continuous elevation of plasma lactic acid and the involvement of multiple systems, we speculate that compound heterozygote with mutation c.424G > A (p. E142K) and the novel mutation c.785A > C (p.Q262P) in *GTPBP3* are the cause for COXPD23 with recessive inheritance (**Table 1**).

DISCUSSION

In this report, we described three cases of COXPD23 caused by mutations in *GTPBP3* from Chinese population, one of them (patient 1) with severe neonatal presentation and a fatal outcome, carrying the novel mutations c.413C > T (p. A138V) and c.509_510del (p. E170Gfs*42) in compound heterozygotes, and the remaining two (patients 2 and 3) with a mild presentation characterized by developmental delay with no significant improvement of the clinical condition during follow-up. Patient 2 was a compound heterozygote with novel mutations c.544G > T (p. G182X) and c.785A > C (p.Q262P), while patient 3 was a compound heterozygote with c.424G > A (p.E142K) and novel mutation c.785A > C (p.Q262P).

The post-transcriptional modification is essential to the maturation processes of tRNAs to form the cloverleaf structure resulting in a stable and correctly functioning tRNAs, and a variety of modified nucleosides are required in these processes (Van Haute et al., 2015). The 5-taurinomethyluridine (τm^5U) modification, identified in mt-tRNALeu$^{(UUR)}$ and mt-tRNA^{Trp}, is required for accurate decoding of purine-ending codons and prevent misreading of pyrimidine-ending codons, thereby promoting efficient decoding of cognate codon (Suzuki and Suzuki, 2014). Human *GTPBP3* gene encoding the mitochondrial GTP-binding protein Gtpbp3, has been documented to be responsible for the τm^5U synthesis, which involved in the post-transcriptional modification of mt-tRNALeu$^{(UUR)}$ and mt-tRNA^{Trp} (Li and Guan, 2002). A study by Asano et al. (2018) demonstrated that τm^5U was absent from mt-tRNALeu$^{(UUR)}$ and mt-tRNA^{Trp} in *GTPBP3* KO cells. *GTPBP3* KO cells exhibited marked reductions in oxygen consumption rate (OCR) and mitochondrial translation, reduced levels of complex I subunit proteins and deficient complex I activity. Their findings demonstrated that repression of mitochondrial translation due to lack of m^5U34 in *GTPBP3* KO might disrupt maturation and stability of respiratory chain complexes (Asano et al., 2018). Villarroya et al. (2008) found that in comparison with the negative controls, the human *GTPBP3*-silenced cells exhibited significant mitochondrial dysfunction, manifested by a significant decrease of OCR and mitochondrial membrane potential, a 40% (±9) decrease in ATP levels, as well as a 28% (±3) increase in mitochondrial superoxide generation. Taken together, these studies documented that the *GTPBP3* gene is associated with mt-tRNAs post-modification and defects of *GTPBP3* will lead to mitochondrial dysfunction. In addition, Boutoual et al. (2018) reported that stable silencing of *GTPBP3* triggers an AMPK-dependent retrograde signaling pathway, which downregulates the mitochondrial pyruvate carrier (MPC), while upregulating the expression of the uncoupling protein 2 (UCP2) and genes involved in glycolysis and fatty acid oxidation, leading to an uncoupling of glycolysis and oxidative phosphorylation. The uncoupling is expected to result in lactic acidosis, a common clinical trait presents in *GTPBP3* patients.

The association between *GTPBP3* mutations and mitochondrial disease was first described in 2014. Kopajtich et al. (2014) reported 11 individuals from 9 families, carrying homozygous or compound heterozygous mutations in *GTPBP3*. These individuals presented with lactic acidosis, hypertrophic cardiomyopathy, and encephalopathy, consistent with the

TABLE 2 | Clinical and Genetic Findings in Patients with *GTPBP3* Mutations.

Patient ID	Sex	Ethic origin	Onset age	Presenting symptoms	Plasma lactate	TTE	Brain MRI	Outcomes, follow-up time, cause of death	*GTPBP3* mutations	chromosomal position (hg19)	Domain/site
Severe form											
#72425 (Kopajtich et al., 2014)	F	No data	3.5 months	Poor feeding, failure to thrive, hypoactivity	23.3 mmol/l	DCM	No data	Died, 8 months, CHF	c.[484G > C; 673G > A; 964G > C], p.[Ala162Pro; Glu225Lys; Ala322Pro]	g.[17449443;17449940;17450398]	Ala162Pro and Glu225Lys at position between N-terminus and TrmE-type G domain; Ala322Pro at TrmE-type G domain (249–416)
#75191 (Kopajtich et al., 2014)	F	No data	Birth	Poor feeding, hypotonic, respiratory failure	23 mmol/l	HCM	No data	Died, 1 day, asystolia	c.[1009G > C; 1009G > C], p.[Asp337His; Asp337His]	g.[17451887]	Asp337His at TrmE-type G domain (249–416)
#76671 (Kopajtich et al., 2014)	M	No data	Birth	Poor feeding, hypotonic, CHF, metabolic acidosis	5.2 mmol/l	HCM	Bilateral hyperintensities in thalamus	Died, 10 months, CHF	c.[665-2delA; 665-2delA], p.[Ala222Gly; Asp223_Ser270del; Ala222Gly; Asp223_Ser270del]	g.[17449930]	N/A
#81471 (Kopajtich et al., 2014)	M	Romanian	4 weeks	Hypothermia, recurrent apnea metabolic acidosis	11 mmol/l	HCM	Hyperintensities in subthalamic nuclei	Died, 5 weeks, acidosis	c.[424G > A; 424G > A], p.[Glu142Lys; Glu142Lys]	g.[17449383]	Glu142Lys at GTP-binding protein TrmE N-terminus (35–152)
#83904 (Kopajtich et al., 2014)	F	Turkish	1 week	Cardiogenic shock, metabolic acidosis	20 mmol/l	DCM	No data	Died, 9 months, CHF	c.[32_33delinsGTG; 32_33delinsGTG], p.[Gln11Argfs*98; Gln11Argfs*98]	g.[17448452_17448453]	Gln11Argfs*98 at transit peptide (1–81)/GTP-binding protein TrmE N-terminus (35–152)
#83905 (Kopajtich et al., 2014)	F	Turkish	Birth	Cardiogenic shock, metabolic acidosis	No data	DCM	No data	Died, 10 days, CHF	c.[32_33delinsGTG; 32_33delinsGTG], p.[Gln11Argfs*98; Gln11Argfs*98]	g.[17448452_17448453]	Gln11Argfs*98 at transit peptide (1–81)/GTP-binding protein TrmE N-terminus (35–152)
Our Patient #1	M	Chinese	17 h	Hypothermia, poor response, respiratory failure, cardiogenic shock, metabolic acidosis	26 mmol/l	Normal	No data	Died, 5 days, CHF	c.[413C > T; c.509_510del], p.[Ala138Val; Gln170Glyfs*42]	g.[17449372;17449468_17449469delAG]	Ala138Val at GTP-binding protein TrmE N-terminus (35–152); Gln170Glyfs*42 localized between the SH3 domain (101–118) and GTP-binding domain (283–301)
Mild form											
#49665 (Kopajtich et al., 2014)	M	Arab	10 years	Intellectual disability, fatigability, visual impairment, slight dyspnea with climbing stairs	3∼7 mmol/l	HCM	Lactate peaks in parietal and precentral cortex	Alive, 14 years	c.[1291dupC; 1375G > A], p.[Pro430Argfs*86; Glu459Lys]	g.[17452324;17452408]	C-terminal
#36349 (Kopajtich et al., 2014)	M	Arab	No data	Intellectual disability, fatigability, visual impairment, slight dyspnea with climbing stairs	No data	HCM	Lactate peaks in parietal and precentral cortex	Alive, 17 years	c.[1291dupC; 1375G > A], p.[Pro430Argfs*86; Glu459Lys]	g.[17452324;17452408]	C-terminal
#66143 (Kopajtich et al., 2014)	M	Arab	2 years	Sudden respiratory failure, CHF	No data	HCM	No data	Alive, 5 years	c.[476A > T; 964G > C], p.[Glu159Val; Ala322Pro]	g.[17449435;17450398]	Glu159Val at position between N-terminus and TrmE-type G domain; Ala322Pro at TrmE-type G domain (Switch II region (302–312, 314–328)
#75168 (Kopajtich et al., 2014)	F	Indian	2 years	Developmental delay, epileptic seizures	>10 mmol/l	No data	Bilateral hyperintensities in thalamus	Alive, 5 years	c.[770C > A; 770C > A], p.[Pro257His; Pro257His]	g.[17450037]	Pro257His at GTP binding region (256–263); Pro257His at TrmE-type G domain (249–416)
#82790 (Kopajtich et al., 2014)	F	Japanese	1 year	Developmental delay, epileptic seizures, hypotonia	5.7∼6.5 mmol/l	Normal	Bilateral hyperintensities in thalamus	Alive, 2 years	c.[8G > T; 934_957del], p.[Arg3Leu; Gly312_Val319del]	g.[17448428;17450368_17450391]	Arg3Leu at transit peptide (1–81); Gly312_Val319del at TrmE-type G domain (249–416); Gly312_Val319del at Switch II region (302–312, 314–328)
Patient No. 24 (Elmas et al., 2019)	F	Turkish	3 weeks	Mental motor retardation, seizure, hearing disability, thrombocytopenia	No data	Normal	Delayed myelination	Alive, 10years	c.[932C > T,932C > T], p.[Pro311Leu, Pro311Leu]	g.[17450270;17450270]	Pro311Leu at TrmE-type G domain (249–416)
Our Patient #2	F	Chinese	1 year	Developmental delay, hypotonia	7.7∼14 mmol/l	No data	Bilateral lesions in brain stem, thalamus and cerebellum	Alive, 3 years	c.[544G > T; c.785A > C], p.[Gly182X; Gln262Pro]	g.[17449503;17449956]	Gly182X at position between N-terminus and TrmE-type G domain which cause the loss of TrmE-type G domain and C terminal; Gln262Pro at GTP binding region (256–263)
Our Patient #3	F	Chinese	1 year	Developmental delay, intellectual disability, fatigability,	4.26∼16 mmol/l	HCM	Bilateral lesions in brain stem, thalamus and cerebellum	Alive, 3 years	c.[424G > A; c.785A > C], p.[Glu142Lys; Gln262Pro]	g.[17449383;17449956]	Glu142Lys at GTP-binding protein TrmE N-terminus (35–152); Gln262Pro at GTP binding region (256–263)

CHF, congestive heart failure; DCM, dilated cardiomyopathy; HCM, hypertrophic cardiomyopathy; N/A, not applicable; TTE, transthoracic echocardiography.

impaired activity of respiratory complexes (I and IV), and defective translation of mitochondrial proteins, providing strong evidence for the pathological role of mutant *GTPBP3* in mitochondrial disease. Elmas et al. (2019) also described a 10-year- old girl with *GTPBP3* mutations, characterized by early childhood onset of mental motor retardation, seizure, hearing disability, and delayed myelination. These 12 patients came from five ethnic groups, including Romanian, Turkish, Arab, Indian, and Japanese, sharing some similar phenotypes, which might be classified into two forms. The first is the severe form, usually presented within the period of infancy and characterized by acute metabolic decompensation with a rapid deterioration, often presenting with CHF, severe hyperlactacidemia, and consequently early death. Six mutants were identified in this form, including c.484G > C, c.673G > A, c.1009G > C, c.665-2delA, c.424G > A, and c.32_33delinsGTG, causing the loss of TrmE-type G domain, the missense *GTPBP3* variants in TrmE-type G domain, or missense variant in N-terminus of Gtpbp3 protein. The second is the mild form with encephalopathy, cardiomyopathy, and hyperlactacidemia, usually presented in early childhood though it may survive into the second decade. Seven mutants were identified in this form, including c.1291dupC, c.1375G > A, c.476A > T, c.770C > A, c.8G > T, c.934_957del, and c.932C > T, while mutant c.964G > C was observed in both severe and mild forms. These causative mutations mainly concentrate on the C-terminus and N-terminus, and only three carry missense variants in the G domain (**Table 2**). Our three cases were born to unrelated parents of Chinese origin. Our patient 1 presented with a severe form, with remarkably hyperlactacidemia, metabolic acidosis, and progressive heart damage and died of CHF on the 4th day of life. Patients 2 and 3 presented with a mild form, with developmental delay, fatigability, and hyperlactacidemia. The brain MRI preformed in patients 2 and 3 and showed an involvement of the thalamus, brainstem, and cerebellum, resembling the findings in Leigh syndrome. The clinical status of these two patients is stable and did not show improvement during their follow-up period. Additionally, a grossly increased level of serum alanine was detected in patient 1, along with a mild hyperalaninemia in patient 2. Of note, the hyperalaninemia has not been described in previously reported cases of COXPD23. The elevation in amino acids such as alanine, glycine, proline, and threonine is due to the altered redox state created by respiratory chain dysfunction, and the notable elevation usually occurs during the course of clinical deterioration (Parikh et al., 2015). The hyperalaninemia accompanied by hyperlactacidemia is an important clue for clinical suspicion of mitochondrial disorders, and the marked hyperalaninemia might serve as a red flag for the severe form of mitochondrial diseases.

Diagnosis of mitochondrial disease is challenging. The next-generation sequence (NGS) is recommended to accurately confirm mitochondrial disease. Two options are currently being implemented—WES and targeted panels of candidate genes including both mt-DNA and known pathogenic nDNA genes (Wong, 2013; Alston et al., 2017). In our patients, we implemented WES and targeted panels of candidate mitochondrial gene and identified five heterozygous rare mutations in *GTPBP3*, among which mutation c.424G > A (p. E142K) was reported previously (**Table 2**, patient #81471). The other four mutations were novel, including c.413C > T (p. A138V) and c.509_510del (p. E170Gfs*42) in patient 1, c.544G > T (p. G182X), c.785A > C (p.Q262P), and c.785A > C (p.Q262P) in patients 2 and 3. Mutation c.413C > T (p. A138V) causes Ala to Val at GTP-binding protein TrmE N-terminus of Gtpbp3 protein, and c.509_510del (p. E170Gfs*42) causes a frame shift that leads to no translation of GTP domains thereafter. The GTP binding domain participates in binding of guanine nucleotides and Mg^{2+}, hydrolysis of GTP or regulates the functional state of GTPases through conformational alteration (Villarroya et al., 2008). Mutations c.544G > T (p. G182X), c.785A > C (p.Q262P) and c.785A > C (p.Q262P) in patients 2 and 3 cause the loss of TrmE-type G domain and C terminal or an impaired GTP domain. Interestingly, the impaired GTP domains were also observed in 9 of 12 previously reported cases with both severe and mild forms (**Table 2**). Therefore, we speculate that mutations in GTP binding domain may cause different degrees of Gtpbp3 functional impairment.

In conclusion, we first report three Chinese individuals with COXPD23 caused by mutations in *GTPBP3* from severe to mild phenotype. Apart from a previously reported mutation c.424G > A (p. E142K), four novel mutations c.413C > T (p. A138V), c.509_510del (p. E170Gfs*42), c.544G > T (p. G182X) and c.785A > C (p.Q262P) were identified. Our findings provide novel information in the molecular diagnosis and genetic counseling of patients with COXPD23. Admittedly, the sample size is small, and more in-depth investigations are needed to further elucidate the genotype-phenotype correlations in COXPD23.

DATA AVAILABILITY STATEMENT

The data presented in the study are deposited in the (GSA-Human) repository (https://bigd.big.ac.cn/gsa-human/browse/HRA000939), accession number (HRA000939).

ETHICS STATEMENT

The studies involving human participants were reviewed and approved by the Ethical Committees of Beijing Children's Hospital and Hunan Provincial Maternal and Child Health Care Hospital. Written informed consent to participate in this study was provided by the participants' legal guardian/next of kin.

AUTHOR CONTRIBUTIONS

H-MY and Z-ML participated in the treatment for the patients, analyzed, and interpreted the data, acquired the literature data, wrote the manuscript, and created **Table 2**. BC cared for the patients, provided clinical data, and performed clinical assessments. VZ and Y-DH performed genetic analysis, reviewed the data, and helped to revise the manuscript for molecular

genetics analysis content. Z-JJ, HX, and JL reviewed the data and helped to draft the manuscript. FF and HW cared for the patients, performed clinical assessments, revised the final version of the manuscript, and supervised the study. All the authors reviewed the final version of the manuscript.

FUNDING

This work is supported by the Major Scientific and Technological Projects for collaborative prevention and control of birth defects in Hunan Province (2019SK1010), the Major Medical Collaboration and Innovation Program of Guangzhou Science Technology and Innovation Commission (Grant Nos. 201604020020 and 201604020009).

ACKNOWLEDGMENTS

We sincerely appreciate the patients' families for their cooperation and giving their written informed consent to publish this case series.

REFERENCES

Alston, C. L., Rocha, M. C., Lax, N. Z., Turnbull, D. M., and Taylor, R. W. (2017). The genetics and pathology of mitochondrial disease. *J. Pathol.* 241, 236–250. doi: 10.1002/path.4809

Asano, K., Suzuki, T., Saito, A., Wei, F. Y., Ikeuchi, Y., Numata, T., et al. (2018). Metabolic and chemical regulation of tRNA modification associated with taurine deficiency and human disease. *Nucleic Acids Res.* 46, 1565–1583. doi: 10.1093/nar/gky068

Boutoual, R., Meseguer, S., Villarroya, M., Martín-Hernández, E., Errami, M., Martín, M. A., et al. (2018). Defects in the mitochondrial-tRNA modification enzymes MTO1 and GTPBP3 promote different metabolic reprogramming through a HIF-PPARγ-UCP2-AMPK axis. *Sci. Rep.* 8:1163. doi: 10.1038/s41598-018-19587-5

Craven, L., Alston, C. L., Taylor, R. W., and Turnbull, D. M. (2017). Recent Advances in Mitochondrial Disease. *Annu. Rev. Genomics Hum. Genet.* 18, 257–275. doi: 10.1146/annurev-genom-091416-035426

Elmas, M., Yıldız, H., Erdoğan, M., Gogus, B., Avcı, K., and Solak, M. (2019). Comparison of clinical parameters with whole exome sequencing analysis results of autosomal recessive patients; a center experience. *Mol. Biol. Rep.* 46, 287–299. doi: 10.1007/s11033-018-4470-7

Jiang, Y., Pan, J., Guo, D., Zhang, W., Xie, J., Fang, Z., et al. (2017). Two novel mutations in the PPIB gene cause a rare pedigree of osteogenesis imperfecta type IX. *Clin. Chim. Acta* 469, 111–118. doi: 10.1016/j.cca.2017.02.019

Kopajtich, R., Nicholls, T. J., Rorbach, J., Metodiev, M. D., Freisinger, P., Mandel, H., et al. (2014). Mutations in GTPBP3 cause a mitochondrial translation defect associated with hypertrophic cardiomyopathy, lactic acidosis, and encephalopathy. *Am. J. Hum. Genet.* 95, 708–720. doi: 10.1016/j.ajhg.2014.10.017

Li, X., and Guan, M. X. (2002). A human mitochondrial GTP binding protein related to tRNA modification may modulate phenotypic expression of the deafness-associated mitochondrial 12S rRNA mutation. *Mol. Cell Biol.* 22, 7701–7711. doi: 10.1128/mcb.22.21.7701-7711.2002

Murayama, K., Shimura, M., Liu, Z., Okazaki, Y., and Ohtake, A. (2019). Recent topics: the diagnosis, molecular genesis, and treatment of mitochondrial diseases. *J. Hum. Genet.* 64, 113–125. doi: 10.1038/s10038-018-0528-6

Parikh, S., Goldstein, A., Koenig, M. K., Scaglia, F., Enns, G. M., Saneto, R., et al. (2015). Diagnosis and management of mitochondrial disease: a consensus statement from the Mitochondrial Medicine Society. *Genet. Med.* 17, 689–701. doi: 10.1038/gim.2014.177

Rahman, S., and Wolf, N. I. (2017). "Diagnostic Workup of Patients with Mitochondrial Diseases," in *Inherited Metabolic Diseases*, eds G. F. Hoffmann, J. Zschocke, and W. L. Nyhan (Berlin: Springer), 521–535.

Richards, S., Aziz, N., Bale, S., Bick, D., Das, S., Gastier-Foster, J., et al. (2015). Standards and guidelines for the interpretation of sequence variants: a joint consensus recommendation of the American College of Medical Genetics and Genomics and the Association for Molecular Pathology. *Genet. Med.* 17, 405–424. doi: 10.1038/gim.2015.30

Skladal, D., Halliday, J., and Thorburn, D. R. (2003). Minimum birth prevalence of mitochondrial respiratory chain disorders in children. *Brain* 126, 1905–1912. doi: 10.1093/brain/awg170

Suzuki, T., and Suzuki, T. (2014). A complete landscape of post-transcriptional modifications in mammalian mitochondrial tRNAs. *Nucleic Acids Res.* 42, 7346–7357. doi: 10.1093/nar/gku390

Van Haute, L., Pearce, S. F., Powell, C. A., D'Souza, A. R., Nicholls, T. J., and Minczuk, M. (2015). Mitochondrial transcript maturation and its disorders. *J. Inherit. Metab. Dis.* 38, 655–680. doi: 10.1007/s10545-015-9859-z

Villarroya, M., Prado, S., Esteve, J. M., Soriano, M. A., Aguado, C., Pérez-Martínez, D., et al. (2008). Characterization of human GTPBP3, a GTP-binding protein involved in mitochondrial tRNA modification. *Mol. Cell Biol.* 28, 7514–7531. doi: 10.1128/mcb.00946-08

Wong, L. J. (2013). Next generation molecular diagnosis of mitochondrial disorders. *Mitochondrion* 13, 379–387. doi: 10.1016/j.mito.2013.02.001

Conflict of Interest: The authors declare that the research was conducted in the absence of any commercial or financial relationships that could be construed as a potential conflict of interest.

Advantages of publishing in Frontiers

OPEN ACCESS
Articles are free to read for greatest visibility and readership

FAST PUBLICATION
Around 90 days from submission to decision

HIGH QUALITY PEER-REVIEW
Rigorous, collaborative, and constructive peer-review

TRANSPARENT PEER-REVIEW
Editors and reviewers acknowledged by name on published articles

Frontiers
Avenue du Tribunal-Fédéral 34
1005 Lausanne | Switzerland

Visit us: www.frontiersin.org
Contact us: frontiersin.org/about/contact

REPRODUCIBILITY OF RESEARCH
Support open data and methods to enhance research reproducibility

DIGITAL PUBLISHING
Articles designed for optimal readership across devices

FOLLOW US
@frontiersin

IMPACT METRICS
Advanced article metrics track visibility across digital media

EXTENSIVE PROMOTION
Marketing and promotion of impactful research

LOOP RESEARCH NETWORK
Our network increases your article's readership